

Rowan University

Rowan Digital Works

Theses and Dissertations

6-17-2016

Synthesis and biological activity of novel quorum sensing compounds

Joseph Nicholas Capilato

Follow this and additional works at: <https://rdw.rowan.edu/etd>



Part of the [Bacteriology Commons](#), and the [Organic Chemistry Commons](#)

Recommended Citation

Capilato, Joseph Nicholas, "Synthesis and biological activity of novel quorum sensing compounds" (2016). *Theses and Dissertations*. 1649.
<https://rdw.rowan.edu/etd/1649>

This Thesis is brought to you for free and open access by Rowan Digital Works. It has been accepted for inclusion in Theses and Dissertations by an authorized administrator of Rowan Digital Works. For more information, please contact graduateresearch@rowan.edu.

**SYNTHESIS AND BIOLOGICAL ACTIVITY OF NOVEL QUORUM SENSING
COMPOUNDS**

by

Joseph N. Capilato

A Thesis

Submitted to the
Department of Chemistry & Biochemistry
College of Science and Mathematics
In partial fulfillment of the requirement
For the degree of
Master of Science in Pharmaceutical Sciences
at
Rowan University
June 1, 2016

Thesis Chair: Lark J. Perez, Ph.D

© 2016 Joseph N. Capilato

Dedication

This paper is dedicated to my parents, who worked tirelessly to be able to provide me with the best education possible.

Acknowledgments

I would like to acknowledge my family and friends for their constant support of me throughout the course of this research and beyond. Additionally, I would like to thank my research advisor for the significant time and effort he devoted towards teaching me and developing me into the scientist I am today. I would not be where I am today without the aid of all of these people.

Abstract

Joseph N. Capilato
SYNTHESIS AND BIOLOGICAL ACTIVITY OF NOVEL QUORUM SENSING
COMPOUNDS
2015-2016
Lark J. Perez, Ph.D
Master of Science in Pharmaceutical Science

Bacteria communicate with chemical signals in a process known as quorum sensing. This population density-dependent process involves the bacterial production, release and detection of structurally specific small molecules and enables the bacterial pathogen to regulate its virulence on a population-wide level. Using a variety of chemical and biological techniques, I have studied various quorum sensing systems in several bacteria, including *Vibrio cholera* and *Pseudomonas aeruginosa*. A key principle of this research involves the design, synthesis and testing of novel compounds for their biological activity. These molecules are typically based off of an initial lead target, which is often identified from a high-throughput screen and serves as a template for further optimization. Specifically, I have researched quorum sensing compounds that affect Hfq-RNA interactions in *V. cholera*, the LasR receptor in *P. aeruginosa* and HapR in *V. cholera*. Taken together, the results of these studies provide a basis for future investigations involving quorum sensing, and demonstrate how organic chemistry can be employed to study these fascinating biochemical systems.

Table of Contents

Abstract	v
List of Figures	vii
List of Tables	viii
Chapter 1: Design of Small Molecule Inhibitors of a Protein-RNA Interaction in Vibrio Cholera	1
Introduction.....	1
Results and Discussion	2
The Dose-Response Relationship for Compound 1 is a Bell Curve	2
An Amino Acid is Required for Biological Activity	3
Development of Truncated Analogs Establishes the Unimportance of the Aryl Sulfonamide Moiety	4
Development of Oxazolidinone Derivatives Addresses Issue of Stability and Toxicity.....	6
Identification of a Higher Potency Compound.....	7
Chemistry	8
Conclusion	12
Experimental Section	20
Bacterial Reporter Strain Assay	20
General Chemistry.....	20
Chapter 2: Development of Photolabile Protecting Groups for a Bioactive Compound.....	60
Introduction.....	60
Results and Discussion	61
Development of the HapR-Riboswitch Construct.....	61

Table of Contents (continued)

Analysis of NPOM-Caged Theophylline	62
Discovery and Evaluation of new Photocages	63
Chemistry	64
Conclusion	65
Experimental Section	66
General Chemistry.....	66
Chapter 3: Gem-Dinitro Enols: Discovery and Application of a new Reaction for Methyl Ketones.....	80
Introduction.....	80
Results and Discussion	81
Isolation of Key Intermediates Leads to the Elucidation of the Reaction Mechanism	81
Nucleophile Substrate Scope is Wide-Ranging.....	83
Ketone Substrate Scope Includes Both Aromatic and Alkyl Methyl Ketones...84	
Application of This new Reaction to Produce Medicinally Relevant Compounds.....	86
Conclusion	87
Experimental Section	89
General Chemistry.....	89
Chapter 4: Structure-Activity Relationship of a Triphenyl Scaffold for the LasR Receptor in Pseudomonas Aeruginosa	106
Introduction.....	106
Results and Discussion	110
Synthesis.....	110
"A-Ring" Structure Activity Relationship Studies	111

Table of Contents (continued)

"C-Ring" Structure Activity Relationship Series	112
Conclusion	120
Experimental Section	121
Bacterial Reporter Strain Assay	121
General Chemistry	121
Chapter 5: Reduction of Virulence in <i>P. Aeruginosa</i> Through Quorum Sensing Inhibition by Lipoxin A ₄	190
Introduction	190
Results	193
Blood Bacterial Load	193
Neutrophil Apoptosis and Free Radical Production	193
Neutrophil Phagocytic Ability and CD64 Expression	193
Inhibition of Pyocyanin Expression by LXA ₄	195
Inhibition of LasR QS by LXA ₄	196
Discussion	199
Experimental Section	202
Conclusion	208
References	211

List of Figures

Figure	Page
Figure 1. Structure of HTS (1) and examples of some analogs prepared	14
Figure 2. Dose response curve for 1	14
Figure 3. Analogs developed using stable linkers	15
Figure 4. Dose response curve for 2	15
Figure 5. OD ₆₀₀ plot for 1 and 2	16
Figure 6. Biological activity of three truncated analogs	16
Figure 7. Dose response curve for the oxazolidinone analog	17
Figure 8. OD ₆₀₀ plot for the oxazolidinone analog	17
Figure 9. Dose response curve for 4	18
Figure 10. Methods employed for the synthesis of 2-substituted benzimidazoles	18
Figure 11. Synthesis of acetal intermediates	19
Figure 12. Various methods utilized to form N, N-acetals	19
Figure 13. TheoRS-hapR-mKate construct in V.c	74
Figure 14. Photolysis of new nitrile photocage	74
Figure 15. Photolysis of big-PEG analog	75
Figure 16. Synthesis of caged-theophylline	75
Figure 17. Reaction scheme and examples of nucleophile substrate scope	88
Figure 18. Proposed reaction mechanism	88
Figure 19. Crystal structure and synthetic details	108
Figure 20. Effect of amide bond configuration and identification of potent LasR antagonists	118
Figure 21. Hybrid analogs containing optimized structural features	118

List of Figures (continued)

Figure 22. LXA ₄ inhibits the expression of <i>P. aeruginosa</i> virulence factor, pyocyanin.....	209
Figure 23. LXA ₄ inhibits the LasR QS receptor	209
Figure 24. Competition binding assay for LXA ₄ inhibition of LasR	210

List of Tables

Table	Page
Table 1. Structure-activity relationship of “A-ring” analogs.....	116
Table 2. Structure-activity relationship of “C-ring”	117
Table 3. Structure-activity relationship of alternative linkers	118
Table 4. Chloropyridine analogs as antagonists of LasR.....	118

Chapter 1

Design of small molecule inhibitors of a protein-RNA interaction in *Vibrio cholera*

Introduction

Protein-RNA interactions facilitate various biochemical processes that are fundamental for life^{1,2,3}. Chief among these is the translation of proteins, in which gene expression can be regulated by a specific protein-RNA interaction^{2,3}. In theory, many of these protein-RNA complexes should represent a potential target for medicinal chemists, as the ability to modulate gene expression is scientifically and medically useful. For that reason, it is surprising how few drugs that are currently on the market take advantage of this untapped interaction. The ability to discover small molecules that interact specifically with protein-RNA complexes is of growing interest and while not entirely trouble-free, has been shown to be at the very least, possible.

Recently, my collaborator Prof. Ng at Tufts University developed an assay to identify inhibitors of a specific protein-RNA interaction in *V. cholera*. Using high-throughput screening, Prof. Ng tested a library of small molecules and found several hit compounds that inhibit a protein-RNA complex of the protein Hfq. This widely conserved bacterial protein mediates the expression of important quorum sensing proteins through the binding of sRNAs known as the Qrrs^{2,3,4}. In *V. cholera*, Hfq bound to sRNAs known as the Qrrs results in destabilization of the quorum sensing master regulator, HapR². As HapR normally functions to suppress virulence, the inhibitory action of the Hfq- Qrr complex on HapR serves to upregulate virulence². El-Mowafi et al. published a paper in 2014 on inhibitors of Hfq-RNA interactions, and was the only relevant precedent that could be found on this topic¹. The active compounds from their study, however, were

cyclic peptides rather than small molecules, which benefit from enhanced pharmaceutical properties such as solubility and permeability¹. In fact, the authors mentioned in the discussion section that a small molecule that binds to the site of RI20, their lead peptide, would be a "candidate anti-infective"¹. They go on to mention that the compounds could be rationally designed once the crystal structure of the Hfq complex is known, or they could be discovered via high-throughput screening¹. Having identified a small molecule that inhibits one of these particular protein-RNA interactions, Hfq is now a viable target to reduce bacterial virulence. After synthesizing and retesting the original hit compound **1**, I prepared a library of analogs and ultimately identified a derivative with significantly improved efficacy and reduced toxicity.

Results and Discussion

The dose-response relationship for Compound 1 is a bell curve. During the early attempts to test the biological activity of compound **1**, the maximum concentration tested was 100 μM . The dose-response curves for these trials appeared to have a sigmoidal shape, increasing in magnitude up to 100 μM , and therefore, it was hypothesized that these curves would flatten out in a sigmoidal fashion if higher concentrations were tested. Upon performing another assay that included concentrations up to 300 μM , it was discovered that the dose-response relationship was not sigmoidal, but was actually a bell curve (or an inverted-U) (Fig. 2). For compound **1**, before 100 μM seems to be the optimal concentration in which the highest response level is reached, while concentrations higher than 100 μM are in the decline section of the bell curve (Fig. 2). To explain this phenomenon we looked at the luminescence and OD₆₀₀ data separately, each plotted as a dose-response. From the OD₆₀₀ plot (Fig. 5) it is apparent

that there is some growth inhibition at concentrations leading up to 100 μM , and the low OD_{600} values for concentrations higher than 100 μM suggest that those cells are dead. While it was discouraging to learn of this problem with toxicity at high concentrations, this was a critical observation that helped explain the unique dose-response relationship for compound **1**. Other analogs that were synthesized and tested all repeated this bell curve effect, and accordingly also suffered from growth inhibition at high concentrations (some to a lesser extent, however).

An aminal is required for biological activity. After becoming aware of how significantly instable the N, N-acetal truly was, a series of experiments were performed to test if the aminal was actually necessary for activity. Firstly, the breakdown products from the hydrolysis of the aminal, the free benzimidazole and piperazine portions, were tested individually in the assay along with **1**. Neither of these fragments produced a significant response compared to **1**, and therefore it was concluded that the coupled molecule is required for activity. However, while this assay supported the notion that the coupled benzimidazole-piperazine compound is required, it was still uncertain whether those portions needed to be coupled via the N, N-acetal. To test this, three new analogs were designed and synthesized, which utilized different linkers to couple the two portions of the molecule (Fig. 3). The first of these compounds is identical to **1**, but with a carbonyl on the carbon involved in the aminal, resulting in a urea-type analog. This change has a negligible effect on the molecule's properties such as size, but the compound now becomes significantly more stable, no longer containing the acid-labile aminal. Similarly, two other new analogs of **1** were prepared, one that utilizes a sulfonamide linker, and another that contains a two-carbon linker (Fig. 3). These three

linker-derivatives were tested against **1** in the assay, and surprisingly none of them produced any measurable level of activity. Ultimately, these experiments taken together leads us to a somewhat paradoxical notion, that the coupled benzimidazole-piperazine molecule is required for activity but these two portions must be linked together via an N, N-acetal. Since the aminal is known to readily hydrolyze even under mild conditions, it is peculiar that this functional group would behave as a pharmacophore. One possible explanation is that the coupled aminal is not actually the active compound, but rather a pro-drug, which during hydrolysis generates reactive intermediates that function as the true biologically active species. Concluding that we could not avoid incorporating the aminal into the structure, we focused our attention on developing methods to synthesize, purify and handle these sensitive molecules as best as possible.

Development of truncated analogs establishes the unimportance of the aryl sulfonamide moiety. The initial SAR (structure-activity relationship) we obtained informed us that changes to the benzyl group of the benzimidazole were not tolerated. Analogs that were prepared and tested modified the benzyl to phenyl, cyclohexyl, pyridine, ortho-methoxybenzyl or para-bromobenzyl (Fig. 1). Of this small series, every compound was inactive with the exception of the pyridine analog, for which a response was observed that was negligible compared to **1**. After this result, our strategy for rationale design of derivatives shifted to modifications of the cyanobenzene group. Being limited to the few aryl sulfonyl chlorides we had available, four analogs that made changes to this ring were synthesized and tested (Fig. 1). While all of these molecules were active in our assay, none of them were more efficacious than **1**, although the ortho-nitro derivative produced the most comparable response. Most interesting was the result that not just small changes (i.e. ortho-nitro) were tolerated but also substantial alterations

(i.e. para-methyl, trichloro, pentafluoro) did not cause a loss in activity. The latter observation caused another reassessment of our synthetic rationale, as the importance of this cyanobenzene group was uncertain. To address this, an analog was designed which removed the aryl sulfanamide group entirely, changing the secondary amine involved in the N, N-acetal from the substituted piperazine to morpholine (**2**). Unexpectedly, this compound was not only active but was equally as potent and slightly more efficacious than **1** at the third highest concentration (Fig. 4). Building off this result, a couple more truncated analogs were prepared and tested in addition to the morpholine derivative, incorporating piperidine, N-methylpiperazine, and dimethylmorpholine into the animal (Fig. 1). These compounds were also active but did not match the response level of **2** (Fig. 6). Unfortunately, the truncated series also suffered from growth inhibition at the same concentrations as **1**, although slightly higher OD₆₀₀ values were recorded for the morpholine analog than for **1** (Fig. 5). Even though the toxicity issue still persisted, the fact that these four compounds maintained (and in one case, somewhat improved) activity after a large part of the molecular structure was removed was remarkable. Furthermore, the chemical properties of these new analogs are superior to **1** in regards to making the compound more drug-like. The truncated analogs are not only smaller molecules but also are more hydrophilic; for instance comparing **1** to **2**, the molecular weight has been reduced from 472 to 323 g/mol and the cLogP value decreased from 4.85 to 3.60. Given the critical SAR that was provided by this series, subsequent analogs did not contain the sulfonamide cyanobenzene moiety.

Development of oxazolidinone derivatives addresses issue of stability and toxicity. Having experimented thoroughly with analogs based off of piperazine, an interest developed in testing N, N-acetals of other NH heterocycles. Attempts to form the aminor from the benzimidazole failed for pyrrole, imidazole, succinimide, tetrazole and several other substrates. Oxazolidinone, on the other hand, was identified to be capable of forming the aminor with benzimidazole, and the product could be isolated in an aqueous workup just as the piperazine-based analogs. Upon testing this new derivative, the somewhat impure sample produced promising data, reaching a higher Lux/OD₆₀₀ value than **1**. This preliminary result led to the development of several other oxazolidinone-based analogs. Several substituted oxazolidinones (isopropyl, phenyl and benzyl) were purchased relatively inexpensively, due to their common use as Evans chiral auxiliaries. Forming the aminor proceeded smoothly with these new substrates, as well as the unsubstituted oxazolidinone, and the coupled product seemed to be a bit more robust than the piperazine-based aminorals such as **1**. The enhanced stability of these derivatives was confirmed via the identification of a purification method that did not hydrolyze the aminor. Using alumina instead of silica, the oxazolidinone-based N, N-acetals could be purified, whereas the piperazine-based aminorals hydrolyze on both alumina and silica. This change in stability is thought to be due to the decreased basicity of the nitrogen of the oxazolidinone, compared to the nitrogen in piperazine which protonates much more readily, thereby initiating the mechanism for hydrolysis of the aminor. Upon testing these more stable analogs it was interesting to see that they experienced significantly reduced growth inhibition at high concentrations in comparison to **1** (Fig. 8). This result supported our initial hypothesis that the instability/reactivity of the N, N-acetal was the cause for the toxicity issue. In regards to the biological response, surprisingly the unsubstituted

oxazolidinone analog was no longer active in its pure form. The other derivatives, however, were active, chief among them being the benzyl-substituted oxazolidinone analog (**3**). Shockingly, this analog produced a drastically higher level of efficacy than **1**, having almost quadrupled the maximum Lux/OD₆₀₀ value of **1** (Fig. 7). Perhaps even more important, though, was the decreased toxicity of this new analog. The OD₆₀₀ plot of **3** depicts no substantial growth inhibition at the three highest concentrations tested, whereas **1** is shown to have decreasing cell density starting at the third highest concentration, and the cells appear to be completely dead by the final two concentrations (Fig. 8). Taking these results together, this oxazolidinone derivative has addressed issues with stability, toxicity and efficacy, and thus has provided a stronger basis for ongoing SAR efforts.

Identification of a higher potency compound. Up to this point in the project, several parameters of **1** had been optimized, including efficacy, toxicity, stability, solubility and molecular weight. Achieving potency that was superior to **1**, however, was difficult and every analog that was tested had either the same potency as **1** or slightly worse. A new compound that I proposed aimed to address this concern by incorporating more than one aminal into the structure - as this reactive functional group was found to be vital for activity. Many potential approaches could be used to introduce an additional N, N-acetal into the structure of **1**; however, the compound that was designed and ultimately synthesized was perhaps the most straightforward. By employing piperazine rather than morpholine or another mono-NH heterocycle, two N, N-acetals can be formed, resulting in a symmetrical molecule. This product was isolated in relatively high yield but could not be purified using alumina to remove the excess benzimidazole, and consequently was

used without purification in the assay. Excitingly, this analog did in fact have increased potency compared to **1** (Fig. 9). At around 10 μM **1** produces essentially no response (less than 1,000 Lux/OD₆₀₀), whereas this new analog was found to be fairly effective at this concentration, having a Lux/OD₆₀₀ value of around 12,000. While a greater increase in potency can likely still be obtained, this was a significant breakthrough as it was the first and only compound in the library to improve upon the potency of **1**.

Chemistry

Although initially assumed to be relatively straightforward, synthesizing the high-throughput hit proved to be a complicated task. Retrosynthetically, the desired molecule is the coupled product of two different secondary amines linked via a methylene group, which originates from formaldehyde. The resulting N, N-acetal (or aminal) proved to be a major synthetic difficulty due to its acid lability, the degree of which was not initially understood until attempting to make these molecules. After many unsuccessful attempts to synthesize the high-throughput screen hit, it was assumed that the Mannich reaction that forms that aminal was not occurring for these substrates. To our surprise, it was discovered that the aminal was indeed forming, however was being fully hydrolyzed during the purification, thus regenerating the two starting materials. This observation was the first indication that these molecules were not particularly stable, since the stationary-phase used during the purifications (silica) is only very slightly acidic. While no universal solution was found to solve this problem of stability, several techniques were identified and developed to make it possible to work with this highly acid-labile functionality.

While forming the N, N-acetal to access the final compound was rather problematic, the prior reactions that form the necessary amines proceeded fairly well. The high-throughput screen hit was retrosynthetically split into two halves, a benzimidazole and a piperazine portion. These are both commonly synthesized heterocycles that are employed throughout medicinal chemistry, and for that reason, various methods were effectively identified to prepare them. The required substituted benzimidazole, 2-benzyl-1H-benzimidazol, was synthesized from ortho-phenylenediamine and phenylacetic acid (Fig. 10). Several methods were explored to facilitate this condensation reaction, each using a different reagent to activate the carboxylic acid for nucleophilic attack. Initially BH_3 was used, in which the borate ester was formed and ultimately gave the desired product in decent yield. Alternatively, borane could be avoided by using a more common coupling reagent, like EDC, but this method was not preferred due to the fact that the monoamide intermediate had to be isolated as opposed to the one-pot approach using borane. A third method to form the benzimidazole that was investigated involved polyphosphoric acid, which was also a one-pot reaction⁷. This became the main approach, as it typically gave high yield and purity without any purification. Its only downside, being a potentially troublesome workup, is what led to the continued use of the other methods described. Typically, forming the benzimidazole was first attempted using polyphosphoric acid, and if the product was not isolated then the other methods were employed. Synthesizing the piperazine portion of the molecule was a bit simpler; the reaction between the various substituted aryl sulfonyl chlorides and excess piperazine proceeded very well (Fig. 11). The desired mono-sulfonamide piperazine derivatives were isolated in extremely high yield and purity via an aqueous workup.

My initial efforts to form the aminor were carried out using common Mannich reaction conditions (Fig. 12, A). The reactions were usually done in methanol at room temperature and formalin was used as the formaldehyde source (37% in water). Two methods were explored in regards to addition of the secondary amines, one in which both are added simultaneously and another where the benzimidazole is added after the piperazine portion reacts with formaldehyde for a short period of time. Using either method, the material was purified using silica-gel flash chromatography after a normal workup, but the product was never isolated. We originally speculated that the aminor was not in fact forming due to the consistent isolation of the benzimidazole starting material. It wasn't until after numerous failed attempts to purify the compound that a crude ^1H NMR was assessed. Surprisingly, it appeared that the aminor was forming as the characteristic methylene peak around 5-6 ppm was present, but since we did not observe this peak after purification it was concluded that the molecule was hydrolyzing on silica. While I did not have a solution for this problem at the time, it was reassuring to discover that the reaction was truly working on these substrates.

After experimenting with those basic Mannich conditions for a while, I began researching new ways of forming N, N-acetals. My initial goals were to optimize the reaction in regard to yield and purity, and potentially identify a highly efficient procedure in which product could be isolated that did not need to be purified. Using SciFinder's *Reaction Structure* search, several interesting papers were found which detailed novel methods of forming aminorals. The first paper we focused on, a paper published in 2010 in *Journal of Organic Chemistry*, described a method to access aminorals via N, O-acetals. The secondary amine (piperazine) is reacted with paraformaldehyde and potassium

carbonate in methanol to generate the corresponding N, O-acetal (Fig. 11). This intermediate is then reacted with a NH heterocycle (benzimidazole in this case) in the presence of hafnium triflate to form the N, N-acetal (Fig. 12, B). According to the paper, if using indole instead of benzimidazole as the NH heterocycle, then using hafnium triflate as a Lewis acid catalyst regioselectively produces amins whereas TMSCl generates 3-aminomethylated indoles. In the case of 2-benzyl-benzimidazole, the hafnium triflate conditions did produce the desired product in 64% yield. This marked the first time we isolated the amina product and while it was exciting to learn that these compounds were at least stable enough to isolate, we still desired to optimize the conditions to improve yield and potency.

The next method to synthesize N, N-acetals that we explored was based off of another Journal of Organic Chemistry paper which was published in 2006. The authors described a route to form amins between secondary amines and NH heterocycles by first forming a bis-aminal of the secondary amine. This is accomplished by reacting two molar equivalence of the amine with 1 eq. of formaldehyde (as formalin) and then extracting the bis-aminal in an aqueous workup (Fig. 11). Subsequent reaction of this bis-aminal with an NH heterocycle in the presence of succinic anhydride provides the desired N, N-acetal (Fig. 12, C). In my attempts using this method, forming the bis-aminal worked well for simple secondary amines (piperazine-based) but not for many other amines that were tested. However, if I was able to produce the bis-aminal then the following step which forms the desired amina always worked in my experience. Importantly, these conditions produced higher yield and purity than the N, O-acetal method, and in some cases the product did not require any further purification. The

limitation to only piperazine-based secondary amines, however, is what led us to further explore alternatives to forming these amins.

A fourth method to prepare relevant N, N-acetals was focused on using chloroaminals as intermediates and therefore accessing the desired amins via an S_N2 reaction. An efficient procedure was identified from a Tetrahedron Letters paper in which a secondary amine is reacted with paraformaldehyde in TMSCl to generate the chloroaminal (Fig. 11). An NH heterocycle is then deprotonated via NaH before the chloroaminal intermediate is introduced to the reaction, which rapidly affords the N, N-acetal (Fig. 12, D). This preparation did not work with every substrate that were tested, as some of the amines did not readily form the chloroaminal. Nevertheless, several secondary amines could be converted to the chloroaminal and then the corresponding N, N-acetal product. Notable among these amines was the oxazolidinone class of heterocycles, which seemed to form N, Cl- and the N, N- acetals with high efficiency. Taking the results of all the aminal-forming methods together, it seems to be very substrate dependent, wherein a given NH substrate (piperazine vs. oxazolidinone) may favor one of the methods over another, or may work for one method but not for another. Luckily, many of the compounds I set out to make were in fact possible to synthesize using one of the methods described here.

Conclusion

Development of small molecule inhibitors of protein-RNA interactions is a difficult task, even when the active compounds are stable. In this study, a series of structurally related N, N-acetals were synthesized and tested for their biological activity.

Structure-activity relationships were determined for the various groups that constitute the target molecule, but ultimately most structural changes caused either a complete loss of activity or a level of activity comparable to the high-throughput screen hit. After many failed attempts, several analogs finally improved upon compound **1** by increasing efficacy, stability, potency and/or decreasing toxicity. Several advances were also made in regards to the synthesis of these compounds. Working with molecules containing unstable aminals presented a learning curve and therefore significant time was dedicated to studying various methods to forming and isolating compounds containing these groups. Eventually, several efficient synthetic approaches to form N, N-acetals were identified and adapted for our substrates, which is what enabled the production of a diverse compound library. In regards to medicinal impact, this project supports the notion that Hfq is a novel target to inhibit bacterial virulence. While more work needs to be done regarding Hfq and specifically Hfq-Qrr complexes, the wide range of activities that were observed throughout this compound library provides promise for future efforts of "drugging" this target. The work described here provides a basis for other projects involving small molecule inhibitors of protein-RNA interactions as well as others in which the lead compound contains an N, N-acetal. This project is currently being prepared for publication, as our collaborators are performing the last studies to identify the mechanism of action.

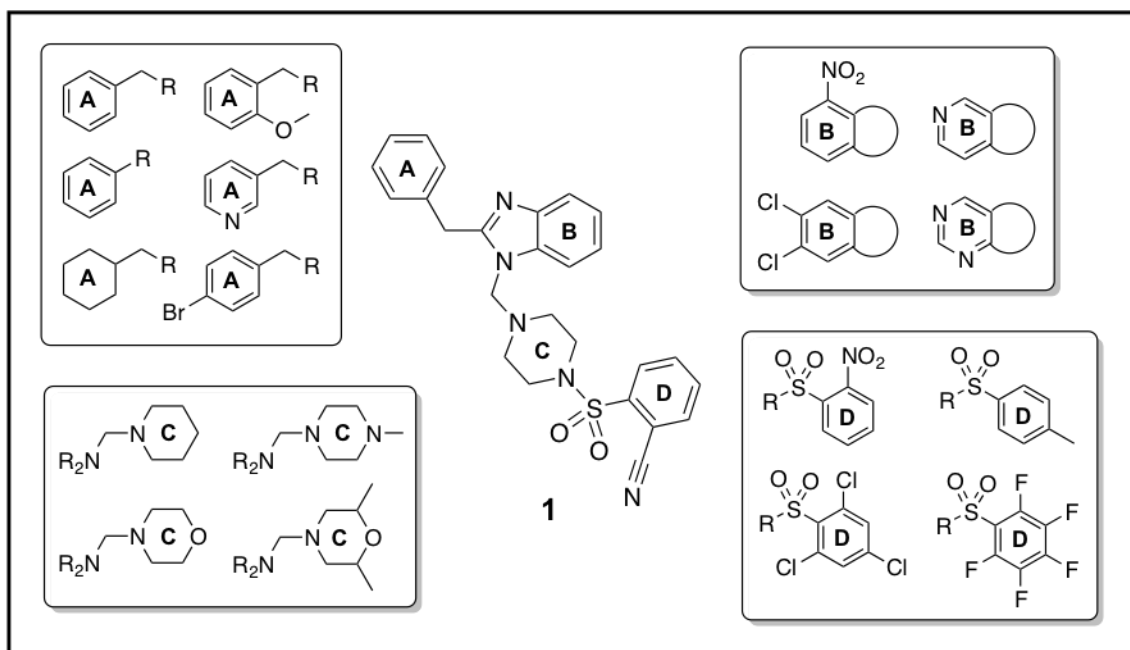


Figure 1. Structure of HTS hit (1) and examples of some analogs prepared

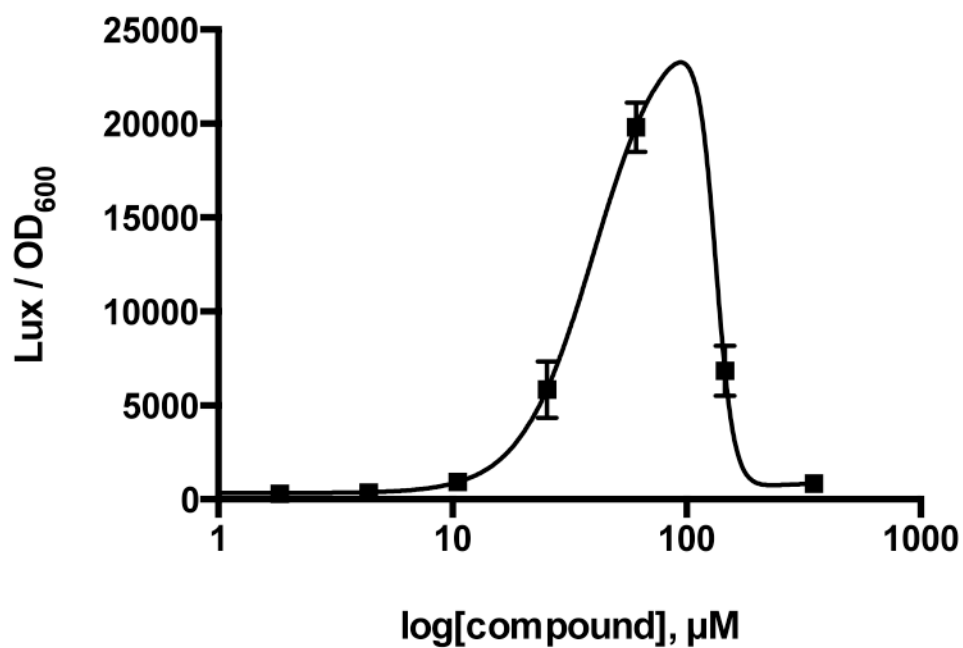


Figure 2. Dose response curve for 1

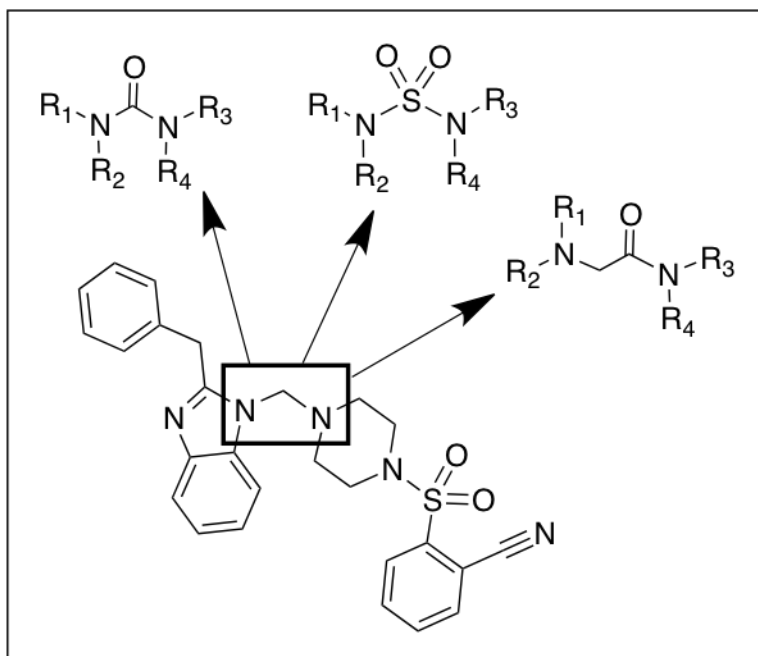


Figure 3. Analogs developed using stable linkers

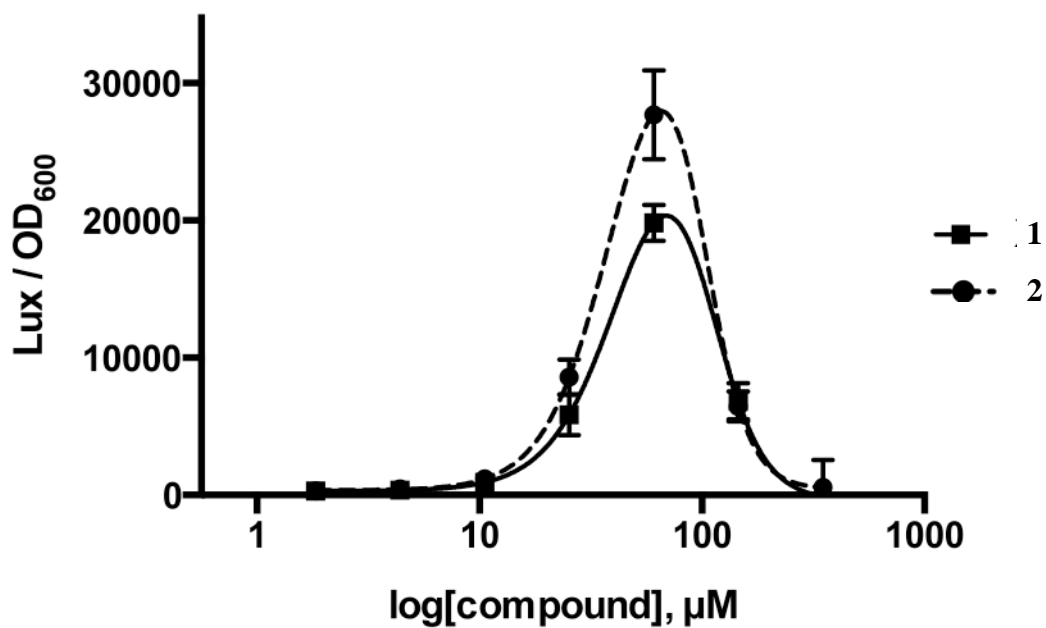


Figure 4. Dose response curve for 2

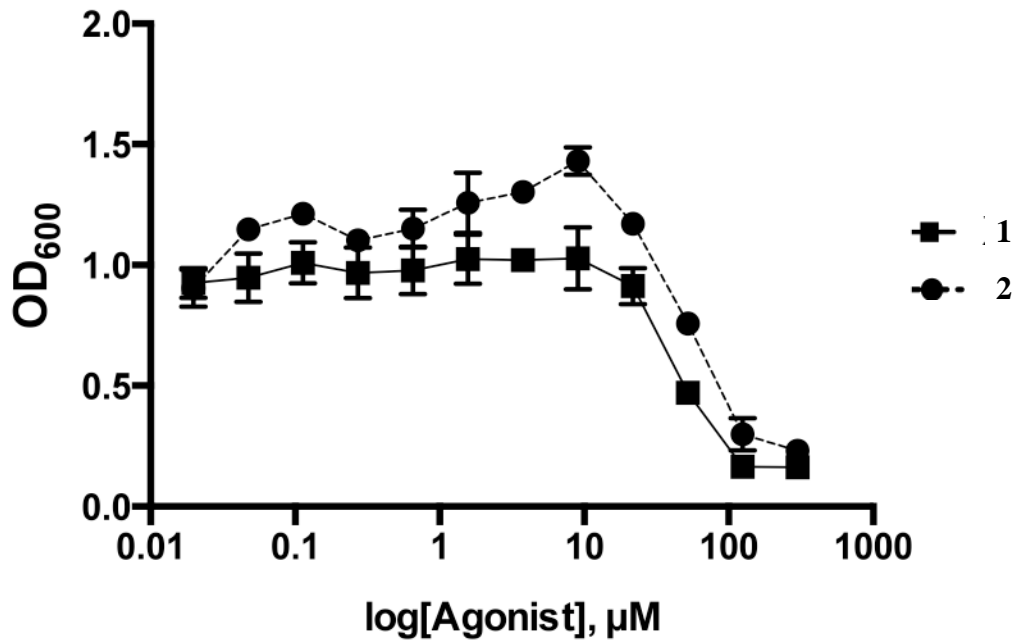


Figure 5. OD₆₀₀ plot for 1 and 2

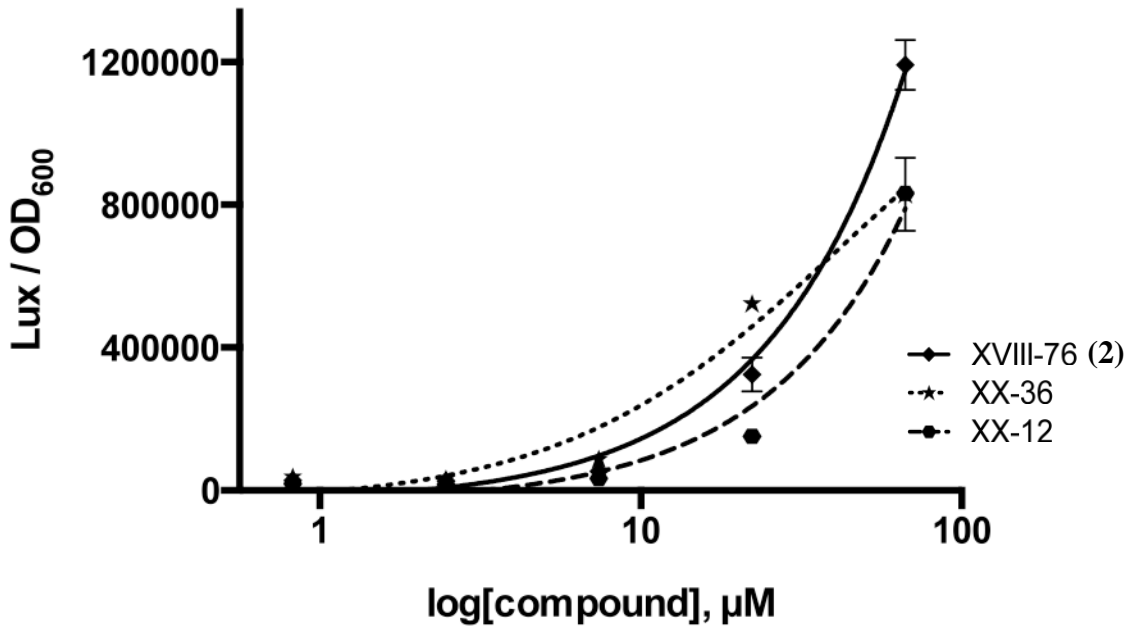


Figure 6. Biological activity of three truncated analogs

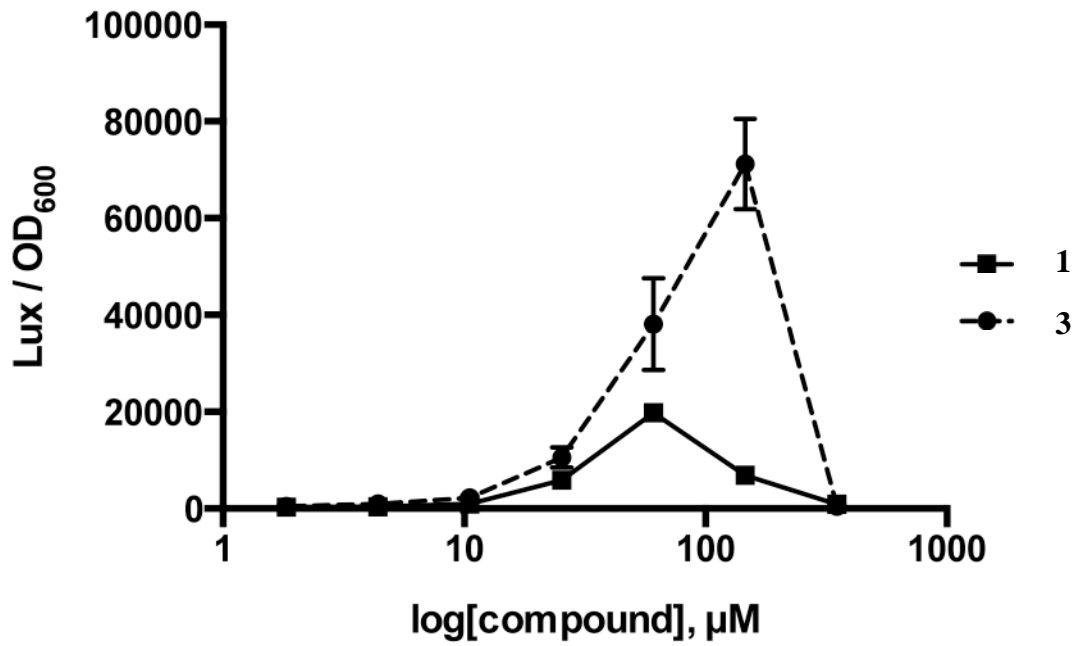


Figure 7. Dose response curve for high-efficacy oxazolidinone analog

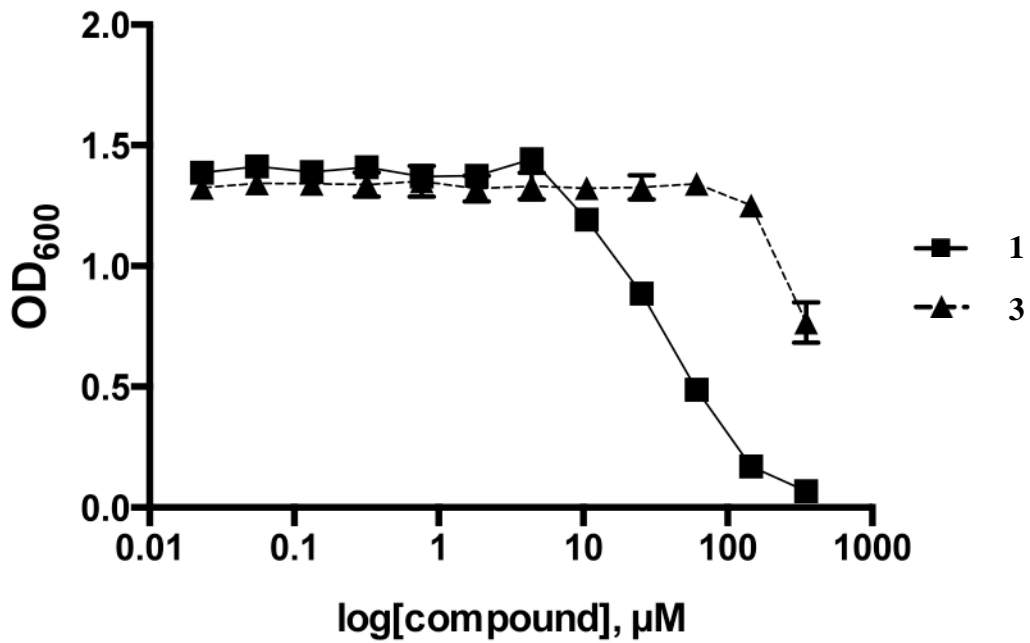


Figure 8. OD₆₀₀ plot of oxazolidinone analog

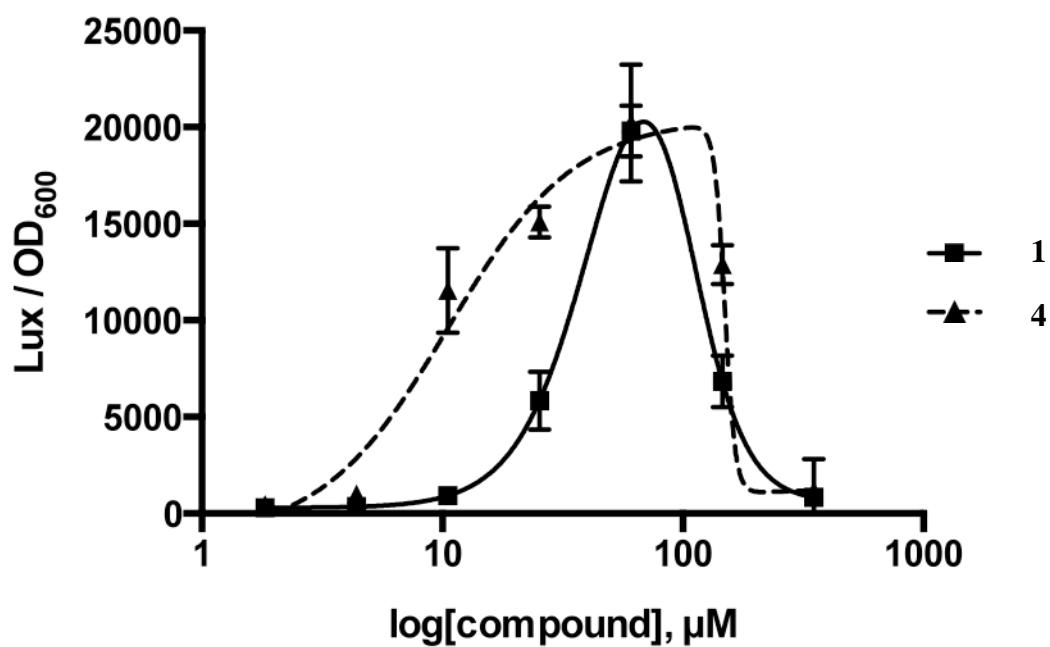


Figure 9. Dose-response curve for 4

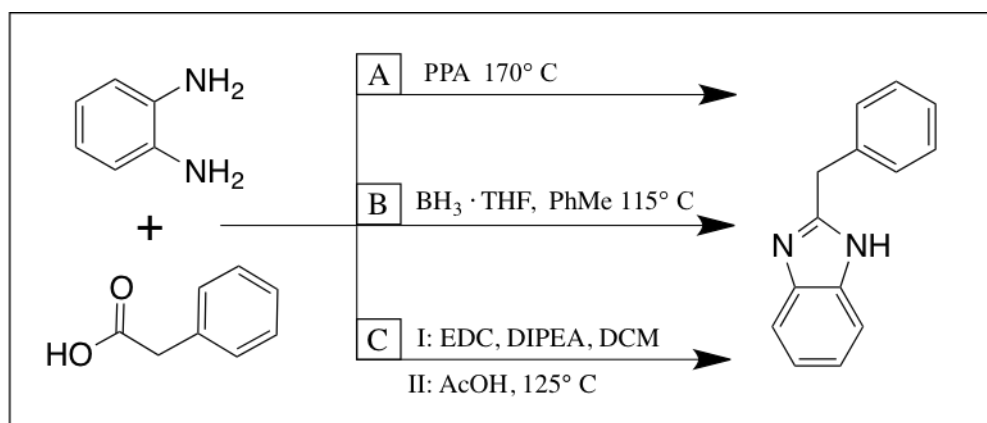


Figure 10. Methods employed for the synthesis of 2-substituted benzimidazoles

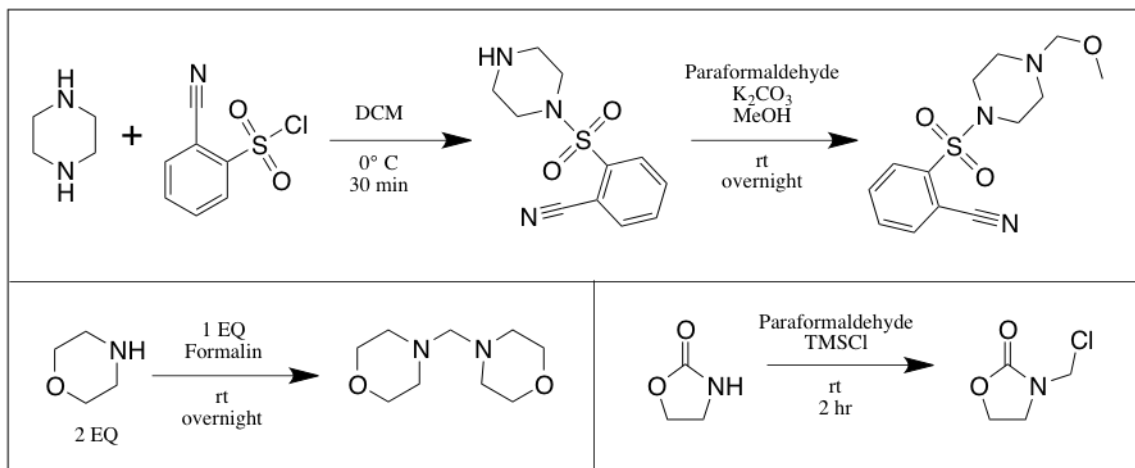


Figure 11. Synthesis of acetal intermediates

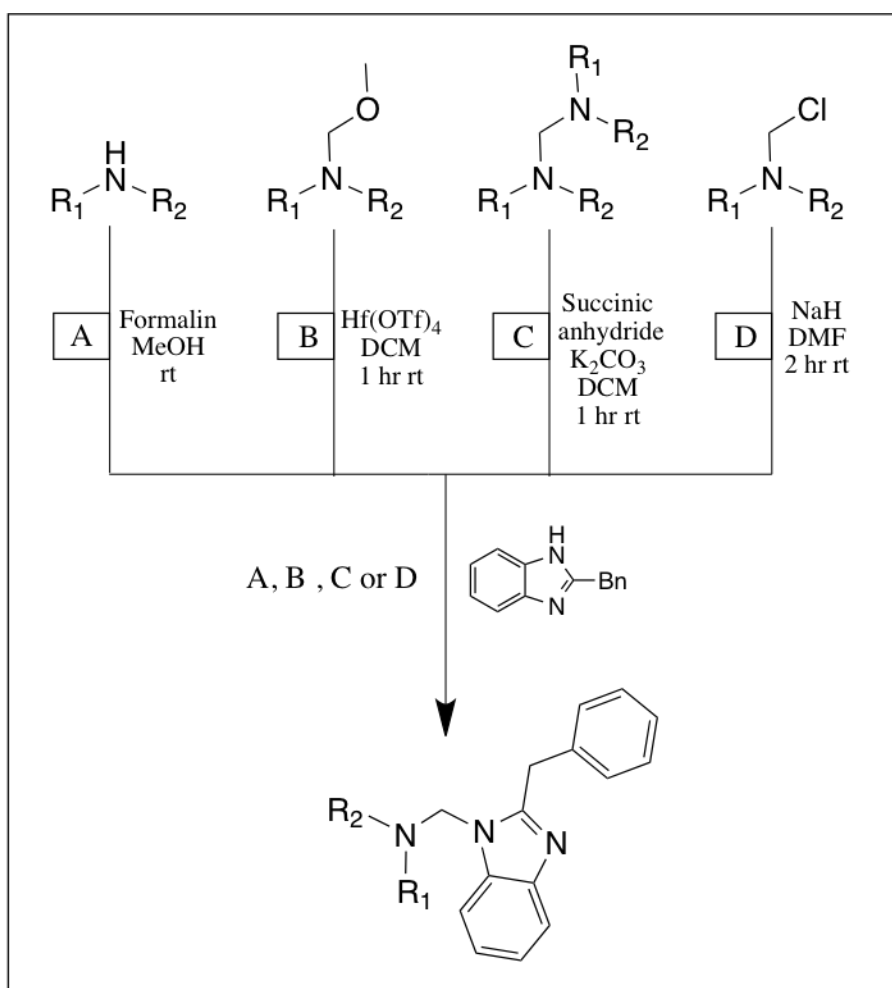


Figure 12. Various methods utilized to form N, N-acetals

Experimental Section

Bacterial reporter strain assay. Our collaborator Prof. Ng developed the biological assay for this project. A reporter strain was first produced using *V. cholera* in which the expression of a luminescent protein is controlled by Hfq-sRNA. For practical purposes, an increase in luminescence (or Lux/OD₆₀₀) corresponds to an increase in inhibition of the Hfq-Qrr complex, whereas compounds that do not effect this protein-RNA interaction do not generate luminescence. To prepare for the assay, an overnight culture of the *V. cholera* reporter strain was incubated at 30 °C in LB media containing 100 µg/mL of Kanamycin and 5 µg/mL of Tetracyclin. Following a 1:50 dilution of this culture into the same LB media, 175 µL was placed into each well of a clear bottom 96-well plate. Next, 10.5 µL of a 10 mM solution of each compound in DMSO was added in triplicate to the wells in the first column. A 2.4 fold dilution was then performed by transferring 125 µL from the first column to the next, and repeating this down the entire plate. Plates were incubated at 30 °C and luminescence (Lux) and OD₆₀₀ were read at 4, 5 and 6 hours. Dose response curves were generated using Prism software, and were plotted as Lux/OD₆₀₀ vs. log[conc.].

General chemistry. All reagents and solvents were obtained from commercial sources and used without further purification or drying. Reactions were performed under a nitrogen gas atmosphere in flame-dried glassware. Unless otherwise noted, compounds were not purified. ¹H and ¹³C NMR data was taken on a Varian AS400 (400 MHz), with chemical shifts being displayed in a ppm scale referenced to residual chloroform.

2-benzyl-1H-benzo[*d*]imidazole. Orthophenylene diamine (1 g, 9.25 mmol) and phenyl acetic acid (1.25 g, 9.25 mmol) was added to poly phosphoric acid (4.4 mL, 1 g/mmol) and the mixture was heated to 180 °C for 12 h. NaOH (1 M, 15 mL x 3) was added, after the flask was saturated with sand (while hot). Combined NaOH portions were neutralized with 1 M HCl, and the resulting aqueous solution was extracted with EtOAc (3 x 50 mL). Combined organic layers were washed with brine and dried with Na₂SO₄ to afford 1.77 g, 92% yield. NMR spectra are consistent with previously published data.

2-phenyl-1H-benzo[*d*]imidazole. Prepared using the procedure described for 2-benzyl-1H-benzo[*d*]imidazole, using the corresponding carboxylic acid. NMR spectra are consistent with previously published data.

2-(cyclohexylmethyl)-1H-benzo[*d*]imidazole. Prepared using the procedure described for 2-benzyl-1H-benzo[*d*]imidazole, using the corresponding carboxylic acid. NMR spectra are consistent with previously published data.

2-(2-methoxybenzyl)-1H-benzo[*d*]imidazole. Prepared using the procedure described for 2-benzyl-1H-benzo[*d*]imidazole, using the corresponding carboxylic acid. NMR spectra are consistent with previously published data.

2-(pyridin-3-ylmethyl)-1H-benzo[*d*]imidazole. Prepared using the procedure described for 2-benzyl-1H-benzo[*d*]imidazole, using the corresponding carboxylic acid. NMR spectra are consistent with previously published data.

2-(4-bromobenzyl)-1H-benzo[d]imidazole. Prepared using the procedure described for 2-benzyl-1H-benzo[d]imidazole, using the corresponding carboxylic acid. NMR spectra are consistent with previously published data.

2-((2,4-dichlorophenoxy)methyl)-1H-benzo[d]imidazole. Prepared using the procedure described for 2-benzyl-1H-benzo[d]imidazole, using the corresponding carboxylic acid. ¹H NMR (400 MHz, CDCl₃) δ 9.94 (s, 1H), 7.75 (s, 1H), 7.50 (s, 1H), 7.39 (dd, *J* = 2.5, 0.5 Hz, 1H), 7.32 – 7.27 (m, 2H), 7.18 (dd, 1H), 7.01 – 6.96 (m, 1H), 5.43 (s, 2H). ¹³C NMR (101 MHz, CDCl₃) δ 152.14, 149.16, 130.37, 128.15, 127.49, 123.94, 114.94, 65.83.

2-(benzylthio)-5-methoxy-1H-benzo[d]imidazole. Prepared using the procedure described for 2-benzyl-1H-benzo[d]imidazole, using the corresponding carboxylic acid. NMR spectra are consistent with previously published data.

2-benzyl-4-nitro-1H-benzo[d]imidazole. Prepared using the procedure described for 2-benzyl-1H-benzo[d]imidazole, using the corresponding diamine. NMR spectra are consistent with previously published data.

2-benzyl-1H-imidazo[4,5-c]pyridine. Prepared using the procedure described for 2-benzyl-1H-benzo[d]imidazole, using the corresponding diamine. NMR spectra are consistent with previously published data.

8-benzyl-9H-purine. Prepared using the procedure described for 2-benzyl-1H-benzo[d]imidazole, using the corresponding diamine. NMR spectra are consistent with previously published data.

2-benzyl-5,6-dichloro-1H-benzo[d]imidazole. Prepared using the procedure described for 2-benzyl-1H-benzo[d]imidazole, using the corresponding diamine. ¹H NMR (400 MHz, CDCl₃) δ 8.75 (s, 1H), 7.50 (s, 2H), 7.28 – 7.20 (m, 3H), 7.19 – 7.12 (m, 2H), 4.16 (s, 2H). ¹³C NMR (101 MHz, CDCl₃) δ 155.96, 137.67, 135.59, 129.20, 129.00, 127.66, 126.63, 116.11, 35.67.

2-(piperazin-1-ylsulfonyl)benzotrile. 2-cyanobenzene sulfonyl chloride (0.5 g, 2.48 mmol) was added to piperazine (1.07 g, 12.4 mmol) in DCM (24 mL, 0.1 M) at 0 °C. Reaction stirred for 30 min at 0 °C and was quenched with sat. NaHCO₃ (25 mL). The mixture was diluted with DCM (25 mL) and separated, and the organic layer was washed with brine (25 mL) and then dried with Na₂SO₄. The product was used without purification, 0.59 g, 96% yield.

1-((2-nitrophenyl)sulfonyl)piperazine. Prepared using the procedure described for 2-(piperazin-1-ylsulfonyl)benzotrile, using the corresponding sulfonyl chloride. NMR spectra are consistent with previously published data.

1-tosylpiperazine. Prepared using the procedure described for 2-(piperazin-1-ylsulfonyl)benzotrile, using the corresponding sulfonyl chloride. NMR spectra are consistent with previously published data.

1-((2,4,6-trichlorophenyl)sulfonyl)piperazine. Prepared using the procedure described for 2-(piperazin-1-ylsulfonyl)benzotrile, using the corresponding sulfonyl chloride. NMR spectra are consistent with previously published data.

2-((4-(methoxymethyl)piperazin-1-yl)sulfonyl)benzotrile. Paraformaldehyde (2.12 g, 8.82 mmol) was added to a mixture of 2-(piperazin-1-ylsulfonyl)benzotrile

(1.11 g, 4.41 mmol), K₂CO₃ (1.22 g, 8.82 mmol) and Na₂SO₄ (1.25 g, 8.82 mmol) in methanol (14.7 mL, 0.3 M). The mixture stirred at room temperature overnight, and then was filtered and washed with ether. Removal of solvent in vacuo yielded 1.16 g of the N, O-acetal, 89% yield. This intermediate was used crude in the next step.

1-(methoxymethyl)-4-((2-nitrophenyl)sulfonyl)piperazine. Prepared using the procedure described for 2-((4-(methoxymethyl)piperazin-1-yl)sulfonyl)benzotrile, using the corresponding piperazine derivative.

1-(methoxymethyl)-4-tosylpiperazine. Prepared using the procedure described for 2-((4-(methoxymethyl)piperazin-1-yl)sulfonyl)benzotrile, using the corresponding piperazine derivative.

1-(methoxymethyl)-4-((2,4,6-trichlorophenyl)sulfonyl)piperazine. Prepared using the procedure described for 2-((4-(methoxymethyl)piperazin-1-yl)sulfonyl)benzotrile, using the corresponding piperazine derivative.

Dimorpholinomethane. Morpholine (2.0 g, 22.96 mmol) was added to formalin (0.86 mL, 11.48 mmol) at 0 °C and the mixture stirred at room temperature overnight. Water (25 mL) was added to the mixture, which was then extracted with EtOAc (25 mL x 3). The combined organic layers were washed with brine and then dried with Na₂SO₄. Crude bis- N, N-acetal was used without purification, 1.94 g, 91% yield. ¹H NMR (400 MHz, CDCl₃) δ 3.62 (t, 9H), 2.84 (s, 2H), 2.47 – 2.36 (m, 8H). ¹³C NMR (101 MHz, CDCl₃) δ 81.67, 67.02, 52.02.

Di(piperidin-1-yl)methane. Prepared using the procedure described for dimorpholinomethane, using the corresponding secondary amine. ¹H NMR (400 MHz,

CDCl_3) δ 2.78 (s, 2H), 2.40 – 2.30 (m, 8H), 1.54 – 1.44 (m, 8H), 1.42 – 1.33 (m, 4H). ^{13}C NMR (101 MHz, CDCl_3) δ 82.86, 53.14, 26.03, 25.03.

Bis(4-methylpiperazin-1-yl)methane. Prepared using the procedure described for dimorpholinomethane, using the corresponding secondary amine.

Bis(2,6-dimethylmorpholino)methane. Prepared using the procedure described for dimorpholinomethane, using the corresponding secondary amine.

3-(chloromethyl)oxazolidin-2-one. Paraformaldehyde (86 mg, 2.87 mmol) was added to a mixture of 2-oxazolidinone (250 mg, 2.87 mmol) in TMSCl (1.45 mL, 2.0 M). The resulting mixture stirred at room temperature for 2 h. Removal of TMSCl in vacuo afforded the chloro-acetal, which was used crude (quant. yield). ^1H NMR (400 MHz, CDCl_3) δ 5.19 (s, 2H), 4.35 – 4.29 (m, 2H), 3.71 – 3.64 (m, 2H). ^{13}C NMR (101 MHz, CDCl_3) δ 156.94, 62.16, 56.20, 42.50.

(R)-3-(chloromethyl)-4-isopropylloxazolidin-2-one. Prepared using the procedure described for 3-(chloromethyl)oxazolidin-2-one, using the corresponding oxazolidinone derivative.

(S)-3-(chloromethyl)-4-isopropylloxazolidin-2-one. Prepared using the procedure described for 3-(chloromethyl)oxazolidin-2-one, using the corresponding oxazolidinone derivative.

(S)-3-(chloromethyl)-4-phenylloxazolidin-2-one. Prepared using the procedure described for 3-(chloromethyl)oxazolidin-2-one, using the corresponding oxazolidinone derivative.

(R)-4-benzyl-3-(chloromethyl)oxazolidin-2-one. Prepared using the procedure described for 3-(chloromethyl)oxazolidin-2-one, using the corresponding oxazolidinone derivative.

2-bromo-1-(4-((2-nitrophenyl)sulfonyl)piperazin-1-yl)ethan-1-one. To 1-((2-nitrophenyl)sulfonyl)piperazine (0.150 g, 0.553 mmol) in DCM (2.6 mL, 0.2 M) was added DIPEA (0.1 mL, 0.553 mmol). The mixture was cooled to 0 °C and bromoacetyl chloride (0.05 mL, 0.608 mmol) was added dropwise, and then the mixture reacted overnight at room temperature. After quenching with HCl (5 mL, 0.1 M), more water was added and the product was extracted with EtOAc (25 mL x 3). The combined organic layers were washed with brine and then dried with Na₂SO₄. Silica-gel column chromatography (product elutes at 65% EtOAc) yielded 181 mg of the desired compound, 83% yield. ¹H NMR (400 MHz, CDCl₃) δ 7.97 (dd, 1H), 7.77 – 7.68 (m, 2H), 7.64 (dd, *J* = 7.3, 1.8, 0.8 Hz, 1H), 4.05 (s, 1H), 3.84 (s, 1H), 3.70 (t, *J* = 5.2 Hz, 2H), 3.61 (t, *J* = 5.9, 3.5 Hz, 2H), 3.40 (t, *J* = 5.8 Hz, 2H), 3.30 (t, 2H). ¹³C NMR (101 MHz, CDCl₃) δ 165.50, 148.35, 134.31, 131.94, 131.05, 131.00, 124.42, 46.58, 45.93, 45.74, 45.57, 25.49.

2-((4-(2-bromoacetyl)piperazin-1-yl)sulfonyl)benzotrile. Prepared using the procedure described for 2-bromo-1-(4-((2-nitrophenyl)sulfonyl)piperazin-1-yl)ethan-1-one, using the corresponding piperazine derivative.

4-((2-cyanophenyl)sulfonyl)piperazine-1-sulfonyl chloride. Chlorosulfonic acid (0.400 mL, 5.88 mmol) was added dropwise to 2-(piperazin-1-ylsulfonyl)benzotrile (0.492 g, 1.96 mmol) in chloroform at 0 °C. The reaction was allowed to warm to room

temperature as it stirred for 30 min. Sat. NaHCO₃ was added and the mixture was extracted with EtOAc (25 mL x 3), and then the combined organic layers were washed with brine and dried with Na₂SO₄. This intermediate (0.152 g, 0.459 mmol) was dissolved in benzene (9.2 mL, 0.05 M) and PCl₅ (0.096 g, 0.459 mmol) was added. The resulting mixture was refluxed for 24 h, filtered and concentrated to dryness, and the sulfonyl chloride was used crude without purification.

4-((2-cyanophenyl)sulfonyl)piperazine-1-carbonyl chloride. Triphosgene (0.082 g, 0.277 mmol) was dissolved in DCM (4.1 mL) and pyridine (0.045 mL, 0.553 mmol) was added at 0 °C. 2-(piperazin-1-ylsulfonyl)benzotrile (0.150 g, 0.553 mmol) in DCM (4.1 mL) was slowly added and the mixture stirred at room temperature overnight. After quenching with HCl (5 mL, 1 M) the product was extracted with DCM, washed with brine and dried with Na₂SO₄. The product was used crude without purification.

2-((4-((2-benzyl-1H-benzo[d]imidazol-1-yl)methyl)piperazin-1-yl)sulfonyl)benzotrile. To 2-benzyl-1H-benzo[d]imidazole (43 mg, 0.207 mmol) and 2-((4-(methoxymethyl)piperazin-1-yl)sulfonyl)benzotrile (61 mg, 0.207 mmol) in DCM (1.4 mL, 0.15 M) was added Hf(OTf)₄ (8 mg, 0.0104 mmol). The reaction was allowed to stir at room temperature for 2 h and then was quenched with sat. NaHCO₃. The mixture was diluted with more DCM, and the organic layer was separated and then dried with Na₂SO₄. The product was obtained as a mixture of the desired aminal and starting materials, and could not be purified.

2-benzyl-1-((4-((2-nitrophenyl)sulfonyl)piperazin-1-yl)methyl)-1H-benzo[d]imidazole. Prepared using the procedure described for 2-((4-((2-benzyl-1H-benzo[d]imidazol-1-yl)methyl)piperazin-1-yl)sulfonyl)benzotrile, using the corresponding benzimidazole and N,O-acetal.

2-benzyl-1-((4-tosylpiperazin-1-yl)methyl)-1H-benzo[d]imidazole. Prepared using the procedure described for 2-((4-((2-benzyl-1H-benzo[d]imidazol-1-yl)methyl)piperazin-1-yl)sulfonyl)benzotrile, using the corresponding benzimidazole and N,O-acetal. ¹H NMR (400 MHz, CDCl₃) δ 7.85 (dd, *J* = 6.3, 1.9, 1.0 Hz, 1H), 7.73 – 7.63 (m, 2H), 7.49 – 7.17 (m, 10H), 4.58 (s, 2H), 4.40 (s, 2H), 2.97 (t, 4H), 2.55 (t, 4H), 2.55 (s, 3H). ¹³C NMR (101 MHz, CDCl₃) δ 153.69, 143.97, 142.44, 136.43, 136.01, 132.60, 129.88, 128.79, 128.54, 127.91, 127.03, 122.84, 122.38, 119.77, 109.70, 64.89, 49.73, 45.70, 34.79, 21.71.

2-benzyl-1-((4-((2,4,6-trichlorophenyl)sulfonyl)piperazin-1-yl)methyl)-1H-benzo[d]imidazole. Prepared using the procedure described for 2-((4-((2-benzyl-1H-benzo[d]imidazol-1-yl)methyl)piperazin-1-yl)sulfonyl)benzotrile, using the corresponding benzimidazole and N,O-acetal.

2-((4-((2-(2-methoxybenzyl)-1H-benzo[d]imidazol-1-yl)methyl)piperazin-1-yl)sulfonyl)benzotrile. Prepared using the procedure described for 2-((4-((2-benzyl-1H-benzo[d]imidazol-1-yl)methyl)piperazin-1-yl)sulfonyl)benzotrile, using the corresponding benzimidazole and N,O-acetal.

2-(2-methoxybenzyl)-1-((4-((2-nitrophenyl)sulfonyl)piperazin-1-yl)methyl)-1H-benzo[d]imidazole. Prepared using the procedure described for 2-((4-((2-benzyl-1H-

benzo[d]imidazol-1-yl)methyl)piperazin-1-yl)sulfonyl)benzotrile, using the corresponding benzimidazole and N,O-acetal.

2-(2-methoxybenzyl)-1-((4-tosylpiperazin-1-yl)methyl)-1H-

benzo[d]imidazole. Prepared using the procedure described for 2-((4-((2-benzyl-1H-benzo[d]imidazol-1-yl)methyl)piperazin-1-yl)sulfonyl)benzotrile, using the corresponding benzimidazole and N,O-acetal.

2-(benzylthio)-5-methoxy-1-((4-tosylpiperazin-1-yl)methyl)-1H-

benzo[d]imidazole. Prepared using the procedure described for 2-((4-((2-benzyl-1H-benzo[d]imidazol-1-yl)methyl)piperazin-1-yl)sulfonyl)benzotrile, using the corresponding benzimidazole and N,O-acetal.

2-((4-((2-(benzylthio)-5-methoxy-1H-benzo[d]imidazol-1-yl)methyl)piperazin-1-yl)sulfonyl)benzotrile. Prepared using the procedure described for 2-((4-((2-benzyl-1H-benzo[d]imidazol-1-yl)methyl)piperazin-1-yl)sulfonyl)benzotrile, using the corresponding benzimidazole and N,O-acetal.

2-(benzylthio)-5-methoxy-1-((4-((2-nitrophenyl)sulfonyl)piperazin-1-yl)methyl)-1H-benzo[d]imidazole. Prepared using the procedure described for 2-((4-((2-benzyl-1H-benzo[d]imidazol-1-yl)methyl)piperazin-1-yl)sulfonyl)benzotrile, using the corresponding benzimidazole and N,O-acetal.

2-((4-((2-phenyl-1H-benzo[d]imidazol-1-yl)methyl)piperazin-1-yl)sulfonyl)benzotrile. Prepared using the procedure described for 2-((4-((2-benzyl-1H-benzo[d]imidazol-1-yl)methyl)piperazin-1-yl)sulfonyl)benzotrile, using the corresponding benzimidazole and N,O-acetal.

2-((4-((2-((2,4-dichlorophenoxy)methyl)-1H-benzo[d]imidazol-1-yl)methyl)piperazin-1-yl)sulfonyl)benzotrile. Prepared using the procedure described for 2-((4-((2-benzyl-1H-benzo[d]imidazol-1-yl)methyl)piperazin-1-yl)sulfonyl)benzotrile, using the corresponding benzimidazole and N,O-acetal.

2-((2,4-dichlorophenoxy)methyl)-1-((4-tosylpiperazin-1-yl)methyl)-1H-benzo[d]imidazole. Prepared using the procedure described for 2-((4-((2-benzyl-1H-benzo[d]imidazol-1-yl)methyl)piperazin-1-yl)sulfonyl)benzotrile, using the corresponding benzimidazole and N,O-acetal.

4-((2-benzyl-1H-benzo[d]imidazol-1-yl)methyl)morpholine. 2-benzyl-1H-benzo[d]imidazole (42 mg, 0.205 mmol), dimorpholinomethane (42 mg, 0.226 mmol) and K₂CO₃ (31 mg, 0.226 mmol) were suspended in DCM (1.25 mL, 0.167 M). Succinic anhydride (23 mg, 0.226 mmol) was added and the reaction stirred at room temperature for 1 h. The reaction was diluted with more DCM (25-50 mL) and washed with 1 M NaOH (25 mL x 2), followed by brine (10 mL). The organic layer was dried over Na₂SO₄ and concentrated to dryness, affording the desired product, which was not purified. ¹H NMR (400 MHz, CDCl₃) δ 7.79 – 7.72 (m, 1H), 7.42 – 7.34 (m, 1H), 7.32 – 7.16 (m, 7H), 4.46 (s, 2H), 4.40 (s, 2H), 3.59 (t, 4H), 2.37 (t, 4H). ¹³C NMR (101 MHz, CDCl₃) δ 153.78, 142.31, 136.36, 136.05, 128.73, 128.53, 126.93, 122.57, 122.10, 119.50, 109.74, 66.47, 65.44, 50.81, 34.71.

2-benzyl-1-(piperidin-1-ylmethyl)-1H-benzo[d]imidazole. Prepared using the procedure described for 4-((2-benzyl-1H-benzo[d]imidazol-1-yl)methyl)morpholine, using the corresponding bis- N, N-acetal. ¹H NMR (400 MHz, CDCl₃) δ 7.81 – 7.72 (m,

1H), 7.43 – 7.34 (m, 1H), 7.31 – 7.15 (m, 7H), 4.43 (s, 4H), 2.36 (t, $J = 5.2$ Hz, 4H), 1.56 – 1.45 (m, 4H), 1.46 – 1.37 (m, 2H). ^{13}C NMR (101 MHz, CDCl_3) δ 154.08, 142.37, 136.59, 136.32, 128.68, 128.66, 126.82, 122.35, 121.86, 119.39, 109.90, 66.01, 51.85, 34.75, 25.58, 24.21.

2-benzyl-1-((4-methylpiperazin-1-yl)methyl)-1H-benzo[*d*]imidazole. Prepared using the procedure described for 4-((2-benzyl-1H-benzo[*d*]imidazol-1-yl)methyl)morpholine, using the corresponding bis- N, N-acetal. ^1H NMR (400 MHz, CDCl_3) δ 7.81 – 7.71 (m, 1H), 7.43 – 7.34 (m, 1H), 7.35 – 7.17 (m, 7H), 4.47 (s, 2H), 4.41 (s, 2H), 2.49 – 2.31 (m, 8H), 2.26 (s, 3H). ^{13}C NMR (101 MHz, CDCl_3) δ 153.68, 142.02, 136.19, 135.84, 128.52, 128.41, 126.70, 122.34, 121.85, 119.15, 109.69, 65.00, 54.33, 50.15, 45.71, 34.43.

4-((2-benzyl-1H-benzo[*d*]imidazol-1-yl)methyl)-2,6-dimethylmorpholine. Prepared using the procedure described for 4-((2-benzyl-1H-benzo[*d*]imidazol-1-yl)methyl)morpholine, using the corresponding bis- N, N-acetal. ^1H NMR (400 MHz, CDCl_3) δ 7.70 – 7.63 (m, 1H), 7.34 – 7.26 (m, 1H), 7.22 – 7.02 (m, 7H), 4.36 (s, 2H), 4.29 (s, 2H), 3.50 – 3.36 (m, 2H), 2.46 – 2.35 (m, 2H), 1.65 (t, 2H), 0.98 (d, 6H). ^{13}C NMR (101 MHz, CDCl_3) δ 153.73, 142.25, 136.35, 135.97, 128.73, 128.57, 126.96, 122.61, 122.15, 119.37, 110.05, 71.37, 65.25, 56.44, 34.63, 18.97.

4-((2-(cyclohexylmethyl)-1H-benzo[*d*]imidazol-1-yl)methyl)morpholine. Prepared using the procedure described for 4-((2-benzyl-1H-benzo[*d*]imidazol-1-yl)methyl)morpholine, using the corresponding benzimidazole and bis- N, N-acetal. ^1H NMR (400 MHz, CDCl_3) δ 7.73 – 7.68 (m, 1H), 7.42 – 7.37 (m, 1H), 7.24 – 7.19 (m, 2H), 4.66 (s, 2H), 3.65 (t, 4H), 2.80 (d, $J = 7.1$ Hz, 2H), 2.51 (t, $J = 5.7, 3.7$ Hz, 4H), 2.05

– 1.94 (m, 1H), 1.83 – 1.60 (m, 4H), 1.30 – 0.99 (m, 6H). ¹³C NMR (101 MHz, CDCl₃) δ 155.25, 142.60, 135.74, 122.19, 122.05, 119.26, 109.85, 66.69, 65.49, 51.08, 37.54, 35.39, 33.56, 26.39, 26.24.

4-((2-(2-methoxybenzyl)-1H-benzo[d]imidazol-1-yl)methyl)morpholine.

Prepared using the procedure described for 4-((2-benzyl-1H-benzo[d]imidazol-1-yl)methyl)morpholine, using the corresponding benzimidazole and bis- N, N-acetal.

4-((2-(pyridin-3-ylmethyl)-1H-benzo[d]imidazol-1-yl)methyl)morpholine.

Prepared using the procedure described for 4-((2-benzyl-1H-benzo[d]imidazol-1-yl)methyl)morpholine, using the corresponding benzimidazole and bis- N, N-acetal.

4-((2-(4-bromobenzyl)-1H-benzo[d]imidazol-1-yl)methyl)morpholine.

Prepared using the procedure described for 4-((2-benzyl-1H-benzo[d]imidazol-1-yl)methyl)morpholine, using the corresponding benzimidazole and bis- N, N-acetal.

4-((2-benzyl-4-nitro-1H-benzo[d]imidazol-1-yl)methyl)morpholine. Prepared using the procedure described for 4-((2-benzyl-1H-benzo[d]imidazol-1-yl)methyl)morpholine, using the corresponding benzimidazole and bis- N, N-acetal.

4-((2-benzyl-1H-imidazo[4,5-c]pyridin-1-yl)methyl)morpholine. Prepared using the procedure described for 4-((2-benzyl-1H-benzo[d]imidazol-1-yl)methyl)morpholine, using the corresponding benzimidazole and bis- N, N-acetal.

4-((8-benzyl-9H-purin-9-yl)methyl)morpholine. Prepared using the procedure described for 4-((2-benzyl-1H-benzo[d]imidazol-1-yl)methyl)morpholine, using the corresponding benzimidazole and bis- N, N-acetal.

4-((2-benzyl-5,6-dichloro-1H-benzo[d]imidazol-1-yl)methyl)morpholine.

Prepared using the procedure described for 4-((2-benzyl-1H-benzo[d]imidazol-1-yl)methyl)morpholine, using the corresponding benzimidazole and bis- N, N-acetal.

3-((2-benzyl-1H-benzo[d]imidazol-1-yl)methyl)oxazolidin-2-one. 2-benzyl-1H-

benzo[d]imidazole (58 mg, 0.279 mmol) was dissolved in DMF (1.4 mL, 0.2 M) and NaH was added in two portions (7 mg, 0.294 mmol). The mixture was allowed to stir at room temperature for 30-45 min. 3-(chloromethyl)oxazolidin-2-one (40 mg, 0.294 mmol) was added dropwise (in DMF) and the reaction stirred at room temperature for 2 h. Water (50 mL) was added and the product was extracted with EtOAc (25 mL x3), and then the combined organic layers were washed with brine (50 mL x 3). After drying on Na₂SO₄ the product was purified using alumina column chromatography. ¹H NMR (400 MHz, CDCl₃) δ 7.83 – 7.76 (m, 1H), 7.49 – 7.43 (m, 1H), 7.37 – 7.21 (m, 7H), 5.53 (s, 2H), 4.41 (s, 2H), 4.07 (t, 2H), 3.01 (t, 2H). ¹³C NMR (101 MHz, CDCl₃) δ 157.65, 153.15, 142.66, 136.21, 134.95, 129.07, 128.70, 127.40, 123.49, 122.98, 119.94, 109.67, 61.95, 52.57, 42.73, 34.28.

3-((2-(pyridin-3-ylmethyl)-1H-benzo[d]imidazol-1-yl)methyl)oxazolidin-2-

one. Prepared using the procedure described for 3-((2-benzyl-1H-benzo[d]imidazol-1-yl)methyl)oxazolidin-2-one, using the corresponding benzimidazole.

3-((2-benzyl-3H-imidazo[4,5-c]pyridin-3-yl)methyl)oxazolidin-2-one. Prepared

using the procedure described for 3-((2-benzyl-1H-benzo[d]imidazol-1-yl)methyl)oxazolidin-2-one, using the corresponding benzimidazole.

3-((8-benzyl-7H-purin-7-yl)methyl)oxazolidin-2-one. Prepared using the procedure described for 3-((2-benzyl-1H-benzo[*d*]imidazol-1-yl)methyl)oxazolidin-2-one, using the corresponding benzimidazole.

(R)-3-((2-benzyl-1H-benzo[*d*]imidazol-1-yl)methyl)-4-isopropylloxazolidin-2-one. Prepared using the procedure described for 3-((2-benzyl-1H-benzo[*d*]imidazol-1-yl)methyl)oxazolidin-2-one, using the corresponding oxazolidinone derivative. ¹H NMR (400 MHz, CDCl₃) δ 7.79 – 7.73 (m, 1H), 7.43 – 7.37 (m, 1H), 7.30 – 7.17 (m, 7H), 5.81, 5.20 (ABq, *J*_{AB}= 14.9 Hz, 2H), 4.46, 4.31 (ABq, *J*_{AB}= 15.9 Hz, 2H), 3.96 (dd, *J* = 9.1, 3.8 Hz, 1H), 3.77 (t, *J* = 9.0 Hz, 1H), 3.35 – 3.28 (m, 1H), 1.98 - 1.86 (m, 1H), 0.73 (dd, *J* = 19.8, 6.9 Hz, 6H). ¹³C NMR (101 MHz, CDCl₃) δ 157.73, 153.05, 142.66, 136.05, 135.05, 128.97, 128.33, 127.19, 123.38, 122.82, 119.93, 109.38, 62.69, 57.69, 50.50, 33.91, 27.56, 17.77, 13.72.

(S)-3-((2-benzyl-1H-benzo[*d*]imidazol-1-yl)methyl)-4-isopropylloxazolidin-2-one. Prepared using the procedure described for 3-((2-benzyl-1H-benzo[*d*]imidazol-1-yl)methyl)oxazolidin-2-one, using the corresponding oxazolidinone derivative. ¹H NMR (400 MHz, CDCl₃) δ 7.79 – 7.72 (m, 1H), 7.42 – 7.36 (m, 1H), 7.32 - 7.15 (m, 7H), 5.81, 5.20 (ABq, *J*_{AB}= 14.9 Hz, 2H), 4.46, 4.29 (ABq, *J* = 15.8 Hz, 2H), 3.97 (dd, *J* = 9.1, 3.7 Hz, 1H), 3.77 (t, *J* = 9.0 Hz, 1H), 3.35 - 3.27 (m, 1H), 1.96 – 1.87 (m, 1H), 0.73 (dd, *J* = 20.8, 6.8 Hz, 6H). ¹³C NMR (101 MHz, CDCl₃) δ 157.78, 153.11, 142.72, 136.10, 135.11, 129.03, 128.38, 127.25, 123.45, 122.90, 120.01, 109.41, 62.74, 57.73, 50.54, 33.99, 27.63, 17.83, 13.78.

(S)-3-((2-benzyl-1H-benzo[*d*]imidazol-1-yl)methyl)-4-phenylloxazolidin-2-one. Prepared using the procedure described for 3-((2-benzyl-1H-benzo[*d*]imidazol-1-

yl)methyl)oxazolidin-2-one, using the corresponding oxazolidinone derivative. ^1H NMR (400 MHz, CDCl_3) δ 7.77 – 7.72 (m, 1H), 7.52 – 7.46 (m, 2H), 7.33 – 7.27 (m, 2H), 7.24–7.15 (m, 7H), 6.97 – 6.91 (m, 2H), 5.79, 4.97 (ABq, $J_{\text{AB}} = 14.8$ Hz, 2H), 4.43 – 4.31 (m, 2H), 4.24, 3.61 (ABq, $J_{\text{AB}} = 15.9$ Hz, 2H), 4.01 (dd, $J = 7.4, 5.1$ Hz, 1H). ^{13}C NMR (101 MHz, CDCl_3) δ 157.82, 153.43, 142.73, 136.97, 136.12, 130.08, 130.05, 129.27, 129.24, 129.03, 128.35, 127.25, 127.06, 123.44, 123.05, 119.88, 110.16, 70.42, 58.07, 50.63, 33.91.

(R)-4-benzyl-3-((2-benzyl-1H-benzo[d]imidazol-1-yl)methyl)oxazolidin-2-one.

Prepared using the procedure described for 3-((2-benzyl-1H-benzo[d]imidazol-1-yl)methyl)oxazolidin-2-one, using the corresponding oxazolidinone derivative. ^1H NMR (400 MHz, CDCl_3) δ 7.86 – 7.78 (m, 1H), 7.46 – 7.39 (m, 1H), 7.36 – 7.19 (m, 10H), 6.98 – 6.91 (m, 2H), 5.83, 5.41 (ABq, $J_{\text{AB}} = 15.0$ Hz, 2H), 4.49, 4.31 (ABq, $J_{\text{AB}} = 15.8$ Hz, 2H), 3.89 (dd, $J = 8.9, 3.6$ Hz, 1H), 3.70 (t, $J = 8.5$ Hz, 1H), 3.65 – 3.56 (m, 1H), 2.97 (dd, $J = 13.6, 4.2$ Hz, 1H), 2.50 (dd, $J = 13.6, 9.4$ Hz, 1H). ^{13}C NMR (101 MHz, CDCl_3) δ 157.60, 153.50, 142.93, 136.27, 135.32, 134.82, 129.37, 129.34, 129.19, 128.66, 127.79, 127.43, 127.19, 123.63, 123.20, 120.32, 109.50, 67.01, 54.94, 51.13, 38.35, 34.06.

2-((4-(2-benzyl-1H-benzo[d]imidazole-1-carbonyl)piperazin-1-

yl)sulfonyl)benzotrile. To 2-benzyl-1H-benzo[d]imidazole (173 mg, 0.832 mmol) in DCM (2.8 mL, 0.3 M) was added 4-((2-cyanophenyl)sulfonyl)piperazine-1-carbonyl chloride (261 mg, 0.832 mmol) and DIPEA (0.3 mL, 1.664 mmol). The mixture was heated in a sealed flask overnight at 40 °C and then cooled to room temperature, diluted with more DCM and washed with sat. NaHCO_3 . The organic layer was dried on Na_2SO_4 ,

concentrated and purified via silica-gel column chromatography. ^1H NMR (400 MHz, CDCl_3) δ 8.00 (dd, 1H), 7.88 (dd, 1H), 7.80 – 7.68 (m, 3H), 7.32 – 7.08 (m, 8H), 3.72 (s, 2H), 3.72 (t, $J = 5.0$ Hz, 2H), 3.55 (t, $J = 5.1$ Hz, 2H), 3.15 (t, $J = 5.1$ Hz, 2H), 3.06 (t, $J = 5.0$ Hz, 2H). ^{13}C NMR (101 MHz, CDCl_3) δ 169.71, 139.85, 135.79, 134.48, 133.17, 130.56, 129.03, 128.81, 128.59, 127.59, 127.21, 126.91, 116.15, 111.03, 109.56, 49.88, 45.79, 45.74, 45.61, 41.17.

2-((4-((2-benzyl-1H-benzo[*d*]imidazol-1-yl)sulfonyl)piperazin-1-yl)sulfonyl)benzotrile. To 2-benzyl-1H-benzo[*d*]imidazole (152 mg, 0.730 mmol) in DMF (3.0 mL, 0.25 M) was added NaH (21 mg, 0.876 mmol). The reaction stirred at room temperature for 30 min and then 4-((2-cyanophenyl)sulfonyl)piperazine-1-sulfonyl chloride (255 mg, 0.730 mmol) was added dropwise (in DMF), after which the reaction was allowed to stir overnight. Water (50 mL) was added and the product was extracted with EtOAc (25 mL x3), and then the combined organic layers were washed with brine (50 mL x 3). After drying on Na_2SO_4 the product was purified using silica-gel column chromatography.

2-((4-(2-(2-benzyl-1H-benzo[*d*]imidazol-1-yl)acetyl)piperazin-1-yl)sulfonyl)benzotrile. To 2-((4-(2-bromoacetyl)piperazin-1-yl)sulfonyl)benzotrile (83 mg, 0.223 mmol) in acetone (2.5 mL, 0.09 M) was added 2-benzyl-1H-benzo[*d*]imidazole (47 mg, 0.223 mmol) and KOH (25 mg, 0.446 mmol). The reaction stirred at 60 °C for 2 h. Solvent was removed in vacuo, and the residue was diluted in water and extracted with chloroform (25 mL x 3). The combined organic layers were dried on Na_2SO_4 and concentrated to dryness. Silica-gel column chromatography yielded the desired product, 42% yield. ^1H NMR (400 MHz, CDCl_3) δ 8.04 (dd, $J = 7.7, 1.4$ Hz,

1H), 7.92 (dd, 1H), 7.83 – 7.69 (m, 3H), 7.25 – 7.05 (m, 8H), 4.60 (s, 2H), 4.26 (s, 2H), 3.54 (t, 2H), 3.31 (t, 2H), 3.20 (t, 2H), 3.08 (t, 2H). ¹³C NMR (101 MHz, CDCl₃) δ 164.20, 153.10, 142.50, 139.91, 135.93, 135.85, 133.40, 133.32, 130.66, 128.99, 128.70, 127.22, 122.83, 122.34, 119.83, 116.21, 110.90, 108.98, 45.58, 45.39, 44.89, 44.39, 41.55, 34.95.

2-(2-benzyl-1H-benzo[d]imidazol-1-yl)-1-(4-((2-nitrophenyl)sulfonyl)piperazin-1-yl)ethanone. Prepared using the procedure described for 2-((4-(2-(2-benzyl-1H-benzo[d]imidazol-1-yl)acetyl)piperazin-1-yl)sulfonyl)benzotrile, using the corresponding alkyl bromide derivative. ¹H NMR (400 MHz, CDCl₃) δ 7.91 (dd, 1H), 7.74 – 7.65 (m, 3H), 7.61 (dd, *J* = 7.1, 2.1 Hz, 1H), 7.21 – 7.03 (m, 8H), 4.55 (s, 2H), 4.21 (s, 2H), 3.47 (t, *J* = 4.8 Hz, 2H), 3.20 (t, *J* = 4.8 Hz, 2H), 3.15 – 3.08 (m, 4H). ¹³C NMR (101 MHz, CDCl₃) δ 164.11, 153.19, 148.25, 142.39, 135.85, 134.38, 131.93, 131.03, 128.84, 128.67, 128.64, 127.07, 124.28, 122.67, 122.17, 119.58, 109.09, 45.52, 45.42, 44.65, 44.36, 41.56, 34.73.

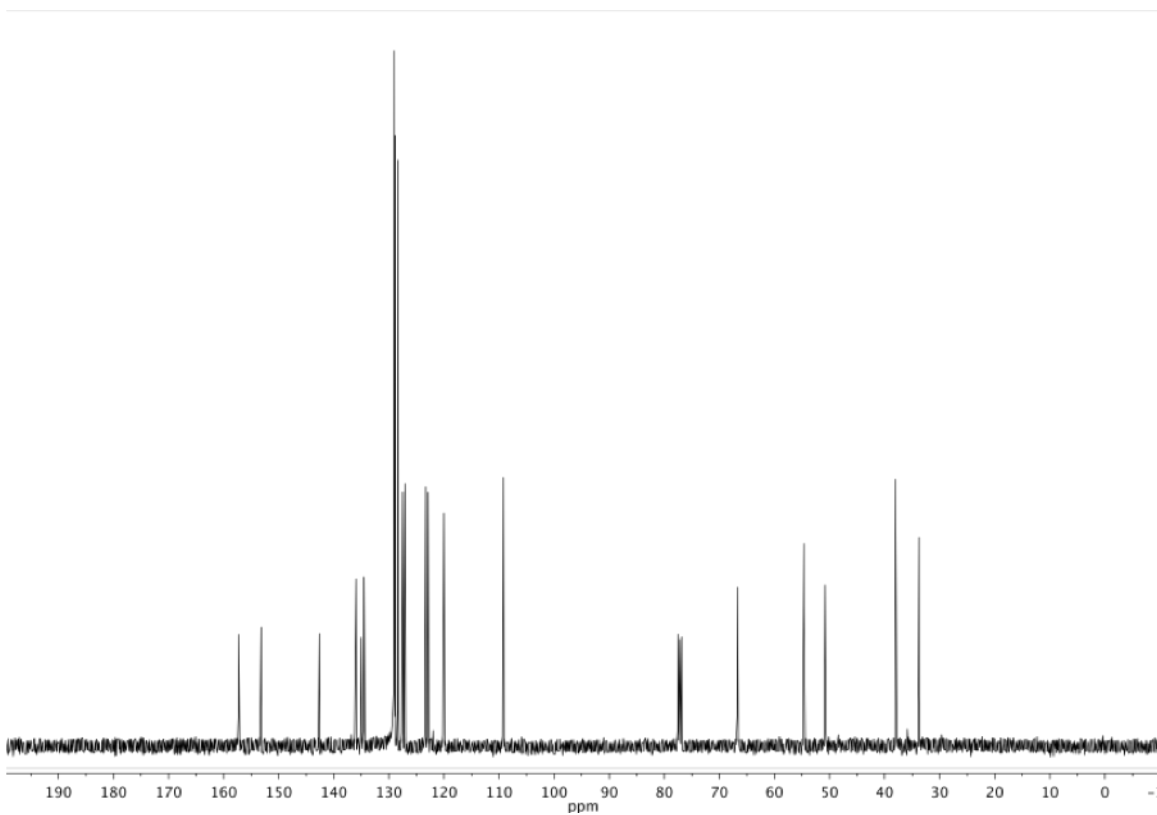
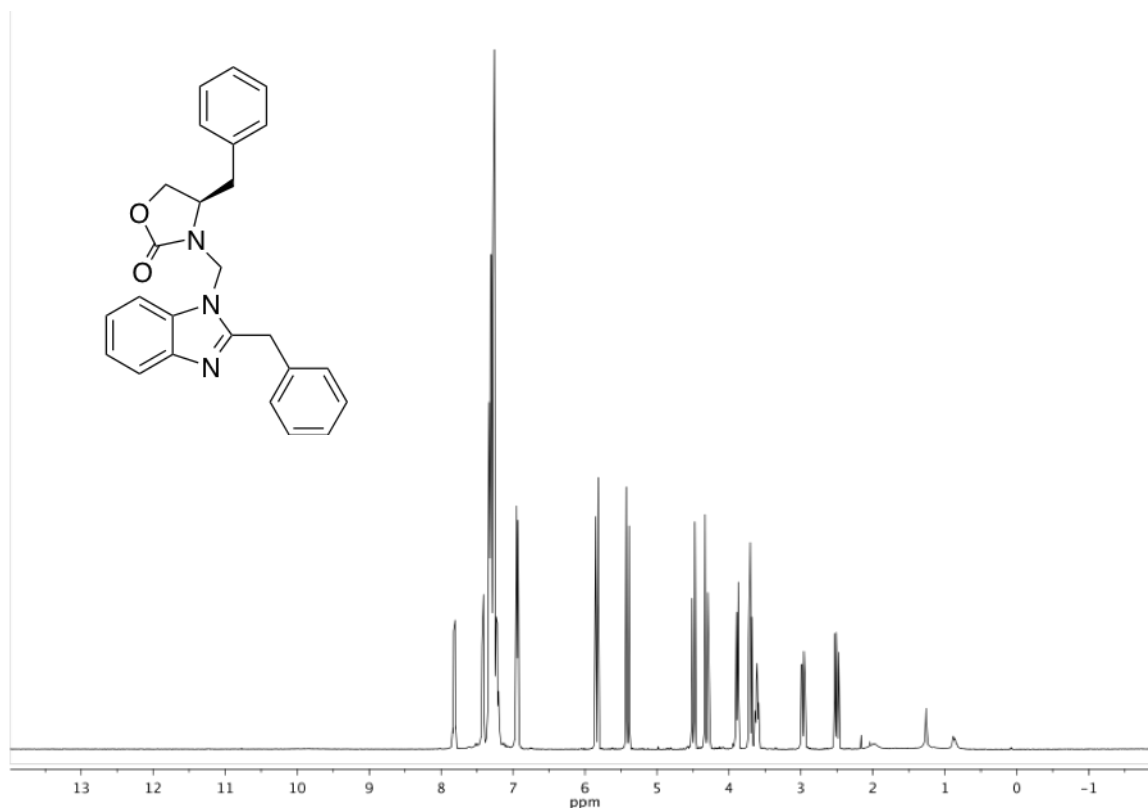
1,4-bis(methoxymethyl)piperazine. Paraformaldehyde (697 mg, 23.22 mmol) was added to a mixture piperazine (500 mg, 5.81 mmol), K₂CO₃ (3.21 g, 23.22 mmol) and Na₂SO₄ (3.30 g, 23.22 mmol) in methanol (20 mL, 0.3 M). The mixture stirred at room temperature overnight, and then was filtered and washed with ether. Removal of solvent in vacuo yielded 613 mg of the bis- N, O-acetal, 71% yield. This intermediate was used crude in the next step.

1,4-bis((2-benzyl-1H-benzo[d]imidazol-1-yl)methyl)piperazine. To 2-benzyl-1H-benzo[d]imidazole (196 mg, 0.941 mmol) and 1,4-bis(methoxymethyl)piperazine (82 mg, 0.471 mmol) in DCM (3.2 mL, 0.15 M) was added Hf(OTf)₄ (36 mg, 0.0471 mmol).

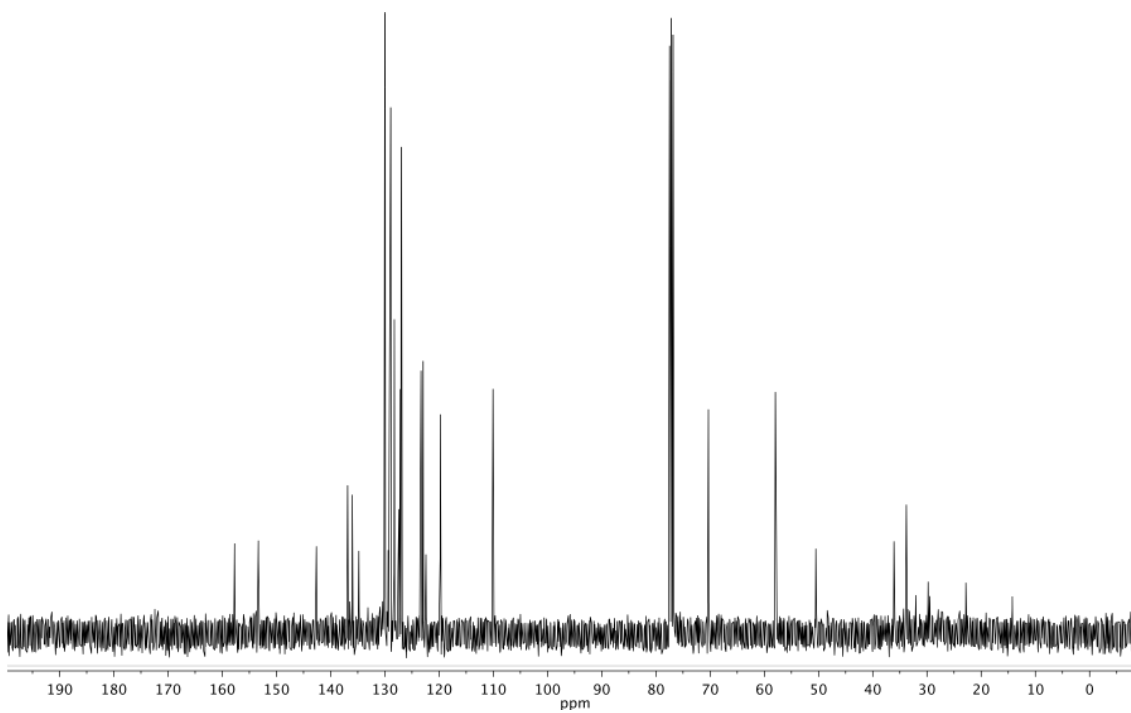
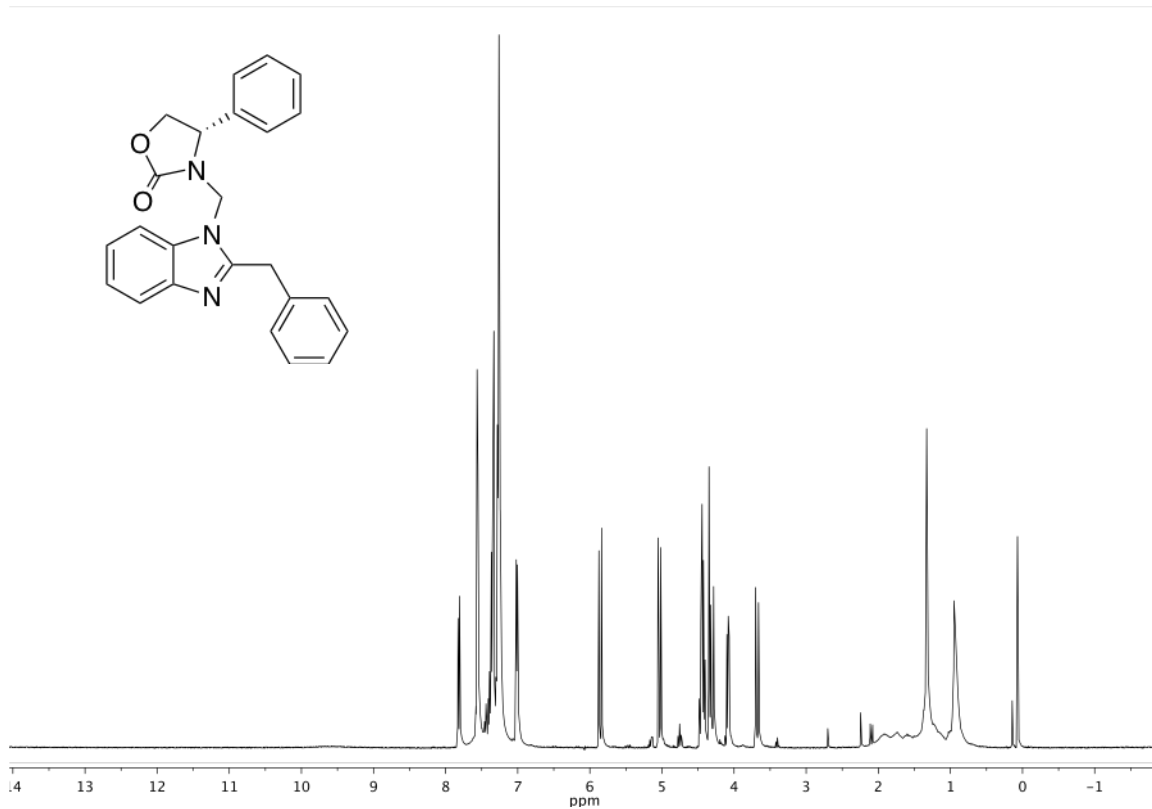
The reaction was allowed to stir at room temperature for 2 h and then was quenched with sat. NaHCO₃. The mixture was diluted with more DCM, and the organic layer was separated and then dried with Na₂SO₄. The product was obtained as a mixture of the desired aminal and starting materials, and could not be purified.

4-((5-benzyl-1H-tetrazol-1-yl)methyl)morpholine. To 5-benzyl-1H-tetrazole (94 mg, 0.587 mmol) in methanol (3 mL, 0.2 M) at 0 °C was added morpholine (0.056 mL, 0.645 mmol). The mixture stirred at 0 °C for 15 min and then formalin (0.053 mL, 0.704 mmol) was added. Reaction was kept at 0 °C for 1 h and then was allowed to warm to room temperature overnight. The product was obtained after removal of solvent in vacuo, and was not purified.

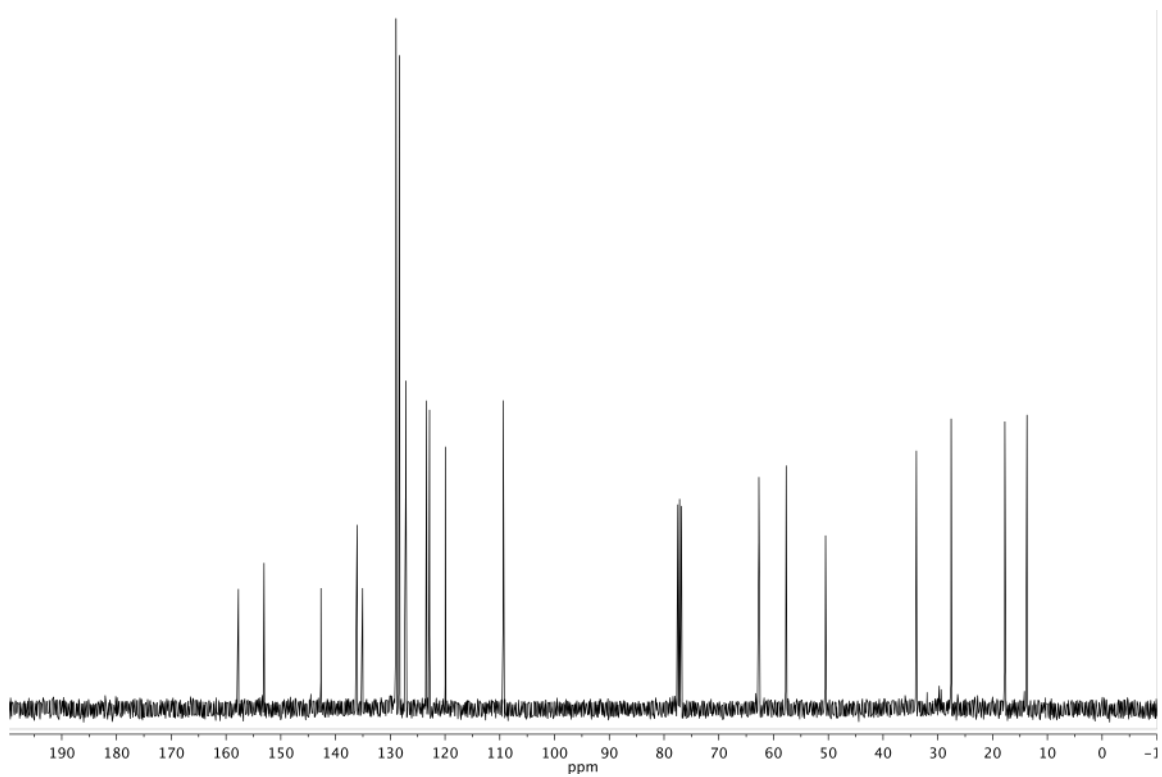
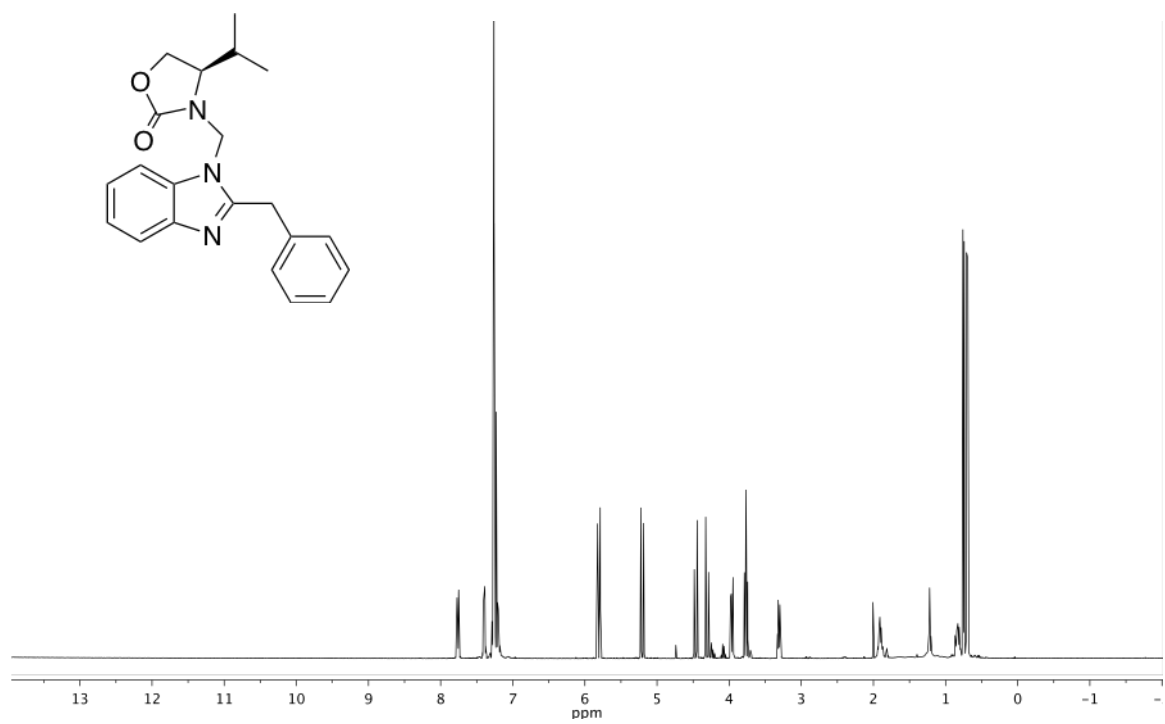
(R)-4-benzyl-3-((2-benzyl-1H-benzo[d]imidazol-1-yl)methyl)oxazolidin-2-one



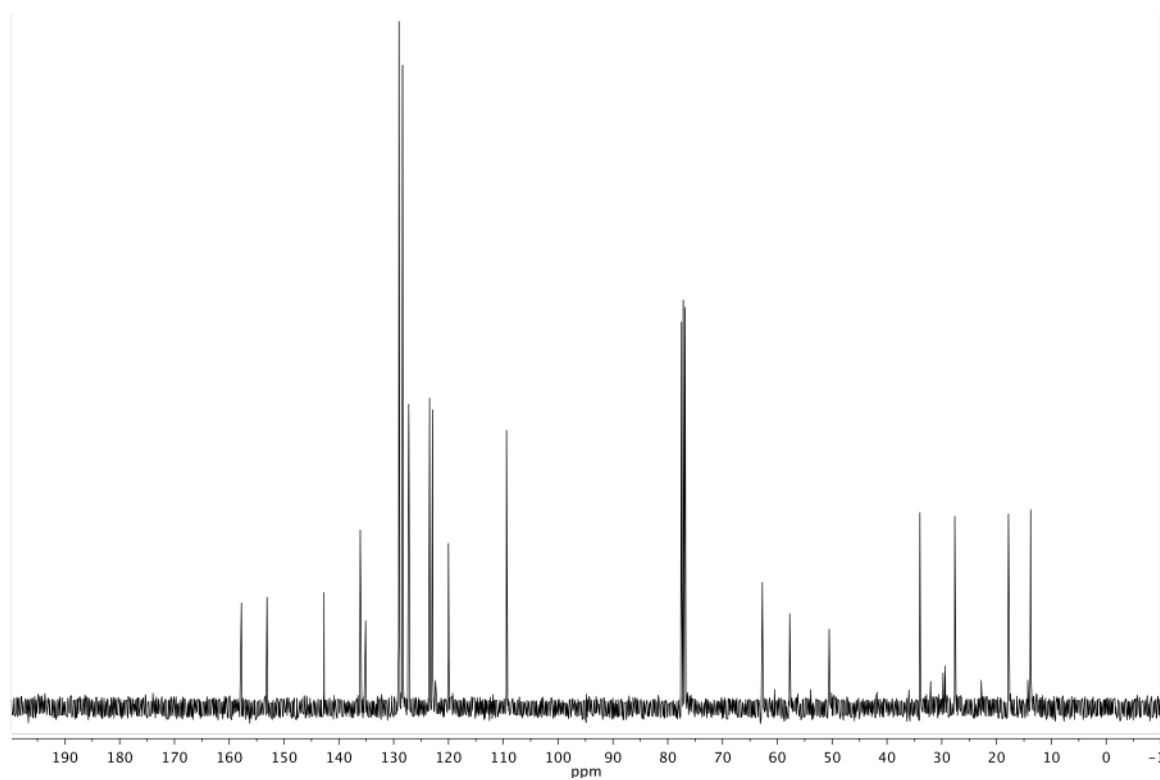
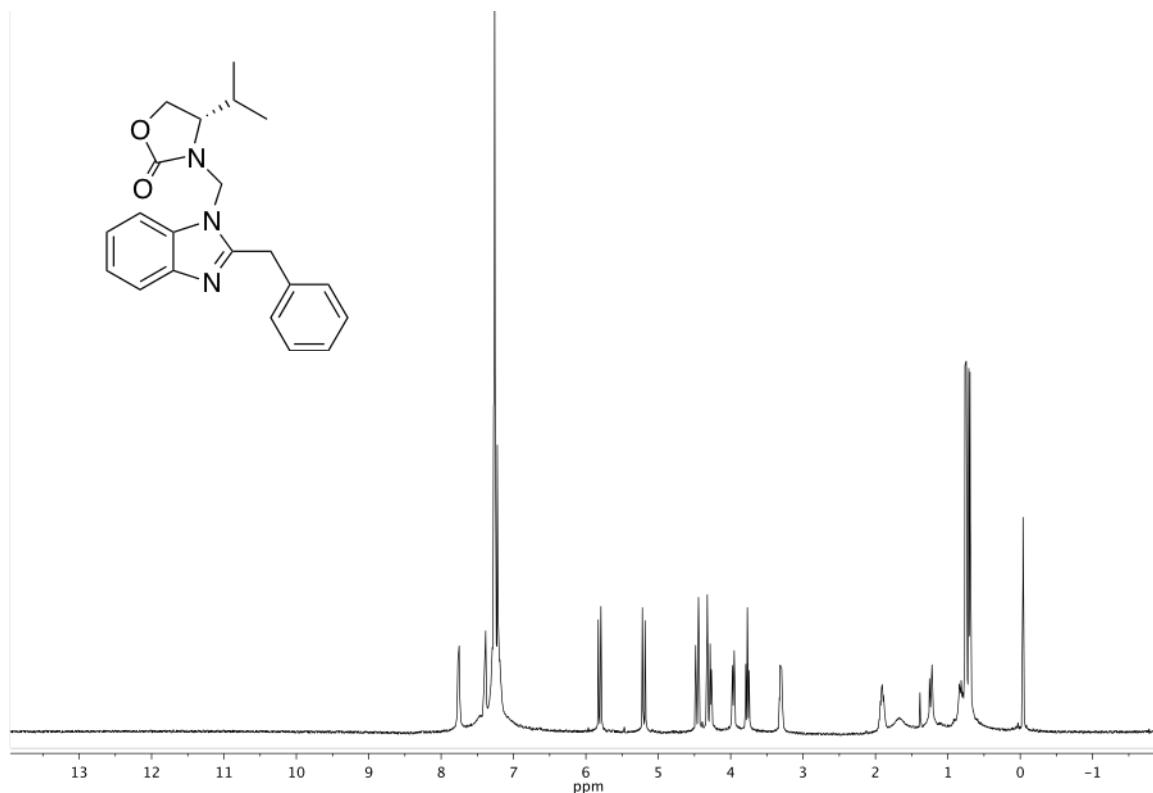
(S)-3-((2-benzyl-1H-benzo[d]imidazol-1-yl)methyl)-4-phenyloxazolidin-2-one



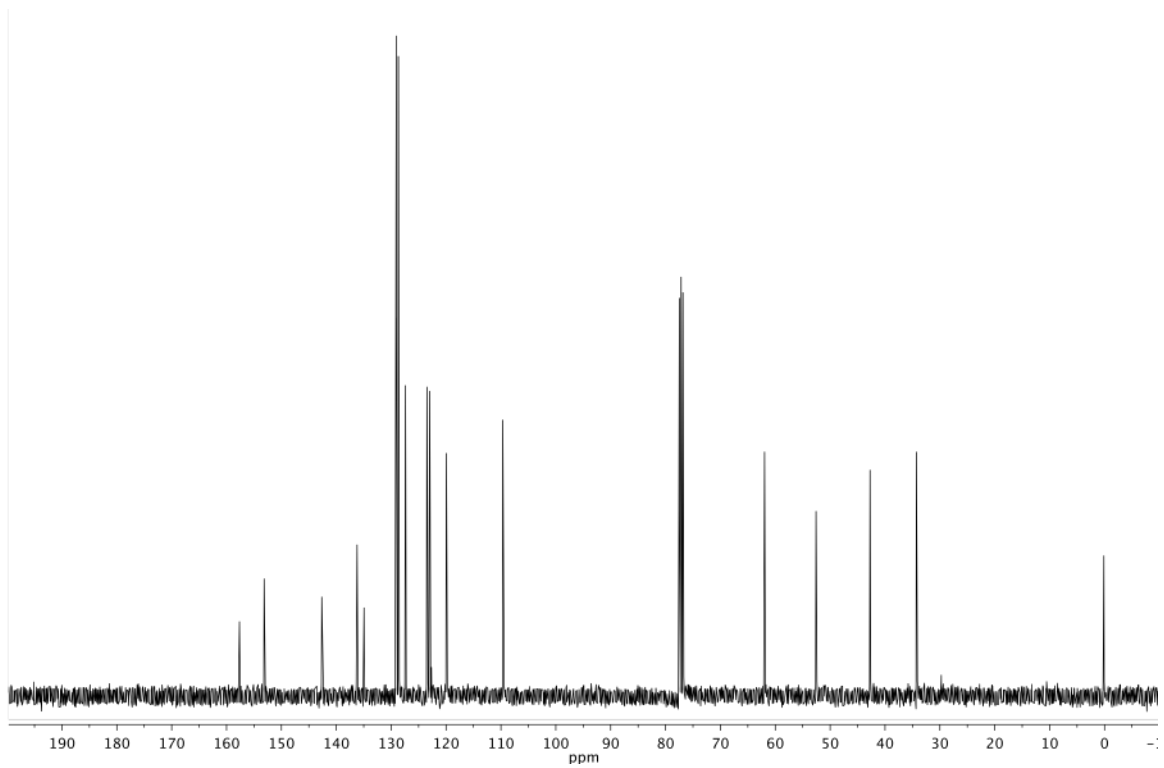
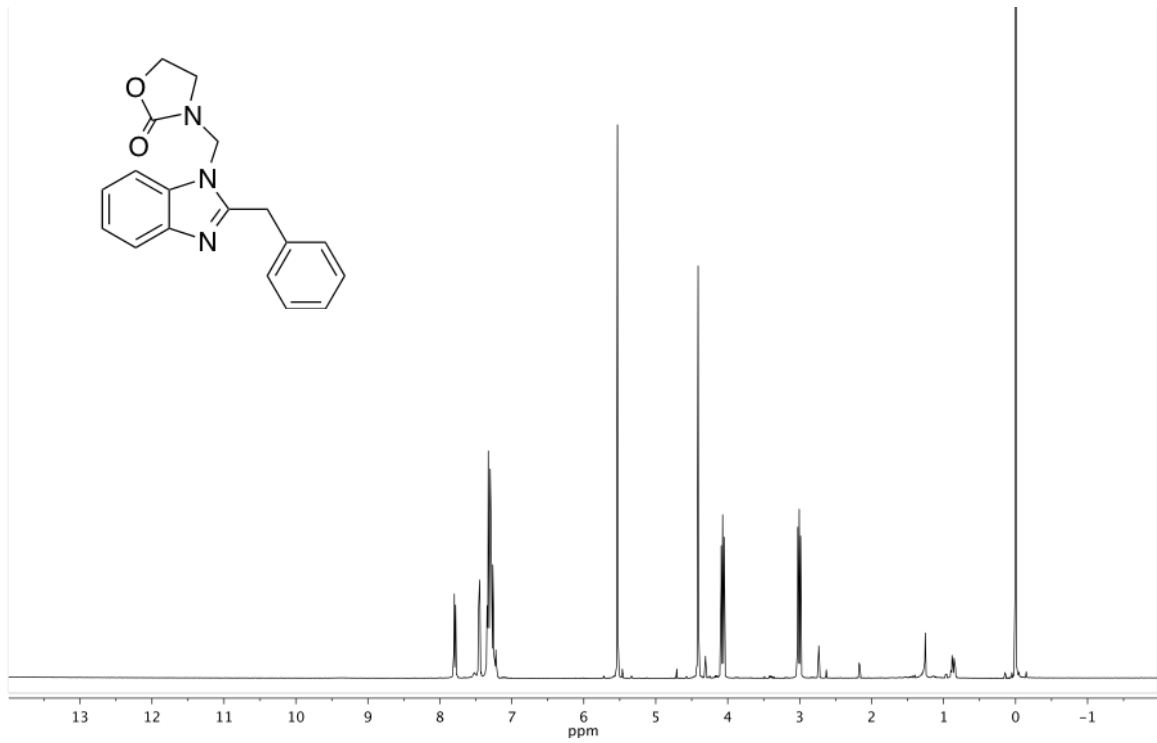
(R)-3-((2-benzyl-1H-benzo[d]imidazol-1-yl)methyl)-4-isopropylloxazolidin-2-one



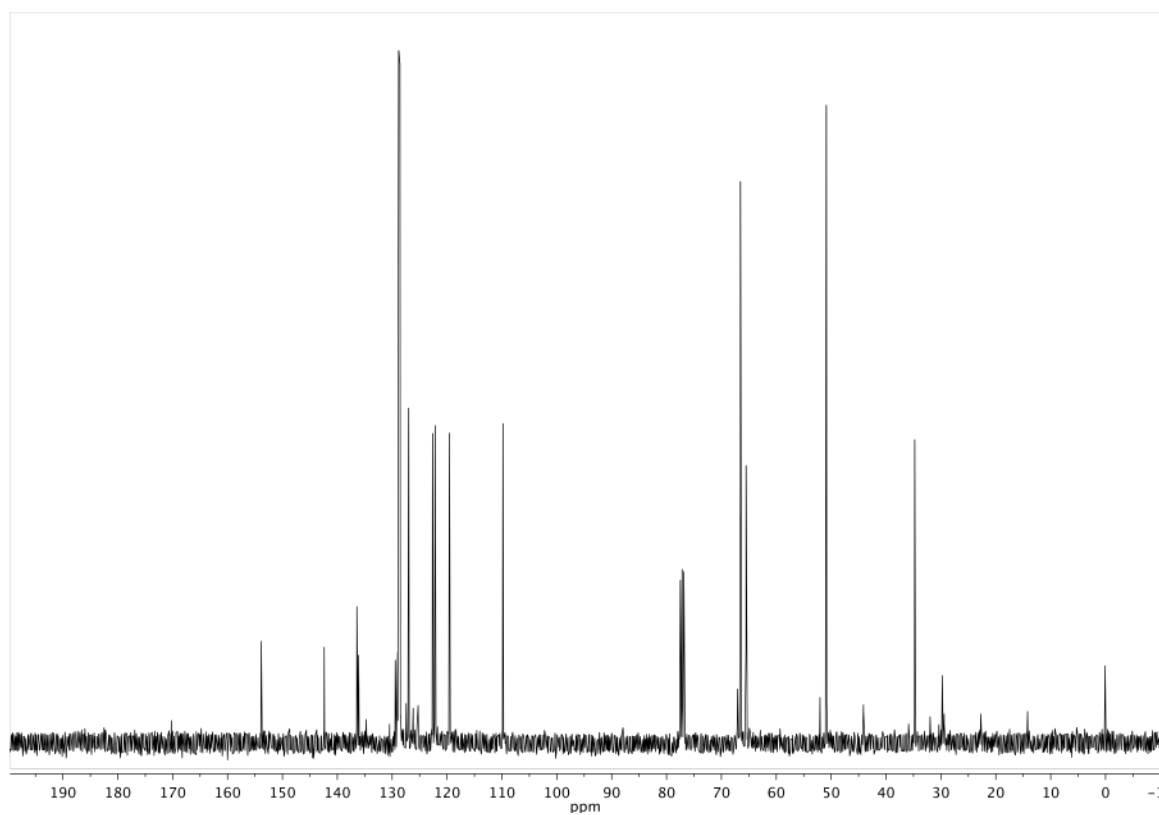
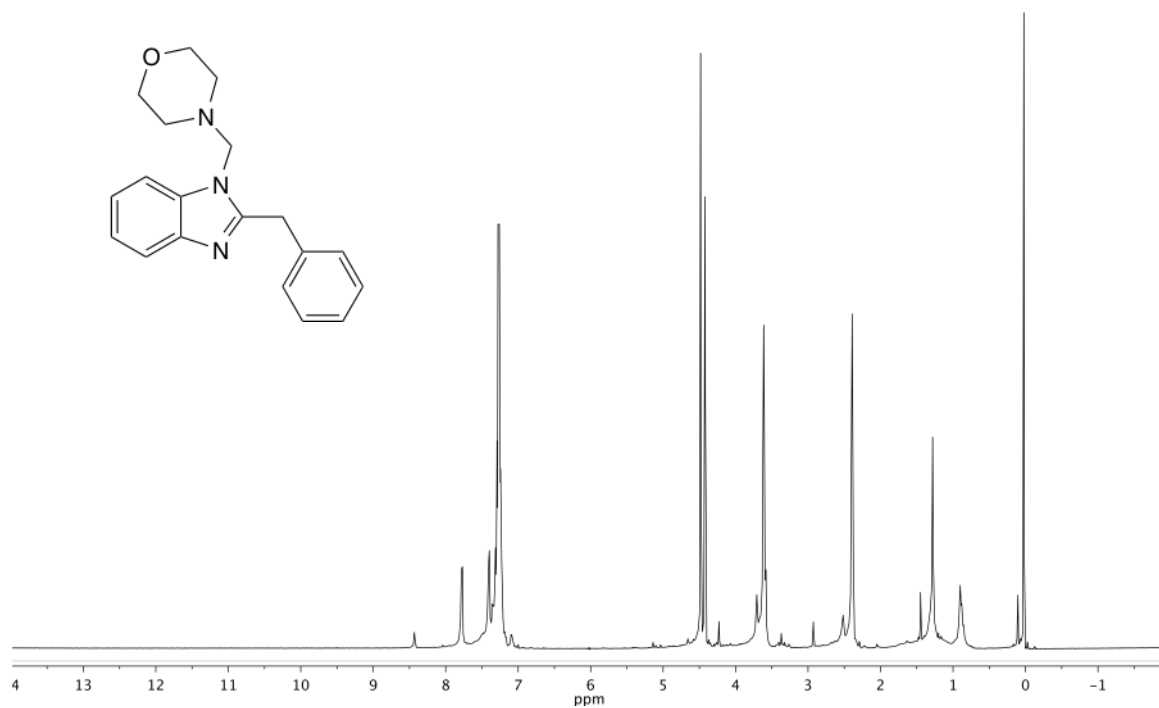
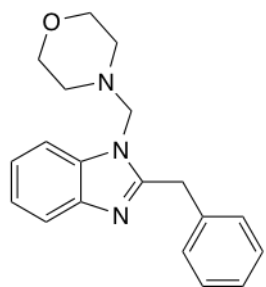
(S)-3-((2-benzyl-1H-benzo[d]imidazol-1-yl)methyl)-4-isopropylloxazolidin-2-one



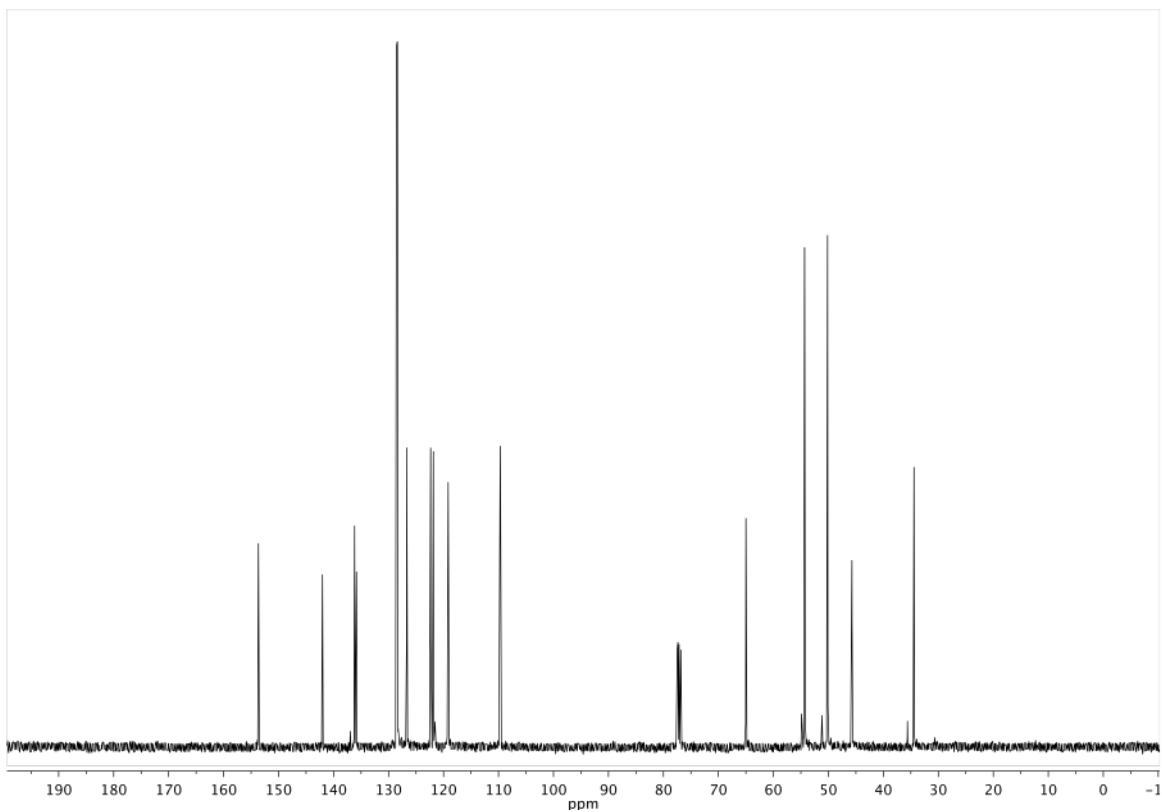
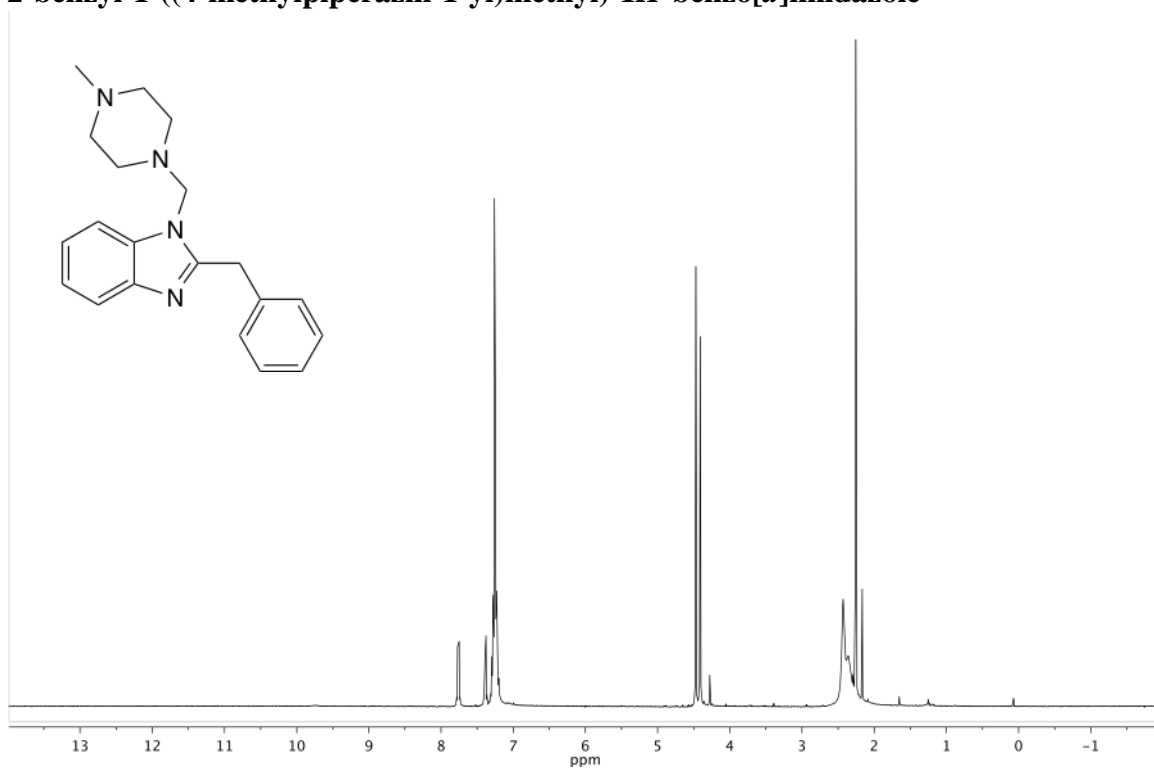
3-((2-benzyl-1H-benzo[d]imidazol-1-yl)methyl)oxazolidin-2-one



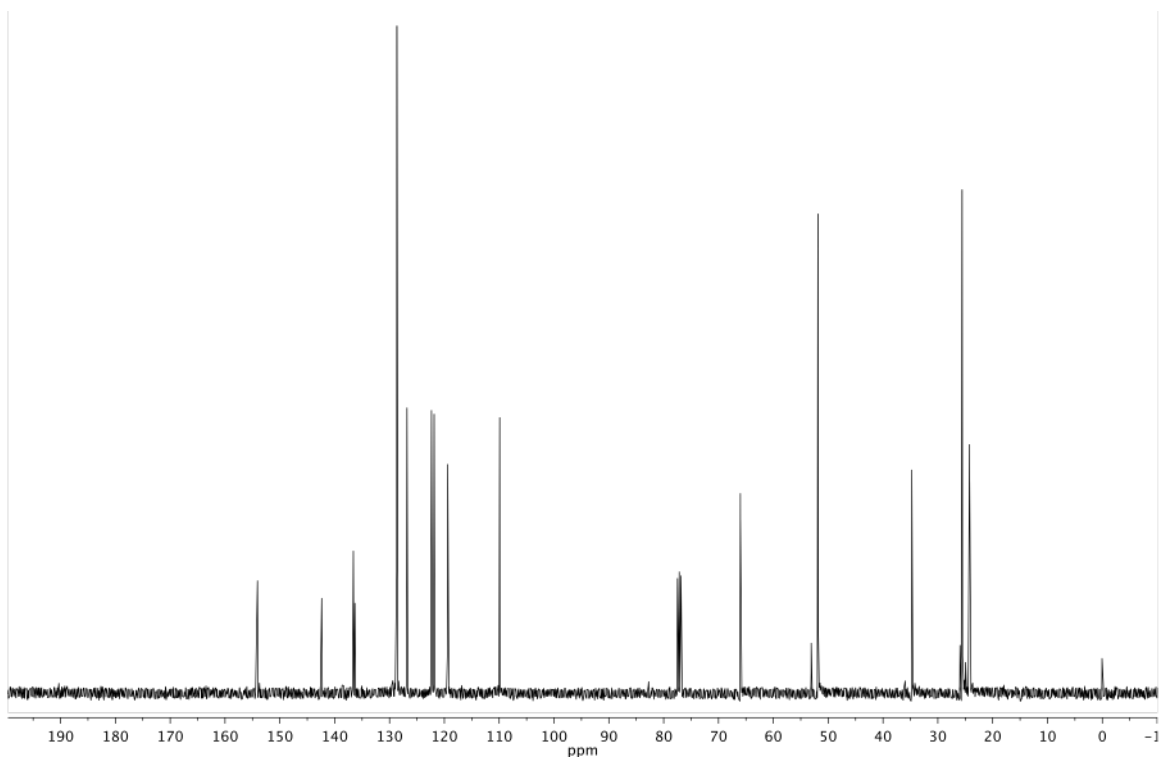
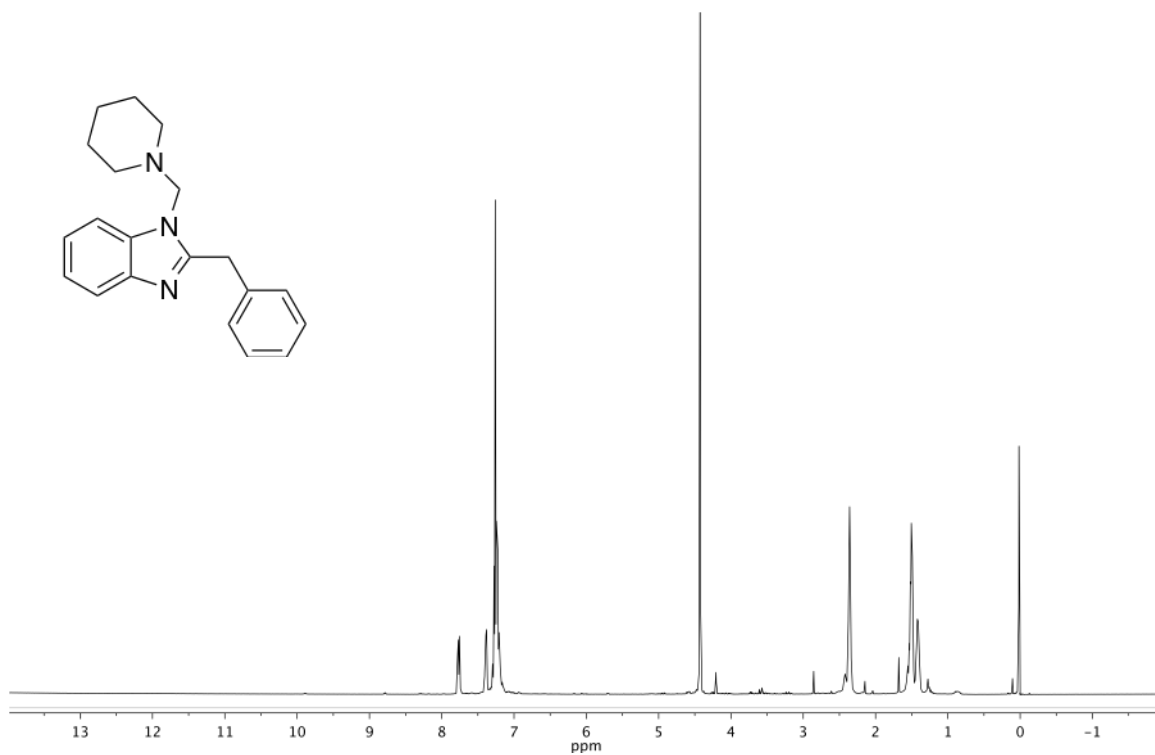
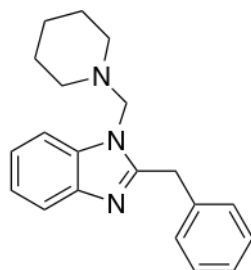
4-((2-benzyl-1H-benzo[d]imidazol-1-yl)methyl)morpholine



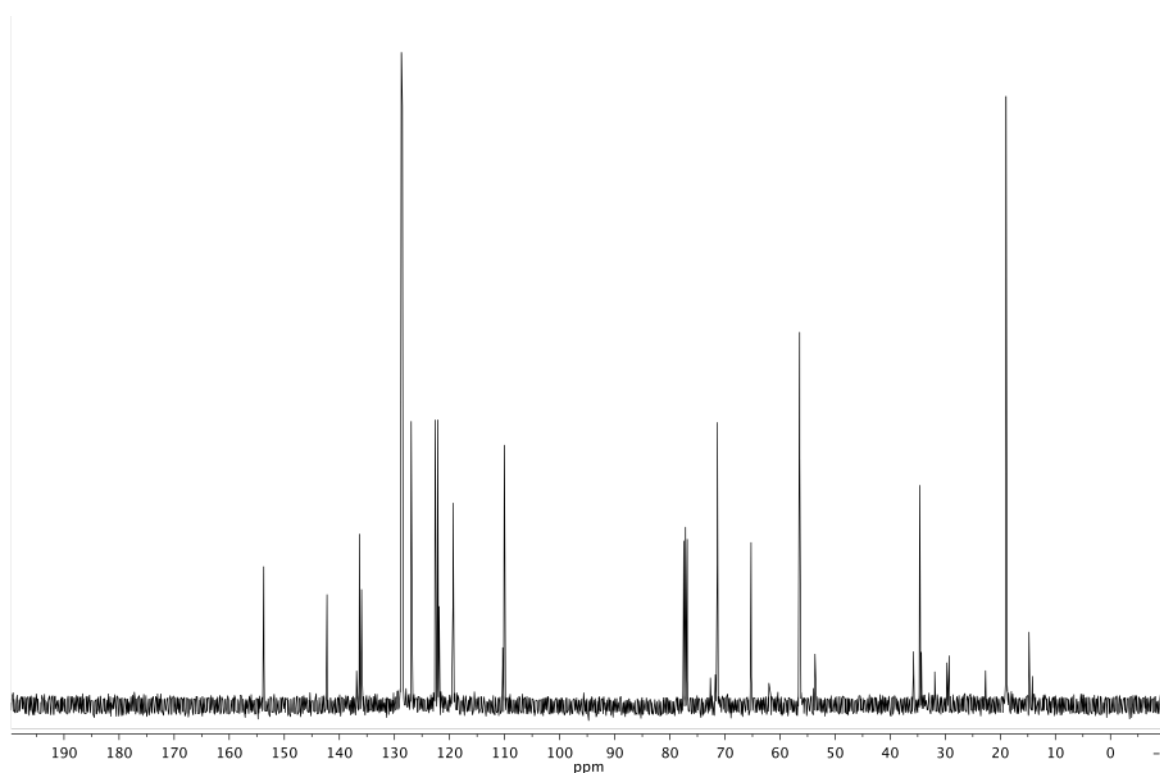
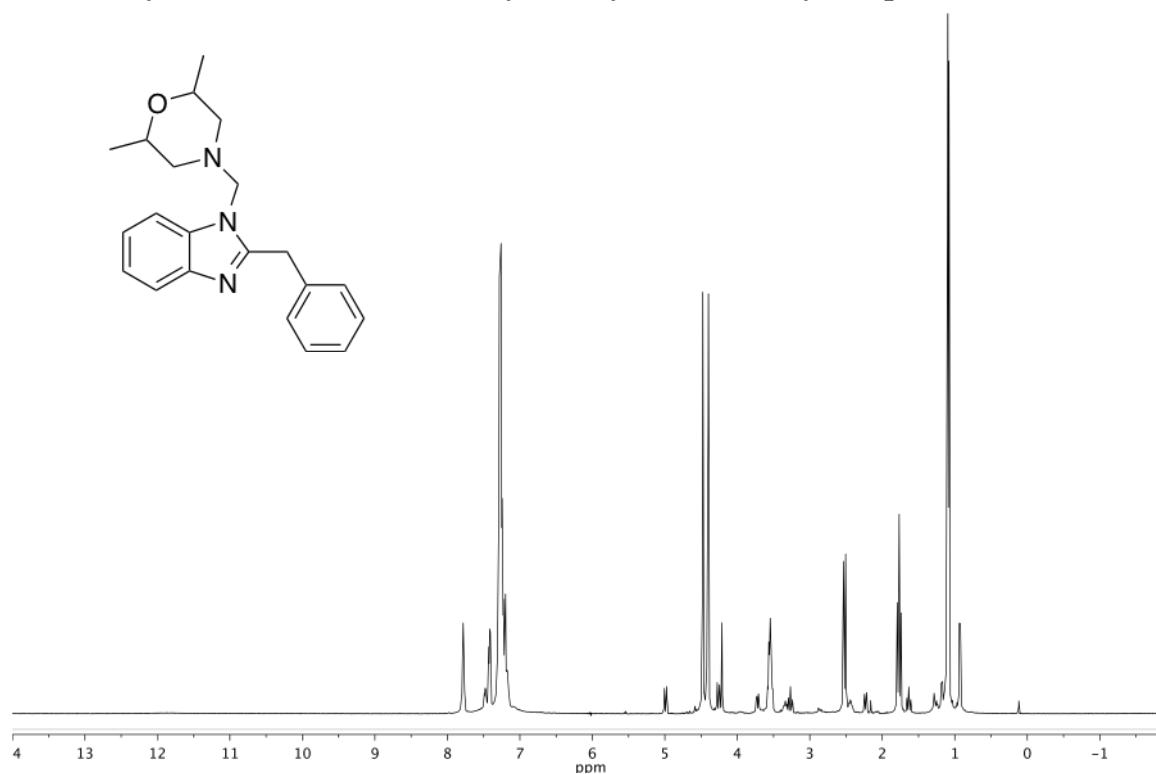
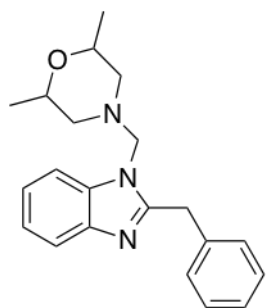
2-benzyl-1-((4-methylpiperazin-1-yl)methyl)-1H-benzo[d]imidazole



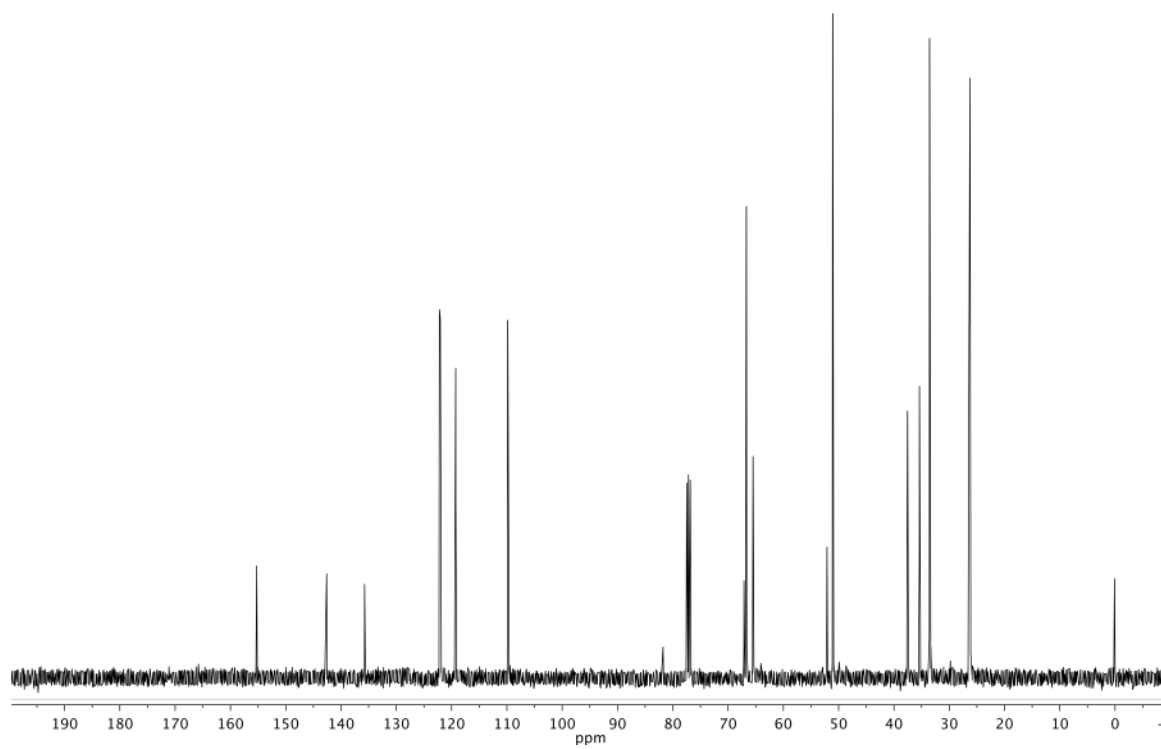
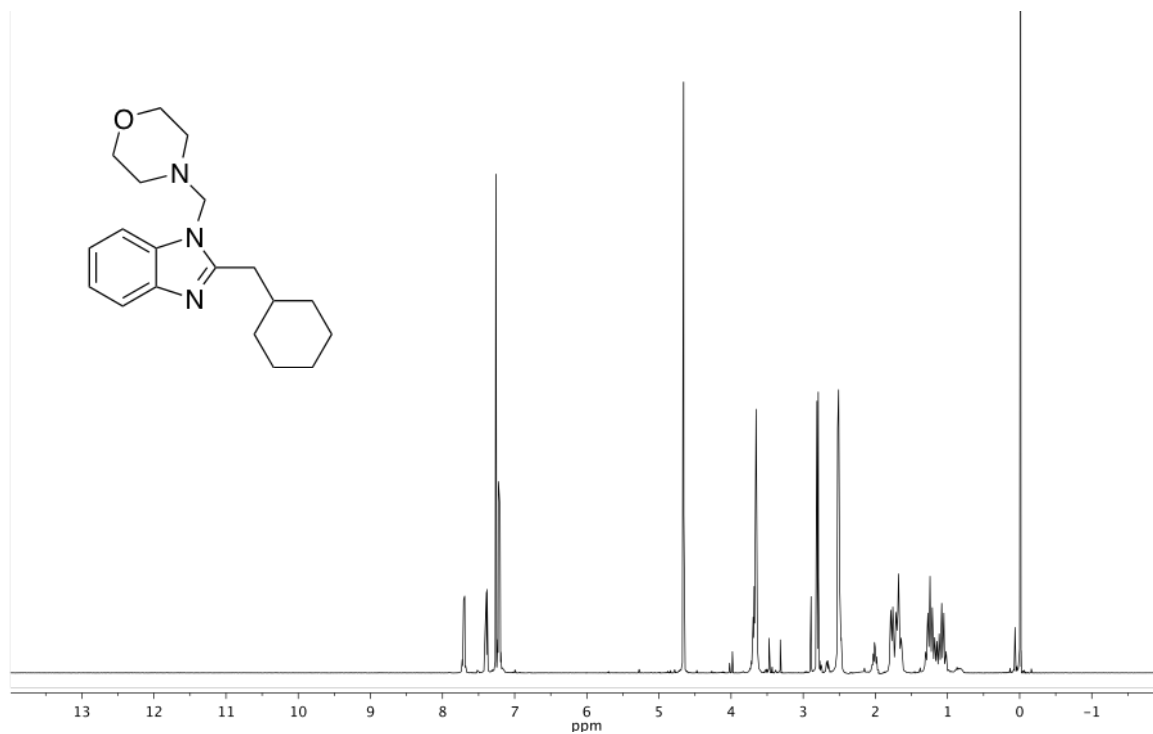
2-benzyl-1-(piperidin-1-ylmethyl)-1H-benzo[d]imidazole



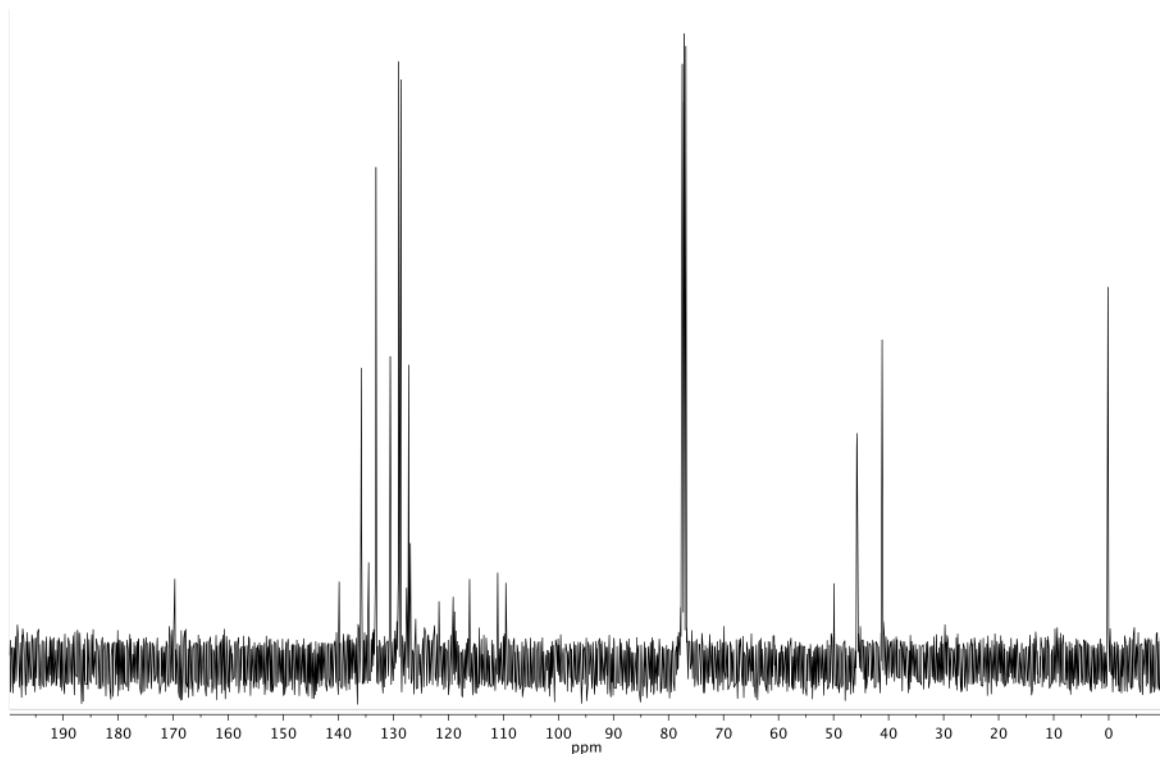
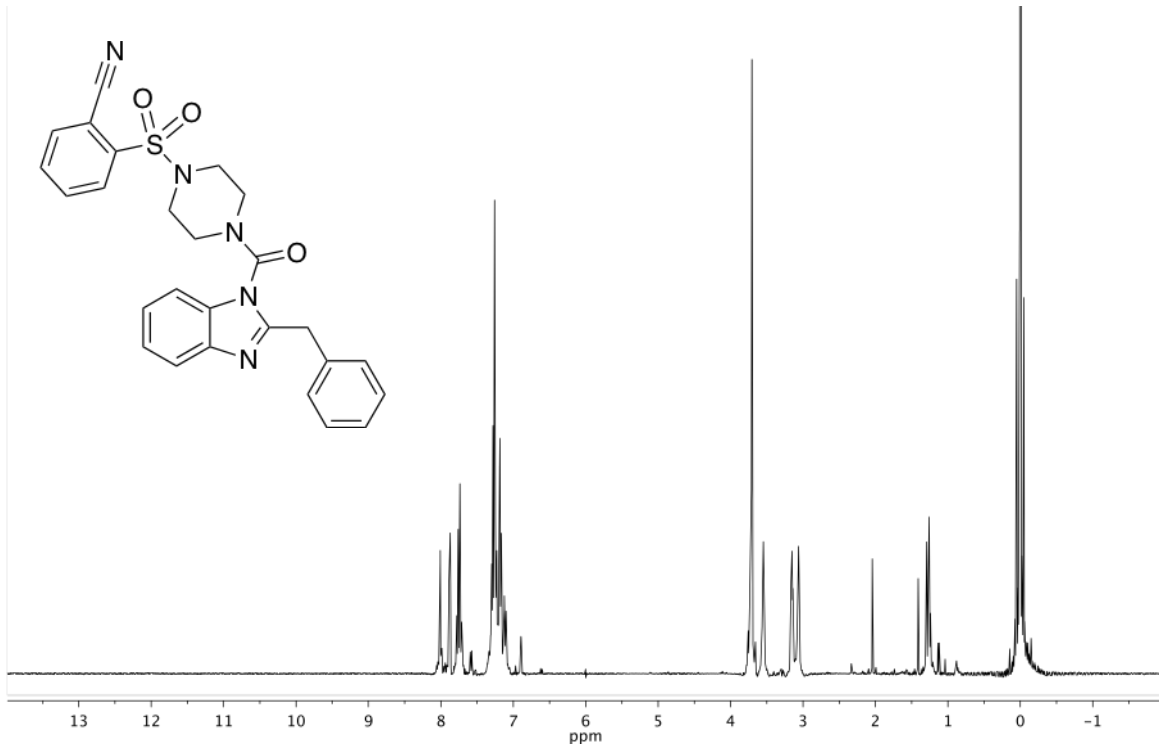
4-((2-benzyl-1H-benzo[d]imidazol-1-yl)methyl)-2,6-dimethylmorpholine



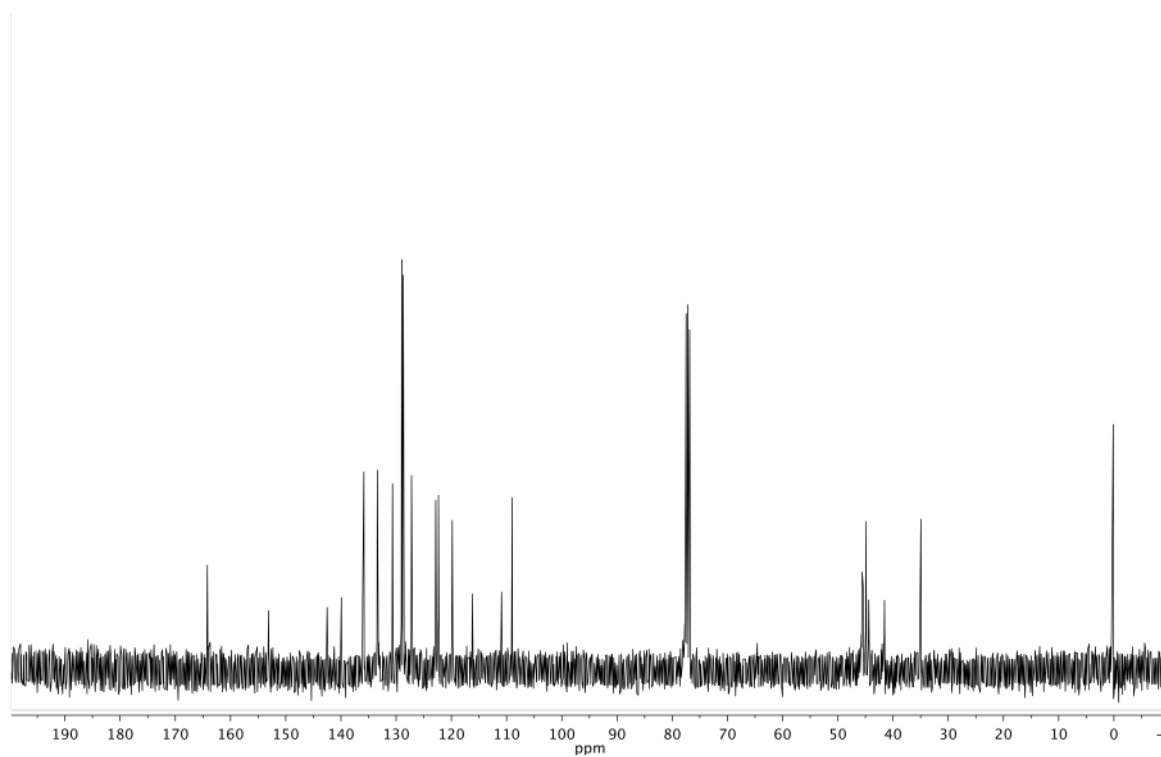
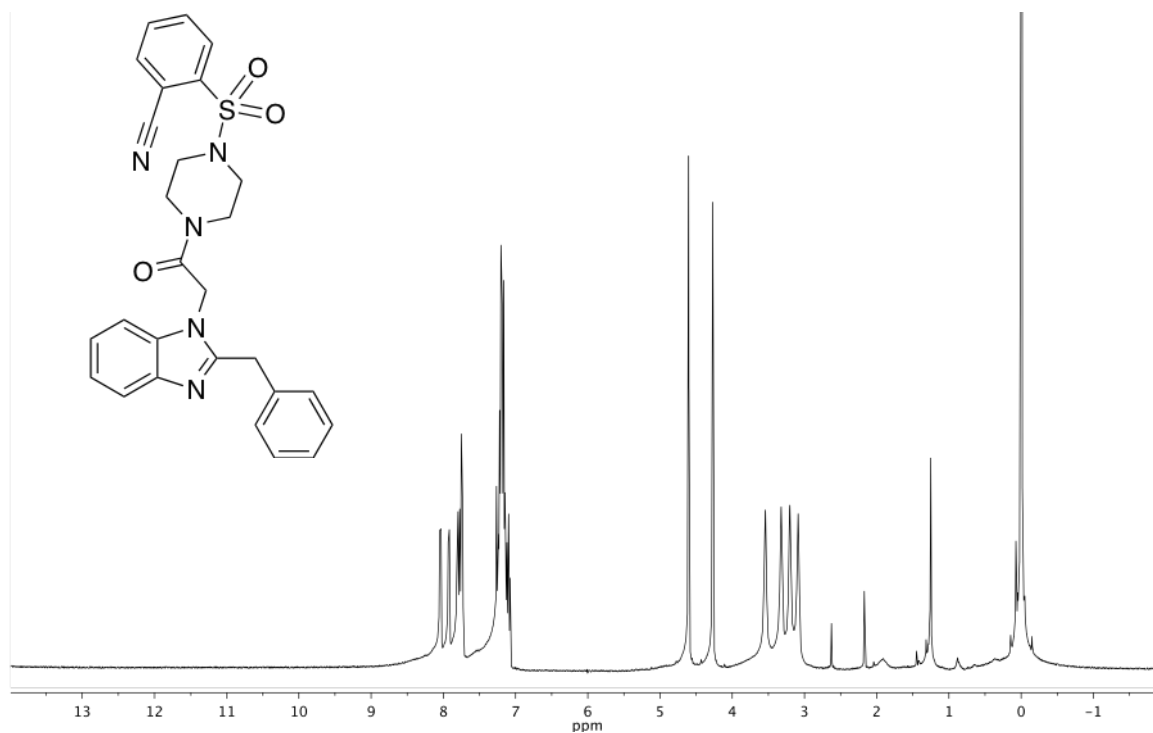
4-((2-(cyclohexylmethyl)-1H-benzo[d]imidazol-1-yl)methyl)morpholine



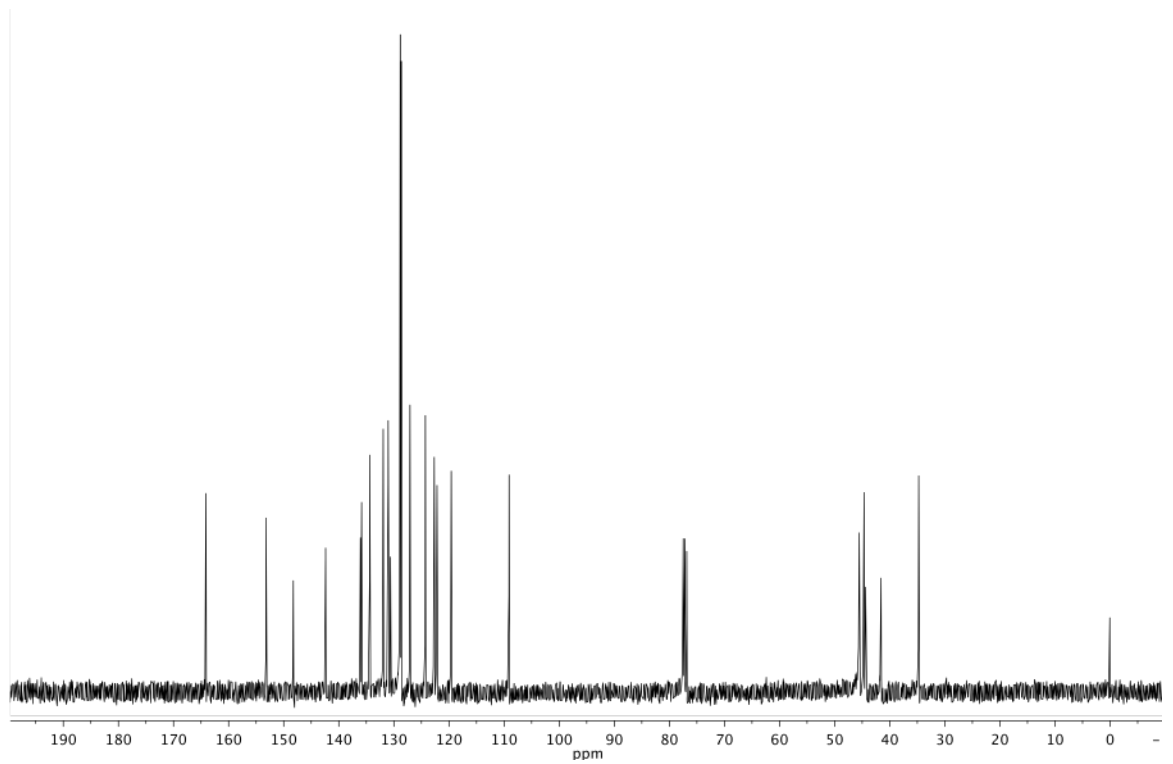
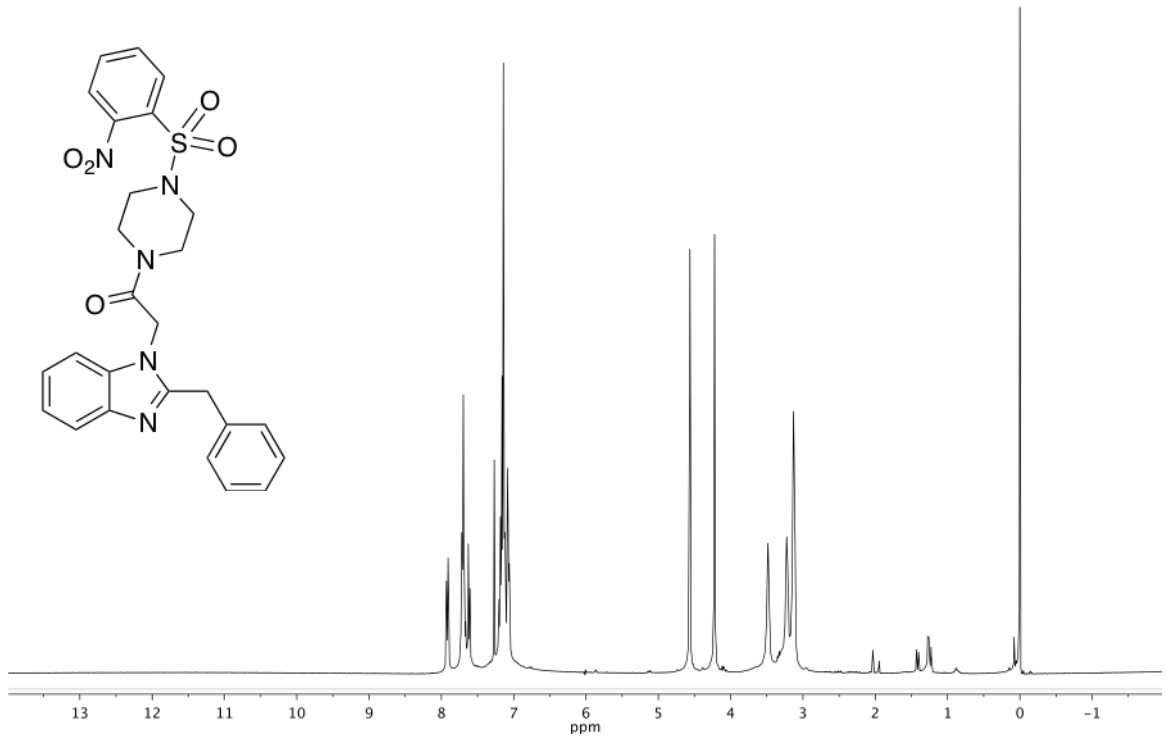
2-((4-(2-benzyl-1H-benzo[d]imidazole-1-carbonyl)piperazin-1-yl)sulfonyl)benzonitrile



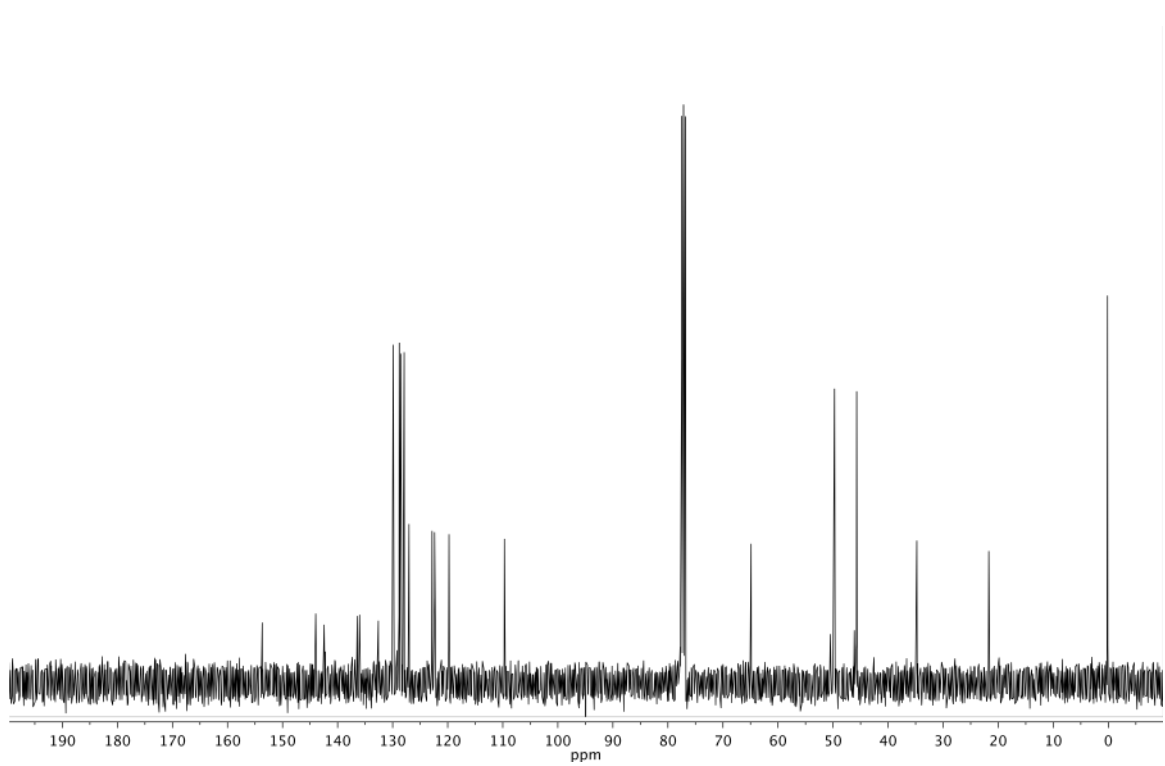
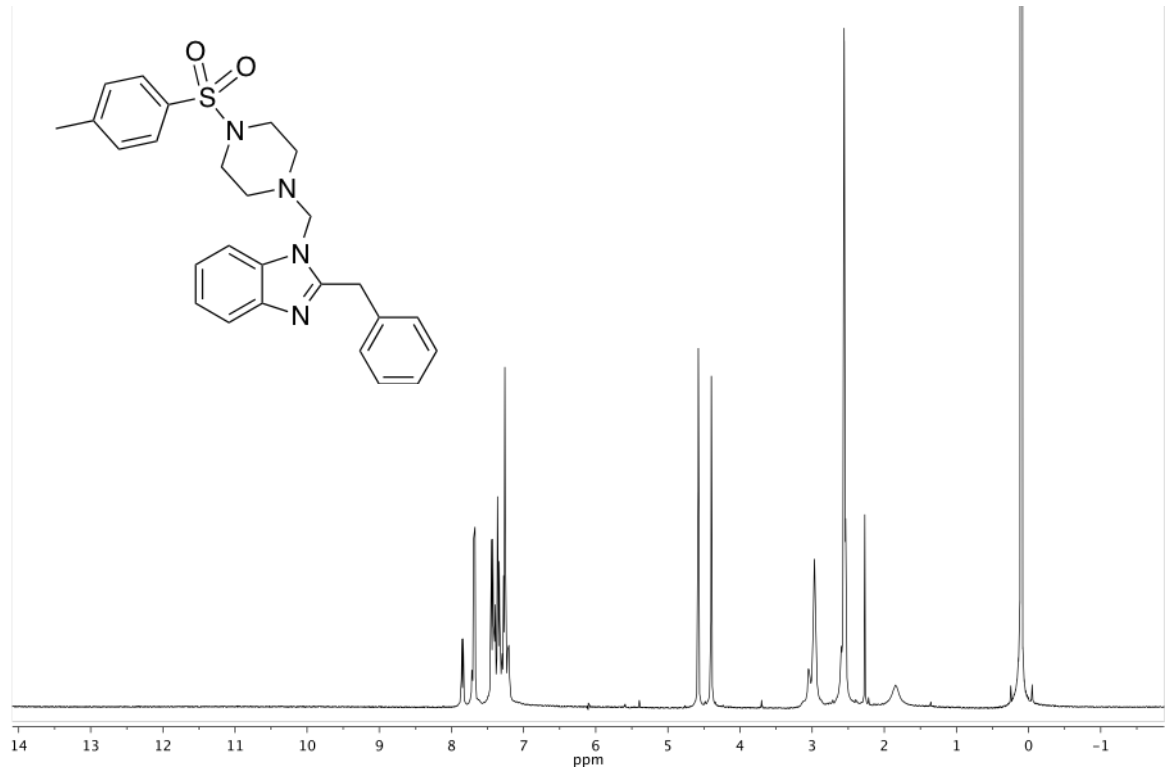
2-((4-(2-(2-benzyl-1H-benzo[d]imidazol-1-yl)acetyl)piperazin-1-yl)sulfonyl)benzonitrile



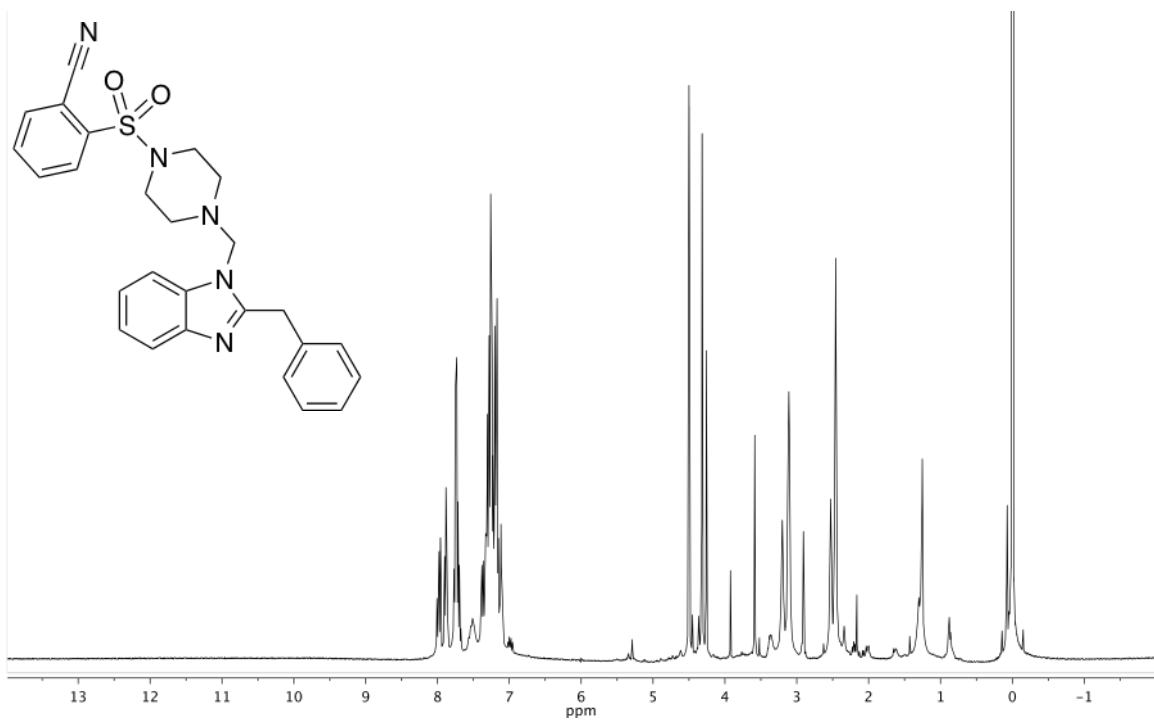
2-(2-benzyl-1H-benzo[d]imidazol-1-yl)-1-(4-((2-nitrophenyl)sulfonyl)piperazin-1-yl)ethanone



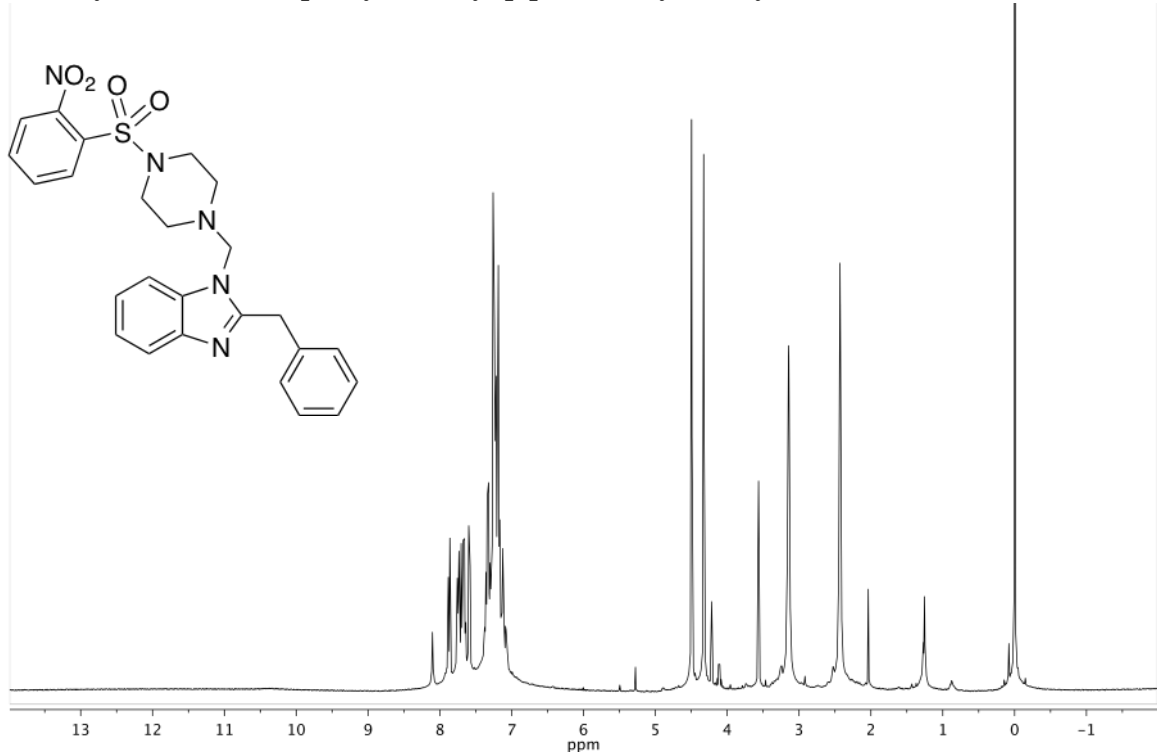
2-benzyl-1-((4-tosylpiperazin-1-yl)methyl)-1H-benzo[d]imidazole



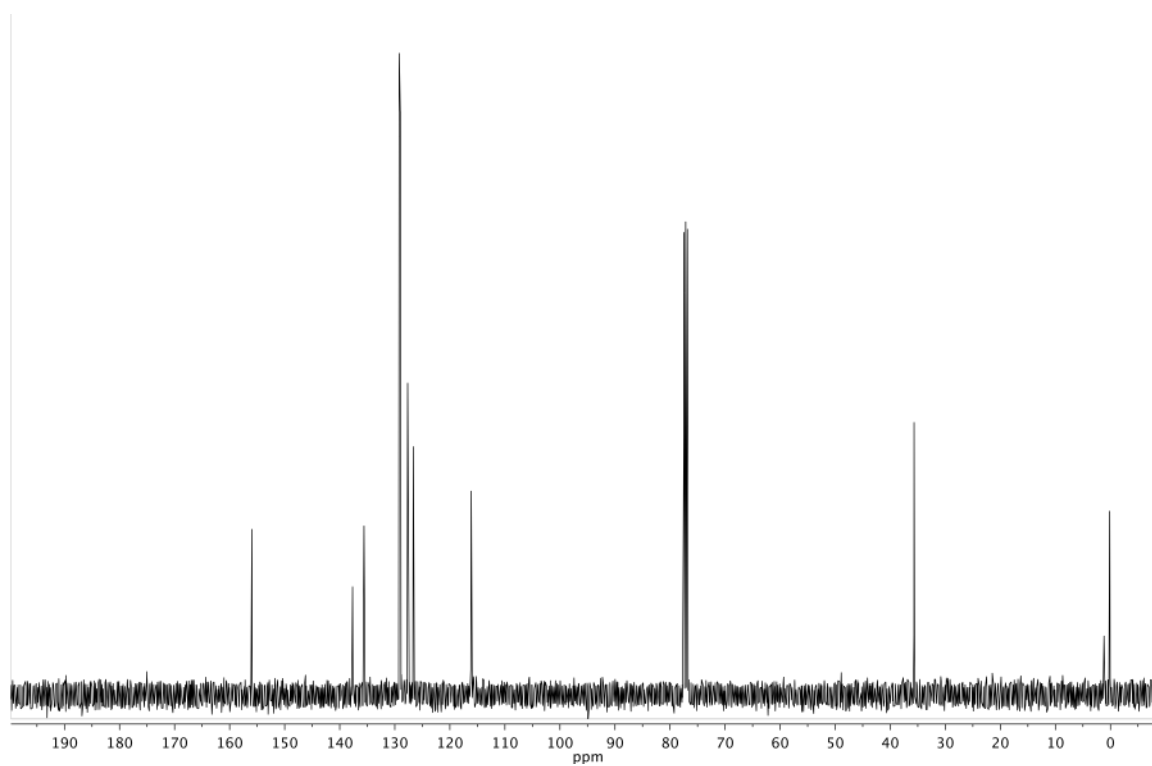
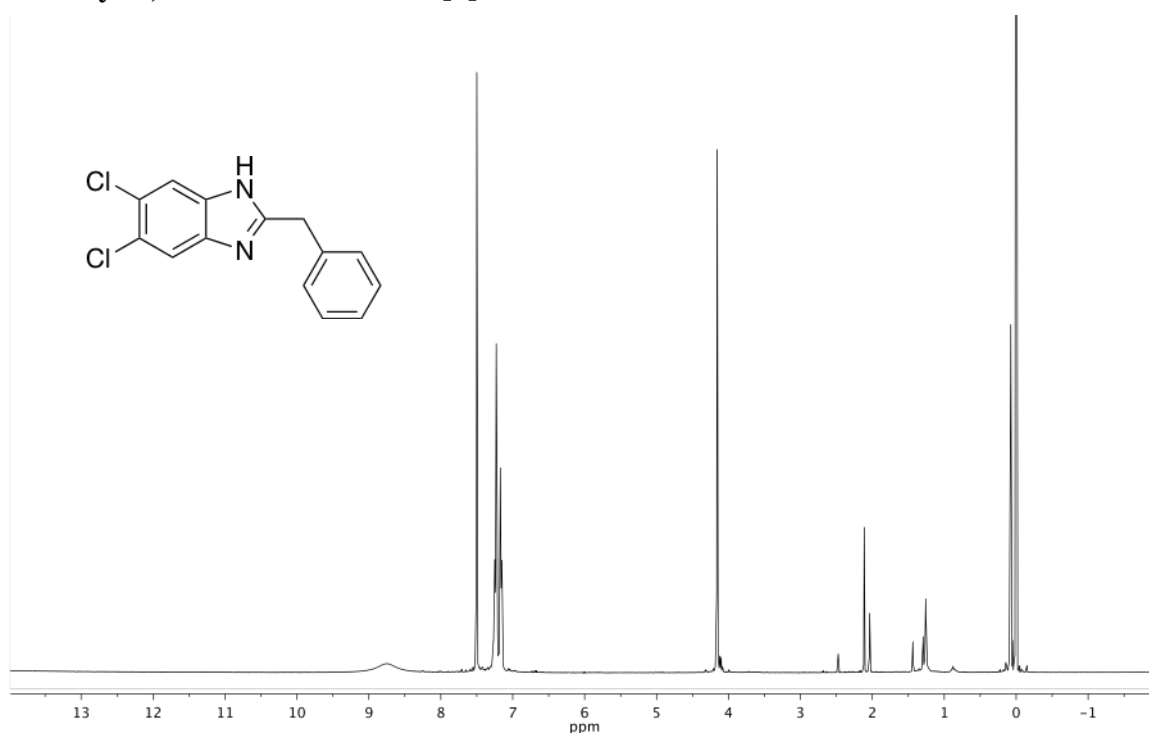
2-((4-((2-benzyl-1H-benzo[d]imidazol-1-yl)methyl)piperazin-1-yl)sulfonyl)benzonitrile



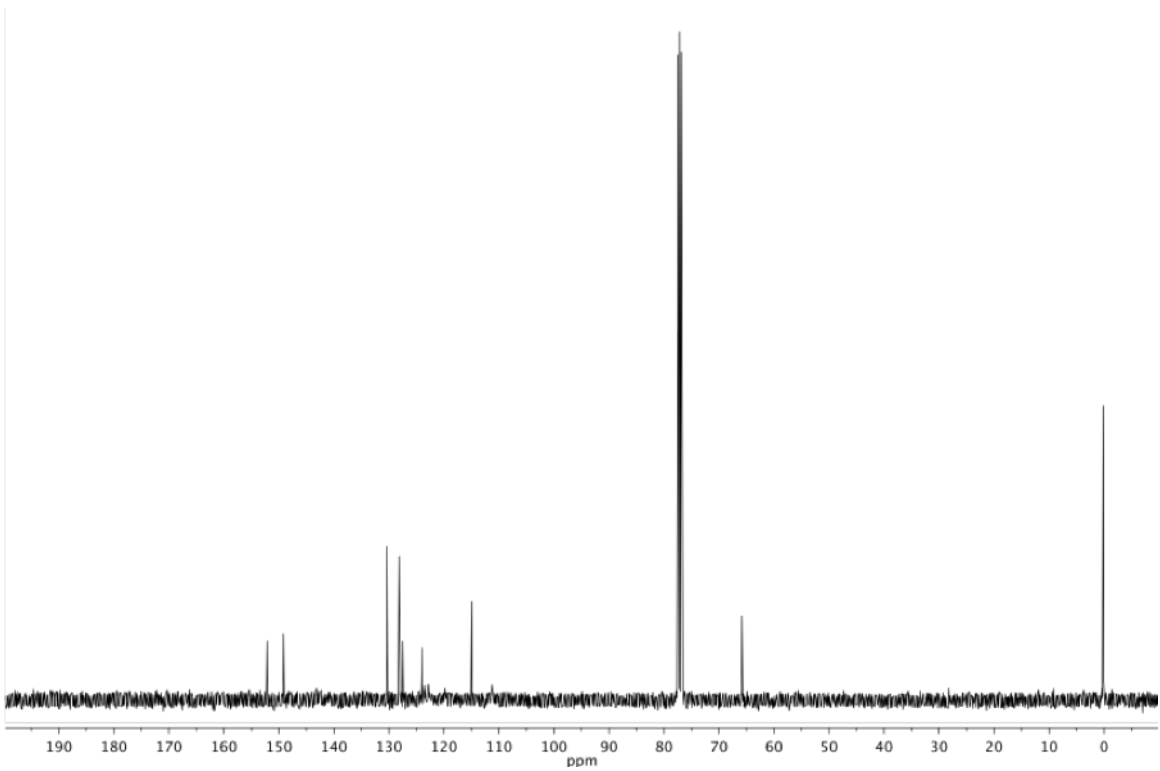
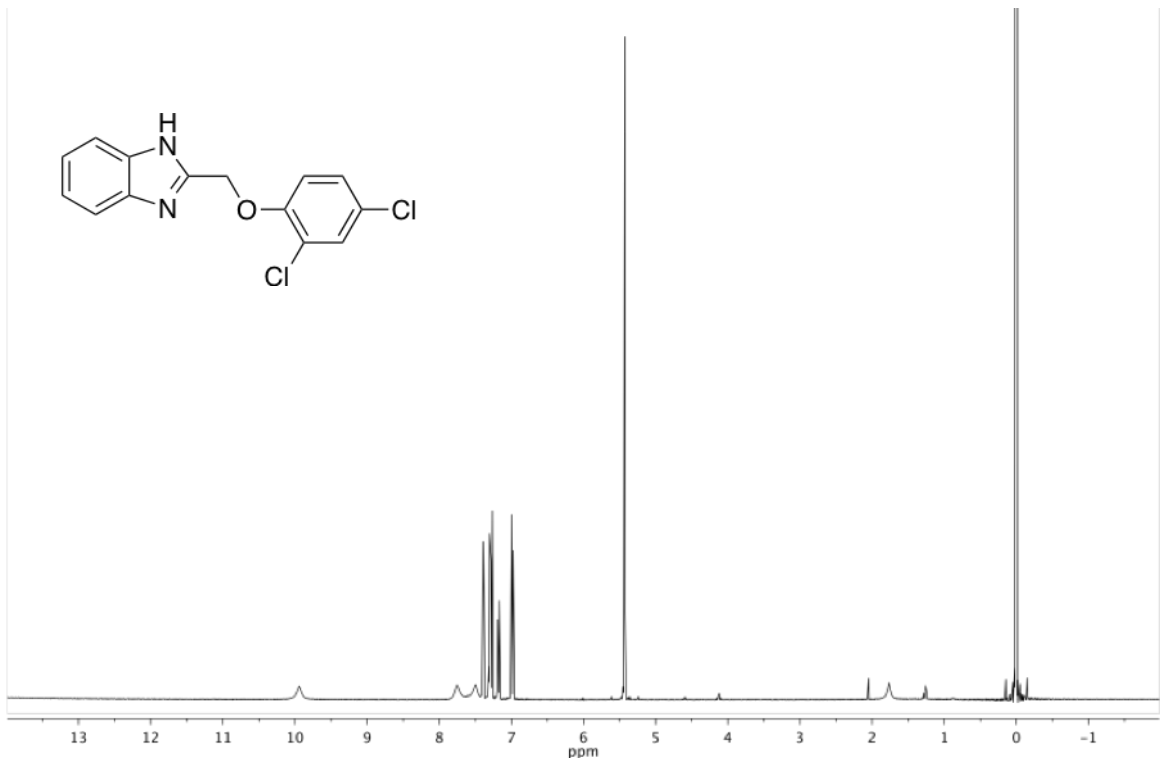
2-benzyl-1-((4-((2-nitrophenyl)sulfonyl)piperazin-1-yl)methyl)-1H-benzo[d]imidazole



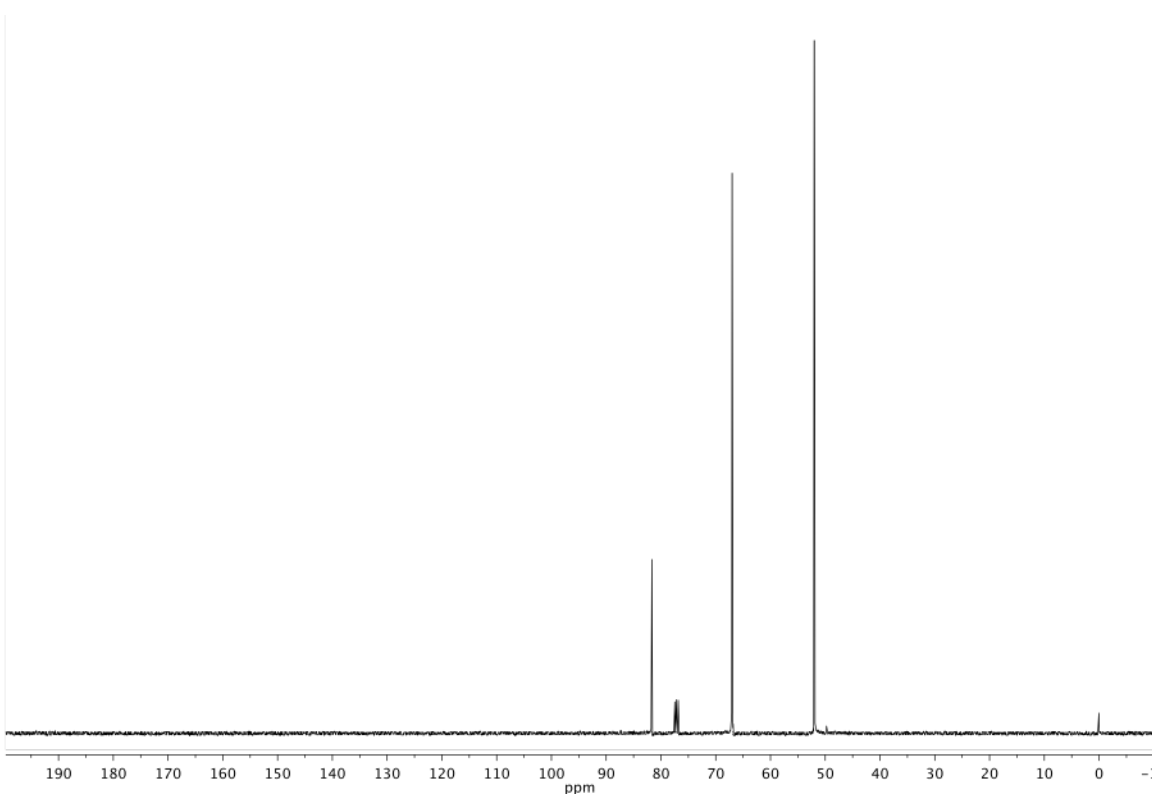
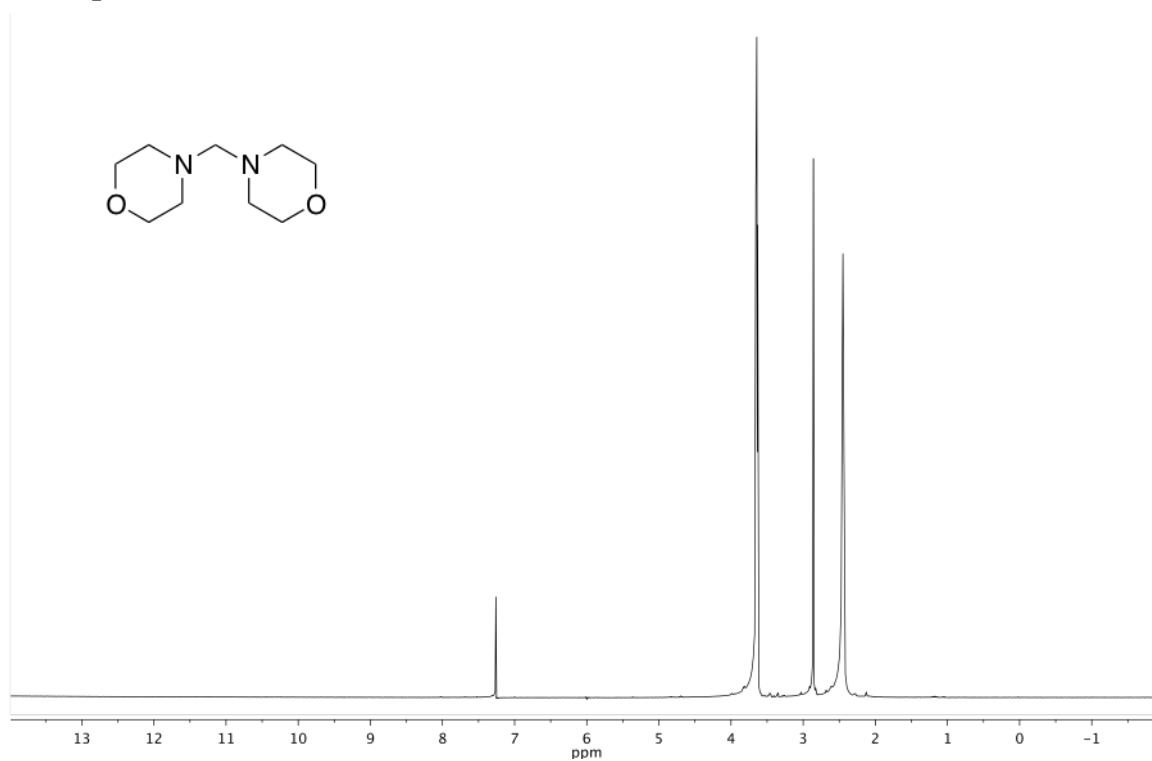
2-benzyl-5,6-dichloro-1H-benzo[d]imidazole



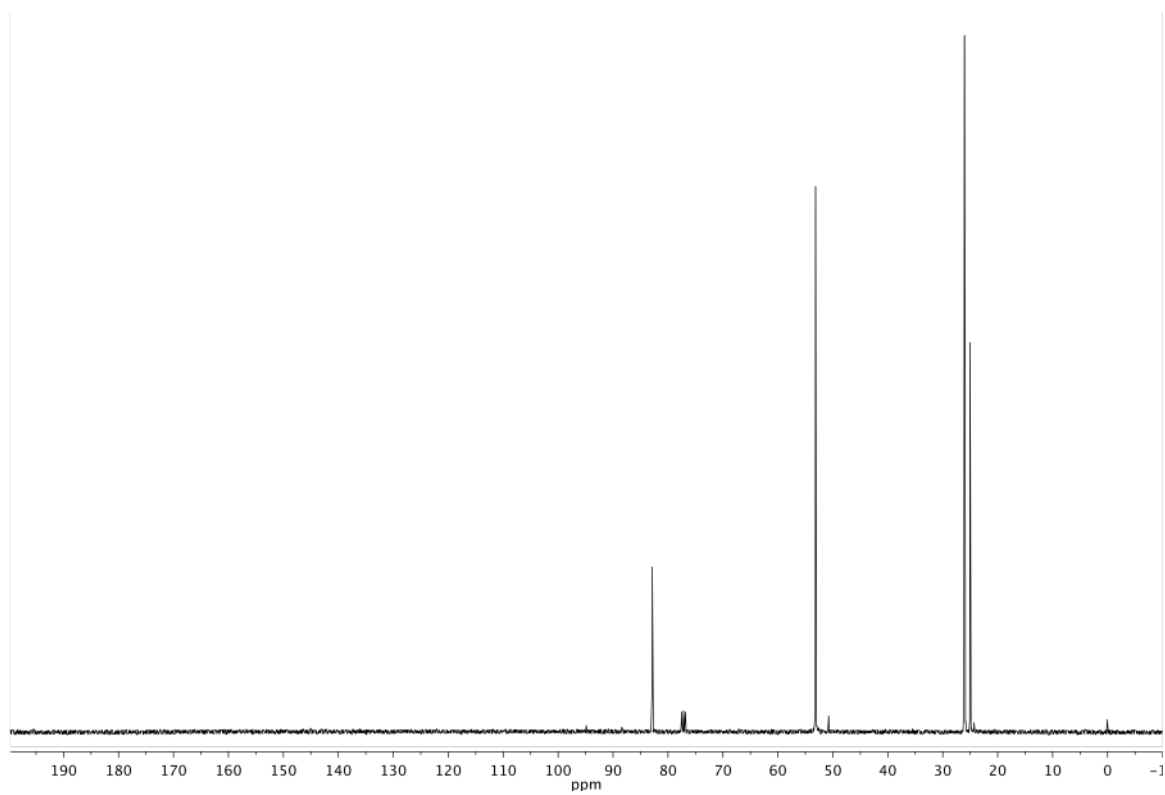
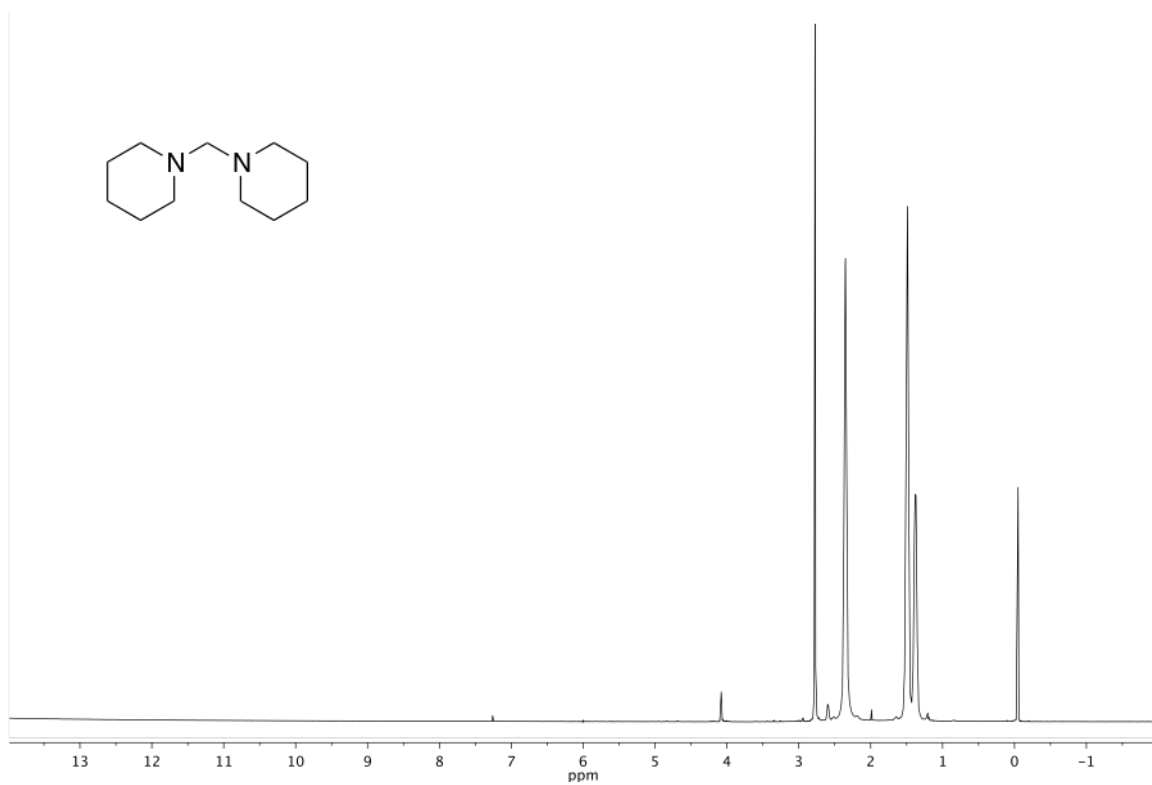
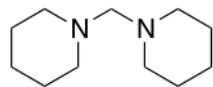
2-((2,4-dichlorophenoxy)methyl)-1H-benzo[d]imidazole



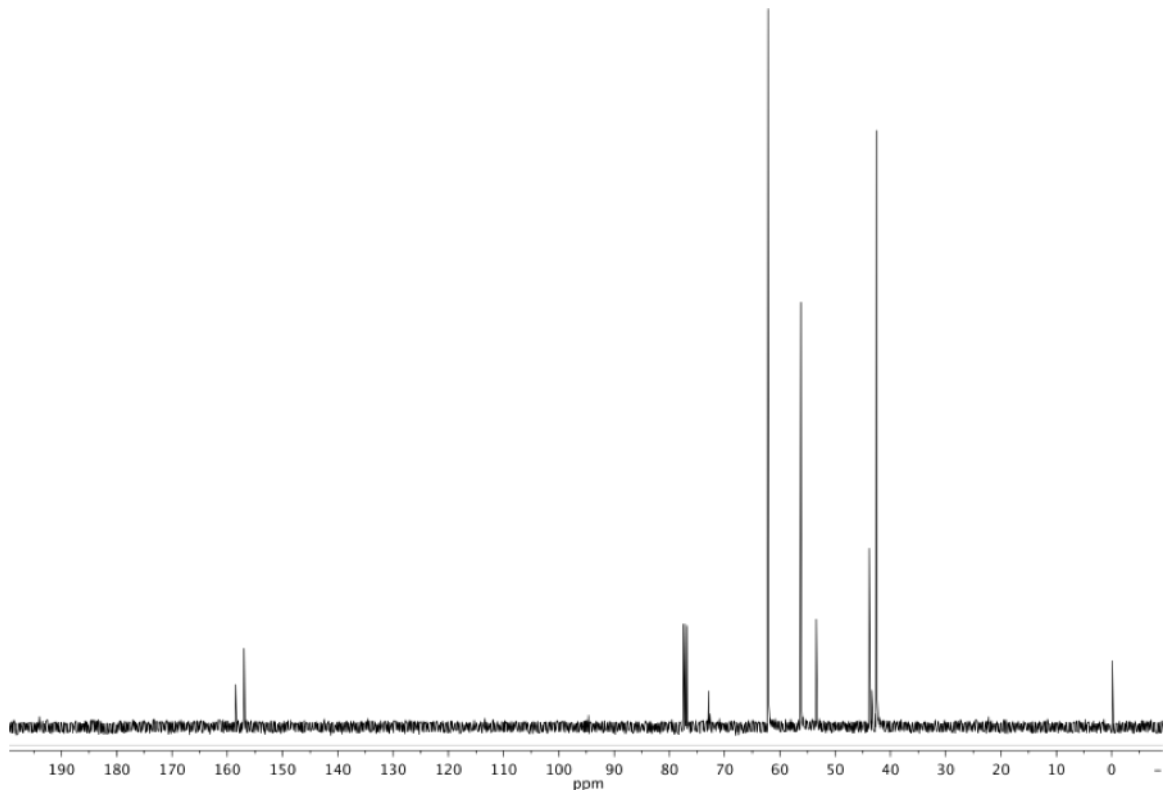
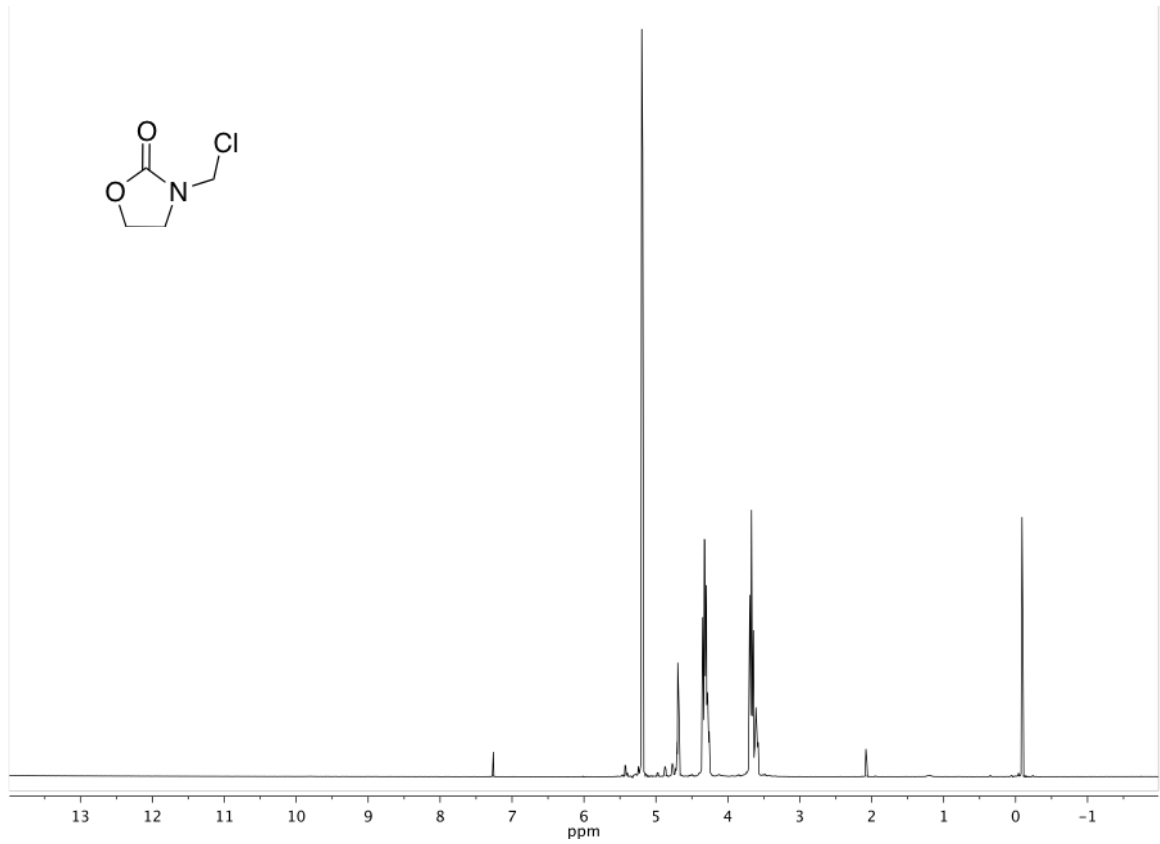
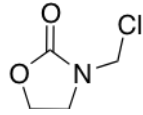
Dimorpholinomethane



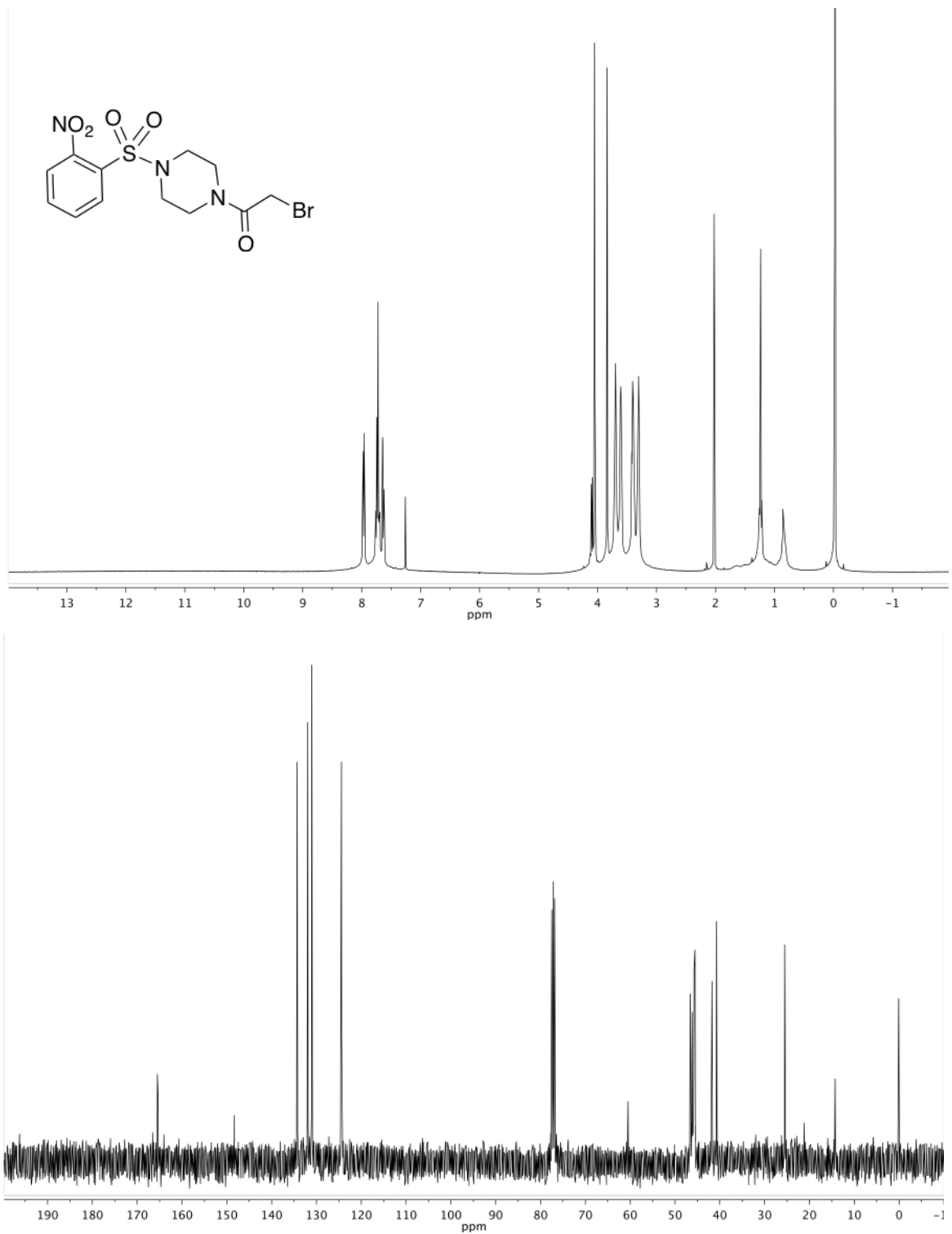
Di(piperidin-1-yl)methane



3-(chloromethyl)oxazolidin-2-one



2-bromo-1-(4-((2-nitrophenyl)sulfonyl)piperazin-1-yl)ethan-1-one



Chapter 2

Development of photolabile protecting groups for a bioactive compound

Introduction

Quorum sensing (QS) is a communication mechanism that occurs in many bacteria. An underlying principle of QS is that bacteria utilize their population density to modify the collective behavior of the group. Organisms that are involved in QS produce small molecule signals known as autoinducers, which are released into their environment after they are synthesized intracellularly. The bacteria, using specific receptors, can then recognize these autoinducers in order to probe the population density. Binding of these signal molecules typically brings forth changes to gene expression, which is the driving factor that allows a given population of cells to modify their behavior in unison.

Importantly, many known virulence factors are produced as a result of QS, and so this signaling mechanism controls how/when a bacterium becomes pathogenic or virulent.

Coupled to the issue of growing antibiotic resistance, QS has recently gained exposure as a potential alternative to these medicines. While no QS drugs are currently on the market, much research has been published on the topic, and several studies have provided support for the idea of using these molecules as a novel means of dealing with bacterial infections.

Photoremovable protecting groups, or "photocages", are a relatively new tool that has successfully been employed to study various biological and biochemical systems^{1,15,16}. After a photocage has been applied to a biologically active molecule, that compound is said to be "caged", and decaging (photorelease) is achieved via irradiation of light at a certain wavelength. Light-activation is an optimal control element, as it can

be managed in regard to location, timing, and magnitude^{1,2,3}. Additionally, photodecaging provides a concentration surge, in which the amount of active compound jumps from zero to a maximum level in seconds (or even milli/micro seconds). While the concept as a whole is without doubt scientifically practical, the degree of effectiveness usually depends on the specific photocage that is chosen for the given assay. Many examples of photocages are known and most differ in the various photorelease characteristics, such as optimal release wavelength, quantum yield, time required for photorelease and solubility. Ortho-nitrobenzyl (ONB) photocages are a class that has been widely explored due to the fact that they possess several ideal properties, including synthetic straightforwardness¹. A subset of this ONB class was employed in this investigation to study QS.

The specific goals of this experiment were to utilize a riboswitch, which is activated by a photocaged organic molecule (theophylline), to study QS in biofilms. The riboswitch controls production of a protein known as HapR, an important QS regulator in *V. cholera*^{5,6}. We were interested in caging theophylline with a certain ONB known as NPOM, which was developed as a cage for NH heterocycles that improved upon similar cages in regards to stability, decaging time, and the production of less toxic byproducts. A previous study has employed NPOM-caged theophylline to activate a ribozyme, and thus has provided a basis for a similar system to be used to photochemically control gene expression¹.

Results and Discussion

Development of the HapR-riboswitch construct. Initial attempts to set up the riboswitch with the other necessary components proved to be somewhat problematic. The riboswitch was first linked to a fluorescent protein, mKate, in *E. coli*. While this was

successful, the ultimate goal was to have a construct consisting of the riboswitch with mKate and HapR in *V. cholera*. Conjugating the plasmid containing the HapR riboswitch from *E. coli* to *V. cholera* was an issue, and as a result, initial assays were performed in the *E. coli* strain. Eventually, a *V. cholera* strain was produced that contained the desired construct (the riboswitch connected to HapR and mKate), and phenotypic data was produced for confirmation. The characteristic rugose morphology of the HapR strain is complemented when grown on plates containing theophylline, changing to a smooth morphology as a result of the expression of HapR. Having constructed the necessary bacterial strain, we focused our attention on developing a means of photochemical control for the riboswitch.

Analysis of NPOM-caged theophylline. Early trials involving the NPOM-caged theophylline produced promising results; the compound degraded as hoped and photorelease could indeed be monitored via fluorescence measurements. The compound, unfortunately, was only able to produce a modest increase in gene expression (4-5 fold) when tested in vitro. In comparison, free theophylline induced a 150-fold increase in gene expression. The level of response from the caged molecules most likely does not need to be this intense, and so we aimed for around a 20-fold increase. As we further assessed the NPOM-caged theophylline it was observed to be poorly soluble in polar solvents, specifically methanol (used to make stock solutions) and water (used in the LB media). The compound was only partially soluble at the working concentration (2 mM), and thus it was hypothesized that this lack of solubility was causing the caged theophylline to under-perform in the assay. Photorelease was tested in solution without cells and determined to occur to an appreciable extent, which supported the idea that aqueous

solubility was limiting the caged compound's ability to cause a significant biological response.

Discovery and evaluation of new photocages. To test this theory, several new photocages were prepared and linked to theophylline. Since the NPOM cage experienced poor solubility in polar solvents, these new cages were designed to contain some type of polar functionality. Since the ortho-nitro group is essential for photorelease, we decided to focus on the substituents on the other side of the ring. Initially, it was thought that changing the methylenedioxy group to a diol (a catechol derivative) would significantly increase polarity. This analog was ultimately abandoned due to synthetic difficulties, as it was determined that the cage could not contain any exposed nucleophiles in order to complete the last steps of the route. Following this revelation, three new photocages were successfully prepared, each derived from the NPOM starting material. Surprisingly, these derivatives all underwent decaging at 365 nm, and produced a range of both solubility and riboswitch activation. 2, theophylline caged by an ONB analog containing an ortho-methoxy-thiomethyl moiety, was found to have the lowest solubility of the four compounds prepared, and accordingly, caused the smallest increase of gene expression. In contrast, 4, another ONB analog that contained an ortho-di-diethyleneglycol-monomethyl ether group, was observed to be fully soluble in polar solvents at a range of concentrations, including the working concentration of the assay. Unfortunately, the fluorescence response level of this compound was not substantially different from that of the original NPOM-theophylline. Finally, an additional ONB cage was synthesized and linked to theophylline, containing an ortho-methoxy nitrile moiety (2). Similar to 4, this new nitrile compound also possessed improved aqueous solubility, being fully soluble at

2 mM. On the other hand, this molecule was found to have unique photorelease properties, producing a biological response that was nearly quadruple that of NPOM-theophylline, after one minute of irradiation. Since the highly polar diethyleneglycol derivative did not perform well in vitro, it can be assumed that solubility does not entirely explain the high response level in 2. Instead, the electronic effect of the nitrile on the decaging process is likely to play an important role as well.

Chemistry

Synthesis of NPOM-theophylline was based of a previously published route to NPOM-Cl, with minor adjustments. Rather than starting with the nitrated secondary alcohol substrate, which was fairly expensive (>\$100/g), we choose start a few steps prior, with 3',4'-(Methylenedioxy)acetophenone, which is significantly cheaper. Nitration at the desired position ortho to the ketone was achieved in 74% yield. Although selectivity was a concern, no other regioisomers were isolated after purification. Reduction of the ketone to the secondary alcohol via sodium borohydride proceeded either very well or poorly, depending on the batch of NaBH₄ that was used. Ultimately it was concluded that the reaction would give all product if one had access to fresh sodium borohydride. Converting the alcohol to the chloro-acetal proved to be somewhat troublesome. Initial attempts focused on obtaining the desired intermediate in one step from the alcohol, using paraformaldehyde and TMSCl. After a couple failed trials, this transformation was performed via a two step procedure, first converting the alcohol to a O, S-acetal (using a MTM ether protecting group), and then reacting this O, S-acetal with sulfuryl chloride to obtain the chloro-acetal. Finally, theophylline was reacted with NaH

in order to facilitate the S_N2 reaction with NPOM-Cl, which typically proceeded very smoothly.

Analogs of NPOM were prepared using NPOM (or one of its precursors) as a starting material, keeping the ONB core consistent. Initial efforts focused on cleaving the methylenedioxy group to the diol, forming a catechol derivative. After several failed attempts using BBr_3 , we switched focuses to making the ortho-methoxy phenol. While this compound was indeed obtained, it was discovered that the sulfonyl chloride step of the route did not tolerate any exposed nucleophiles, as sulfonyl esters/amides formed preferentially to the S, O-acetal reacting to give the desired chloro-acetal. Accordingly, other NPOM analogs were designed and prepared that did not possess any exposed nucleophiles, yet still maintained the desired photorelease characteristics. Performing nucleophilic aromatic substitution on NPOM, three new analogs were synthesized using either, sodium cyanide, sodium methoxide or the alkoxide salt of diethyleneglycol monomethylether. Interestingly, it found that S_NAr occurred selectively at the position para to the nitro group. The resulting free phenol that was produced in each case was functionalized with either a methyl group or another diethyleneglycol monomethylether chain.

Conclusion

Based off of precedent for the activation of a ribozyme using NPOM-caged theophylline, a similar study was performed. The previous paper was expanded upon by using the concept to photochemically control gene expression in a *V. cholera* strain consisting of a riboswitch connected to a QS master regulator, HapR, and a fluorescent protein, mKate. In addition to developing novel biological methods, several new

photocages were prepared based off of the common NPOM cage, some of which improved upon solubility as well as in vitro photorelease. These new cages are likely to be useful in other studies that utilize NPOM-caged compounds, or ONB cages in general, although they are not completely synthetically straightforward to make. Current goals include a more detailed investigation into QS in biofilms (specifically in *V. cholera* HapR) using the photochemical approach described here. Meanwhile, additional nitrile-containing ONB caging groups are being developed and will be assessed, as the presence of that functional group appears to have a positive effect on the decaging process.

Experimental Section

General chemistry

1-(6-nitrobenzo[*d*][1,3]dioxol-5-yl)ethanone. 3,4-methylenedioxyacetophenone (750 mg, 4.57 mmol) was dissolved in TFA (6.75 ml, 0.67 M) and the solution was cooled to 0 °C. Sodium nitrite (946 mg, 13.71 mmol) was added portion wise (in 3 portions, CAUTION: very exothermic, reaction foams up significantly after third addition of NaNO₂). The mixture stirred at room temperature for 4 h and then was quenched with water (50 mL). Product was extracted with EtOAc (25 mL x 3) and the combined organic layers were washed with sat. NaHCO₃ and brine, and then dried with Na₂SO₄. Purification via silica-gel flash chromatography (product elutes around 30% EtOAc) afforded 649 mg of the desired product, 68% yield.

1-(6-nitrobenzo[*d*][1,3]dioxol-5-yl)ethanol. To 1-(6-nitrobenzo[*d*][1,3]dioxol-5-yl)ethanone (350 mg, 1.67 mmol) in a mixture of ethanol and THF (1:1, 18 mL total, 0.1 M) was added NaBH₄ (69.5 mg, 1.84 mmol). The reaction stirred overnight at room

temperature and then HCl was added (5 mL, 1 M). After removal of solvent in vacuo, the residue was dissolved in EtOAc, washed with brine and dried over Na₂SO₄. Purification via silica-gel flash chromatography (product elutes around 30% EtOAc) afforded 342 mg of the desired alcohol, 97% yield.

5-(1-((methylthio)methoxy)ethyl)-6-nitrobenzo[*d*][1,3]dioxole. To 1-(6-nitrobenzo[*d*][1,3]dioxol-5-yl)ethanol (224 mg, 1.06 mmol) dissolved in acetic acid (2.5 mL, 42.43 mmol) was added DMSO (1.51 mL, 21.22 mmol), followed by acetic anhydride (2.0 mL, 21.22 mmol) dropwise. The reaction stirred at room temperature for 72 h. Sat. NaHCO₃ (50 mL) was added dropwise and the mixture was then extracted with EtOAc (25 mL x 3). The combined organic layers were washed with brine and dried over Na₂SO₄. Purification via silica-gel flash chromatography (product elutes around 25% EtOAc) afforded 240 mg of the desired alcohol, 83% yield.

5-(1-(chloromethoxy)ethyl)-6-nitrobenzo[*d*][1,3]dioxole. 5-(1-((methylthio)methoxy)ethyl)-6-nitrobenzo[*d*][1,3]dioxole (240 mg, 0.885 mmol) was dissolved in DCM (6 mL, 0.15 M) and the solution was cooled to 0 °C. Sulfuryl chloride (0.07 mL, 0.885 mmol) was added dropwise and the reaction stirred at 0 °C for 1 h. Solvent was removed in vacuo, and the product was used crude in the subsequent reaction, without a workup or purification.

2-hydroxy-5-(1-hydroxyethyl)-4-nitrobenzotrile. To 1-(6-nitrobenzo[*d*][1,3]dioxol-5-yl)ethanol (116 mg, 0.549 mmol) in HMPA (1.1 mL, 0.5 M) was added NaCN (27 mg, 0.549 mmol). The reaction stirred at 150 °C for 3 min and then three additional portions of NaCN was added (0.275 mmol x 3) every 5 minutes. After

stirring an additional 10 minutes at 150 °C, the reaction was quenched with water and NaOH. The product was extracted with EtOAc (25 mL x 3) and the combined organic layers were washed with brine and dried on Na₂SO₄. Purification via silica-gel flash chromatography (product elutes around 95% EtOAc) afforded 30 mg of the desired diol, 26% yield.

5-(1-((*tert*-butyldimethylsilyl)oxy)ethyl)-2-hydroxy-4-nitrobenzonitrile. 2-hydroxy-5-(1-hydroxyethyl)-4-nitrobenzonitrile (272 mg, 1.31 mmol) was dissolved in DCM (13 mL, 0.1 M) and cooled to 0 °C. Triethylamine (0.27 mL, 1.97 mmol) was added followed by TBSCl (196 mg, 1.31 mmol) and DMAP (cat.). The mixture was allowed to warm to room temperature as it stirred overnight. Additional DCM (50 mL) was added and the mixture was washed with HCl (25 mL, 1.0 M) and brine, and then was dried over Na₂SO₄. Purification via silica-gel flash chromatography (product elutes around 15% EtOAc) afforded 300 mg of the desired phenol, 71% yield.

5-(1-hydroxyethyl)-2-methoxy-4-nitrobenzonitrile. Prepared using the procedure described for 2-methoxy-5-(1-((methylthio)methoxy)ethyl)-4-nitrobenzonitrile, using the corresponding phenol derivative.

2-hydroxy-5-(1-((methylthio)methoxy)ethyl)-4-nitrobenzonitrile. To 5-(1-((methylthio)methoxy)ethyl)-6-nitrobenzo[*d*][1,3]dioxole (283 mg, 1.05 mmol) in HMPA (2.1 mL, 0.5 M) was added NaCN (51.5 mg, 1.05 mmol). The reaction stirred at 150 °C for 3 min and then three additional portions of NaCN was added (0.502 mmol x 3) every 5 minutes. After stirring an additional 10 minutes at 150 °C, the reaction was quenched with water and NaOH. The product was extracted with EtOAc (25 mL x 3) and the

combined organic layers were washed with brine and dried on Na₂SO₄. Purification via silica-gel flash chromatography (product elutes around 55% EtOAc) afforded 51 mg of the desired phenol, 17% yield.

2-methoxy-5-(1-((methylthio)methoxy)ethyl)-4-nitrobenzonitrile. To 2-hydroxy-5-(1-((methylthio)methoxy)ethyl)-4-nitrobenzonitrile (51 mg, 0.181 mmol) in DMF (2 mL, 0.1 M) was added K₂CO₃ (50 mg, 0.362 mmol) and methyl iodide (0.02 mL, 0.362 mmol). The mixture stirred at room temperature overnight, and then the reaction was quenched with water. The product was extracted with EtOAc (25 mL x 3), and the combined organic layers were washed with brine (50 mL x 3).

5-(1-(chloromethoxy)ethyl)-2-methoxy-4-nitrobenzonitrile. Prepared using the procedure described for 5-(1-(chloromethoxy)ethyl)-6-nitrobenzo[*d*][1,3]dioxole, using the corresponding MTM ether derivative.

2-(methylthio)-4-(1-((methylthio)methoxy)ethyl)-5-nitrophenol. To 5-(1-((methylthio)methoxy)ethyl)-6-nitrobenzo[*d*][1,3]dioxole (283 mg, 1.05 mmol) in HMPA (2.1 mL, 0.5 M) was added NaCN (51.5 mg, 1.05 mmol). The reaction stirred at 150 °C for 3 min and then three additional portions of NaCN was added (0.502 mmol x 3) every 5 minutes. After stirring an additional 10 minutes at 150 °C, the reaction was quenched with water and NaOH. The product was extracted with EtOAc (25 mL x 3) and the combined organic layers were washed with brine and dried on Na₂SO₄. Purification via silica-gel flash chromatography (product elutes around 45% EtOAc) afforded 65 mg of the desired phenol, 20% yield.

(2-methoxy-5-(1-((methylthio)methoxy)ethyl)-4-nitrophenyl)(methyl)sulfane.

Prepared using the procedure described for 2-methoxy-5-(1-((methylthio)methoxy)ethyl)-4-nitrobenzotrile, using the corresponding phenol derivative.

(5-(1-(chloromethoxy)ethyl)-2-methoxy-4-nitrophenyl)(methyl)sulfane.

Prepared using the procedure described for 5-(1-(chloromethoxy)ethyl)-6-nitrobenzo[*d*][1,3]dioxole, using the corresponding MTM ether derivative.

4-(1-hydroxyethyl)-2-(2-(2-methoxyethoxy)ethoxy)-5-nitrophenol. To

diethylene glycol monomethylether (0.28 mL, 2.38 mmol) in DMSO (1.5 mL, 0.5 M) was added NaH (114 mg, 2.86 mmol) in two portions. The mixture was stirred at 150 °C for 20 min and then 5-(1-((methylthio)methoxy)ethyl)-6-nitrobenzo[*d*][1,3]dioxole (323 mg, 1.191 mmol) was added dropwise (in 1 mL DMSO). After stirring at 150 °C for an additional 15 min, the mixture was cooled to room temperature and quenched with water and 1 M HCl. The product was extracted with EtOAc (30 mL x 3) and then the combined organic layers were washed with NaHCO₃ and brine (x 2), and then dried over Na₂SO₄, affording 326 mg of the desired phenol, 90% yield.

4-(1-((*tert*-butyldimethylsilyl)oxy)ethyl)-2-(2-(2-methoxyethoxy)ethoxy)-5-

nitrophenol. Prepared using the procedure described for 5-(1-((*tert*-butyldimethylsilyl)oxy)ethyl)-2-hydroxy-4-nitrobenzotrile, using the diol derivative. Purification via silica-gel flash chromatography (product elutes around 15% EtOAc) afforded 179.4 mg of the desired phenol, 40% yield.

2-(2-methoxyethoxy)ethyl 4-methylbenzenesulfonate. Solid NaOH (0.583 g,

14.56 mmol) was dissolved in water (2.91 mL) and the solution was chilled to 0 °C.

Diethyleneglycol monomethylether (500 mg, 0.489 mL, 4.16 mmol) was added dropwise (in 1.25 mL THF), followed by tosyl chloride (0.952 g, 4.994 mmol) also dropwise, in 2.9 mL THF. The mixture stirred overnight at room temperature and then the solvent was removed in vacuo. EtOAc (50 mL) was added and the mixture was washed with 1 M NaOH and then brine. After drying over Na₂SO₄ the product was used crude in the subsequent step.

1-(4,5-bis(2-(2-methoxyethoxy)ethoxy)-2-nitrophenyl)ethanol. A solution of 2-(2-methoxyethoxy)ethyl 4-methylbenzenesulfonate (85 mg, 0.3084 mmol) in 2 mL ACN was added to a mixture of 4-(1-((*tert*-butyldimethylsilyl)oxy)ethyl)-2-(2-(2-methoxyethoxy)ethoxy)-5-nitrophenol (106.6 mg, 0.257 mmol) and K₂CO₃ (43 mg, 0.384 mmol) in 3.2 mL ACN. The reaction was refluxed at 70 °C overnight and then was concentrated to dryness. EtOAc (50 mL) was added and then the mixture was washed with sat. NaHCO₃ and then brine. Drying over Na₂SO₄ and concentration in vacuo afforded 122.2 mg of the desired product, which was used crude without purification.

((1-(4,5-bis(2-(2-methoxyethoxy)ethoxy)-2-nitrophenyl)ethoxy)methyl)(methyl)sulfane. Prepared using the procedure described for 5-(1-((methylthio)methoxy)ethyl)-6-nitrobenzo[*d*][1,3]dioxole, using the corresponding alcohol derivative.

1-(1-(chloromethoxy)ethyl)-4,5-bis(2-(2-methoxyethoxy)ethoxy)-2-nitrobenzene. Prepared using the procedure described for 5-(1-(chloromethoxy)ethyl)-6-nitrobenzo[*d*][1,3]dioxole, using the corresponding MTM ether derivative.

1,3-dimethyl-7-((1-(6-nitrobenzo[*d*][1,3]dioxol-5-yl)ethoxy)methyl)-1*H*-purine-2,6(3*H*,7*H*)-dione. NaH (25.5 mg, 1.062 mmol) was added (in two portions) to theophylline (160 mg, 0.885 mmol) in DMF (3 mL) and the mixture stirred at room temperature for 45 min. 5-(1-(chloromethoxy)ethyl)-6-nitrobenzo[*d*][1,3]dioxole (229 mg, 0.885 mmol) was dissolved in DMF (1.5 mL) and added dropwise to the stirring mixture, and then the reaction continued stirring for 1.5 h at room temperature. EtOAc (50 mL) was added and the mixture was washed with sat. NaHCO₃ and brine (30 mL x 3). After drying over Na₂SO₄ the product was purified via alumina flash chromatography, eluting after 75% EtOAc. ¹H NMR (400 MHz, CDCl₃) δ 7.65 (s, 1H), 7.41 (s, 1H), 7.02 (s, 1H), 6.07 (s, 2H), 5.63 (s, 2H), 5.35 (q, *J* = 6.3 Hz, 1H), 3.54 (s, 3H), 3.37 (s, 3H), 1.48 (d, *J* = 6.3 Hz, 3H). ¹³C NMR (101 MHz, CDCl₃) δ 155.12, 152.27, 151.58, 148.69, 147.19, 141.97, 141.75, 136.52, 106.18, 106.14, 105.00, 103.16, 74.25, 73.32, 29.94, 28.16, 23.75.

7-((1-(4-methoxy-5-(methylthio)-2-nitrophenyl)ethoxy)methyl)-1,3-dimethyl-1*H*-purine-2,6(3*H*,7*H*)-dione. Prepared using the procedure described for 1,3-dimethyl-7-((1-(6-nitrobenzo[*d*][1,3]dioxol-5-yl)ethoxy)methyl)-1*H*-purine-2,6(3*H*,7*H*)-dione, using the corresponding chloro-acetal derivative. ¹H NMR (400 MHz, CDCl₃) δ 7.64 (s, 1H), 7.30 (s, 1H), 7.02 (s, 1H), 5.74, 5.63 (ABq, *J*_{AB} = 11.2 Hz, 2H), 5.44 (q, 1H), 3.89 (s, 3H), 3.49 (s, 3H), 3.33 (s, 3H), 2.40 (s, 3H), 1.53 (d, *J* = 6.4 Hz, 3H). ¹³C NMR (101 MHz, CDCl₃) δ 155.07, 154.18, 151.39, 148.52, 143.95, 141.53, 137.20, 132.79, 121.11, 121.08, 104.32, 75.18, 74.81, 56.50, 29.84, 28.03, 24.05, 13.88.

5-(1-((1,3-dimethyl-2,6-dioxo-2,3-dihydro-1*H*-purin-7(6*H*)-yl)methoxy)ethyl)-2-methoxy-4-nitrobenzotrile. Prepared using the procedure described for 1,3-

dimethyl-7-((1-(6-nitrobenzo[*d*][1,3]dioxol-5-yl)ethoxy)methyl)-1*H*-purine-2,6(3*H*,7*H*)-dione, using the corresponding chloro-acetal derivative. ¹H NMR (400 MHz, CDCl₃) δ 7.83 (s, 1H), 7.73 (s, 1H), 7.49 (s, 1H), 5.63, 5.59 (ABq, *J*_{AB} = 11.2 Hz, 2H), 5.25 (q, *J* = 6.3 Hz, 1H), 4.00 (s, 3H), 3.56 (s, 3H), 3.35 (s, 3H), 1.49 (d, *J* = 6.3 Hz, 3H). ¹³C NMR (101 MHz, CDCl₃) δ 160.33, 155.27, 151.44, 150.90, 148.74, 142.11, 133.50, 131.89, 114.31, 107.12, 106.98, 106.66, 73.73, 72.48, 57.08, 29.95, 28.10, 23.82.

7-((1-(4,5-bis(2-(2-methoxyethoxy)ethoxy)-2-nitrophenyl)ethoxy)methyl)-1,3-dimethyl-1*H*-purine-2,6(3*H*,7*H*)-dione. Prepared using the procedure described for 1,3-dimethyl-7-((1-(6-nitrobenzo[*d*][1,3]dioxol-5-yl)ethoxy)methyl)-1*H*-purine-2,6(3*H*,7*H*)-dione, using the corresponding chloro-acetal derivative. ¹H NMR (400 MHz, CDCl₃) δ 7.66 (s, 1H), 7.51 (s, 1H), 6.96 (s, 1H), 5.71, 5.55 (ABq, *J*_{AB} = 11.0 Hz, 2H), 5.44 (q, *J* = 6.2 Hz, 1H), 4.26 – 4.11 (m, 4H), 3.93 – 3.84 (m, 4H), 3.76 – 3.69 (m, 4H), 3.60 – 3.53 (m, 4H), 3.51 (s, 3H), 3.38 (s, 6H), 3.33 (s, 3H), 1.48 (d, *J* = 6.3 Hz, 3H). ¹³C NMR (101 MHz, CDCl₃) δ 155.04, 153.36, 151.48, 148.61, 147.50, 141.77, 140.13, 134.30, 109.78, 109.75, 109.29, 74.58, 73.86, 72.06, 70.98, 69.53, 69.41, 69.15, 68.83, 59.17, 29.82, 28.05, 23.80.

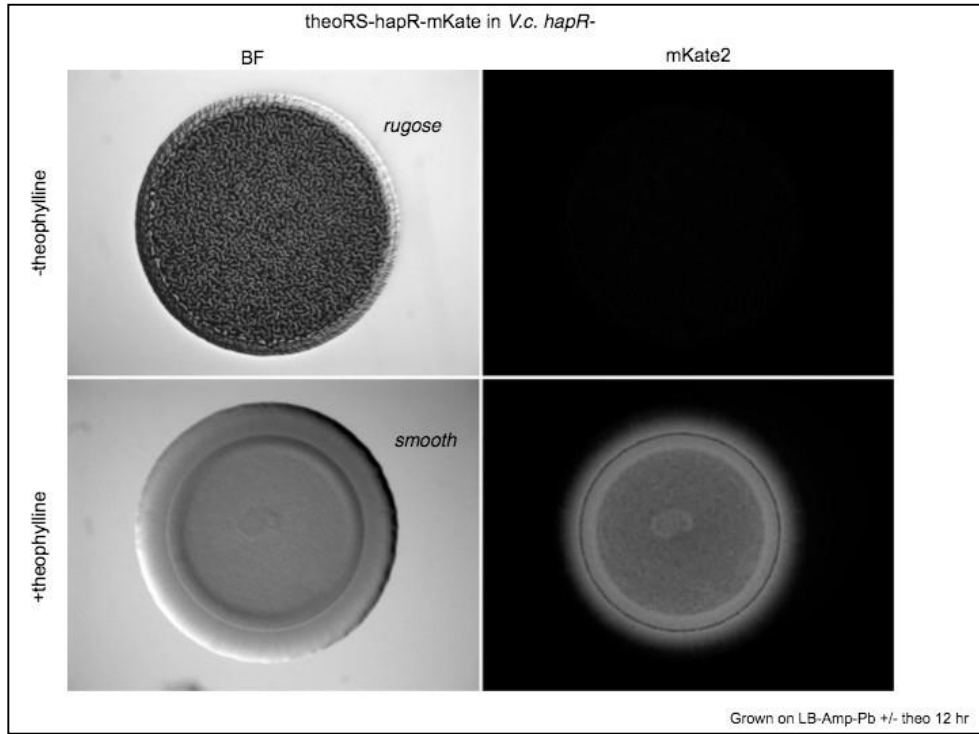


Figure 13. TheoRS-hapR-mKate construct in *V.c.*

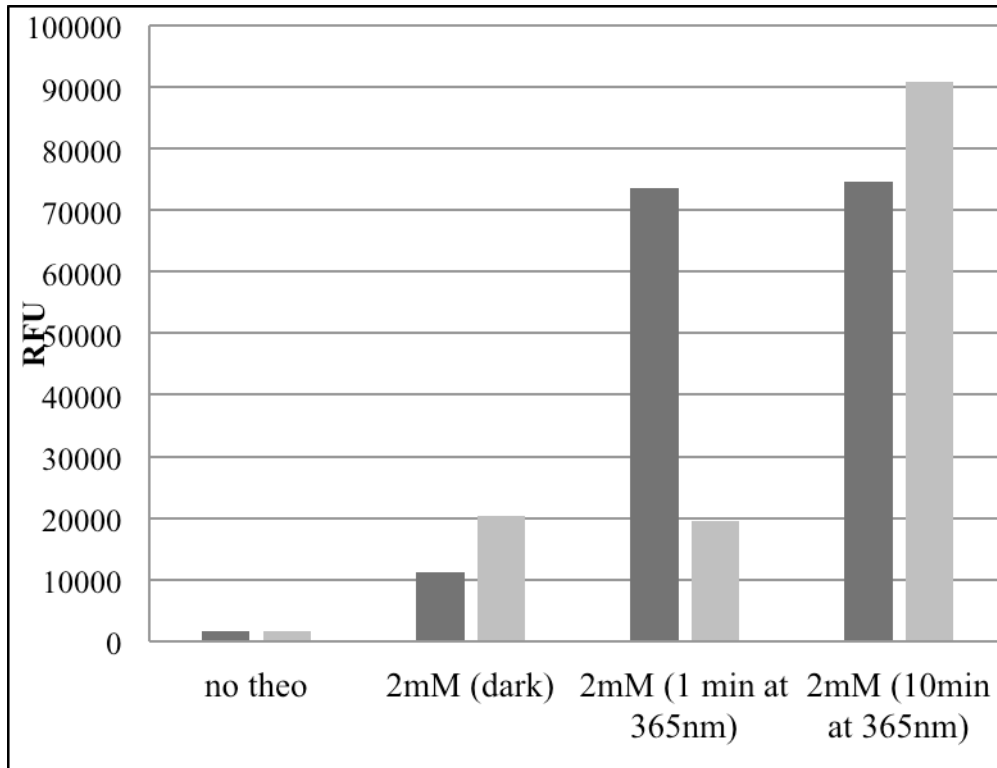


Figure 14. Photolysis of new nitrile photocage

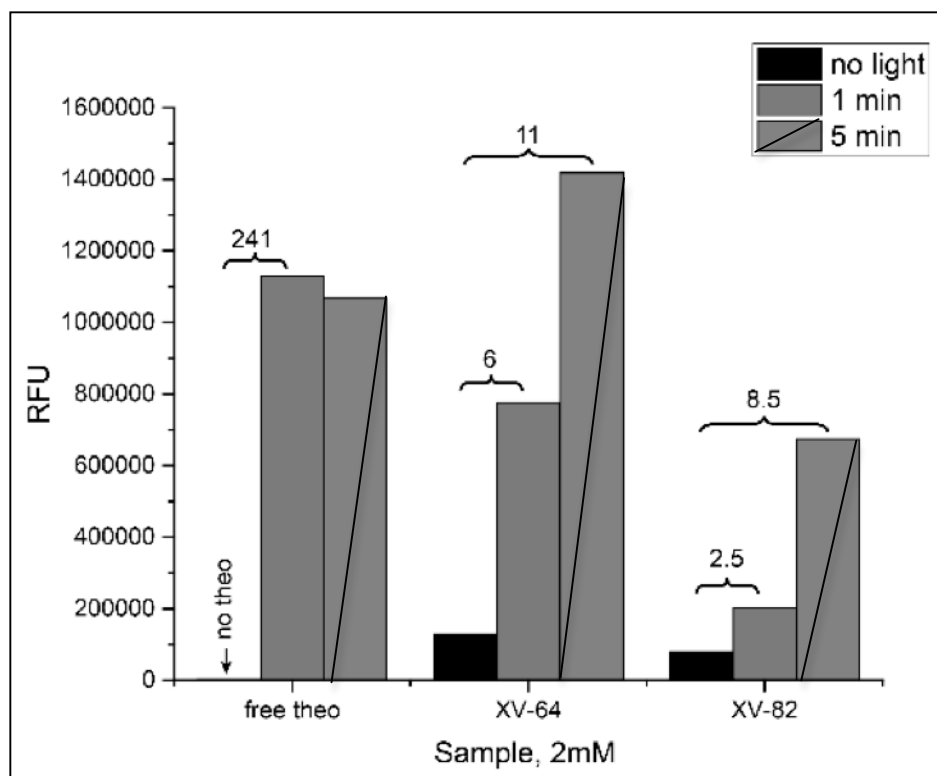


Figure 15. Photolysis of bis-PEG analog

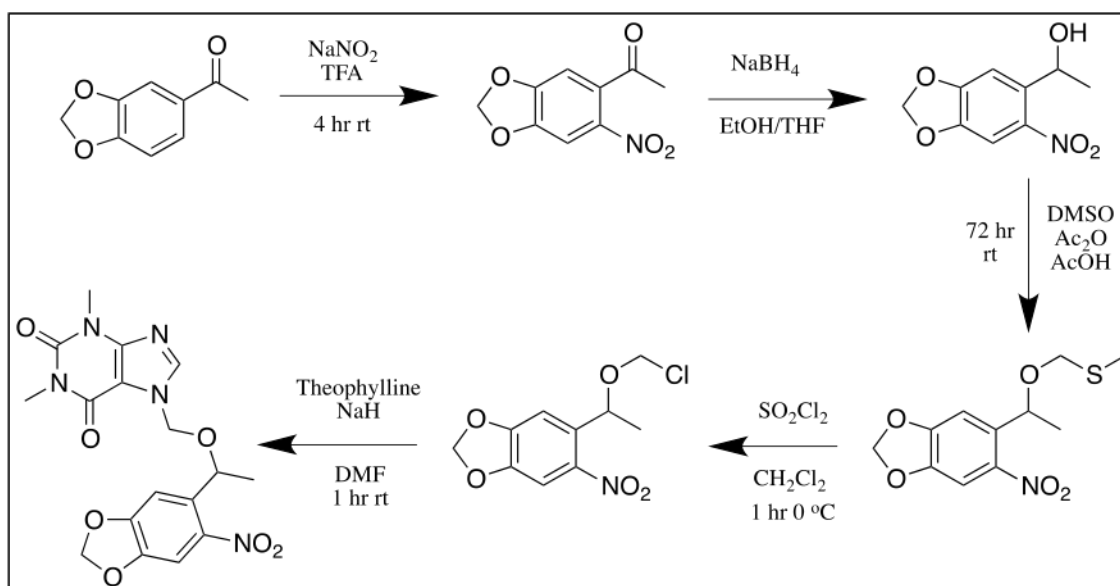
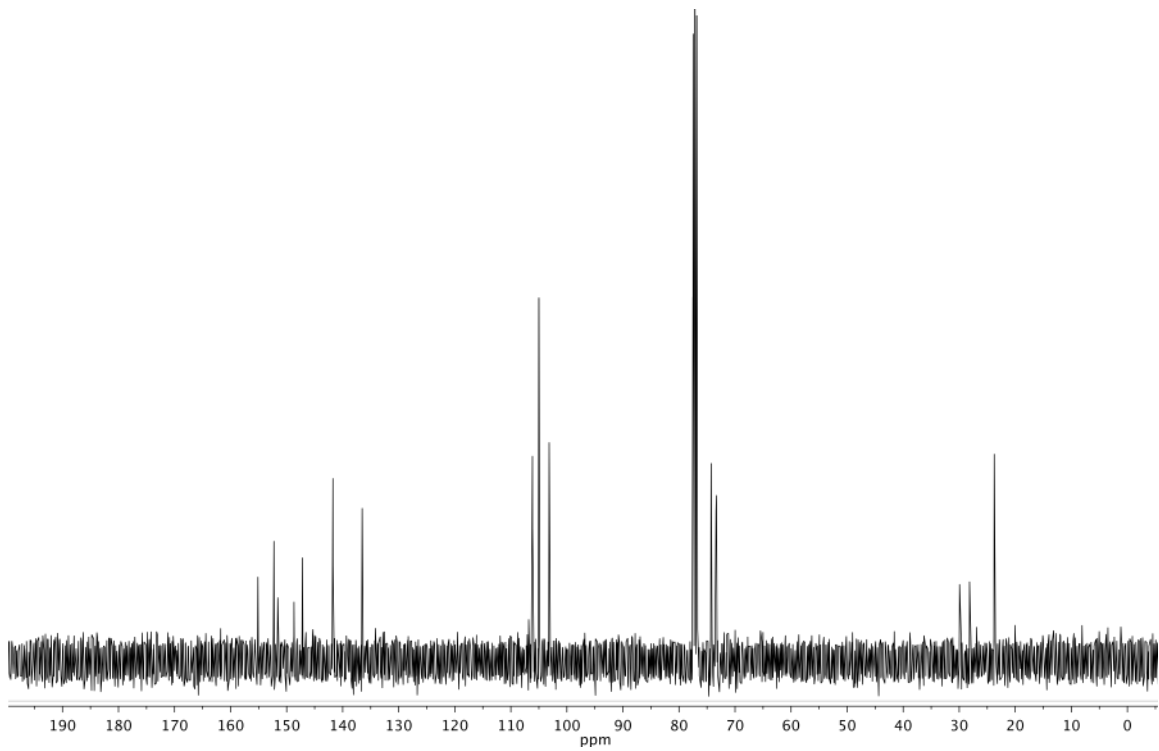
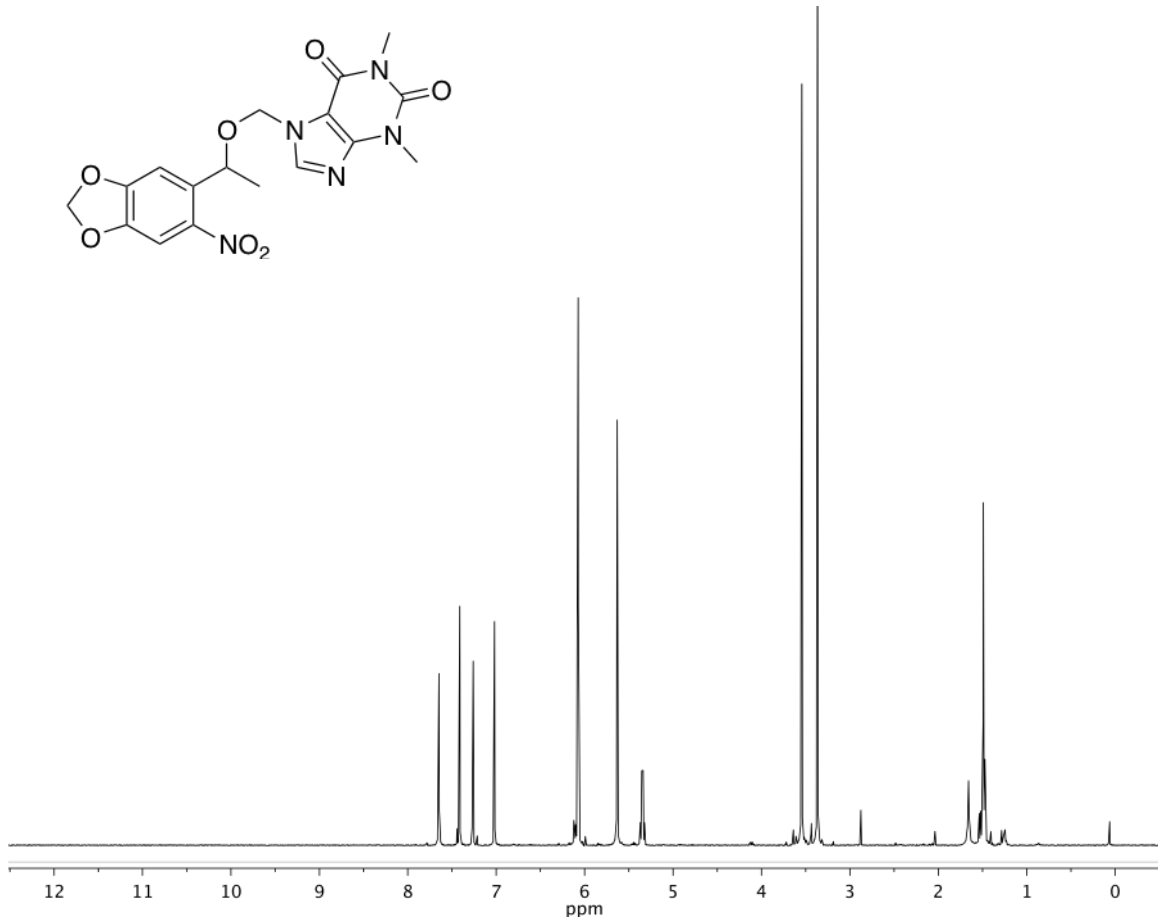
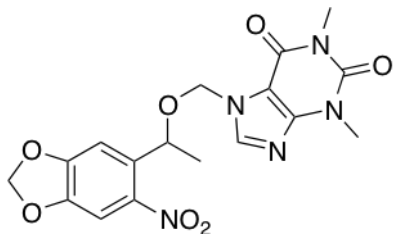
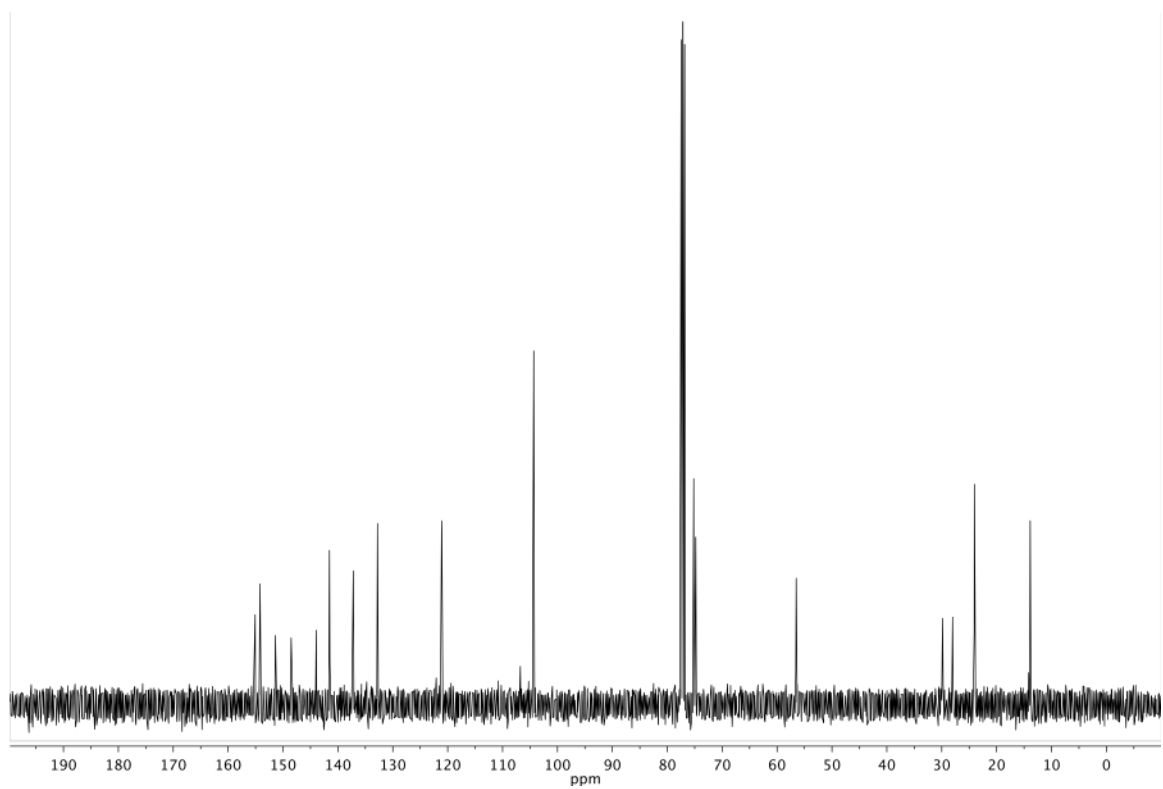
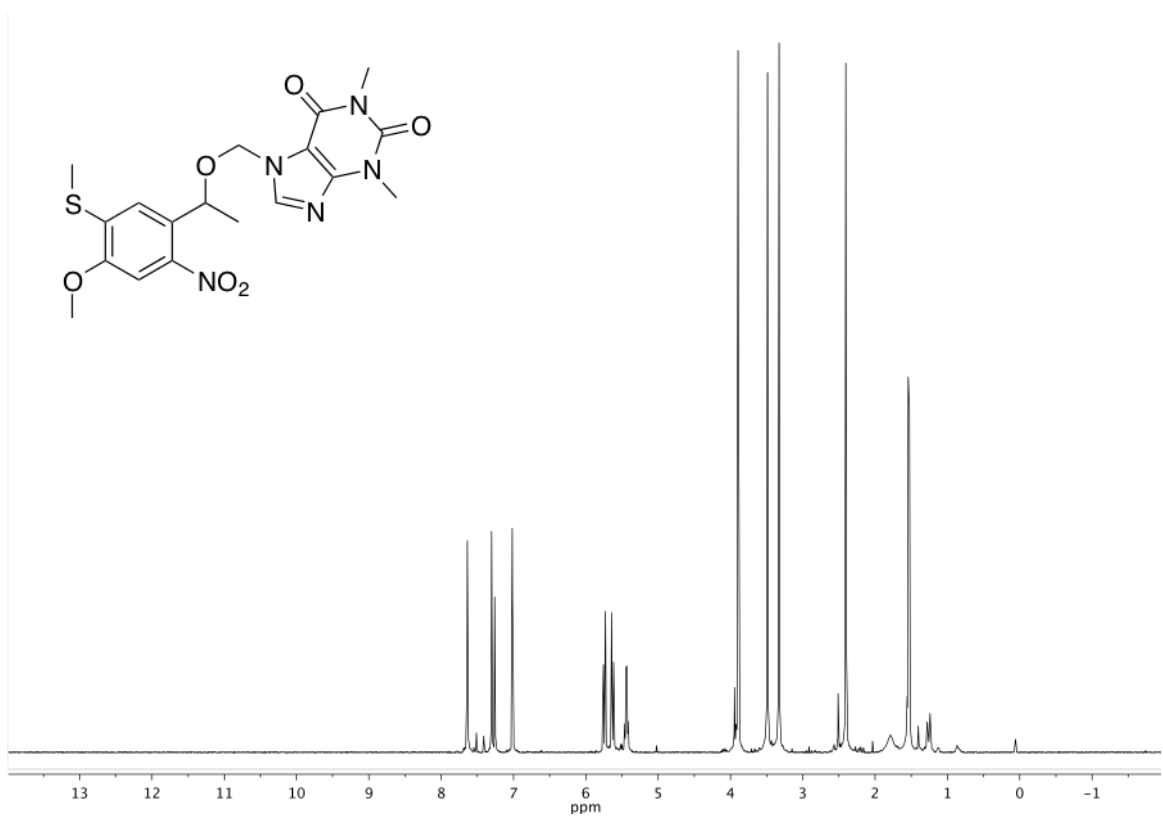
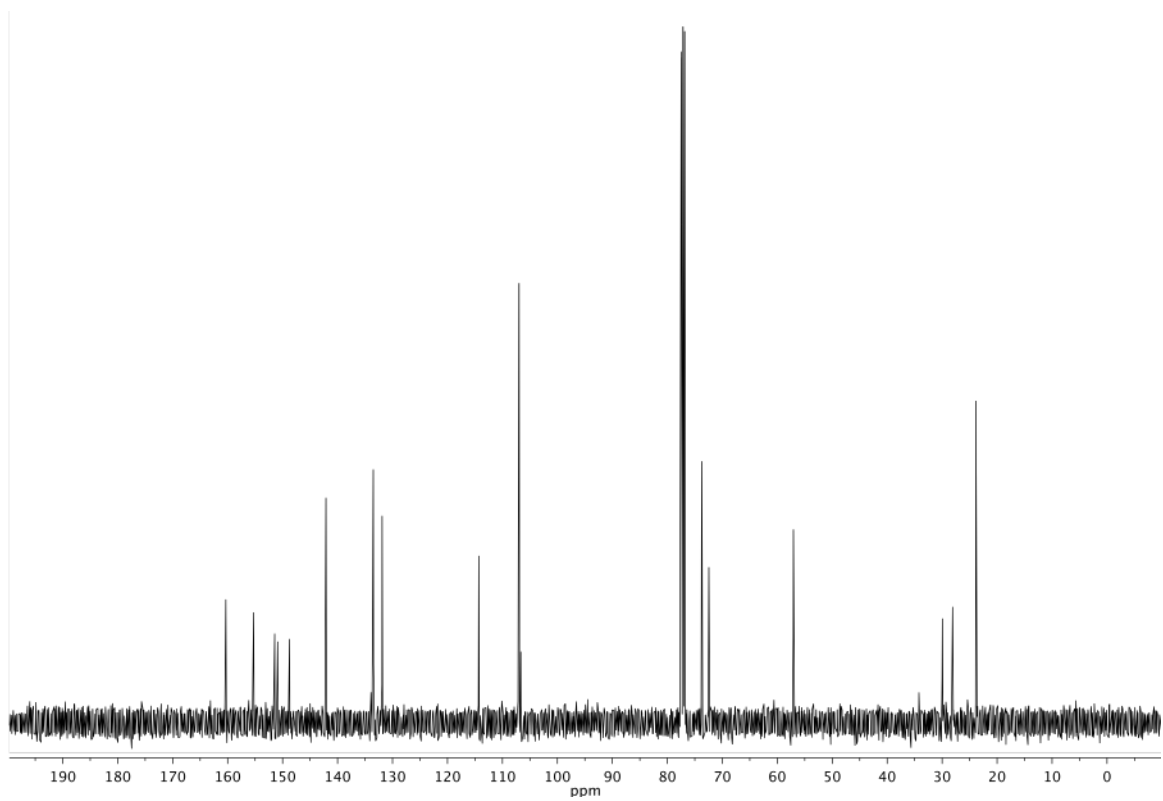
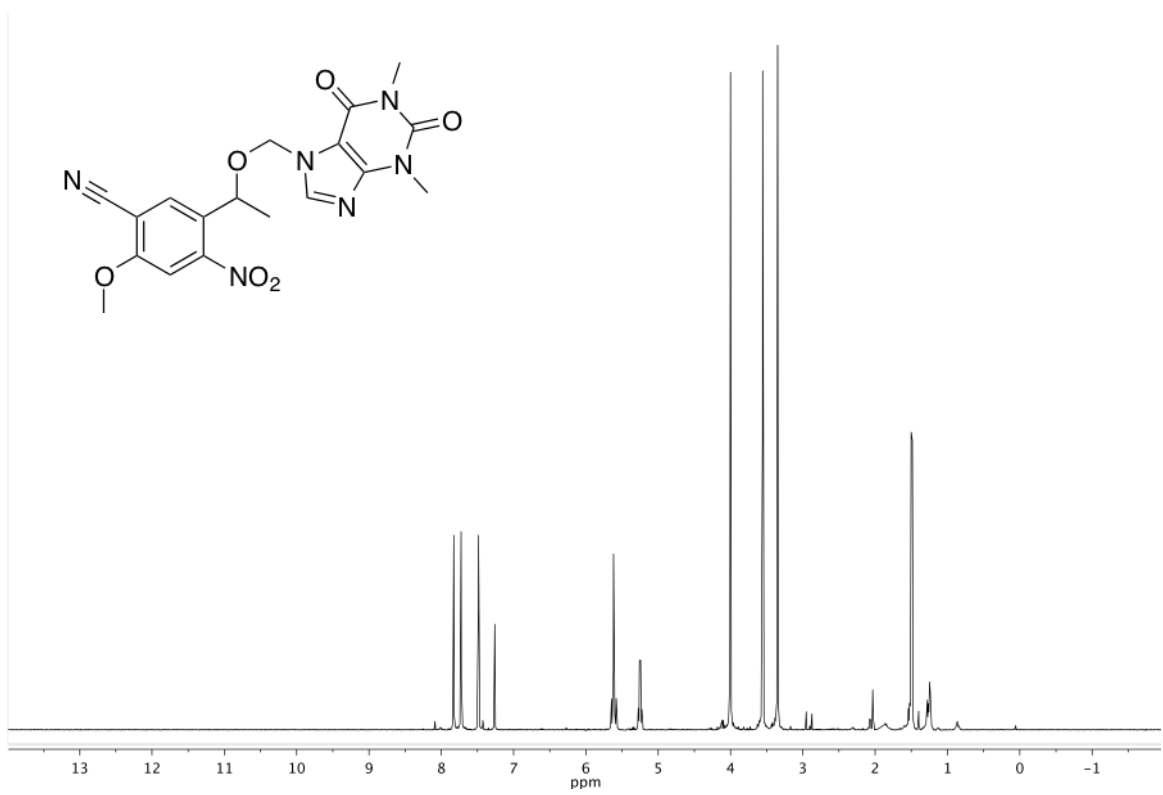
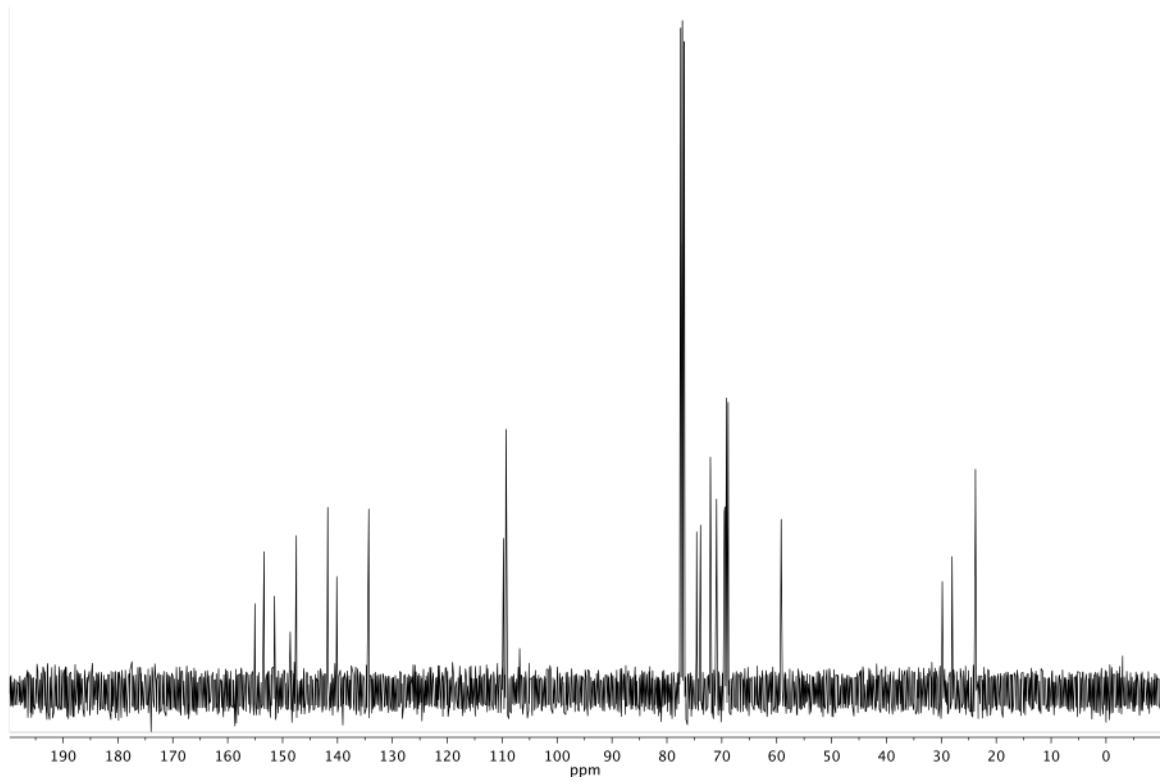
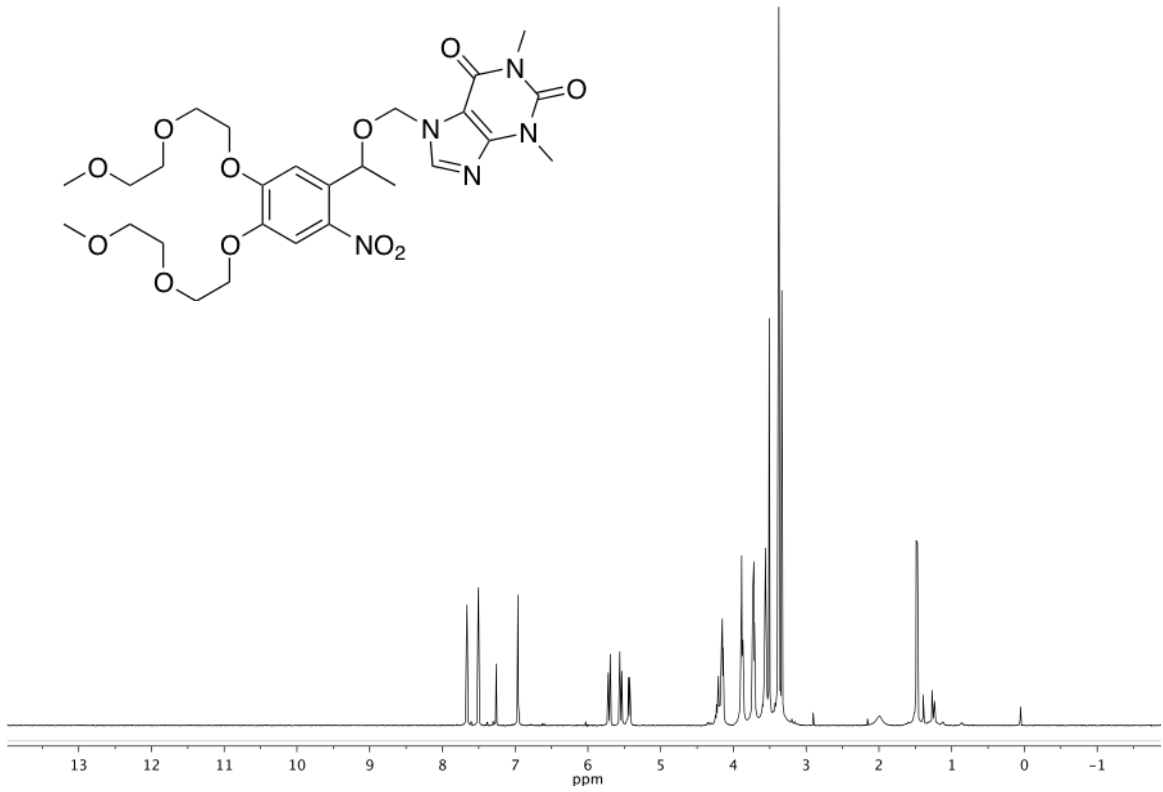
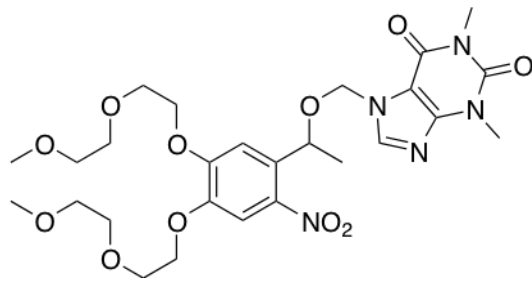


Figure 16. Synthesis of caged-theophylline









Chapter 3

Gem-dinitro enols: Discovery and application of a new reaction for methyl ketones

Introduction

Due to the promising results of the nitrile-containing ONB photocage, additional efforts were focused on optimizing the synthesis of this compound. The original synthetic route employed a nucleophilic aromatic substitution on 1-(6-nitrobenzo[*d*][1,3]dioxol-5-yl)ethanol and suffered from a low yield (<30%) and a difficult workup/purification. Accordingly, a new substrate was identified and purchased in an attempt to improve both the yield and overall efficiency of the route. This starting material, 1-(3-fluoro-4-methoxyphenyl)ethanone, was superior in regard to possessing a better leaving group, being a fluorine atom rather than a methylene dioxy group, and also already had the methoxy substituent that was required for the final compound, thus eliminating the methylation of the phenol step.

A major assumption that this new substrate depended on was that the first step of the route, an aromatic nitration, would be selective and high yielding to the extent that it was for the original methylene dioxy substrate. Upon performing a nitration on the fluoro substrate however, it was observed that nitration of the ring did not occur. While all three aromatic hydrogen atoms were accounted for by H^1 NMR, the hydrogens on the alpha carbon of the methyl ketone were absent. At this point in time this unknown product was assumed to be the carboxylic acid, although this idea was not fully consistent with the polarity and solubility of this compound, which seemed to be much less polar than the acid would likely be.

Several reactions and publications were identified after an in-depth search for similar types of C-C bond cleavage reactions. The haloform reaction was discovered by Adolf Lieben in 1870, although its history goes back a bit further to 1822¹. Employing successive halogenation of an alpha carbon under basic conditions, the reaction is used to produce carboxylic acids from methyl ketones, with a trihalomethane serving as a leaving group. Similar to this, for our reaction we envisioned nitration of an alpha carbon resulting with either mono/di/tri-nitromethane acting as a leaving group. Some precedent exists for the transformation of mono alpha-nitro methyl ketones into esters and amides from Sarma et al and Ballini et al^{2,3}. After review of these publications, it seemed unlikely that the mechanism of our reaction proceeded through the same mono-nitro ketone intermediate, due to differences in conditions and substrate scope. An additional paper was found regarding the conversion of methyl ketones in esters via an oxidative mechanism using CuO₂ that provided another example of this type of reaction, but also likely differs in mechanism from ours⁴.

Results and Discussion

Isolation of key intermediates leads to the elucidation of the reaction mechanism. A key possibility that was being explored in regard to mechanism included mono, di and tri nitration of the alpha carbon, leading to mono, di or tri-nitro methane serving as the leaving group. While precedent existed for the conversion of alpha mono-nitro ketones to amides, the conditions for this reaction were significantly different and harsher than those for our reaction. Additionally, these alpha mono-nitro ketones were commercially available and thus stable enough to isolate. Through dozens of reactions and purifications, I had not isolated or observed any of these compounds, which are easily identified by a singlet around 5-6 ppm in H¹ NMR. In the case of alpha gem-di and

tri-nitro ketones, little to no precedent exists in the literature which gave us doubts that either of these were the intermediate that we have been looking for.

During the course of exploring the nucleophile substrate scope for para-bromo acetophenone, an unknown molecule was obtained from a purification as a minor byproduct, although in high purity. This compound looked like the corresponding carboxylic acid by H^1 NMR, having the four hydrogen atoms in the aromatic ring but lacking the three hydrogens of the methyl. A C^{13} NMR, on the other hand, suggested that this mystery product was not the carboxylic acid, as it did indeed still have the carbon of the methyl (in addition to the carbonyl carbon). Based off of the specific locations of the peaks in the C^{13} NMR it was determined that this sample was the gem-di nitro intermediate that was previously hypothesized. Given both the H^1 and C^{13} NMR data, it appears that this ketone derivative exists entirely in the enol form. This idea is consistent with the lack of one hydrogen in the H^1 NMR and the location of the carbonyl carbon in the C^{13} NMR, being around 180 ppm rather than 200.

To further demonstrate that this compound was in fact the gem-di nitro enol and also a competent intermediate, I subjected the molecule to a reaction with an amine in attempt to produce an amide. Surprisingly, two distinct products were isolated after a purification in similar amounts, both of which could be characterized by NMR. As we had hoped, the desired amide product was indeed isolated, providing support for the proposed intermediate. The other isolated product strongly resembled the amide product by H^1 NMR, with the exception that the two sets of doublets (arising from the 1,4-disubstituted benzene ring) were shifted to a much higher ppm. C^{13} NMR spectra for this unknown product did not have a carbonyl or enol peak present, but did have two peaks

around 150 ppm (one of which belonging to the carbon of the dinitromethane). This shift is consistent with an enamine carbon, which in fact is a plausible secondary intermediate that could form after the gem-dinitro enol reacts with an NH-nucleophile. Similarly in the case of the enol, the enamine tautomer seems to be preferred over the imine when the alpha carbon is dinitro substituted.

While we did not necessarily expect to be able to isolate and purify intermediates of this type, this breakthrough does suggest that these gem-dinitro enols and enamines are stable to some degree. Still, more work needs to be done in order to obtain a more complete understanding of the stability and reactivity of these currently unreported intermediates.

Nucleophile substrate scope is wide-ranging. The first nucleophile tested in the reaction was hydroxide, thus generating a carboxylic acid from 4-bromoacetophenone. Due to the inherent difficulties in isolating and purifying acids, I shifted my focus on attempting to produce the methyl ester of 4-bromoacetophenone (using methanol rather than hydroxide as the nucleophile). This reaction proceeded smoothly, providing a product that was both easier to isolate and purify than the carboxylic acid, and in higher yield (81.0% yield instead of 69.6%). Two additional esters were then synthesized, a benzyl and phenyl ester, using benzyl alcohol and phenol, respectively. While these nucleophiles resulted in slightly lower yields than the methanol, the desired ester was indeed produced, demonstrating some substrate inclusiveness for -OH nucleophiles.

Next I turned my attention to -NH nucleophiles in hopes of forming amides from the methyl ketone of 4-bromoacetophenone. The first amine substrate that was attempted

was 1-butylamine, which produced the corresponding amide in high yield (80.8%). After that initial success several other amines were subjected to the reaction, and amides were synthesized from benzyl amine, aniline, piperidine, N,O-dimethyl hydroxylamine, and oxazolidinone. Yields from this series followed a general trend based on expected nucleophilicity; primary amines were better than secondary and poor nucleophiles such as aniline and oxazolidinone produced lower yields. Based off of these six amines, it appears that substrate universality also exists for -NH nucleophiles in this reaction, most of which proceed in moderate to high yields.

In addition to this list of -OH and -NH nucleophiles, a -SH nucleophile was tested in order to produce a thioester. Thiophenol was employed for this purpose, however the desired product was not isolated after several trials and purifications. The major compounds obtained seemed to be the disulfide of thiophenol and another species that could not be characterized. Ultimately, a different thiol (aliphatic) should be tested before concluding that the thioesters are not able to be produced from the reaction.

Ketone substrate scope includes both aromatic and alkyl methyl ketones.

Following the realization of the nucleophile substrate class, I turned my attention to investigating the scope of ketone substrates. Based off of the success using 4-bromoacetophenone, other acetophenone derivatives were the first to be tested. It became apparent almost immediately, however, that many aromatic ketones would not be competent in the reaction. For instance, in the case of acetophenone, para-methoxy acetophenone and ortho-hydroxy acetophenone, nitrations of the aromatic ring were observed thus inhibiting the desired nitration reaction from occurring. Heterocyclic methyl ketones followed the same trend, as substrates containing pyridine, pyrrole, indole,

thiophene and benzothiophene did not produce any desired product. In general, electron-rich aromatics and heteroaromatics appear to be non-ideal for this reaction, as many of these substrates will preferably undergo aromatic nitration rather than alpha nitration.

With this limitation in mind, I focused on identifying new aromatic methyl ketone substrates in order to demonstrate that the reaction does not only work for 4-bromo acetophenone. Accordingly, I performed bromination reactions on the substrates that failed, and was able to isolate and purify several mono-bromo products. After subjecting these new compounds to my reaction it was found that the desired amide was produced in many cases. For example, 1-(3-bromo-4-methylphenyl)ethanone and 1-(3,4-dibromophenyl)ethanone participated in the reaction and produced amides in good yields. Interestingly, in the case of 1-(3-bromo-4-methoxyphenyl)ethanone, while the compound did not nitrate the ring and thus did indeed generate the gem-dinitro enol, addition of an -NH nucleophile and subsequent stirring overnight did not produce the amide as expected. This observation potentially clues us into the effect of the substituent that is para to the ketone, as the para methoxy allows the alpha nitration to occur but not the nucleophilic substitution. Since alpha nitration occurs in the enol form, while the substitution reaction occurs in the keto form, it can be hypothesized that an electron-donating substituent at the para position stabilizes the enol form during the reaction. Ultimately, more aromatic substrates need to be tested to confirm this trend and also to demonstrate better substrate inclusiveness for acetophenones.

Next I became interested in testing aliphatic ketones in the reaction, since these would in theory not be hindered by the side reactions seen in the aromatic substrates.

Pinacolone became the first aliphatic methyl ketone subjected to the reaction and was

shown to be competent in the reaction, producing an amide in 58.4% yield. Acetone, on the other hand, also worked but with much lower yield. This disparity could be due in part to the keto/enol ratio for pinacolone and acetone, as pinacolone would supposedly have lower yield due to the steric hindrance around the carbonyl carbon from the tert butyl group. Nonetheless, these two examples provide good support for the claim that the reaction works for aliphatic methyl ketones and not just aromatic substrates.

Another alkyl methyl ketone substrate that was tested was 4-(4-nitrophenyl)butan-2-one, which produced a very peculiar result. In addition to the desired amide product that was obtained in about 25% yield, an unknown compound was isolated from purification that appeared to have the para nitro-substituted benzene ring but was missing the rest of the structure. It was unable to be determined what the other substituent on the 1,4 disubstituted benzene was or how aromatic dealkylation took place. This remains an area of interest that could potentially lead to a side project after this work gets published, but further investigation of this strange result is not a priority.

Application of this new reaction to produce medicinally relevant compounds. In order to further validate the usefulness of this new reaction, I next utilized it to synthesize pharmaceutically pertinent moieties. Using ortho-phenylene diamine as the nucleophile and heating the reaction overnight, I was able to obtain a benzimidazole from 4-bromoacetophenone in moderate yield. Benzimidazoles are important heterocycles found in a variety of drugs and are almost exclusively synthesized from carboxylic acids or aldehydes. Generation of these molecules from methyl ketones is far less common, with only a small number of procedures existing for this transformation.

For that reason, this has the potential to become a separate publication, pending further investigations regarding substrate scope and practicality.

Another class of biologically relevant compounds that can be produced from this reaction are methyl ketone-containing steroids such as progesterone derivatives. Since several semi-synthetic steroids are/were available as drugs, this one-step transformation from progesterone could provide an assortment of amide and ester analogs with unique properties and applications. A reaction with benzyl amine demonstrated that this substrate was able to participate in the dinitro enol reaction, but the yield is currently not known. At any rate, the fact progesterone is cheap and widely available makes the one-step process worthwhile even if yields are moderately low.

Conclusion

A new reaction for methyl ketones provides carboxylic acids, esters and amides from a simple one-pot procedure. A large variety of -NH and -OH nucleophiles are tolerated, and both aromatic and aliphatic methyl ketones have been demonstrated to participate in the reaction. Through the isolation of previously unreported intermediates, a plausible mechanism has been suggested involving gem-dinitro enols that are formed via alpha-nitration of a methyl ketone. The reaction has great potential to be employed for the synthesis of biologically active compounds such as benzimidazoles and steroid derivatives. Currently, this work is being concluded and will be submitted for publication in due time.

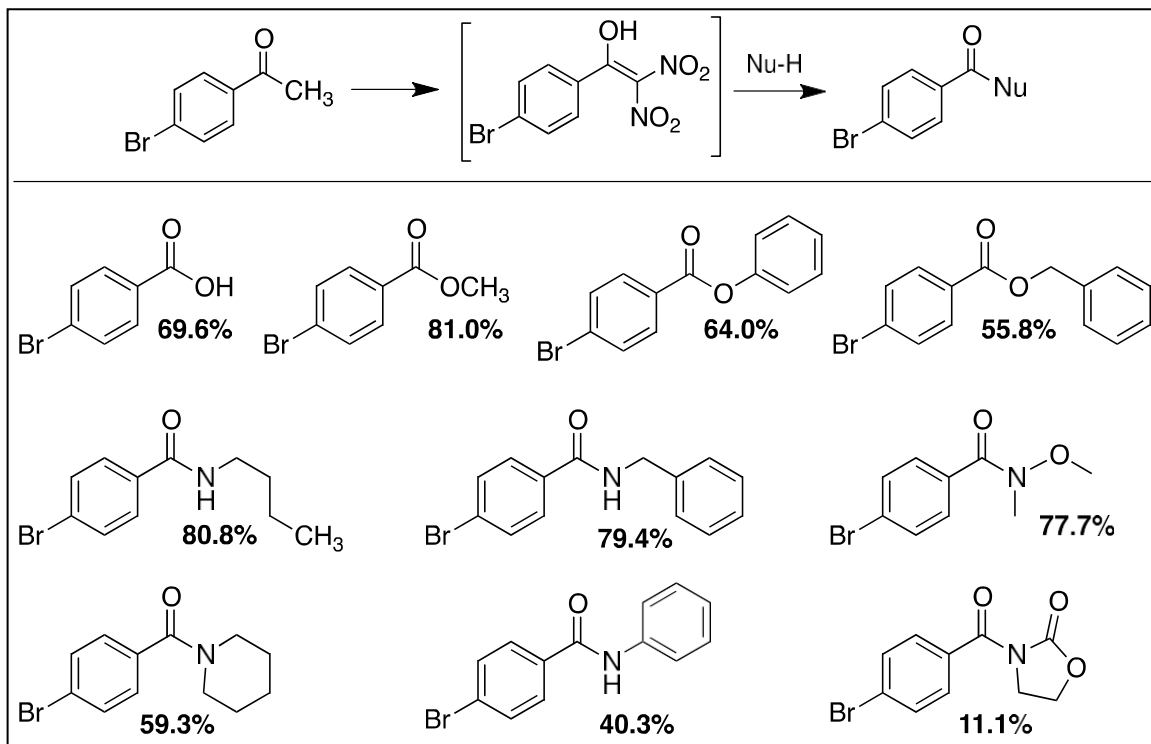


Figure 17. Reaction scheme and examples of nucleophile substrate scope

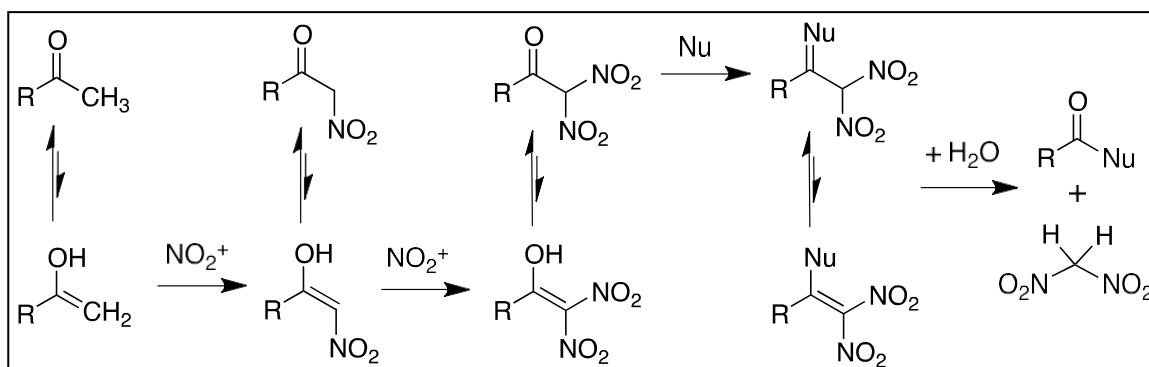


Figure 18. Proposed reaction mechanism

Experimental Section

General chemistry. All reagents and solvents were obtained from commercial sources and used without further purification or drying. Reactions were performed under a nitrogen gas atmosphere in flame-dried glassware. Unless otherwise noted, compounds were not purified. ^1H and ^{13}C NMR data was taken on a Varian AS400 (400 MHz), with chemical shifts being displayed in a ppm scale referenced to residual chloroform.

4-bromobenzoic acid. 4-bromoacetophenone (139.3 mg, 0.700 mmol) was dissolved in ACN (1.4 mL, 0.5 M) and cooled to 0 °C. Acetic anhydride (0.20 mL, 3.0 EQ, 3.58 M) was added, followed by 90% nitric acid dropwise (0.20 mL, 6.0 EQ, 3.58 M). The solution was allowed to warm to room temperature and stir overnight. After cooling to 0 °C, the reaction was quenched with DIPEA dropwise (12 EQ). KOH (19.6 mg, 0.5 EQ) was added and the mixture was allowed to stir at room temperature overnight. The product was isolated after standard workup and purified by silica-gel column chromatography, affording 96.7 mg of the desired product, 69.6% yield.

Methyl 4-bromobenzoate. Prepared using the procedure described for 4-bromobenzoic acid, using the corresponding nucleophile (methanol), 81.0% yield.

Phenyl 4-bromobenzoate. Prepared using the procedure described for 4-bromobenzoic acid, using the corresponding nucleophile (phenol), 64.0% yield.

Benzyl 4-bromobenzoate. Prepared using the procedure described for 4-bromobenzoic acid, using the corresponding nucleophile (benzyl alcohol), 55.8% yield.

4-bromo-N-butylbenzamide. Prepared using the procedure described for 4-bromobenzoic acid, using the corresponding nucleophile (1-butyl amine), 80.8% yield.

***N*-benzyl-4-bromobenzamide.** Prepared using the procedure described for 4-bromobenzoic acid, using the corresponding nucleophile (benzyl amine), 79.4% yield.

(4-bromophenyl)(piperidin-1-yl)methanone. Prepared using the procedure described for 4-bromobenzoic acid, using the corresponding nucleophile (piperidine), 59.3% yield.

4-bromo-*N*-methoxy-*N*-methylbenzamide. Prepared using the procedure described for 4-bromobenzoic acid, using the corresponding nucleophile (N,O dimethyl hydroxylamine HCl), 77.7% yield.

4-bromo-*N*-phenylbenzamide. Prepared using the procedure described for 4-bromobenzoic acid, using the corresponding nucleophile (aniline), 40.3% yield.

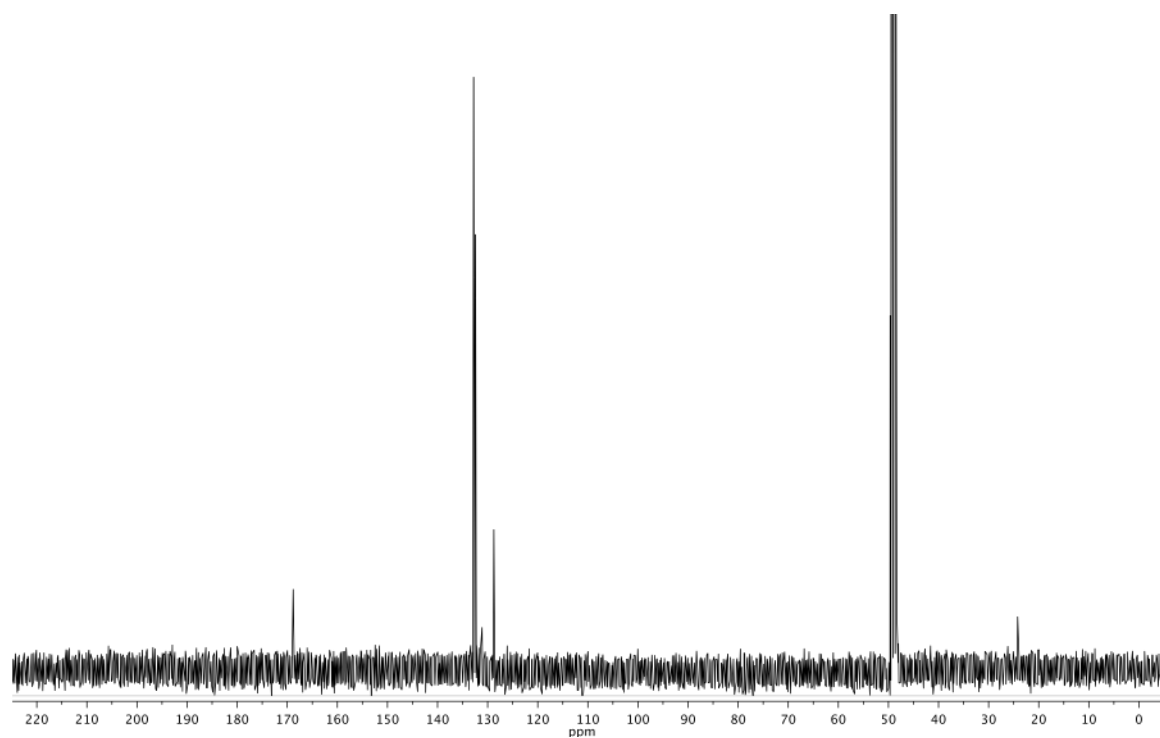
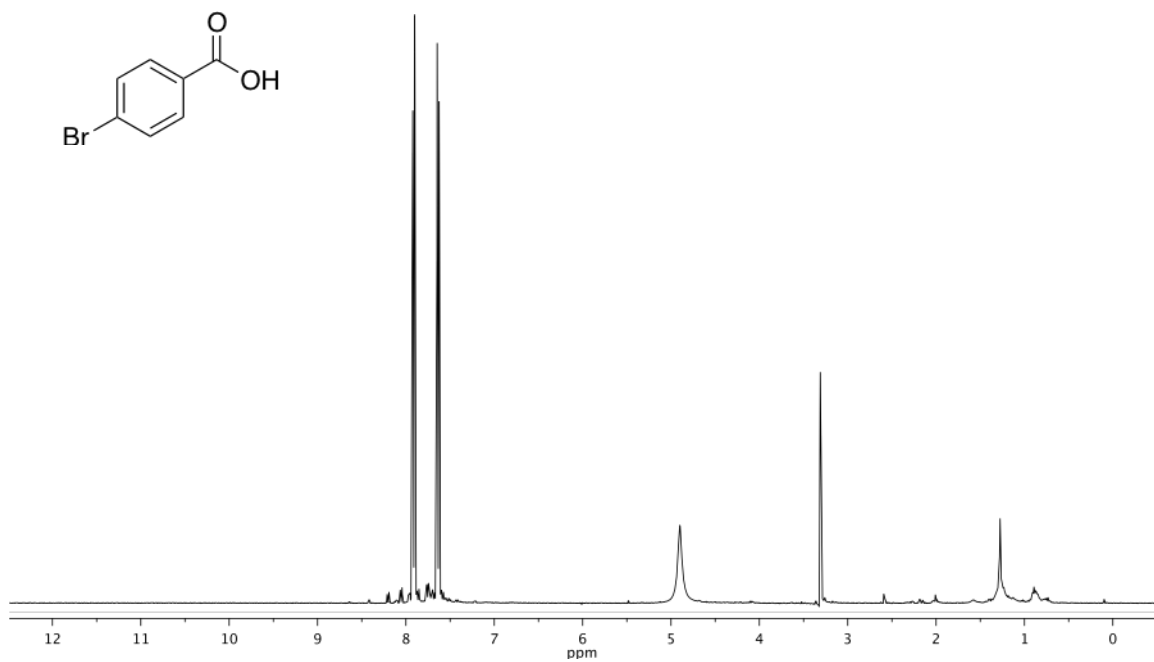
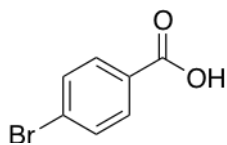
3-(4-bromobenzoyl)oxazolidin-2-one. Prepared using the procedure described for 4-bromobenzoic acid, using the corresponding nucleophile (oxazolidinone), 11.1% yield.

2-(4-bromophenyl)-1*H*-benzo[*d*]imidazole. Prepared using the procedure described for 4-bromobenzoic acid, using the corresponding nucleophile (ortho-phenylene diamine), 35.4% yield.

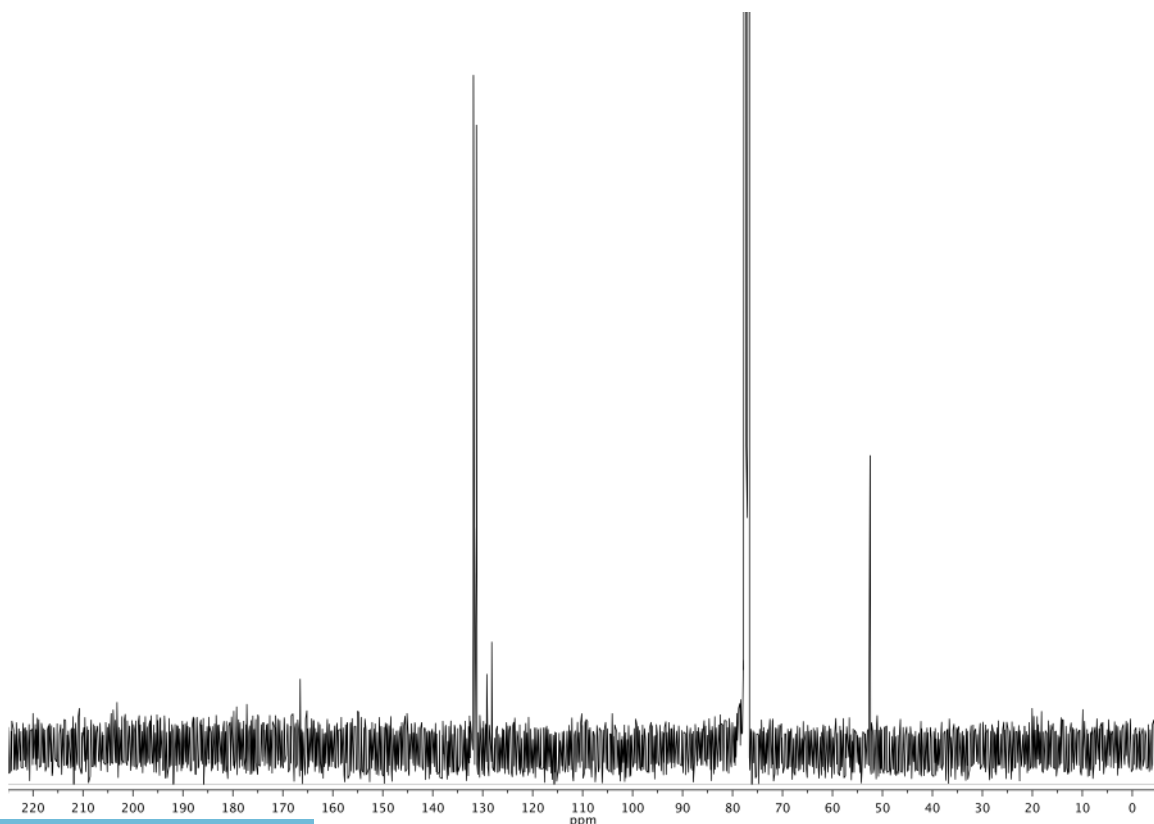
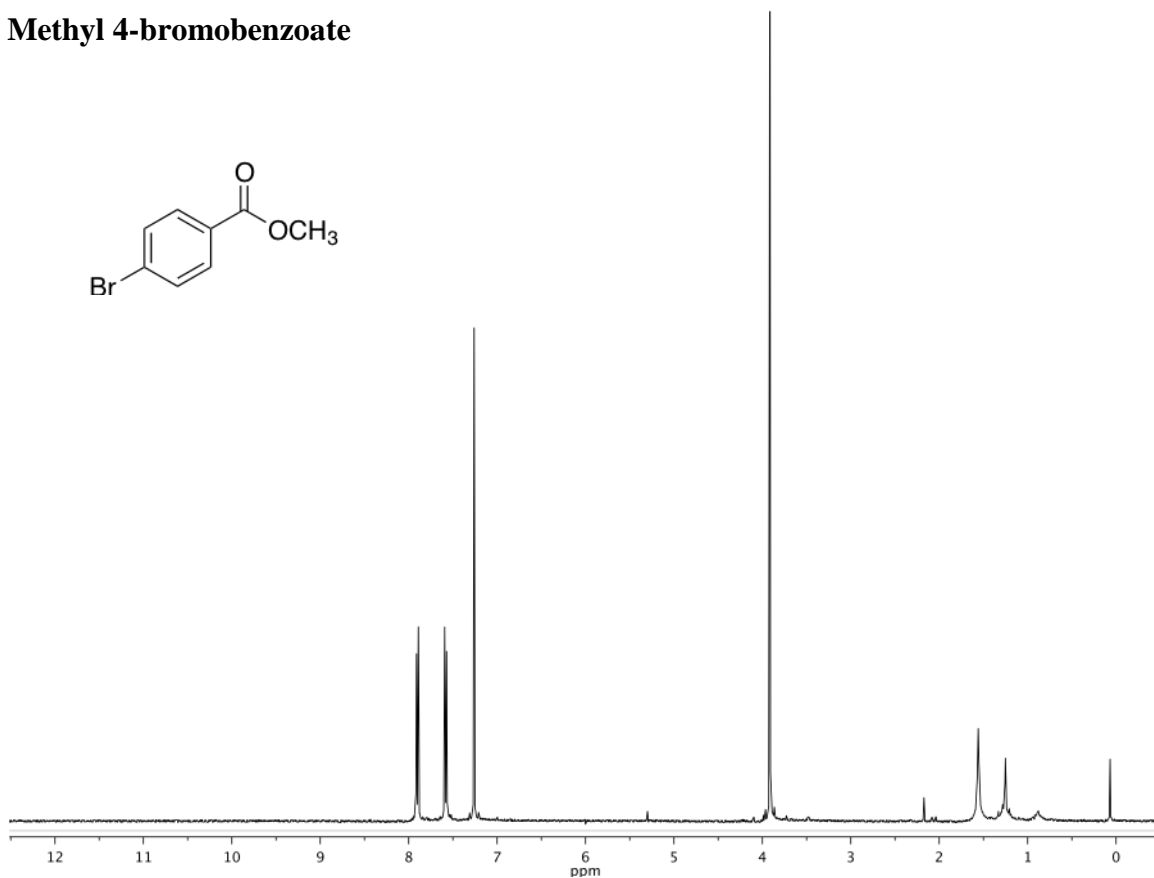
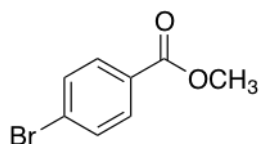
***N*-benzylpivalamide.** Prepared using the procedure described for *N*-benzyl-4-bromobenzamide, using the corresponding ketone (pinacolone), 58.4% yield.

***N*-butyl-3-(4-nitrophenyl)propanamide.** Prepared using the procedure described for 4-bromo-*N*-butylbenzamide, using the corresponding ketone, 25.3% yield.

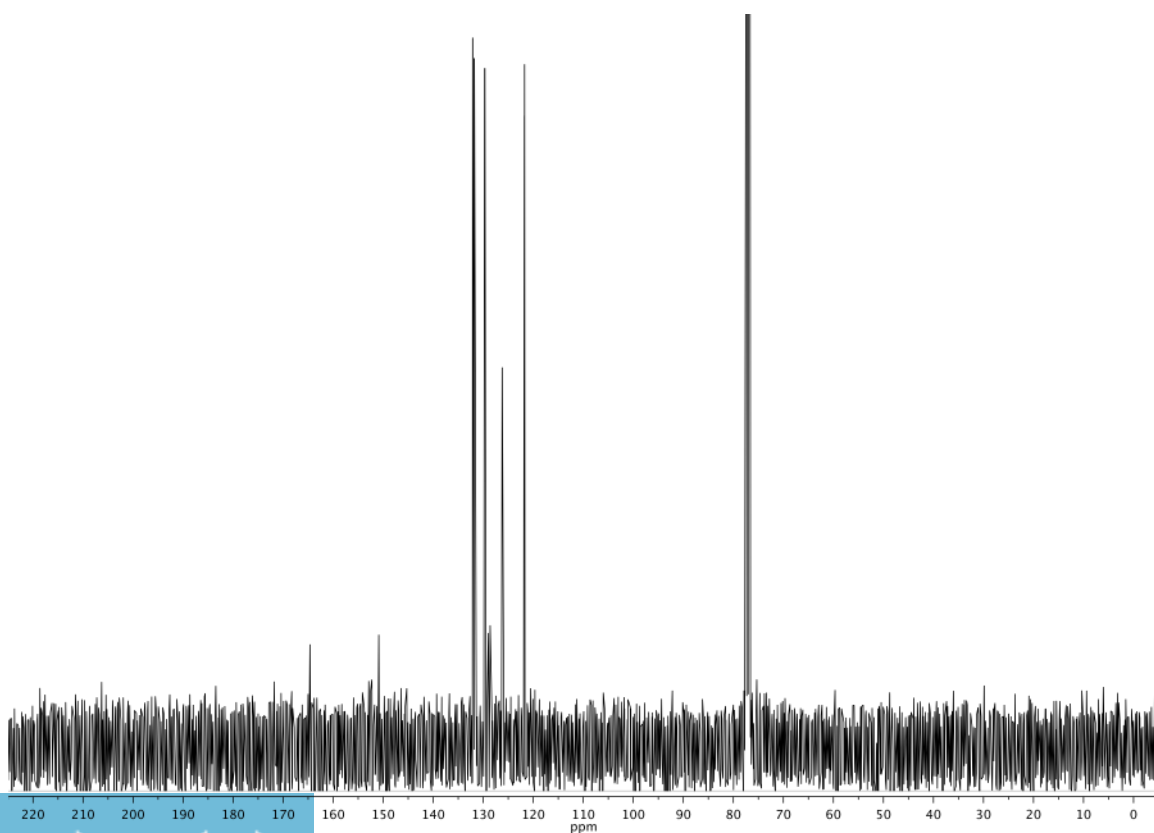
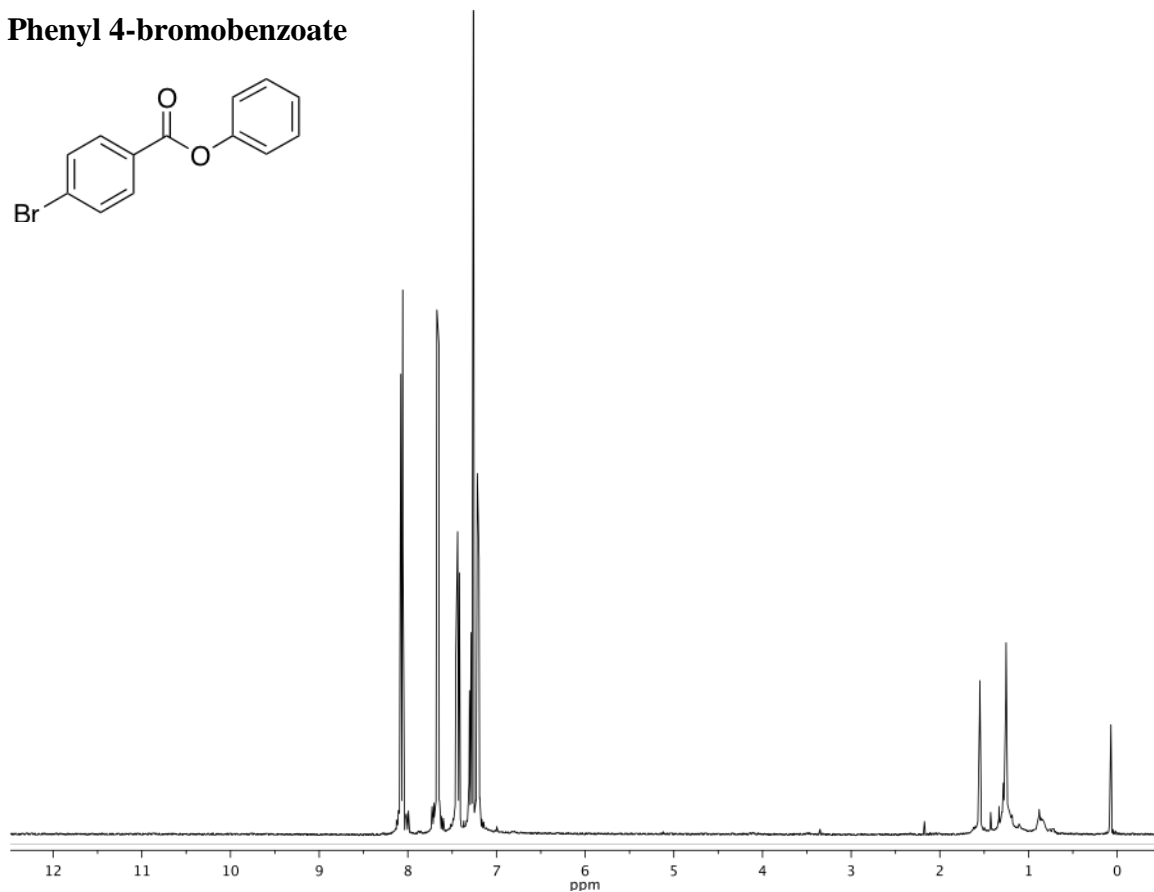
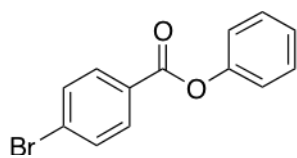
4-bromobenzoic acid



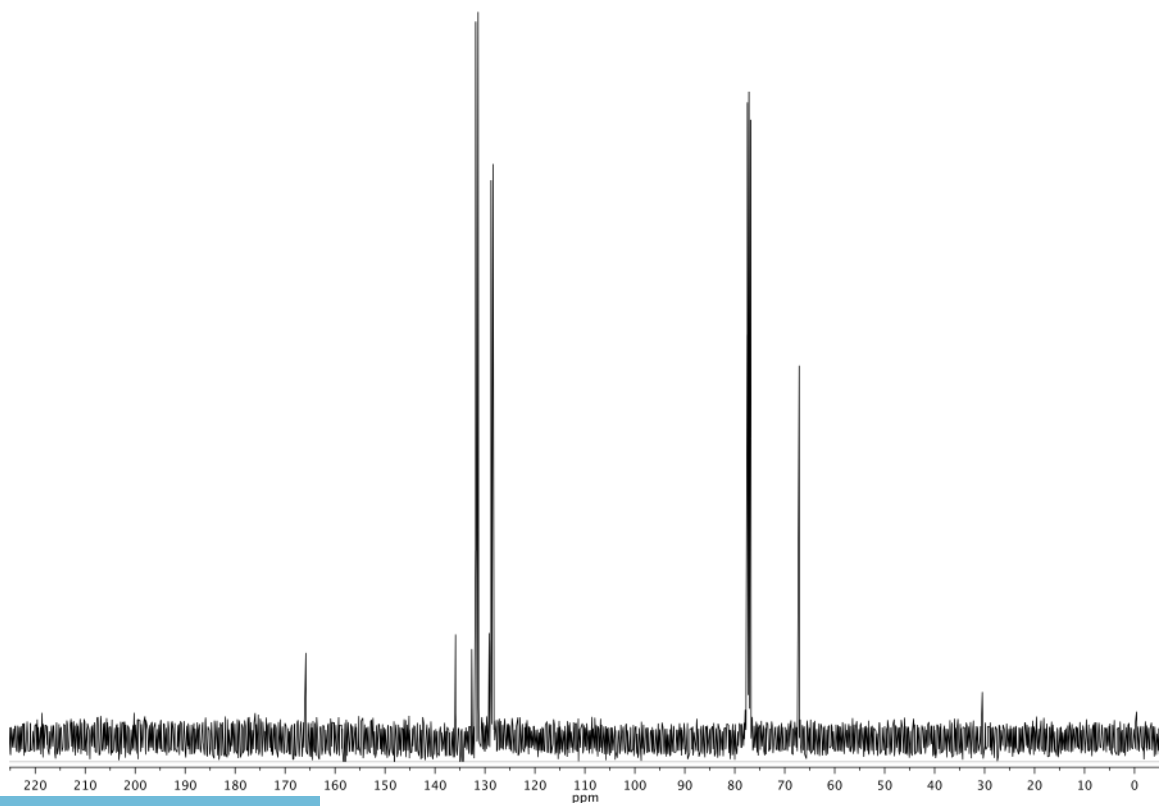
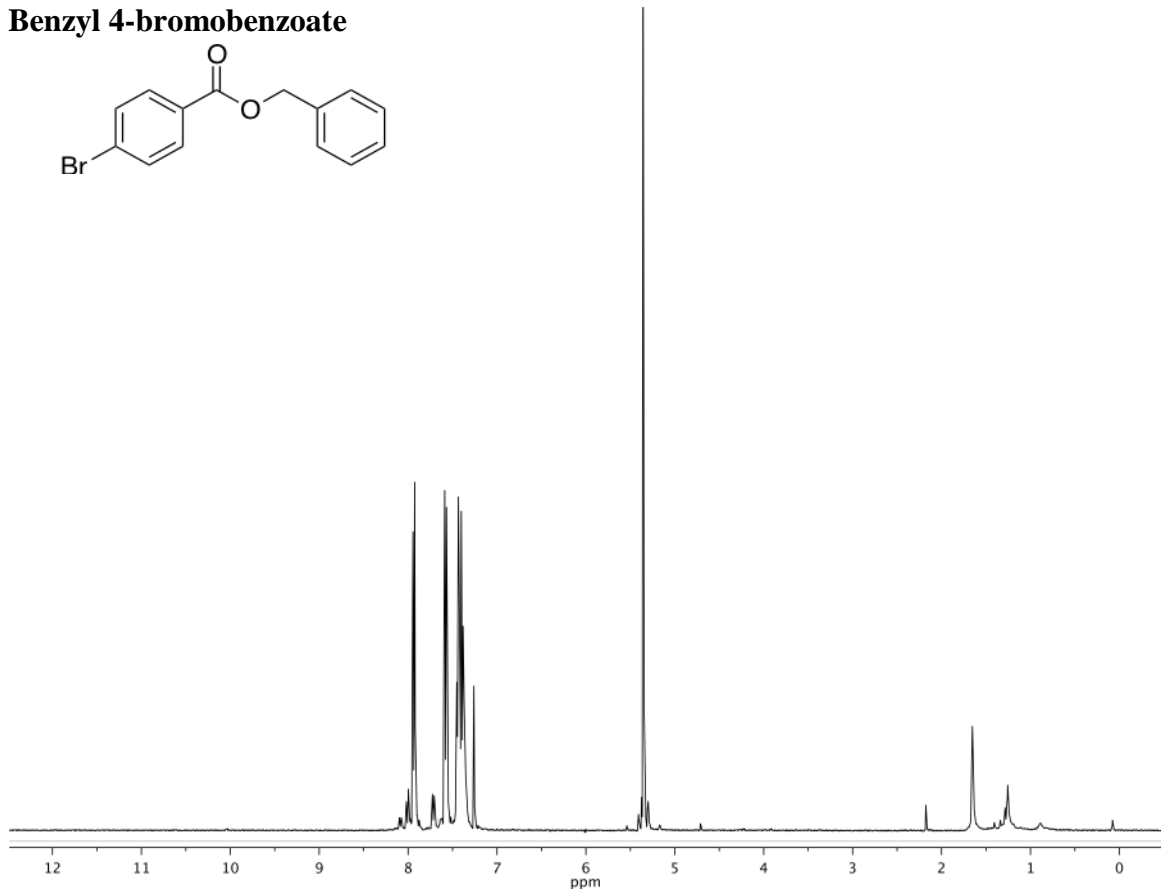
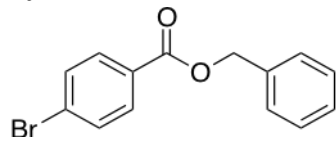
Methyl 4-bromobenzoate



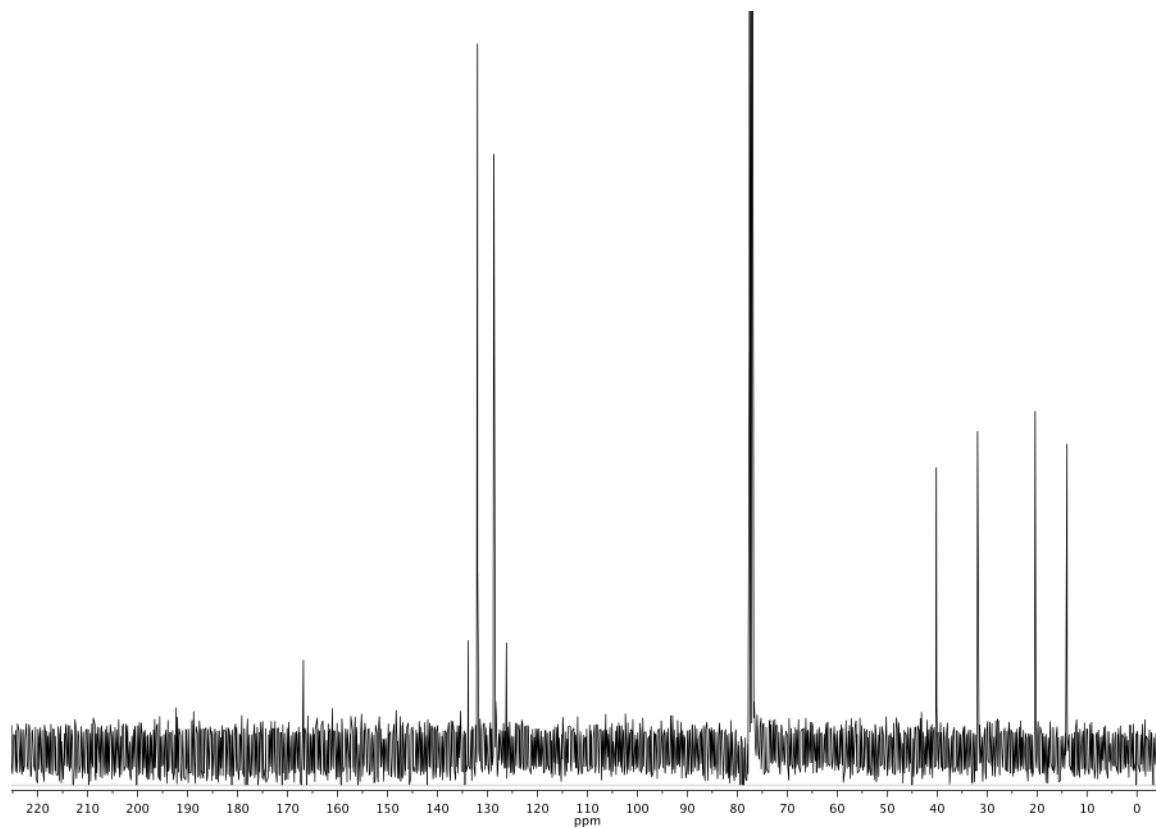
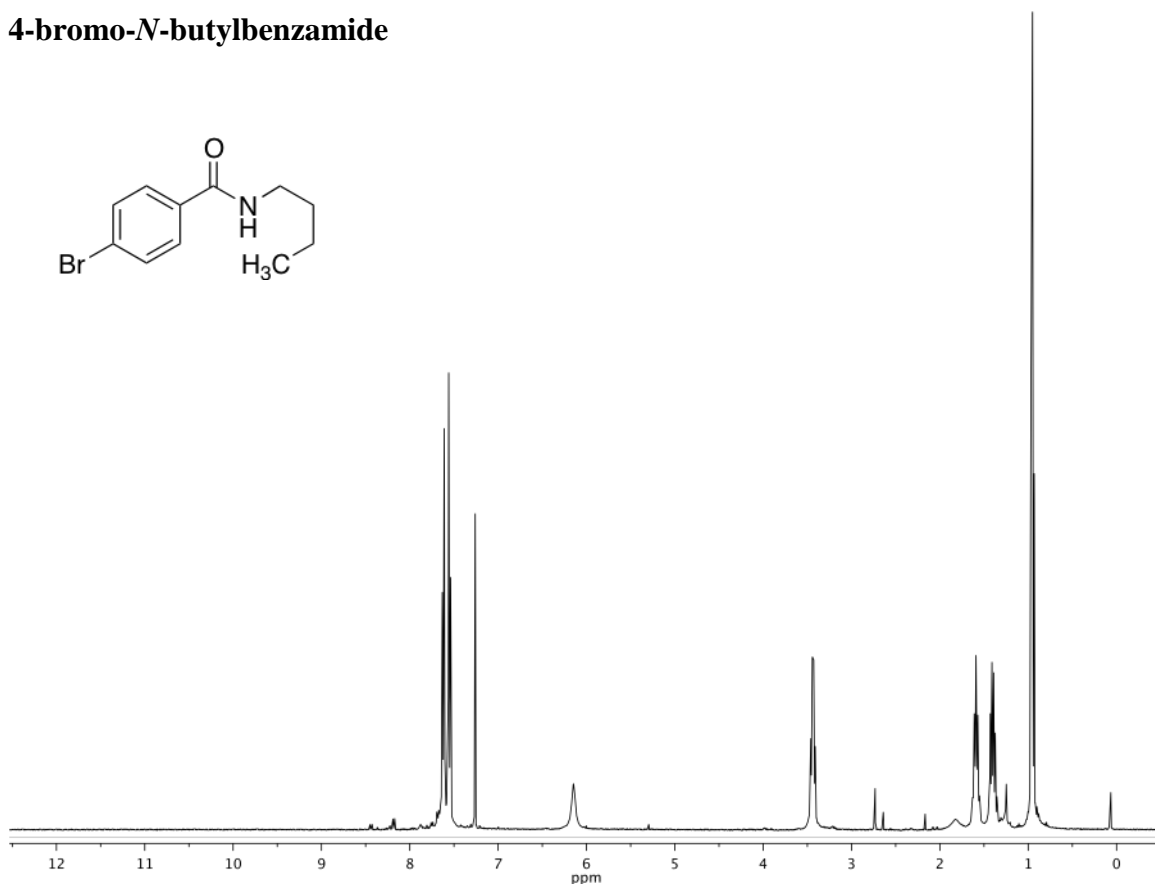
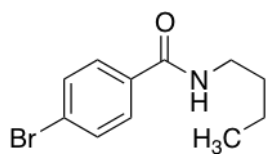
Phenyl 4-bromobenzoate



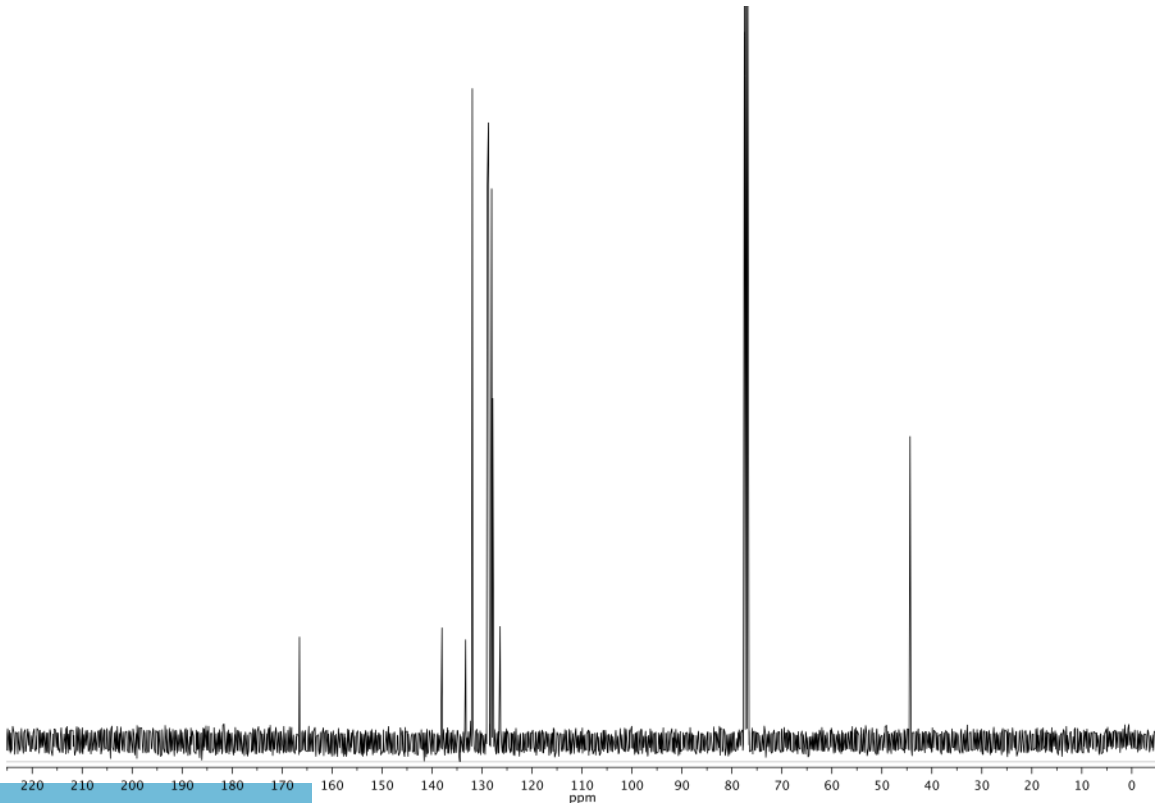
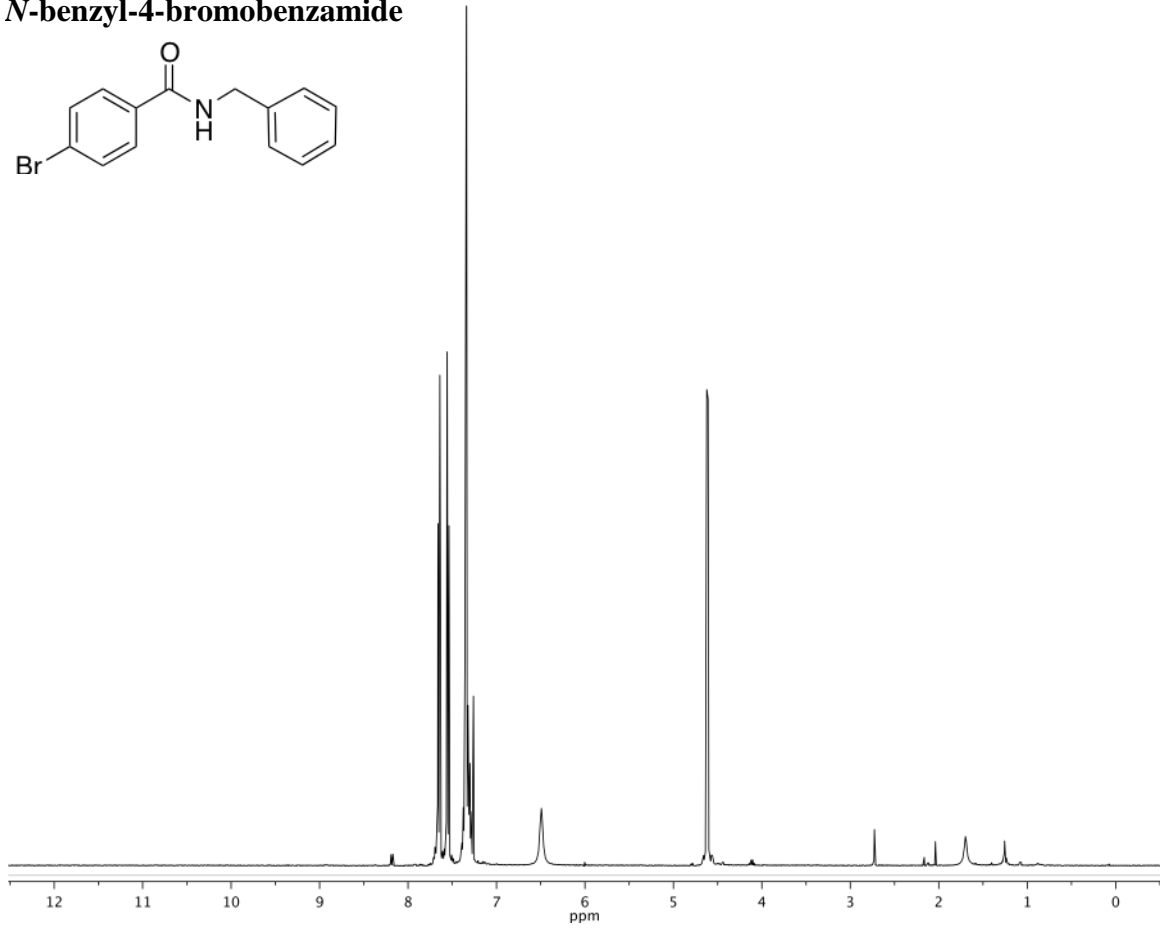
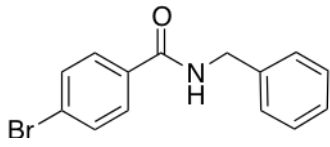
Benzyl 4-bromobenzoate



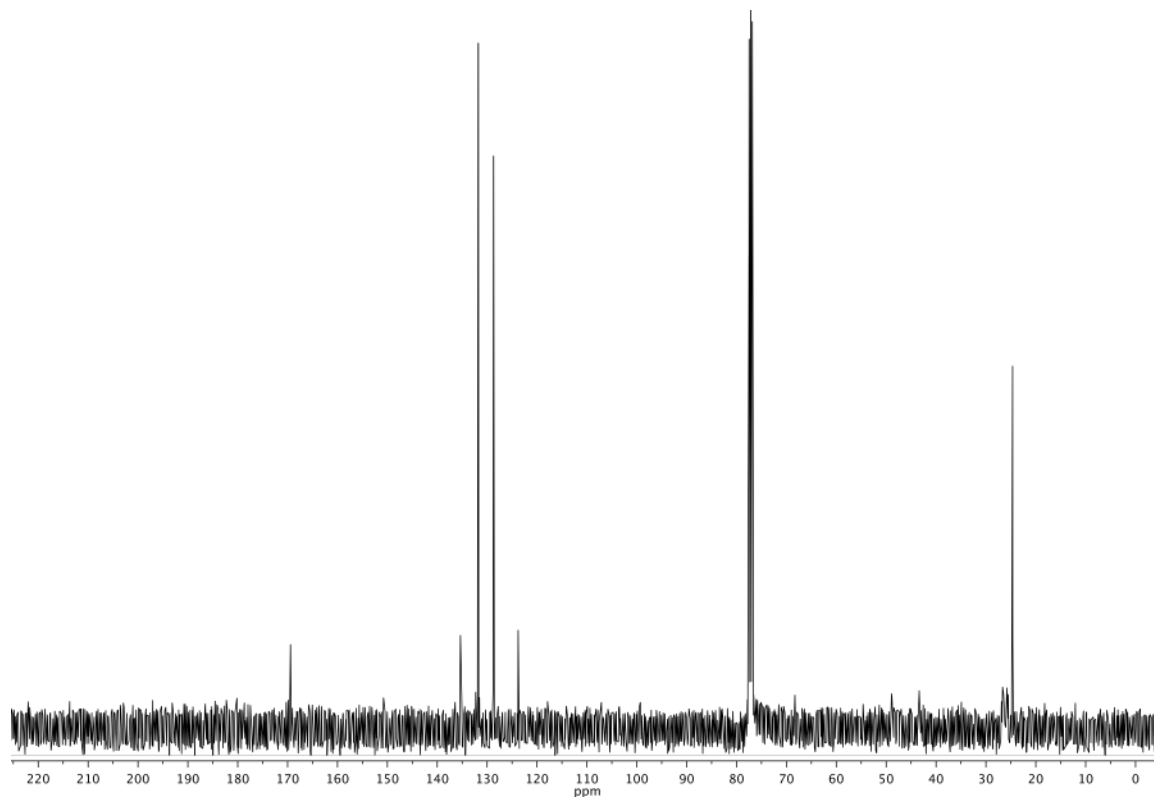
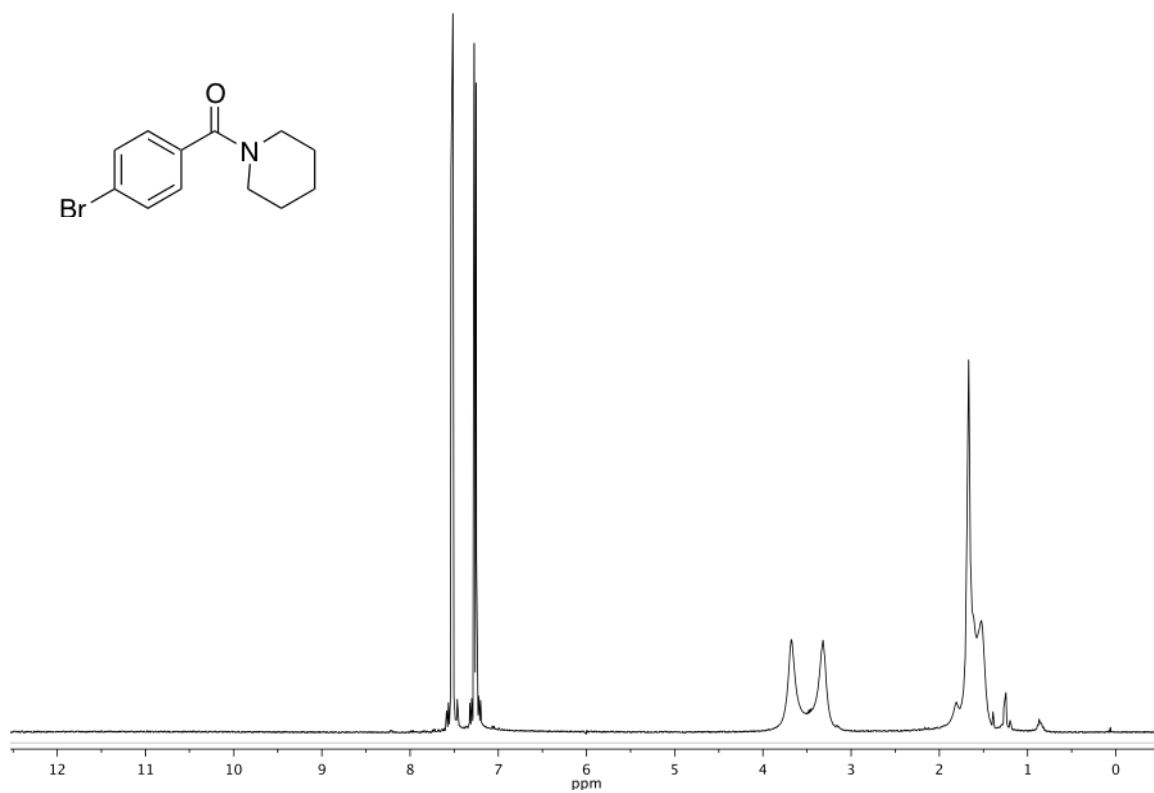
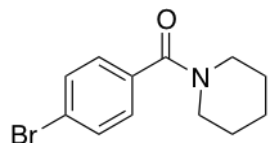
4-bromo-N-butylbenzamide



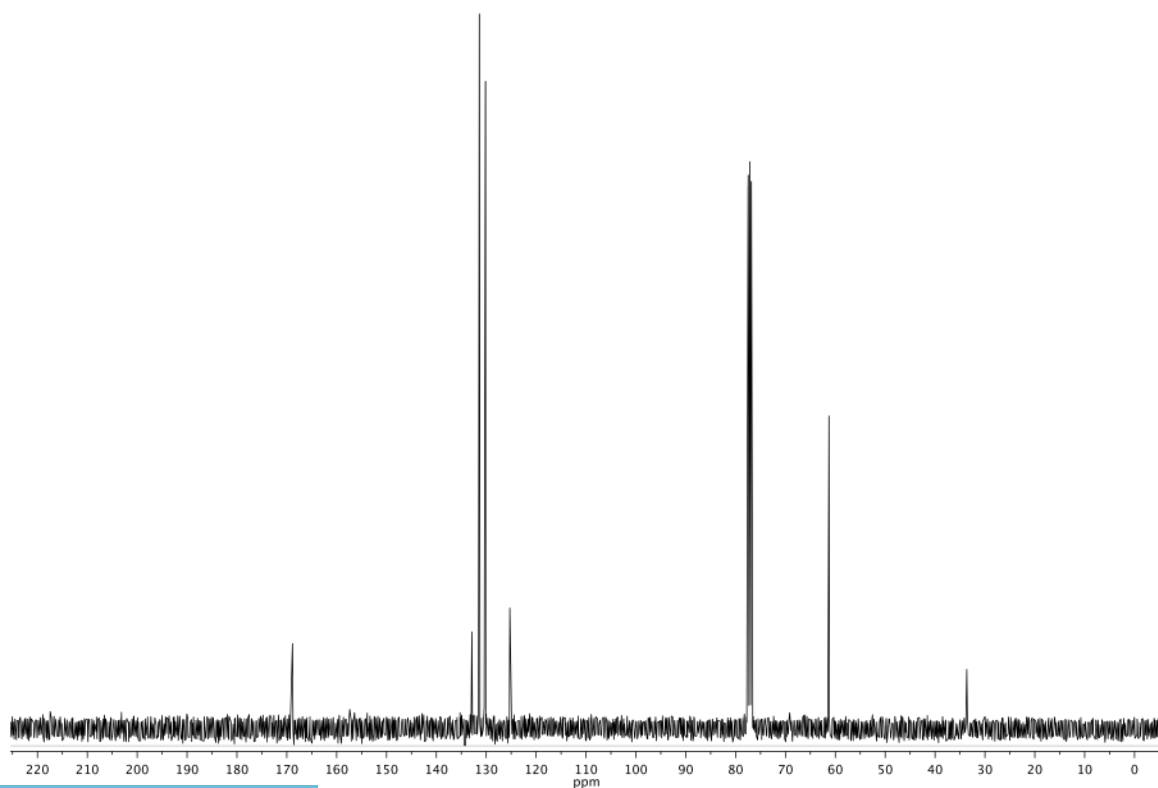
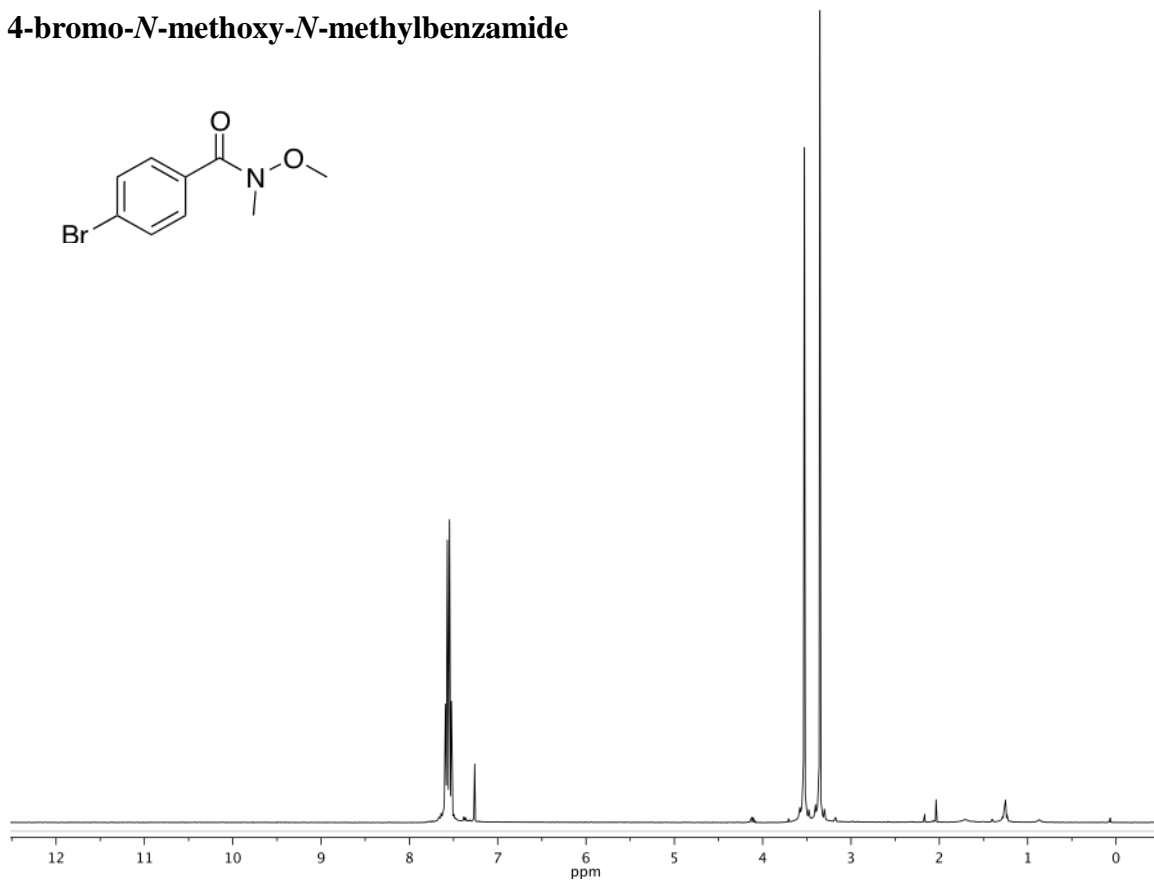
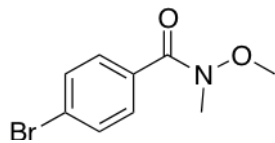
***N*-benzyl-4-bromobenzamide**



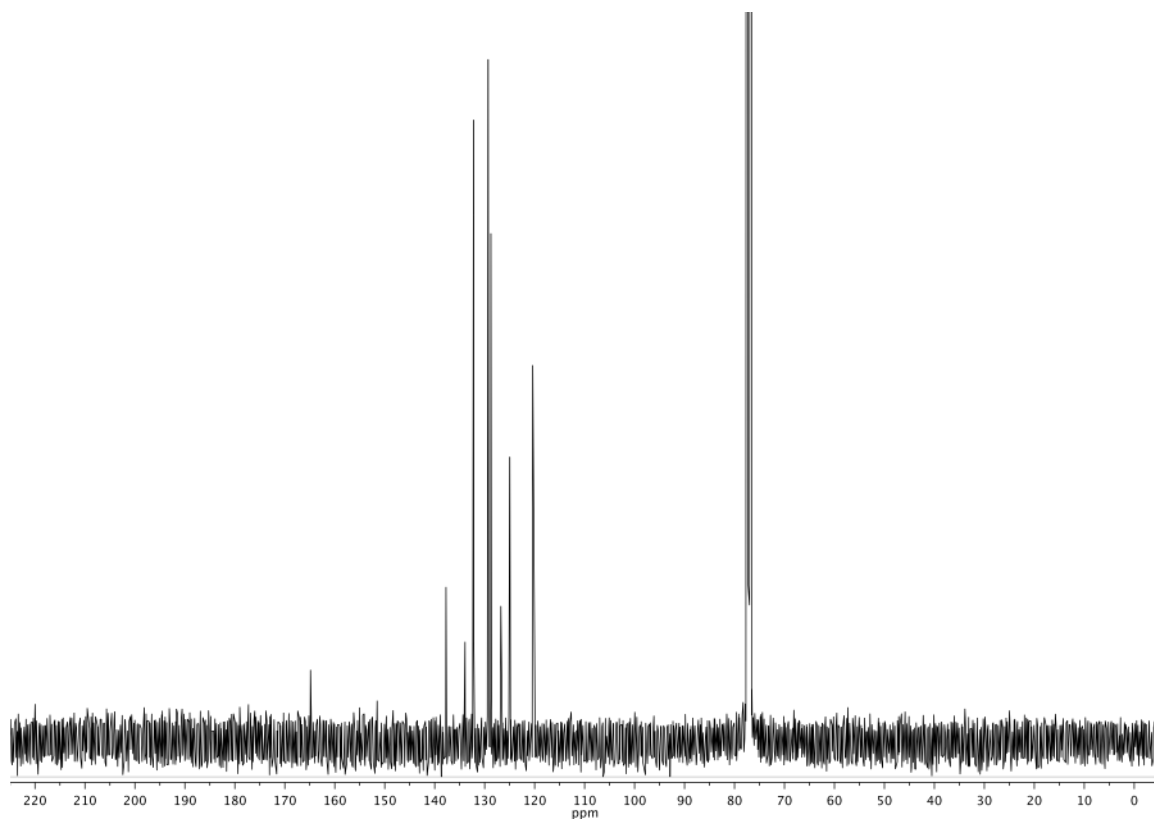
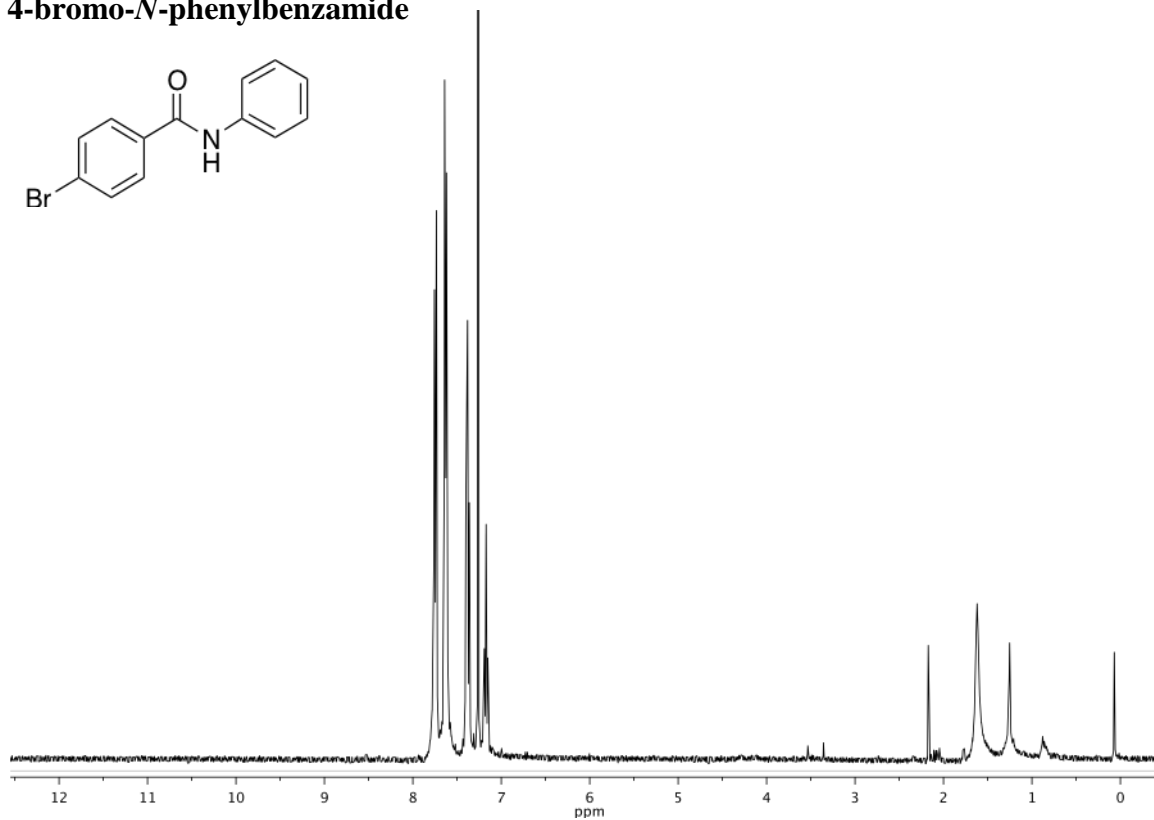
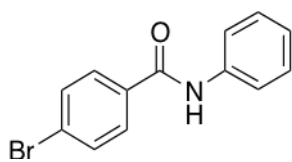
(4-bromophenyl)(piperidin-1-yl)methanone



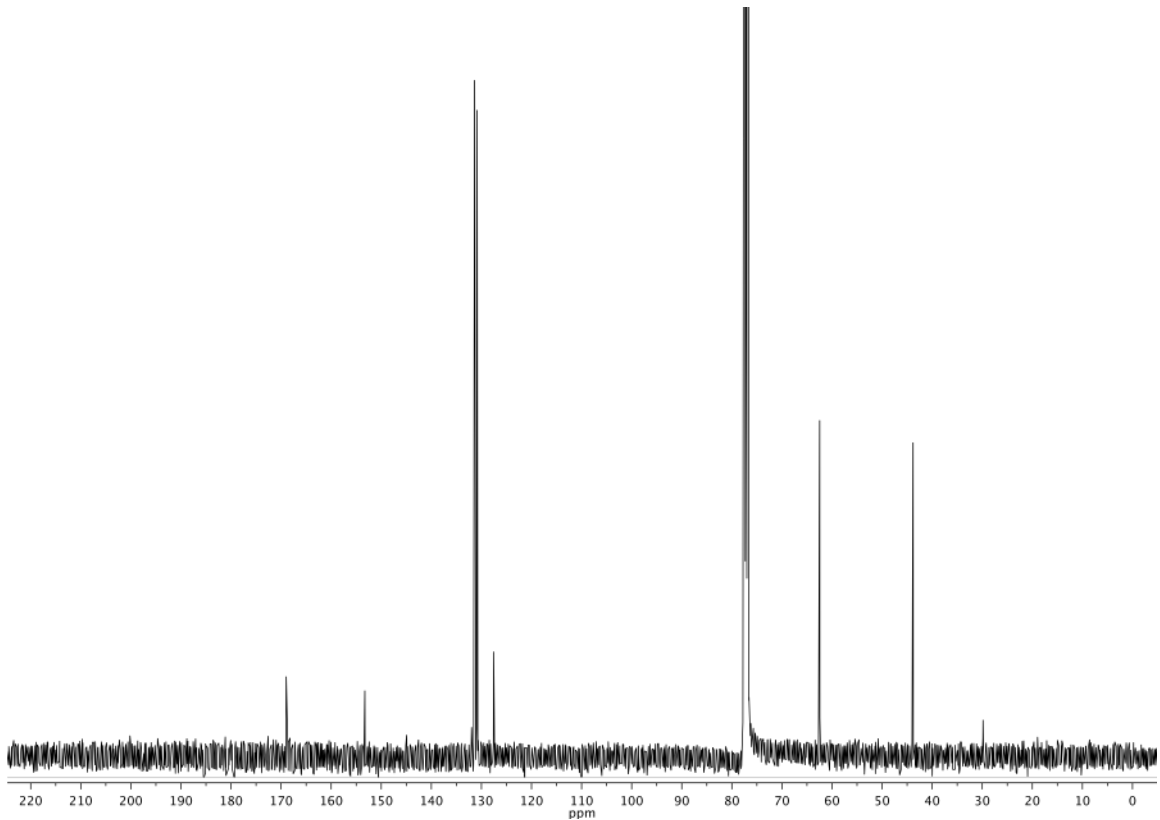
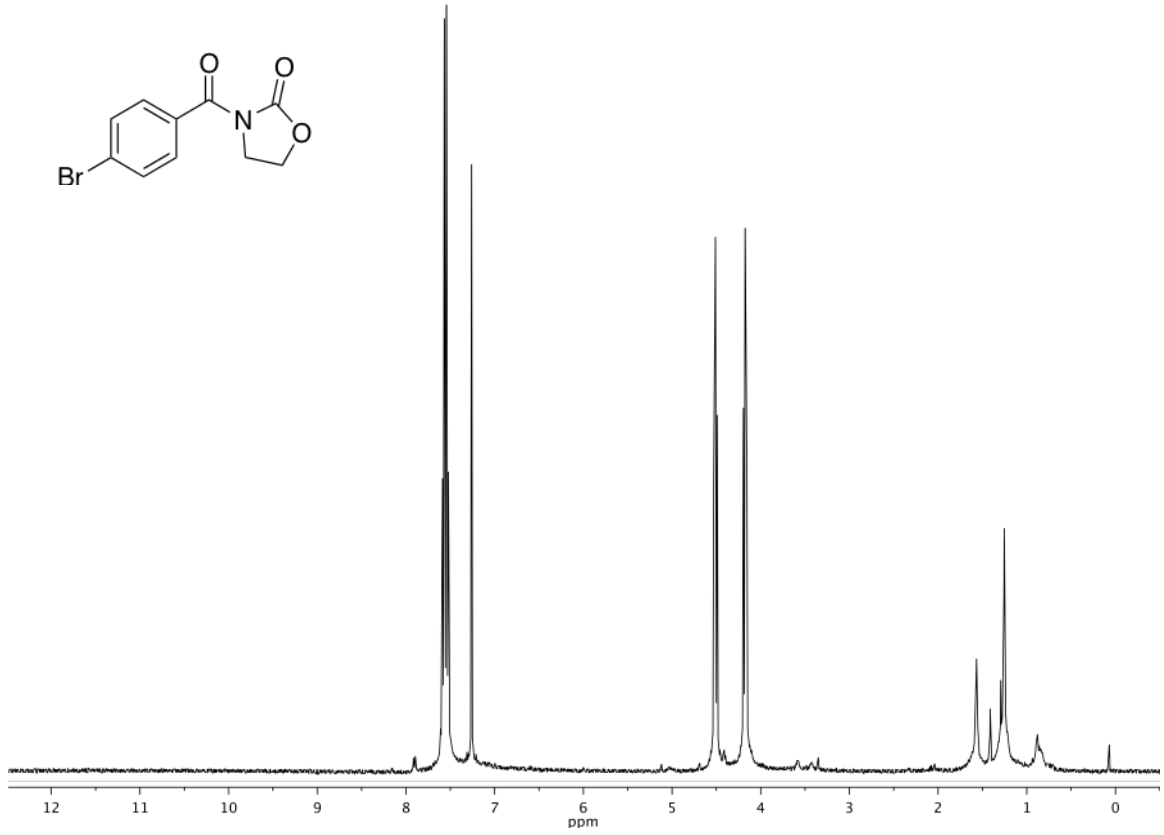
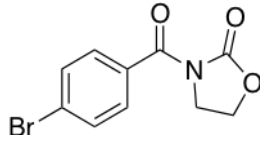
4-bromo-N-methoxy-N-methylbenzamide



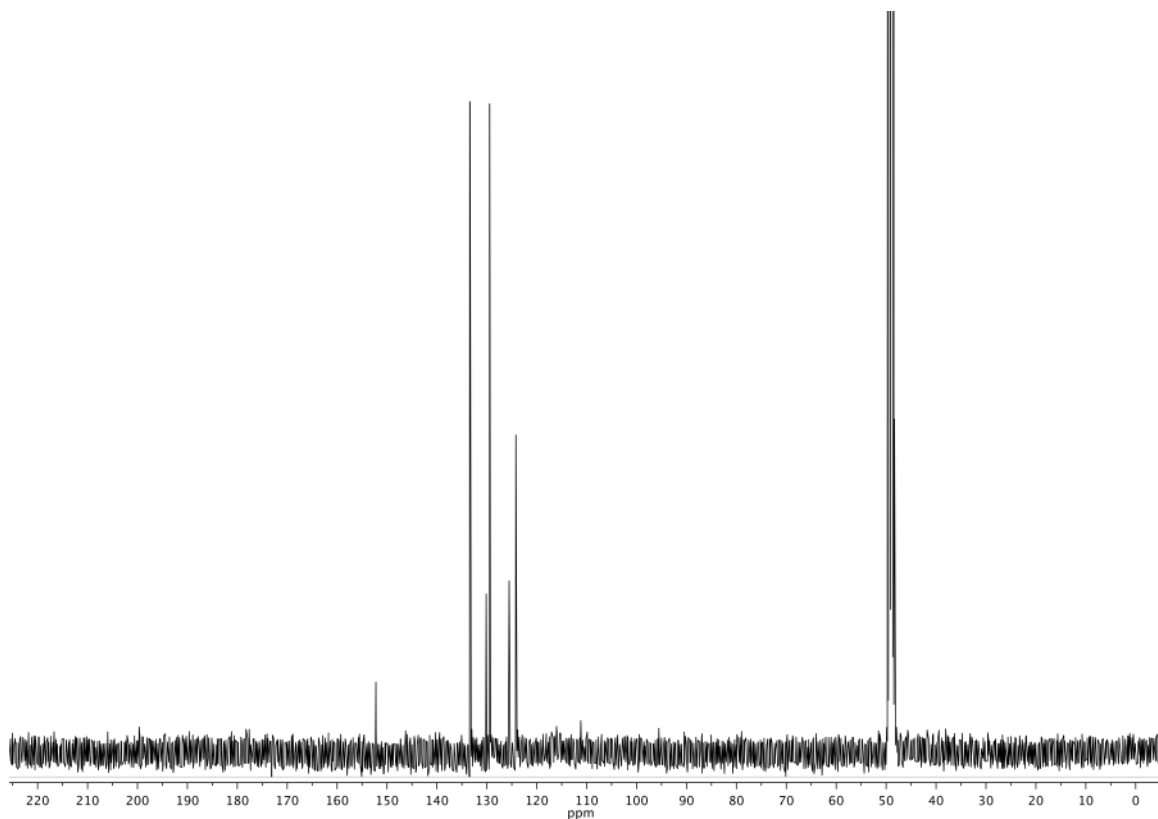
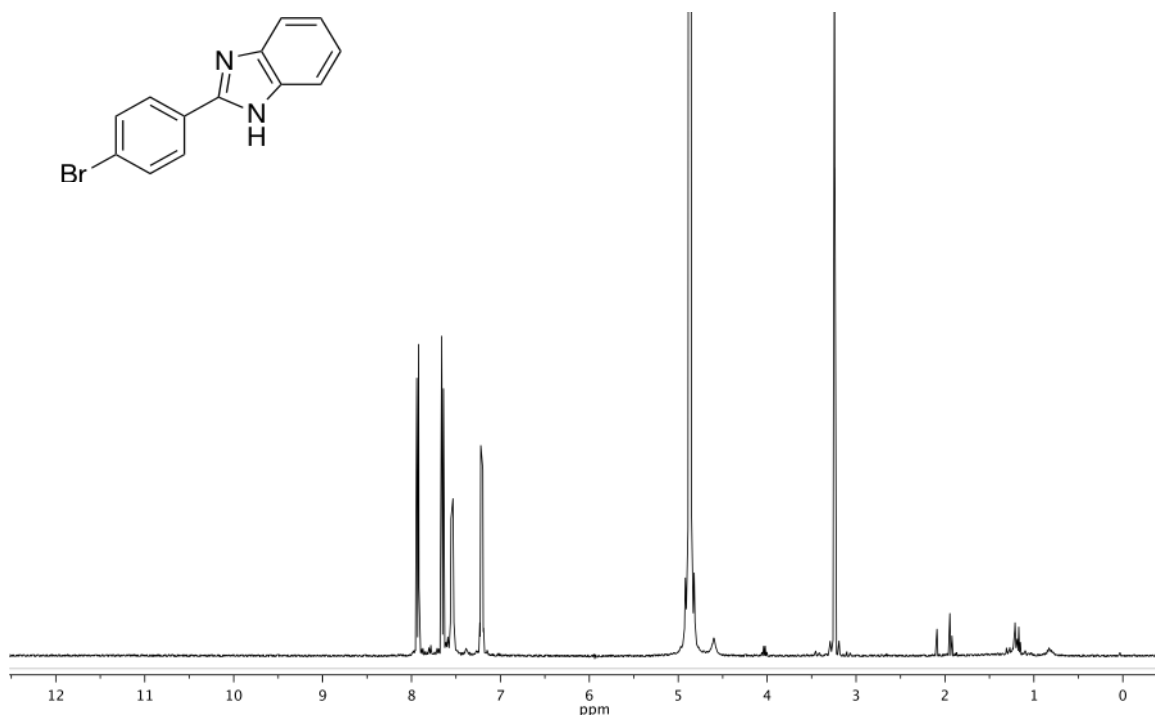
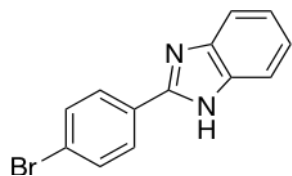
4-bromo-N-phenylbenzamide



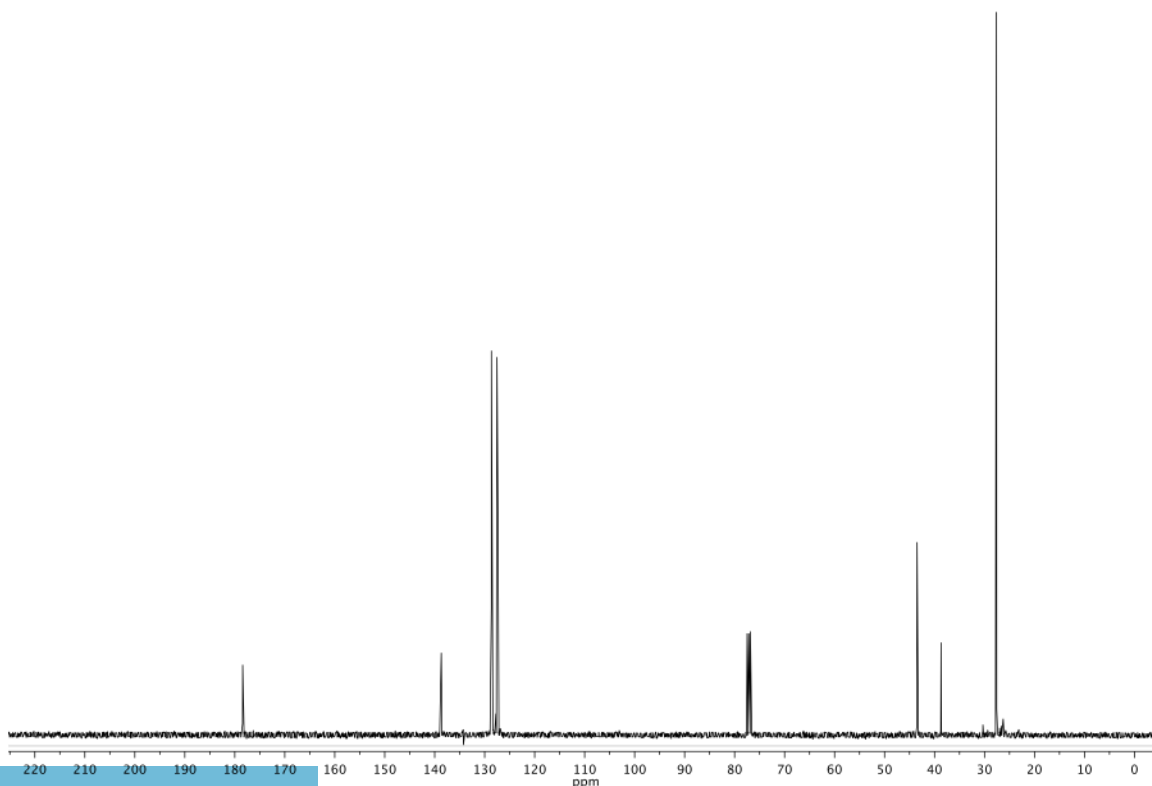
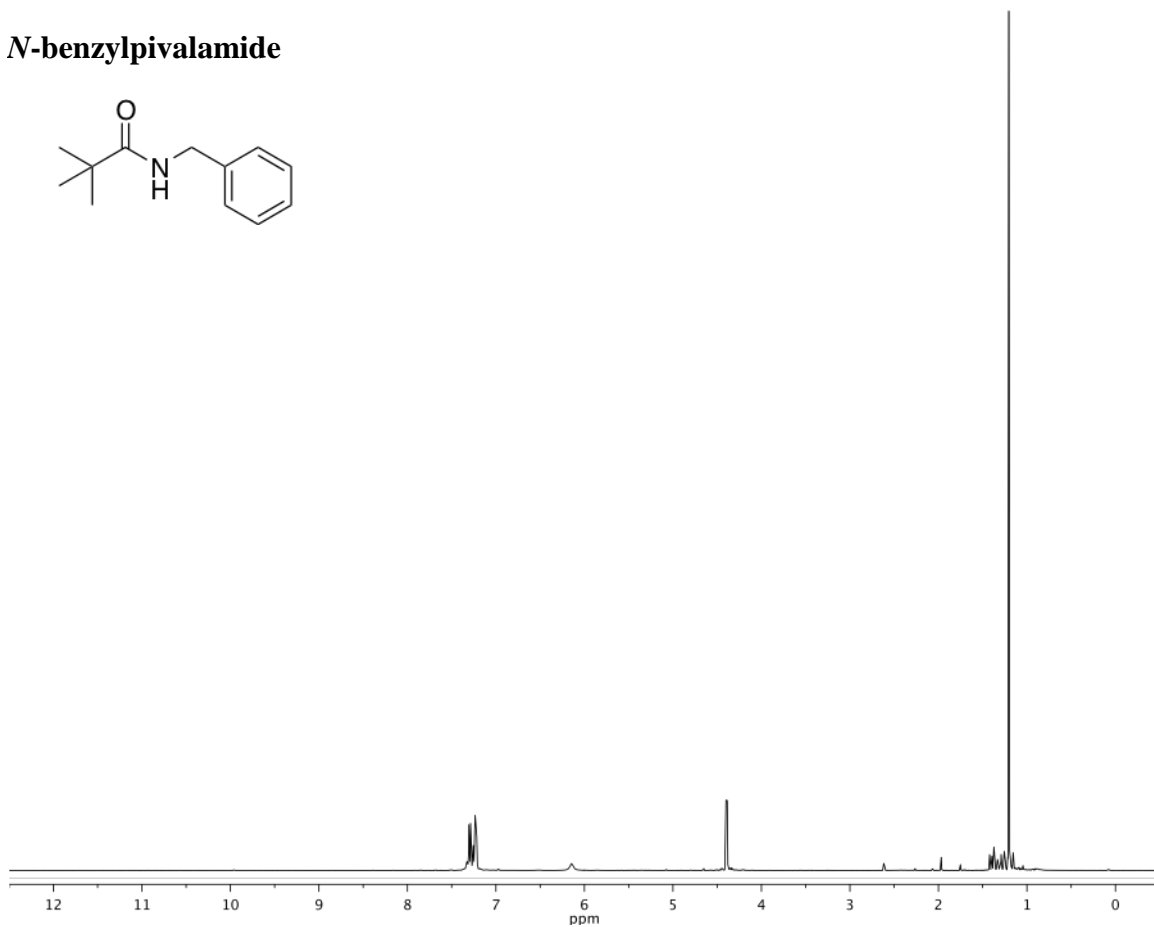
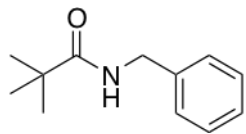
3-(4-bromobenzoyl)oxazolidin-2-one



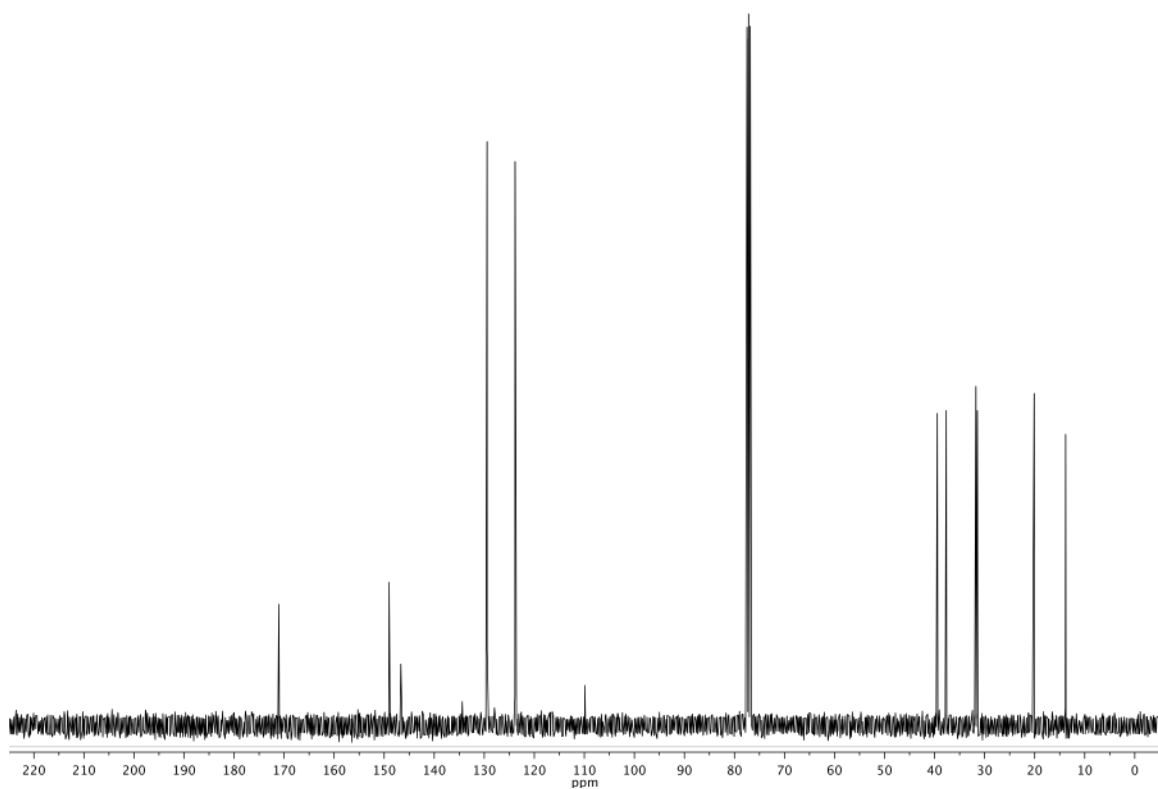
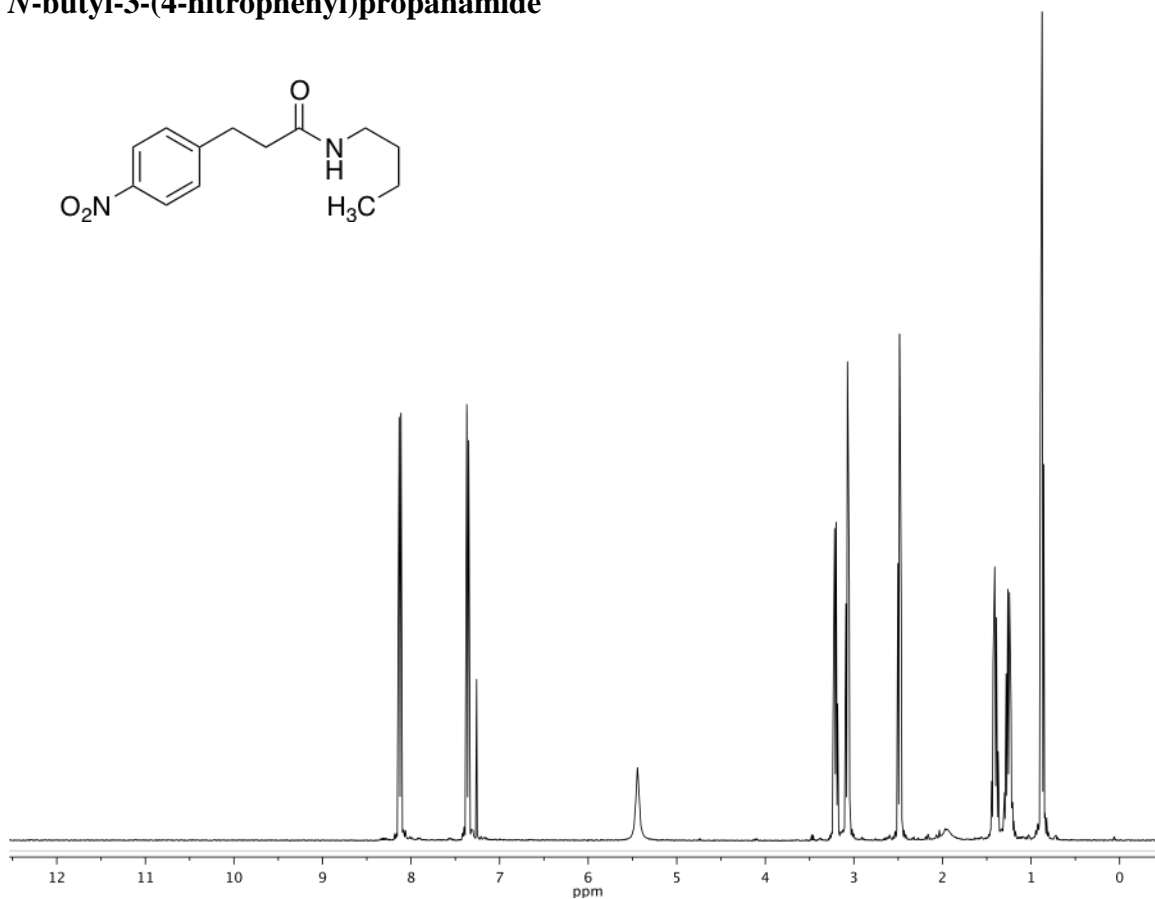
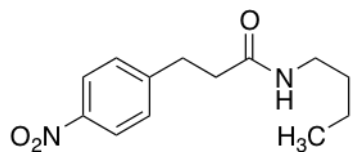
2-(4-bromophenyl)-1H-benzo[d]imidazole



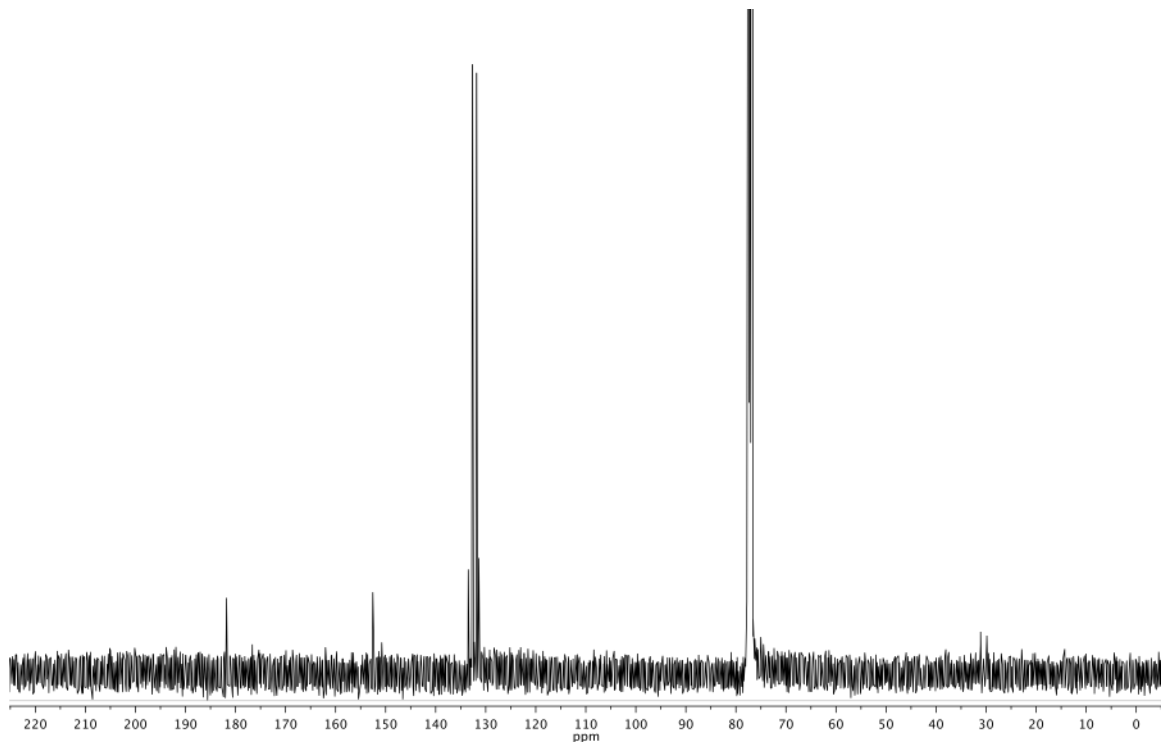
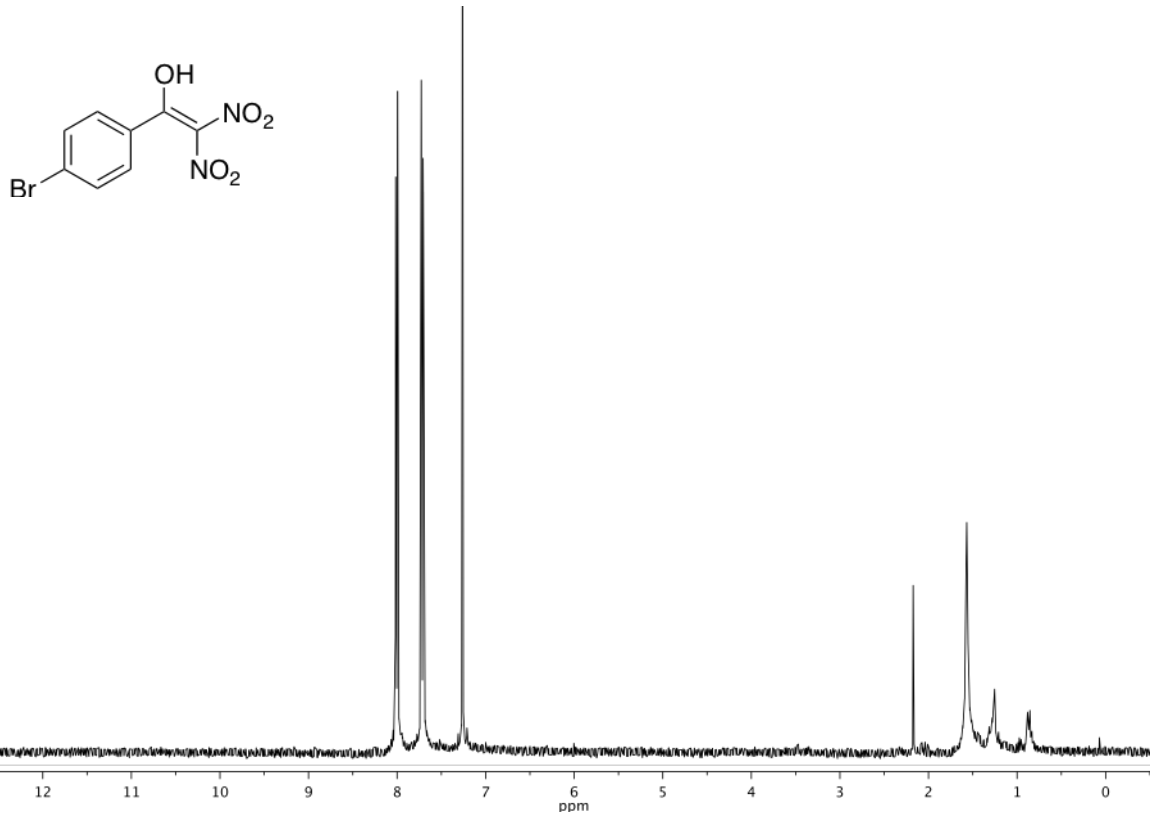
***N*-benzylpivalamide**



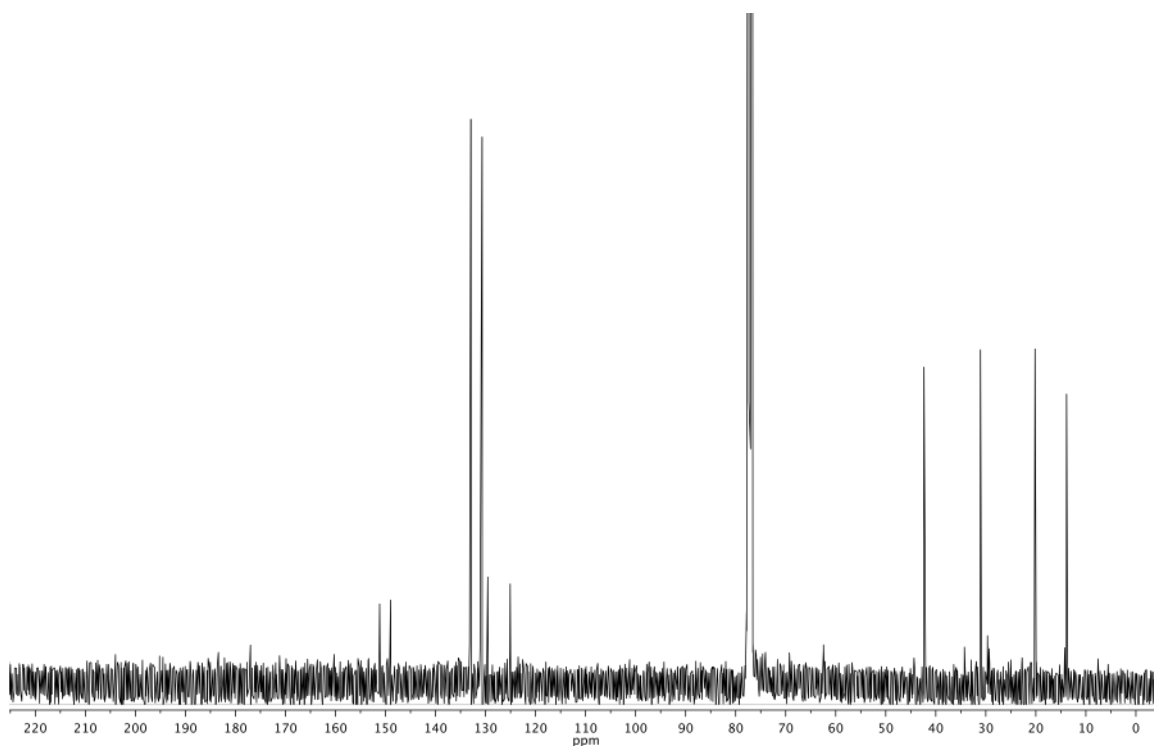
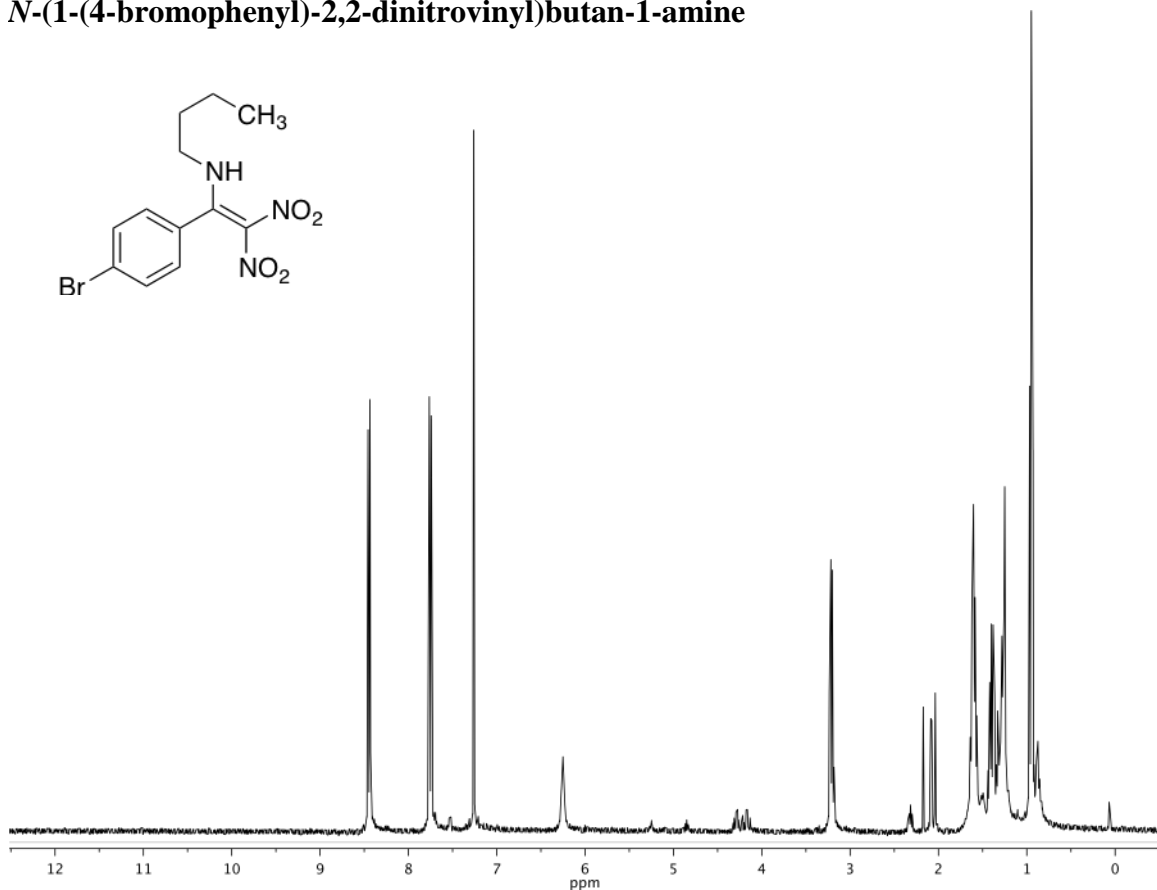
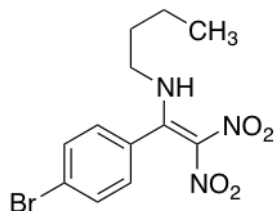
***N*-butyl-3-(4-nitrophenyl)propanamide**



1-(4-bromophenyl)-2,2-dinitroethenol



***N*-(1-(4-bromophenyl)-2,2-dinitrovinyl)butan-1-amine**



Chapter 4

Structure-activity relationship of a triphenyl scaffold for the LasR receptor in *Pseudomonas aeruginosa*

Introduction

Due to the array of medically relevant cellular processes that are under the control of LuxR-type quorum sensing circuits, significant effort has been directed toward the identification of antagonist molecules in several different bacterial pathogens¹⁻³. These efforts have led to the identification of antagonists from natural sources⁴, diversity-oriented compound libraries⁵⁻⁶, and focused library synthesis⁷⁻⁸. The most broadly explored class of LuxR-type receptor antagonists are based on the structural features found in the native HSLs, maintaining the homoserine lactone while changing the functionality of the acyl-tail. Some initial attempts to inhibit HSL-mediated quorum sensing in Gram-negative bacteria have yielded promising results. In studies of *P. aeruginosa*,⁹ a significant bacterial pathogen associated with cystic fibrosis lung infection, bacterial keratitis (eye infection), and third degree burn associated skin infections, several antagonists have been identified that inhibit the HSL receptor, LasR¹⁰⁻¹².

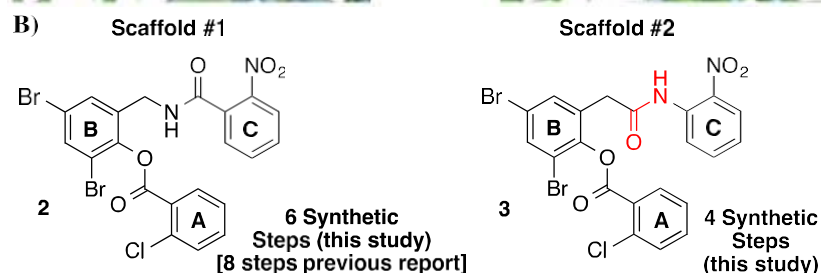
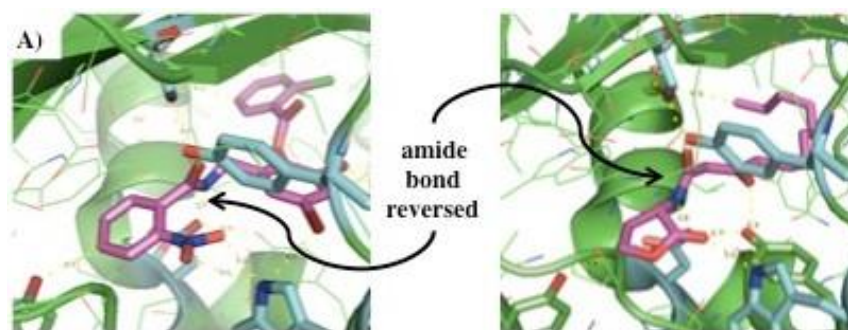
A major obstacle that remains in the development of an anti-quorum sensing strategy targeting LasR and other LuxR-type receptors is ligand potency¹⁰. The high levels of affinity and specificity that the receptor displays for its native HSL ligand complicates this challenge. As the result, studies of antagonism (inhibition) are typically performed using synthase mutants where the native autoinducer is added exogenously at minimal concentrations. The approach of using synthase mutants with minimal concentrations of the quorum sensing agonist provides valuable information about

antagonism of LuxR-type receptors but is misleading in terms of potency as the systems studied are often not representative of wild-type bacteria. Strategies to overcome the limitation of inhibitor potency are expected to be significant in the development of anti-quorum sensing therapeutics. Further, many of the inhibitors that have been identified maintain the physiologically labile homoserine lactone functionality, limiting the potential of these antagonists for development as therapeutic agents.

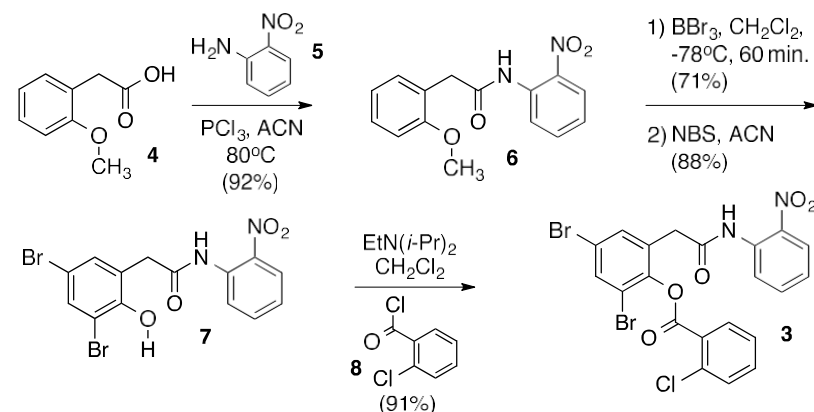
The inhibition of quorum sensing with small molecules offers a unique strategy for the treatment and prevention of a number of acute and chronic bacterial infections, a fact that is of particular significance given the rapid and ongoing spread of antimicrobial-resistant bacteria^{2,13,14}. Research in this area has been defined as a Category C Priority by the NIAID¹⁵. Through the inhibition of quorum sensing, control over expression of virulence factors and biofilm formation is achieved, rendering the bacteria benign while not directly affecting viability. This anti-infective approach is conceptually distinct from traditional approaches for the treatment of bacterial infection that typically utilize bactericidal or bacteriostatic molecules, targeting critical cellular processes. As exemplified by the spread of bacterial resistance, these treatments provide a considerable growth advantage to bacteria that can resist the drug. Contrasting this approach, the inhibition of quorum sensing does not affect cellular viability, decreasing the growth advantage of resistance¹⁶. Rather, this approach targets cellular signaling, inhibiting the expression of virulence factors necessary for successful infection, rendering the bacteria benign until the hosts immune system can clear the pathogen^{2,17-19}.

Recently a highly potent activator of quorum-sensing in *P. aeruginosa* was identified from a high-throughput screen (2, Figure 2)². While the activation of virulence

factor expression in this bacterial pathogen is not therapeutically desirable our rationale to obtain the desired **inhibitory** *function* for this *potent* agonist through analog synthesis is based on precedent. Most notably, a large number of inhibitors have been discovered by systematic modification of HSLs, molecules which serve as natural QS activators. The agonist discovered (2) bears many structural and pharmacological properties that make it superior to HSLs as a lead compound for the development of an anti-virulence therapy, including the absence of a metabolically labile homoserine lactone. Additionally, the potency of this molecule for activation of LasR exceeds the potency of the natural signaling molecule and compounds of this structure type have never been systematically analyzed for the effect of their structure-activity relationships (SARs)⁵⁻²⁰. Accordingly, our goal is to take advantage of the high *potency* and the more desirable pharmacological properties of this lead compound and optimize the structure to possess the *function* that we desire, the inhibition of virulence.



C) Synthesis of Scaffold #1:



Synthesis of Scaffold #2:

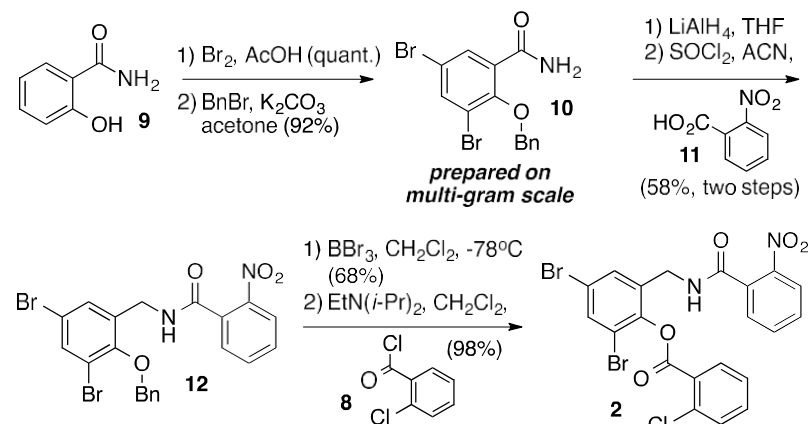


Figure 19. A) Detail of the crystal structure of 3-oxo-C12-HSL (PDB 3IX3) and 2 complexed to LasR (PDB 3IX4). B) Two scaffolds targeted for library synthesis and structure-activity relationship studies. C) Modular chemical synthesis pathways for library assembly.

Results and Discussion

Synthesis. Challenging our efforts toward the goal of identifying inhibitors of LasR based on the structure of **2** is the number of synthetic steps required for its assembly (Figure 2B). To prepare a library of molecules related to **2** requires a more efficient synthetic route. Identification of an effective approach to the synthesis of our target molecules was informed by examination of the recently published crystal structure of the QS receptor in *P. aeruginosa*, LasR, in the presence of **2**²¹. Analysis of the binding pocket for the ligand suggested that a subtle structural change in the orientation of the amide bond in **2** (Figure 2B, highlighted in red) may be tolerated.

Based on these target scaffolds, we have successfully identified two efficient and modular synthetic routes to analogs containing the core scaffold as in **2** (Scaffold #1) analogs containing the core scaffold as in **3** (Scaffold #2) We have begun to systematically optimize the structural features of the targeted molecules to modify the *potency* and the *function* of this class of potential anti-virulence therapeutic agents. To date we have prepared and evaluated the biological activity of more than 50 analogs of **2** and **3**. These efforts will be discussed in greater detail below and additional analogs will be prepared to support and expand on our preliminary findings during the timeframe of this proposal.

Analysis of the crystal structure of LasR complexed to **2**²¹ suggests that the two terminal aromatic rings (Figure 2B, labeled “A” and “C”) play an important role by interacting with LasR whereas the central ring appears to play primarily a scaffolding role in ligand binding. Therefore, we have focused our initial efforts on identifying the

structure activity correlations of the pendant ring structures (“A-ring” and “C-ring”) while maintaining the structure of the central ring (“B-ring”). While the two scaffolds differ only in the orientation of one amide bond, we have observed some notable differences in biological activity for analogs prepared on the two different scaffolds which will be discussed further below.

“A-ring” Structure Activity Relationship Studies. To validate our systematic strategy for optimization of the biological properties of **3**, a small library of structural analogs were prepared. Reaction of intermediate **7** (Figure 2) with a series of structurally related acid chlorides (analogous to **8**) provided library of “A-ring” analogs (Table 1). From this series of structural analogs, we observe a consistent dependence of substitution in this ring structure on the *potency* of the molecules. We discovered that substitution in the *ortho*-position of the arene (entries 1, 4, 7, 9, 10, and 13-15) is critical for *potency*. Substitution in the *meta*- or *para*-position of the “A-ring” (entries 2-3, 5-7 and 11-12) leads to the complete loss of *potency* as measured by comparing the EC₅₀ values of the compounds determined using the bacterial reporter strain described earlier. In support of the significance of *ortho*-substitution, an analog was prepared containing chlorine atoms at both of the *ortho*-positions of the “A-ring” (entry 16) increasing the *potency* of this LasR agonist. Interestingly, the activity of the analogs bearing *ortho*-substitution appears to be largely independent of the nature of the substituent. Analogues with electron-withdrawing substituents (halogen, nitro, trifluoromethyl) and electron-donating groups (methyl, methoxy) in the *ortho*-position all are agonists with EC₅₀ values between 0.1 and 1.3 μ M. Generally we find that analogs with substituents in the *ortho*-position are potent agonists whereas the *meta*- or *para*-substituted analogs are universally not active. This

may suggest that the binding pocket in LasR for this portion of the molecule is not able to accommodate substituents in either the *meta*- or *para*-position. Further, the comparable activities of the analogs containing electronically and sterically diverse substituents in the *ortho*-position suggests that this substitution does not have a direct role interacting with the receptor (no specific hydrogen-bonding or electronic interactions with the receptor) but rather may simply play an anchoring role for the overall positioning of the “A-ring”. In support of this hypothesis, we have found that while the nature of the substituent in the *ortho*-position does not lead to significant changes in *potency* (EC₅₀) or *function* (most are agonists) the absence of an *ortho*-substituent results in the complete loss of activity. Entry 18, in which the “A-ring” bears no substitution is completely inactive.

“C-ring” Structure Activity Relationship Series. While most analogs that we have analyzed with changes in the structure of the “A-ring” were found to be either agonists or to have no activity (i.e. changes in *potency*), analogs with structural changes in the “C-ring” (Table 2) have both changes in *potency* and changes in *function* (agonism vs. antagonism). We first assessed the impact of the position of the nitro-substituent on the activity of the molecules (entries 1-3), revealing the necessity of an *ortho*-nitro substituent. We then prepared a series of analogs in which the *ortho*-nitro group on the “C-ring” of the parent compound (**3**) was exchanged for functionality that had been previously found to be a suitable bioisostere of an aromatic nitro group²². While the 2-pyridine was observed to have no agonist activity (entry 4) the di-fluoro bioisostere was found to show enhanced activity as a LasR agonist (entry 5). Introducing additional electron-withdrawing substituents onto the ring (entry 6) had minimal effect on activity however, interestingly, the pyrimidine analog (entry 7) was found to be active as an

agonist. Combining the 2-nitro substitution with a ring nitrogen at the 4-position (entry 8) also provided an agonist of comparable activity to the parent compound. Therefore within the series of aromatic and heteroaromatic analogs of this ring highest agonist activity was noted with the di-fluoro analog (entry 5) and the 2-pyridine and *meta*- and *para*-nitro analogs were found to be inactive. Based on published crystal-structure analysis from which the *ortho*-nitro ring serves the role of a mimic of the homoserine lactone characteristic of this class of signaling molecules, we replaced this ring with a homoserine lactone. Notably, this analog (entry 10) displays significantly enhanced *potency* to the natural LasR signaling molecule, 3-oxo-C12-HSL, with an EC₅₀ value of 0.9 nM.

We next turned our attention to evaluating the structure-activity relationships surrounding changes to the amide bond linking the “C-ring” to the “B-ring” (Table 3). While we found that converting the amide bond into a benzimidazole linker (entry 2) provided an analog with no activity, several sulfonamides we prepared showed potent agonist activity (entries 5 and 6), successfully serving as structural mimics for the amide bond found in the parent compound.

We next turned our attention to evaluation of the role of the orientation of the amide bond linking the “B-ring” and the “C-ring” on the activity of several of the “C-ring” analogs prepared. We selected the new 2-pyridine, di-fluoro and pyrimidine “C-ring” analogs for this analysis as these analogs displayed a range of agonist activities in our initial library. Therefore, we prepared analogs **XX-XX** and evaluated them for both their agonist and antagonist activity in the LasR quorum sensing reporter strain (Figure 2). In our analysis, we found that 2-pyridine analog **XX**, earlier observed to show no

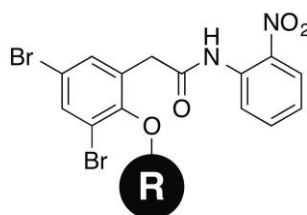
agonist activity against LasR (Table 2, entry 4) possessed potent antagonist activity with an IC_{50} of 42 μ M. The potency of this inhibitor of LasR compares favorably with the “best in class” inhibitors of this quorum sensing circuit and represents one of the most potent inhibitors discovered^{6-8,23-26}. We additionally prepared this analog with the amide linker between the “B-ring” and the “C-ring” reversed and observed that this analog (**XX**) had similarly low LasR agonist and high LasR antagonist activity to **XX**. We next prepared an analog containing a reversed amide corresponding to the potent difluoro arene full LasR agonist **XX** (EC_{50} = 46nM). To our surprise, this analog (**XX**) was not an agonist of LasR, instead it displayed a change in *function*, instead acting as an antagonist of LasR QS with an IC_{50} of 65 μ M (80% maximal inhibition). In contrast to this finding, when we prepared the reversed amide analog of the weak agonist pyrimidine **XX** (EC_{50} = 0.6 μ M) we found the new analog (**XX**) to similarly be a weak agonist of LasR with an EC_{50} of 1.3 μ M.

Given the antagonist activity of the pyridine analog and our previous success with the design of irreversible inhibitors of LasR we evaluated a series of chloropyridines and electron poor arenes as potential irreversible antagonists of LasR (Table 3). While we found two analogs with potent antagonist activity (entries 1,2 and 4) these analogs do not appear to be irreversible inhibitors of LasR based on competition binding assays with the native agonist 3-oxo-C12HSL. While the mechanism of inhibition does not appear to require irreversible attachment to LasR, we note that only analogs containing a chlorine *ortho* to the ester linker showed activity as antagonists. Entry 3, which only has a chlorine *meta* to the ester linkage showed no activity in our assay.

In an effort to enhance the potency of the series of irreversible maleimide

containing LasR antagonists we had previously identified we prepared two targeted inhibitors combining structural changes in the “C-ring” with the appropriate chain-length tether to a maleimide in place of the “A-ring” based on our previous studies. For this investigation we selected the most potent “C-ring” LasR antagonist analog on the reversed amide backbone (amide as in TP-1, **2**) and the most potent “C-ring” LasR agonist analog on the amide backbone as in **3**. We rationalized that we might enhance the antagonist activity of the 2-pyridine analog (**XX**, Figure 2) by combining this feature with the appropriately positioned maleimide for irreversible modification of a conserved cysteine in the LasR ligand binding pocket. In the event, the designed analog **XX** underperformed our expectations, showing antagonist activity however with an increased IC_{50} value (116 μ M with 2-pyridine vs. 1.5 μ M with the 2-nitro analog). We next prepared an analog containing the HSL headgroup as the “C-ring” structure based on an analog which we had observed to provide significant agonist activity against LasR (Table 2, entry 10). We rationalized that if the more potent EC_{50} observed this “C-ring” analog was attributed to a lower K_D , then combining this enhanced binding of the analog effect with the introduction of a maleimide appropriately positioned to irreversibly react with LasR should provide enhanced antagonist activity. In the analysis, the designed analog **XX** did indeed demonstrate potent antagonist activity ($IC_{50} = 13.1\mu$ M). This analog represents one of the most potent antagonists if LasR discovered being comparable to the “best in class” potency we had previously identified for analog **XX**.

Table 1. Structure-activity relationships of "A-ring" analogs.



Entry	Structure	EC ₅₀ (nM)	% Max	Entry	Structure	EC ₅₀ (nM)	% Max
1		371.6±40.7	105	10		757.4±653	85
2		<5000	0	11		<5000	24
3		<5000	0	12		<5000	33
4		271.4±21.5	82	13		246.5±122	45
5		<5000	44	14		489.0±1,280	37
6		<5000	35	15		350.4±138	64
7		1,287±598	76	16		312.6±149	95
8		<5000	39	17		161.3±101	56

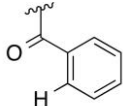
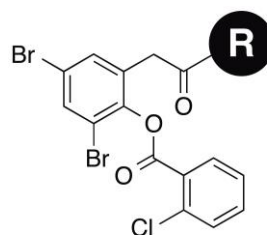
9		157.8±45.6	50	18		<5000	0
---	---	------------	----	----	---	-------	---

Table 2. Structure-activity relationships of “C-ring” analogs.



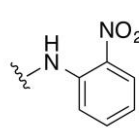
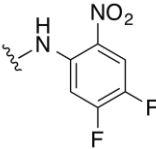
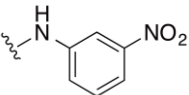
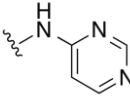
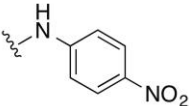
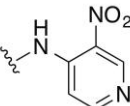
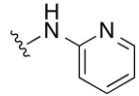
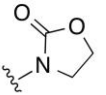
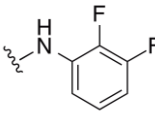
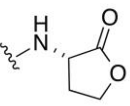
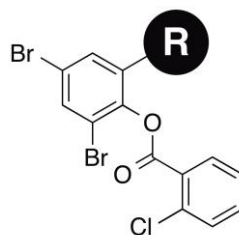
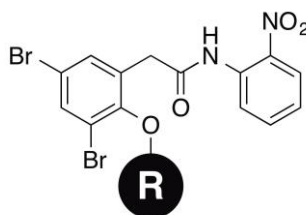
Entry	Structure	EC ₅₀ (nM)	% Max	Entry	Structure	EC ₅₀ (nM)	% Max
1		371±40.7	105	6		335±194	89
2		<5000	0	7		601±464	92
3		<5000	0	8		446±257	112
4		<5000	0	9		<5000	0
5		45.6±2.8	116	10		0.896±2.1	105

Table 3. Structure-activity relationships of alternative linkers.

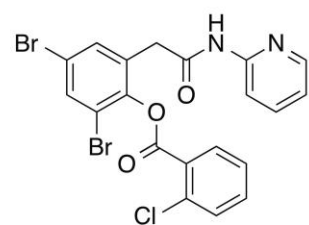


Entry	Structure	EC ₅₀ (nM)	% Max	Entry	Structure	EC ₅₀ (nM)	% Max
1		371±40.7	105	4		<5000	0
2		<5000	0	5		25.2±15.2	77
3		xxx	xxx	6		183±48	72

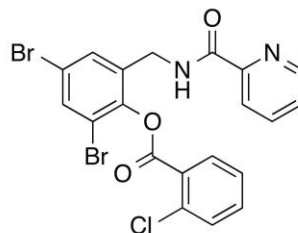
Table 4. Chloropyridine analogs as antagonists of LasR.



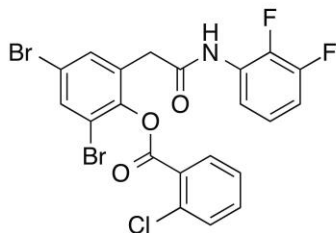
Entry	Structure	IC ₅₀ (μM)	% Max	Entry	Structure	IC ₅₀ (μM)	% Max
1		7.89±8.5	94	3		<100	50
2		33.9±39	107	4		65.0±110	124



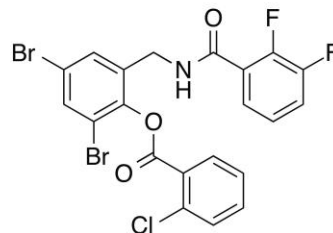
IC₅₀ = 42.0±37.9 (122%)
EC₅₀ > 5000nM (0%)



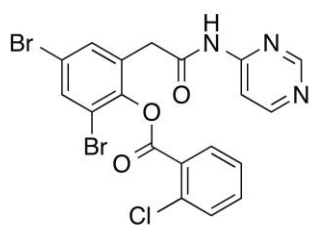
IC₅₀ = 79.3±37.9uM (105%)
EC₅₀ > 5000nM (0%)



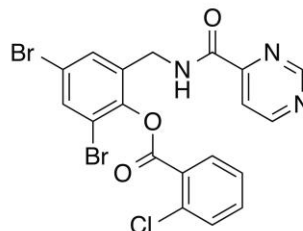
IC₅₀ > 100uM (0%)
EC₅₀=45.6±2.8nM (116%)



IC₅₀ = 64.5±99uM (80%)
EC₅₀ > 5000nM (0%)

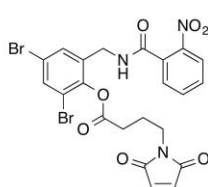


IC₅₀ > 100uM (0%)
EC₅₀=601±464nM (92%)

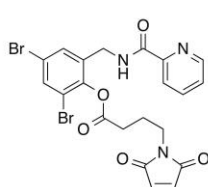


IC₅₀ > 100uM (0%)
EC₅₀=1,630±691nM (90%)

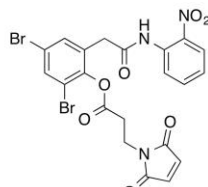
Figure 20. Effect of amide bond configuration and identification of potent LasR antagonists.



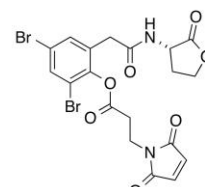
IC₅₀ = 1.5±0.5 (101%) (REF PAPER)



IC₅₀ = 116±46.4uM (164%)



IC₅₀ = 3.6±1.9 (98%) (REF PAPER)



IC₅₀ = 13.1±8.9uM (80%)

Figure 21. Hybrid analogs combining optimized structural features identified in this study with a maleimide for LasR irreversible inhibition.

Conclusion

We have evaluated a series of synthetic libraries of non-natural modulators of LasR-mediated QS in *Pseudomonas aeruginosa*. The compounds prepared are significant as they represent a novel drug-like scaffold for the preparation of inhibitors of bacterial virulence. We have identified several notable structure-activity relationships and in so doing have paved the way for the rational design of potent inhibitors of LasR QS. We have demonstrated several series of analogs which possess the therapeutically desirable LasR antagonist activity and have defined structural features which contribute positively to both this desirable *function* of the ligands evaluated while simultaneously characterizing structural features which positively contribute to the *potency* of the molecules tested.

While I did not prepare all of the compounds presented in this Chapter, I have played an active role in this project since its inception. The summary of our progress described here represents a collaborative effort and I am grateful for the contributions of my co-workers in the Perez group who have worked with me on this project. During the time-period of my Masters thesis research not only did I personally prepare a large percentage of the molecules to complete the analysis described above but I additionally played an active role designing targets, training and trouble-shooting synthetic challenges faced by my co-workers in this project. Therefore, here I present a comprehensive overview of the progress we have made in this area.

Experimental Section

Bacterial reporter strain assay. Our collaborator Prof. Ng developed the biological assay for this project. A reporter strain was first produced using *V. cholera* in which the expression of a luminescent protein is controlled by Hfq-sRNA. For practical purposes, an increase in luminescence (or Lux/OD₆₀₀) corresponds to an increase in inhibition of the Hfq-Qrr complex, whereas compounds that do not effect this protein-RNA interaction do not generate luminescence. To prepare for the assay, an overnight culture of the *V. cholera* reporter strain was incubated at 30 °C in LB media containing 100 µg/mL of Kanamycin and 5 µg/mL of Tetracyclin. Following a 1:50 dilution of this culture into the same LB media, 175 µL was placed into each well of a clear bottom 96-well plate. Next, 10.5 µL of a 10 mM solution of each compound in DMSO was added in triplicate to the wells in the first column. A 2.4 fold dilution was then performed by transferring 125 µL from the first column to the next, and repeating this down the entire plate. Plates were incubated at 30 °C and luminescence (Lux) and OD₆₀₀ were read at 4, 5 and 6 hours. Dose response curves were generated using Prism software, and were plotted as Lux/OD₆₀₀ vs. log[conc.].

General chemistry. All reagents and solvents were obtained from commercial sources and used without further purification or drying. Reactions were performed under a nitrogen gas atmosphere in flame-dried glassware. Unless otherwise noted, compounds were not purified. ¹H and ¹³C NMR data was taken on a Varian AS400 (400 MHz), with chemical shifts being displayed in a ppm scale referenced to residual chloroform.

3,5-dibromo-2-hydroxybenzamide. Salicylamide (10.0 g, 72.9 mmol) was dissolved in glacial acetic acid (146 mL, 0.5 M) and Br₂ (11.2 mL, 218.7 mmol) was added dropwise. The reaction stirred overnight at room temperature and then was quenched with water (500 mL). Product was filtered and washed with a small amount of water and then dried in a dessicator, affording 20.2 g of the desired product, which was used crude in the subsequent step, 93.5% yield.

2-(benzyloxy)-3,5-dibromobenzamide. 3,5-dibromo-2-hydroxybenzamide (10.0 g, 33.7 mmol) was dissolved in acetone (337 mL, 0.1 M) and K₂CO₃ (5.58 g, 40.4 mmol) was added, followed by benzyl bromide (4.80 mL, 40.4 mmol) dropwise. The mixture was stirred at reflux overnight and then was cooled to room temperature. Potassium carbonate was filtered off (filtrate was washed with more acetone) and the solvent was removed in vacuo. The product was recrystallized in acetone, affording 11.3 g of the desired product, 87.1% yield.

(2-(benzyloxy)-3,5-dibromophenyl)methanamine. 2-(benzyloxy)-3,5-dibromobenzamide (1.0 g, 2.58 mmol) was dissolved in BH₃·THF (13.24 mL, 13.24 mmol) under N₂ and the mixture was heated to reflux. The reaction stirred for 48 h at 75 °C and was monitored by TLC (10 mL additional BH₃·THF was added at 30 h). Methanol (10 mL x 2) was added dropwise to quench the reaction, and then the solvent was removed in vacuo. The product was used crude in the subsequent step without purification, quant. yield. ¹H NMR (400 MHz, DMSO-*d*₆) δ 7.95 (d, *J* = 2.5 Hz, 1H), 7.91 (s, 1H), 7.74 (s, 1H), 7.60 (d, *J* = 2.4 Hz, 1H), 7.48 – 7.42 (m, 2H), 7.40 – 7.29 (m, 3H), 4.95 (s, 2H), 4.36 (t, 2H). ¹³C NMR (101 MHz, DMSO-*d*₆) δ 151.79, 136.32, 136.20, 134.68, 131.19, 128.40, 128.39, 119.03, 116.67, 60.79, 29.25.

***N*-(2-(benzyloxy)-3,5-dibromobenzyl)-2-nitrobenzamide.** 2-nitrobenzoic acid (534.8 mg, 3.20 mmol) was dissolved in CH₂Cl₂ and the solution was cooled to 0 °C under N₂. Oxalyl chloride (0.550 mL, 6.40 mmol) was added dropwise, followed by DMF (1 drop). The reaction was allowed to warm to room temperature as it stirred for 2 h. Solvent and excess oxalyl chloride was removed in vacuo and then the residue was resuspended in CH₂Cl₂. This acid chloride was added dropwise to a solution of (2-(benzyloxy)-3,5-dibromophenyl)methanamine (655 mg, 1.60 mmol) in CH₂Cl₂ (32 mL, 0.1 M). Triethylamine (1.56 mL, 11.2 mmol) was added, followed by DMAP (cat.) and the mixture stirred overnight at room temperature. After quenching the reaction with water (25 mL), more CH₂Cl₂ was added (50 mL) and the organic layer was washed with HCl (50 mL, 1 M), sat. NaHCO₃ (50 mL) and then brine (50 mL), and then was dried over Na₂SO₄. Purification via silica-gel column chromatography (product elutes around 30% EtOAc) afforded 354 mg of the desired product, 42.5% yield. ¹H NMR (400 MHz, CDCl₃) δ 8.04 (dd, 1H), 7.69 (d, *J* = 2.4 Hz, 1H), 7.66 – 7.59 (m, 1H), 7.59 – 7.53 (m, 2H), 7.44 – 7.40 (m, 2H), 7.37 – 7.29 (m, 3H), 7.26 – 7.20 (m, 1H), 5.81 (t, *J* = 6.1 Hz, 1H), 5.05 (s, 2H), 4.46 (d, *J* = 6.1 Hz, 2H). ¹³C NMR (101 MHz, CDCl₃) δ 166.46, 153.03, 146.43, 136.07, 135.70, 134.99, 133.83, 132.54, 132.45, 130.73, 129.03, 128.89, 128.87, 128.75, 124.72, 118.29, 117.99, 75.85, 39.21.

***N*-(3,5-dibromo-2-hydroxybenzyl)-2-nitrobenzamide.** *N*-(2-(benzyloxy)-3,5-dibromobenzyl)-2-nitrobenzamide (354 mg, 0.681 mmol) was dissolved in CH₂Cl₂ (4.54 mL, 0.15 M) and cooled to -78 °C in a dry ice/acetone bath. BBr₃ (65 μL, 0.681 mmol) was added dropwise and the mixture stirred for 3 h while the temperature was kept between -20 and -60 °C. The reaction was quenched with sat. NaHCO₃ (25 mL) and was

extracted with CH₂Cl₂ (50 mL). This organic layer was washed with brine and then dried over Na₂SO₄. Purification via silica-gel column chromatography (product elutes around 40% EtOAc) afforded 129.5 mg of the desired product, 30.2% yield. ¹H NMR (400 MHz, DMSO-*d*₆) δ 9.25 (t, *J* = 6.2 Hz, 1H), 7.99 (d, *J* = 8.0 Hz, 1H), 7.75 (t, *J* = 7.5 Hz, 1H), 7.70 – 7.56 (m, 3H), 7.34 (d, *J* = 2.2 Hz, 1H), 4.37 (d, *J* = 5.1 Hz, 2H). ¹³C NMR (101 MHz, DMSO-*d*₆) δ 166.33, 151.20, 147.18, 133.78, 133.02, 131.85, 131.14, 130.27, 130.03, 129.20, 124.28, 112.36, 110.97, 38.51.

2-(2-methoxyphenyl)-*N*-(2-nitrophenyl)acetamide. 2-methoxyphenyl acetic acid (6.75 g, 40.62 mmol) and 2-nitroaniline (3.76 g, 27.07 mmol) were dissolved in ACN (90 mL, 0.3 M). Thionyl chloride (2.86 mL, 40.62 mmol) was added dropwise and the mixture stirred at reflux for 24 h. Solvent was removed in vacuo and the residue was resuspended in EtOAc (150 mL) and washed with sat. NaHCO₃ and then brine. After drying over Na₂SO₄, the product was purified via silica-gel column chromatography (product elutes around 30% EtOAc) affording 5.313 g of the desired product, 68.6% yield. ¹H NMR (400 MHz, CDCl₃) δ 10.37 (s, 1H), 8.76 (dd, *J* = 8.6, 1.3 Hz, 1H), 8.12 (dd, *J* = 8.5, 1.6 Hz, 1H), 7.64 – 7.53 (m, 1H), 7.39 – 7.27 (m, 2H), 7.18 – 7.07 (m, 1H), 7.04 – 6.93 (m, 2H), 3.91 (s, 3H), 3.82 (s, 2H). ¹³C NMR (101 MHz, CDCl₃) δ 170.72, 157.24, 136.58, 135.73, 134.97, 131.43, 129.54, 125.65, 123.09, 122.45, 122.13, 121.19, 110.86, 55.50, 40.69.

2-(2-hydroxyphenyl)-*N*-(2-nitrophenyl)acetamide. 2-(2-methoxyphenyl)-*N*-(2-nitrophenyl)acetamide (6.927 g, 24.2 mmol) was dissolved in CH₂Cl₂ (161.3 mL, 0.15 M) and cooled to -78 °C in a dry ice/acetone bath. BBr₃ (2.29 mL, 24.2 mmol) was added dropwise and the mixture stirred for 4 h while the temperature was kept between -20 and

-60 °C. The reaction was quenched with sat. NaHCO₃ (100 mL) and was extracted with more CH₂Cl₂ (100 mL). This organic layer was washed with brine and then dried over Na₂SO₄. Purification via silica-gel column chromatography (product elutes around 40% EtOAc) afforded 3.98 g of the desired product, 60.5% yield. ¹H NMR (400 MHz, CDCl₃) δ 10.60 (s, 1H), 8.72 (dd, *J* = 8.6, 1.3 Hz, 1H), 8.16 (dd, *J* = 8.4, 1.6 Hz, 1H), 7.66 – 7.59 (m, 1H), 7.50 (s, 1H), 7.24 – 7.13 (m, 3H), 6.98 – 6.90 (m, 2H), 3.84 (s, 2H). ¹³C NMR (101 MHz, CDCl₃) δ 171.92, 154.90, 136.82, 136.01, 134.33, 131.33, 129.68, 125.84, 123.92, 122.63, 121.28, 120.58, 117.08, 41.86.

2-(3,5-dibromo-2-hydroxyphenyl)-*N*-(2-nitrophenyl)acetamide. 2-(2-hydroxyphenyl)-*N*-(2-nitrophenyl)acetamide (2.363 g, 8.68 mmol) was dissolved in glacial acetic acid (173.6 mL, 0.05 M) and Br₂ (1.33 mL, 26.0 mmol) was added dropwise. The reaction stirred for 1 h at room temperature and then was quenched with water (100 mL). The product was extracted with CH₂Cl₂ (50 mL x 3) and then the combined organic layers were washed with sat. NaHCO₃ and then brine, and then dried over Na₂SO₄. Purification via silica-gel column chromatography (product elutes around 40% EtOAc) afforded 3.34 g of the desired product, 89.5% yield. ¹H NMR (400 MHz, CDCl₃) δ 10.58 (s, 1H), 8.73 (dd, *J* = 8.5, 1.3 Hz, 1H), 8.19 (dd, *J* = 8.5, 1.6 Hz, 1H), 7.67 – 7.60 (m, 1H), 7.59 (d, *J* = 2.3 Hz, 1H), 7.37 (d, *J* = 2.3 Hz, 1H), 7.22 – 7.16 (m, 1H), 6.76 (s, 1H), 3.83 (s, 2H). ¹³C NMR (101 MHz, CDCl₃) δ 169.59, 150.37, 136.68, 136.12, 134.46, 134.19, 133.51, 125.93, 123.89, 123.42, 122.45, 113.01, 111.92, 41.18.

2,4-dibromo-6-(2-((2-nitrophenyl)amino)-2-oxoethyl)phenyl 2-chlorobenzoate. To 2-(3,5-dibromo-2-hydroxyphenyl)-*N*-(2-nitrophenyl)acetamide (53.0 mg, 0.123 mmol) in CH₂Cl₂ (2.46 mL, 0.05 M) under N₂ was added 2-chlorobenzoyl

chloride (19 μL , 0.148 mmol), followed by Et_3N (41 μL , 0.295 mmol) and then DMAP (1.5 mg, 0.0123 mmol). The mixture was allowed to stir overnight at room temperature and then was diluted with CH_2Cl_2 (50 mL) and washed with HCl (25 mL, 1 M), sat. NaHCO_3 (25 mL) and then brine (25 mL). After drying over Na_2SO_4 , the material was purified via silica-gel flash chromatography, affording XX mg of the desired product (XX% yield). $^1\text{H-NMR}$ (500MHz, CDCl_3) δ 10.32 (s, 1H), 8.67 (dd, $J = 8.5, 1.1$ Hz, 1H), 8.17-8.10 (m, 2H), 7.81 (d, $J = 2.2$ Hz, 1H), 7.63-7.56 (m, 2H), 7.50-7.45 (m, 2H), 7.36-7.30 (m, 1H), 7.16 (ddd, $J = 8.5, 7.3, 1.3$ Hz, 1H), 3.78 (s, 2H). $^{13}\text{C-NMR}$ (125MHz, CDCl_3) δ 169.8, 162.2, 146.6, 136.6, 136.2, 135.9, 135.1, 134.5, 134.2, 133.8, 132.6, 131.7, 130.7, 127.6, 127.1, 125.9, 123.9, 122.4, 120.6, 118.9, 40.8.

2,4-dibromo-6-(2-((2-nitrophenyl)amino)-2-oxoethyl)phenyl 3-

chlorobenzoate. Prepared according to the procedure provided for 2,4-dibromo-6-(2-((2-nitrophenyl)amino)-2-oxoethyl)phenyl 2-chlorobenzoate, affording XX mg of the desired product (XX% yield). $^1\text{H-NMR}$ (500MHz, CDCl_3) δ 10.35 (s, 1H), 8.68 (d, $J = 8.4$ Hz, 1H), 8.15 (dd, $J = 8.5, 1.3$ Hz, 1H), 8.09-8.05 (m, 1H), 8.02 (d, $J = 7.9$ Hz, 1H), 7.79 (d, $J = 2.2$ Hz, 1H), 7.63 (ddd, $J = 8.5, 7.2, 1.0$ Hz, 1H), 7.60-7.54 (m, 2H), 7.39 (t, $J = 7.9$ Hz, 1H), 7.18 (ddd, $J = 8.4, 7.3, 1.1$ Hz, 1H), 3.71 (s, 2H). $^{13}\text{C-NMR}$ (125MHz, CDCl_3) δ 167.8, 162.6, 146.6, 136.4, 136.3, 135.8, 135.2, 134.6, 134.5, 133.8, 130.8, 130.6, 130.3, 129.7, 128.8, 126.0, 123.9, 122.2, 120.6, 118.8, 41.0.

2,4-dibromo-6-(2-((2-nitrophenyl)amino)-2-oxoethyl)phenyl 4-

chlorobenzoate. Prepared according to the procedure provided for 2,4-dibromo-6-(2-((2-nitrophenyl)amino)-2-oxoethyl)phenyl 2-chlorobenzoate, affording XX mg of the desired product (XX% yield). $^1\text{H-NMR}$ (500MHz, CDCl_3) δ 10.33 (s, 1H), 8.67 (dd, $J = 8.5, 1.1$

Hz, 1H), 8.15 (dd, $J = 8.5, 1.5$ Hz, 1H), 8.08-8.03 (m, 2H), 7.79 (d, $J = 2.2$ Hz, 1H), 7.62 (ddd, $J = 8.6, 7.2, 1.4$ Hz, 1H), 7.57 (d, $J = 2.2$ Hz, 1H), 7.43-7.37 (m, 2H), 7.18 (ddd, $J = 8.5, 7.2, 1.2$ Hz, 1H), 3.71 (s, 3H). $^{13}\text{C-NMR}$ (125MHz, CDCl_3) δ 167.9, 163.0, 146.7, 141.2, 136.4, 136.2, 135.8, 134.5, 133.7, 132.0, 130.8, 129.4, 126.4, 126.0, 123.9, 122.2, 120.5, 118.8, 41.0.

2,4-dibromo-6-(2-((2-nitrophenyl)amino)-2-oxoethyl)phenyl 2-

bromobenzoate. Prepared according to the procedure provided for 2,4-dibromo-6-(2-((2-nitrophenyl)amino)-2-oxoethyl)phenyl 2-chlorobenzoate, affording XX mg of the desired product (XX% yield). $^1\text{H-NMR}$ (500MHz, CDCl_3) δ 10.32 (s, 1H), 8.68 (dd, $J = 8.5, 1.0$ Hz, 1H), 8.17-8.11 (m, 2H), 7.81 (d, $J = 2.2$ Hz, 1H), 7.71-7.66 (m, 1H), 7.63-7.57 (m, 2H), 7.41-7.36 (m, 2H), 7.16 (ddd, $J = 8.5, 7.2, 1.2$ Hz, 1H), 3.79 (s, 2H). $^{13}\text{C-NMR}$ (125MHz, CDCl_3) δ 167.8, 162.7, 146.6, 136.6, 136.1, 135.9, 135.1, 134.5, 134.1, 133.8, 132.7, 130.7, 129.5, 127.6, 126.0, 123.9, 123.1, 122.4, 120.6, 118.8, 40.8.

2,4-dibromo-6-(2-((2-nitrophenyl)amino)-2-oxoethyl)phenyl 3-

bromobenzoate. Prepared according to the procedure provided for 2,4-dibromo-6-(2-((2-nitrophenyl)amino)-2-oxoethyl)phenyl 2-chlorobenzoate, affording XX mg of the desired product (XX% yield). $^1\text{H-NMR}$ (500MHz, CDCl_3) δ 10.35 (s, 1H), 8.68 (dd, $J = 8.5, 1.0$ Hz, 1H), 8.22 (t, $J = 1.0$ Hz, 1H), 8.15 (dd, $J = 8.4, 1.0$ Hz, 1H), 8.06 (d, $J = 8.5$ Hz, 1H), 7.79 (d, $J = 2.2$ Hz, 1H), 7.75-7.71 (m, 1H), 7.64-7.61 (m, 1H), 7.57 (d, $J = 2.1$ Hz, 1H), 7.33 (t, $J = 8.7$ Hz, 1H), 7.18 (t, $J = 8.6$ Hz, 1H), 3.71 (s, 2H). $^{13}\text{C-NMR}$ (125MHz, CDCl_3) δ 167.8, 162.5, 146.6, 137.5, 136.3, 135.8, 134.5, 133.8, 133.5, 130.8, 130.5, 129.9, 129.3, 126.0, 124.0, 123.0, 122.2, 120.6, 118.7, 41.0.

2,4-dibromo-6-(2-((2-nitrophenyl)amino)-2-oxoethyl)phenyl 4-

bromobenzoate. Prepared according to the procedure provided for 2,4-dibromo-6-(2-((2-nitrophenyl)amino)-2-oxoethyl)phenyl 2-chlorobenzoate, affording XX mg of the desired product (XX% yield). ¹H-NMR (500MHz, CDCl₃) δ 10.34 (s, 1H), 8.68 (dd, *J* = 8.5, 0.9 Hz, 1H), 8.16 (dd, *J* = 8.4, 1.0 Hz, 1H), 7.98 (d, *J* = 8.5 Hz), 7.79 (d, *J* = 2.3 Hz, 1H), 7.65-7.54 (m, 3H), 7.18 (t, *J* = 8.4 Hz, 1H), 3.71 (s, 2H). ¹³C-NMR (125MHz, CDCl₃) δ 167.9, 163.1, 146.7, 136.3, 135.8, 134.5, 133.7, 132.4, 132.1, 130.8, 130.0, 126.8, 126.0, 123.9, 122.2, 120.6, 118.8, 41.0.

2,4-dibromo-6-(2-((2-nitrophenyl)amino)-2-oxoethyl)phenyl 2-

fluorobenzoate. Prepared according to the procedure provided for 2,4-dibromo-6-(2-((2-nitrophenyl)amino)-2-oxoethyl)phenyl 2-chlorobenzoate, affording XX mg of the desired product (XX% yield). ¹H-NMR (500MHz, CDCl₃) δ 10.32 (s, 1H), 8.67 (dd, *J* = 8.4, 0.9 Hz, 1H), 8.15 (dd, *J* = 8.5, 1.0 Hz, 1H), 8.06 (dt, *J* = 8.4, 0.9 Hz, 1H), 7.79 (d, *J* = 2.2 Hz, 1H), 7.64-7.55 (m, 2H), 7.24-7.11 (m, 2H), 3.75 (s, 2H). ¹³C-NMR (125MHz, CDCl₃) δ 167.8, 163.7, 161.6, 161.2, 161.1, 136.3, 136.2, 136.2, 135.8, 134.5, 133.7, 133.0, 130.7, 125.9, 124.5, 124.5, 123.9, 122.4, 120.5, 118.8, 117.6, 117.4, 116.7, 116.6, 40.8.

2,4-dibromo-6-(2-((2-nitrophenyl)amino)-2-oxoethyl)phenyl 4-

fluorobenzoate. Prepared according to the procedure provided for 2,4-dibromo-6-(2-((2-nitrophenyl)amino)-2-oxoethyl)phenyl 2-chlorobenzoate, affording XX mg of the desired product (XX% yield). ¹H-NMR (500MHz, CDCl₃) δ 10.33 (s, 1H), 8.67 (d, *J* = 8.3 Hz, 1H), 8.20-8.11 (m, 2H), 7.79 (d, *J* = 1.9 Hz, 1H), 7.62 (t, *J* = 8.4 Hz, 1H), 7.57 (d, *J* = 1.8 Hz, 1H), 7.18 (t, *J* = 8.4 Hz, 1H), 7.14-7.07 (m, 2H), 3.71 (s, 2H). ¹³C-NMR (125MHz,

CDCl₃) δ167.9, 167.8, 165.7, 162.8, 146.7, 136.5, 136.2, 135.7, 134.5, 133.7, 133.5, 133.4, 130.8, 126.0, 124.2, 123.9, 122.2, 120.5, 118.8, 116.4, 116.2, 40.9.

2,4-dibromo-6-(2-((2-nitrophenyl)amino)-2-oxoethyl)phenyl 2-methylbenzoate. Prepared according to the procedure provided for 2,4-dibromo-6-(2-((2-nitrophenyl)amino)-2-oxoethyl)phenyl 2-chlorobenzoate, affording XX mg of the desired product (XX% yield). ¹H-NMR (500MHz, CDCl₃) δ 10.33 (s, 1H), 8.68 (d, *J* = 8.4 Hz, 1H), 8.16 (d, *J* = 8.4 Hz, 1H), 8.13 (dd, *J* = 8.4, 0.9 Hz, 1H), 7.80 (d, *J* = 2.0 Hz, 1H), 7.60 (t, *J* = 8.2 Hz, 1H), 7.57 (d, *J* = 1.9 Hz, 1H), 7.44 (t, *J* = 8.2 Hz, 1H), 7.27-7.13 (m, 2H), 3.73 (s, 2H), 2.53 (s, 3H). ¹³C-NMR (125MHz, CDCl₃) δ168.0, 163.9, 147.0, 142.4, 136.5, 136.1, 135.7, 134.5, 133.7, 133.7, 132.3, 131.8, 130.9, 126.8, 126.2, 125.9, 123.8, 122.2, 120.2, 119.1, 41.0, 22.1.

2,4-dibromo-6-(2-((2-nitrophenyl)amino)-2-oxoethyl)phenyl 3-methylbenzoate. Prepared according to the procedure provided for 2,4-dibromo-6-(2-((2-nitrophenyl)amino)-2-oxoethyl)phenyl 2-chlorobenzoate, affording XX mg of the desired product (XX% yield). ¹H-NMR (500MHz, CDCl₃) δ 10.33 (s, 1H), 8.70 (dd, *J* = 8.4, 0.8 Hz, 1H), 8.13 (dd, *J* = 8.4, 0.9 Hz), 7.94-7.89 (m, 2H), 7.78 (d, *J* = 2.1 Hz, 1H), 7.61 (t, *J* = 8.2 Hz, 1H), 7.56 (d, *J* = 2.1 Hz, 1H), 7.43-7.37 (m, 1H), 7.30 (t, *J* = 8.4 Hz, 1H), 7.16 (t, *J* = 8.4 Hz, 1H), 3.71 (s, 2H), 2.33 (s, 3H). ¹³C-NMR (125MHz, CDCl₃) δ 167.9, 163.9, 146.9, 138.9, 136.4, 136.2, 135.7, 135.4, 134.6, 133.7, 131.1, 130.9, 128.8, 127.9, 127.8, 125.9, 123.8, 122.2, 120.3, 118.9, 40.9, 21.4.

2,4-dibromo-6-(2-((2-nitrophenyl)amino)-2-oxoethyl)phenyl 4-methylbenzoate. Prepared according to the procedure provided for 2,4-dibromo-6-(2-((2-

nitrophenyl)amino)-2-oxoethyl)phenyl 2-chlorobenzoate, affording XX mg of the desired product (XX% yield). ¹H-NMR (500MHz, CDCl₃) δ 10.32 (s, 1H), 8.69 (dd, *J* = 8.4, 0.9 Hz, 1H), 8.13 (dd, *J* = 8.4, 0.9 Hz, 1H), 8.00 (d, *J* = 8.5 Hz, 2H), 7.78 (d, *J* = 2.1 Hz, 1H), 7.61 (t, *J* = 8.3 Hz, 1H), 7.56 (d, *J* = 2.1 Hz, 1H), 7.20 (d, *J* = 8.5 Hz, 2H), 7.17 (t, *J* = 8.4 Hz, 1H), 3.71 (s, 2H), 2.40 (s, 3H). ¹³C-NMR (125MHz, CDCl₃) δ 168.0, 163.8, 146.9, 145.6, 136.4, 136.2, 135.7, 134.6, 133.6, 131.0, 130.8, 129.6, 125.9, 125.1, 123.8, 122.3, 120.2, 118.9, 40.9, 22.1.

2,4-dibromo-6-(2-((2-nitrophenyl)amino)-2-oxoethyl)phenyl 2,6-

dichlorobenzoate. Prepared according to the procedure provided for 2,4-dibromo-6-(2-((2-nitrophenyl)amino)-2-oxoethyl)phenyl 2-chlorobenzoate, affording XX mg of the desired product (XX% yield). ¹H-NMR (500MHz, CDCl₃) δ 10.32 (s, 1H), 8.70 (d, *J* = 8.4 Hz, 1H), 8.16 (dd, *J* = 8.4, 1.0 Hz, 1H), 7.83 (d, *J* = 2.1 Hz, 1H), 7.64-7.57 (m, 2H), 7.41-7.31 (m, 2H), 7.16 (t, *J* = 8.4 Hz, 1H), 3.98 (s, 2H). ¹³C-NMR (125MHz, CDCl₃) δ 167.9, 161.9, 146.1, 136.6, 136.3, 136.2, 134.5, 134.1, 133.0, 132.2, 131.2, 130.5, 128.9, 126.0, 123.9, 122.3, 121.1, 118.6, 40.5.

2,4-dibromo-6-(2-((2-nitrophenyl)amino)-2-oxoethyl)phenyl 2,6-

dibromobenzoate. Prepared according to the procedure provided for 2,4-dibromo-6-(2-((2-nitrophenyl)amino)-2-oxoethyl)phenyl 2-chlorobenzoate, affording XX mg of the desired product (XX% yield). ¹H NMR (400 MHz, CDCl₃) δ 10.32 (s, 1H), 8.72 (dd, *J* = 8.6, 1.3 Hz, 1H), 8.17 (dd, *J* = 8.5, 1.6 Hz, 1H), 7.85 (d, *J* = 2.3 Hz, 1H), 7.65 – 7.59 (m, 4H), 7.24 – 7.13 (m, 2H), 4.06 (s, 2H). ¹³C NMR (101 MHz, CDCl₃) δ 167.97, 145.95, 136.66, 136.20, 136.04, 135.00, 134.45, 133.99, 132.64, 132.56, 130.68, 125.88, 123.79, 122.36, 120.91, 118.45, 40.70. MISSING A C=O & SOME Ar

2,4-dibromo-6-(2-((4,5-difluoro-2-nitrophenyl)amino)-2-oxoethyl)phenyl 2-chlorobenzoate. Prepared according to the procedure provided for 2,4-dibromo-6-(2-((2-nitrophenyl)amino)-2-oxoethyl)phenyl 2-chlorobenzoate, affording XX mg of the desired product (XX% yield). ¹H NMR (400 MHz, CDCl₃) δ 10.41 (s, 1H), 8.74 (dd, *J* = 12.6, 7.5 Hz, 1H), 8.14 (dd, *J* = 7.9, 0.9 Hz, 1H), 8.07 (dd, *J* = 10.1, 7.9 Hz, 1H), 7.85 (d, *J* = 2.3, 0.7 Hz, 1H), 7.59 (d, 1H), 7.55 – 7.49 (m, 2H), 7.41 – 7.35 (m, 1H), 3.81 (s, 2H). ¹³C NMR (101 MHz, CDCl₃) δ 167.90, 162.12, 146.58, 136.02, 135.00, 134.18, 133.71, 132.55, 131.71, 130.14, 127.47, 127.05, 120.64, 118.93, 115.14, 114.93, 111.01, 110.76, 40.75.

2,4-dibromo-6-(2-oxo-2-(pyridin-2-ylamino)ethyl)phenyl 2-chlorobenzoate. Prepared according to the procedure provided for 2,4-dibromo-6-(2-((2-nitrophenyl)amino)-2-oxoethyl)phenyl 2-chlorobenzoate, affording XX mg of the desired product (XX% yield). ¹H NMR (400 MHz, CDCl₃) δ 8.27 – 8.19 (m, 2H), 8.19 – 8.10 (m, 2H), 7.77 (d, *J* = 2.3 Hz, 1H), 7.70 – 7.64 (m, 1H), 7.58 (d, *J* = 2.3 Hz, 1H), 7.53 – 7.48 (m, 2H), 7.40 – 7.32 (m, 1H), 7.05 – 6.99 (m, 1H), 3.73 (s, 2H). ¹³C NMR (101 MHz, CDCl₃) δ 167.23, 162.64, 151.12, 147.96, 146.34, 138.49, 135.47, 135.01, 134.05, 133.44, 132.56, 131.66, 131.15, 127.73, 127.03, 120.48, 120.20, 118.56, 114.21, 39.73.

2,4-dibromo-6-(2-((2-nitrophenyl)amino)-2-oxoethyl)phenyl 2-nitrobenzoate. Prepared according to the procedure provided for 2,4-dibromo-6-(2-((2-nitrophenyl)amino)-2-oxoethyl)phenyl 2-chlorobenzoate, affording XX mg of the desired product (XX% yield). ¹H NMR (400 MHz, CDCl₃) δ 10.35 (s, 1H), 8.68 (dd, *J* = 8.6, 1.3 Hz, 1H), 8.13 (dd, *J* = 8.5, 1.2 Hz, 1H), 8.10 (dd, *J* = 7.4, 1.6 Hz, 1H), 8.01 (dd, *J* = 7.8, 1.4 Hz, 1H), 7.79 (d, 1H), 7.77 – 7.69 (m, 2H), 7.63 (d, 1H), 7.62 – 7.56 (m, 1H), 7.20 –

7.12 (m, 1H), 3.96 (s, 2H). ^{13}C NMR (101 MHz, CDCl_3) δ 167.90, 162.39, 147.98, 145.87, 136.78, 135.86, 135.52, 134.37, 134.16, 133.47, 132.80, 131.18, 130.53, 126.30, 125.74, 124.55, 123.71, 122.51, 120.82, 118.26, 39.85.

2,4-dibromo-6-(2-((2-nitrophenyl)amino)-2-oxoethyl)phenyl benzoate.

Prepared according to the procedure provided for 2,4-dibromo-6-(2-((2-nitrophenyl)amino)-2-oxoethyl)phenyl 2-chlorobenzoate, affording XX mg of the desired product (XX% yield). ^1H NMR (400 MHz, CDCl_3) δ 10.34 (s, 1H), 8.70 (dd, $J = 8.5, 1.3$ Hz, 1H), 8.18 – 8.12 (m, 3H), 7.81 (d, $J = 2.2$ Hz, 1H), 7.67 – 7.57 (m, 3H), 7.49 – 7.41 (m, 2H), 7.22 – 7.15 (m, 1H), 3.74 (s, 2H). ^{13}C NMR (101 MHz, CDCl_3) δ 167.85, 163.71, 136.07, 135.65, 134.50, 134.45, 133.57, 130.85, 130.64, 128.87, 127.94, 125.86, 123.76, 122.23, 120.28, 40.83. POSSIBLY MISSING SOME Ar

2,4-dibromo-6-(2-((2-nitrophenyl)amino)-2-oxoethyl)phenyl 2-methoxybenzoate. Prepared according to the procedure provided for 2,4-dibromo-6-(2-((2-nitrophenyl)amino)-2-oxoethyl)phenyl 2-chlorobenzoate, affording XX mg of the desired product (XX% yield). ^1H NMR (400 MHz, CDCl_3) δ 10.29 (s, 1H), 8.70 (dd, $J = 8.5, 1.3$ Hz, 1H), 8.15 (dd, $J = 8.4, 1.6$ Hz, 1H), 8.02 (dd, $J = 7.8, 1.8$ Hz, 1H), 7.80 (d, $J = 2.3$ Hz, 1H), 7.66 – 7.47 (m, 3H), 7.21 – 7.11 (m, 1H), 7.03 – 6.91 (m, 2H), 3.86 (s, 3H), 3.80 (s, 2H). ^{13}C NMR (101 MHz, CDCl_3) δ 168.09, 162.72, 160.18, 146.93, 136.61, 135.95, 135.60, 135.16, 134.51, 133.54, 132.69, 130.81, 125.82, 123.71, 122.36, 120.40, 120.06, 119.02, 117.52, 112.24, 56.10, 40.65.

2,4-dibromo-6-(2-((2-nitrophenyl)amino)-2-oxoethyl)phenyl 2-iodobenzoate.

Prepared according to the procedure provided for 2,4-dibromo-6-(2-((2-

nitrophenyl)amino)-2-oxoethyl)phenyl 2-chlorobenzoate, affording XX mg of the desired product (XX% yield). ^1H NMR (400 MHz, CDCl_3) δ 10.33 (s, 1H), 8.70 (dt, $J = 8.5, 1.2$ Hz, 1H), 8.23 – 8.13 (m, 2H), 8.05 (dt, $J = 7.9, 1.2$ Hz, 1H), 7.82 (dd, $J = 2.4, 1.1$ Hz, 1H), 7.65 – 7.57 (m, 2H), 7.47 – 7.39 (m, 1H), 7.26 – 7.13 (m, 2H), 3.80 (d, $J = 1.0$ Hz, 2H). ^{13}C NMR (101 MHz, CDCl_3) δ 167.72, 162.75, 142.23, 141.98, 136.02, 135.78, 135.03, 134.46, 134.11, 133.74, 132.34, 132.11, 130.68, 129.74, 128.30, 125.88, 123.80, 122.38, 120.54, 118.79, 40.81.

2,4-dibromo-6-(2-((2-nitrophenyl)amino)-2-oxoethyl)phenyl 3,5-difluoro-2-nitrobenzoate. Prepared according to the procedure provided for 2,4-dibromo-6-(2-((2-nitrophenyl)amino)-2-oxoethyl)phenyl 2-chlorobenzoate, affording XX mg of the desired product (XX% yield). ^1H NMR (400 MHz, CDCl_3) δ 10.34 (s, 1H), 8.67 (dd, $J = 8.6, 1.3$ Hz, 1H), 8.17 (dd, $J = 8.5, 1.6$ Hz, 1H), 7.80 (d, $J = 2.3$ Hz, 1H), 7.75 – 7.71 (m, 1H), 7.67 – 7.59 (m, 2H), 7.32 – 7.26 (m, 1H), 7.23 – 7.17 (m, 1H), 3.78 (s, 2H). ^{13}C NMR (101 MHz, CDCl_3) δ 167.34, 164.11, 163.99, 158.86, 153.63, 145.64, 136.72, 136.08, 135.78, 134.30, 134.10, 133.52, 130.58, 125.85, 123.94, 122.42, 121.33, 118.13, 114.64, 110.54, 40.37.

2,4-dibromo-6-(2-((2-nitrophenyl)amino)-2-oxoethyl)phenyl 2-bromo-3-fluoro-5-nitrobenzoate. Prepared according to the procedure provided for 2,4-dibromo-6-(2-((2-nitrophenyl)amino)-2-oxoethyl)phenyl 2-chlorobenzoate, affording XX mg of the desired product (XX% yield). ^1H NMR (400 MHz, CDCl_3) δ 10.39 (s, 1H), 8.80 (dd, $J = 2.6, 1.5$ Hz, 1H), 8.70 (dd, $J = 8.5, 1.3$ Hz, 1H), 8.21 – 8.15 (m, 2H), 7.86 (d, $J = 2.3$ Hz, 1H), 7.67 – 7.60 (m, 2H), 7.23 – 7.16 (m, 1H), 3.80 (s, 2H). ^{13}C NMR (101 MHz, CDCl_3) δ 167.40, 161.16, 160.05, 158.65, 147.33, 146.06, 136.24, 136.01, 134.32,

134.00, 132.53, 130.44, 125.94, 124.02, 122.51, 122.19, 121.25, 118.48, 115.32, 115.04, 41.16.

(S)-2,4-dibromo-6-(2-oxo-2-((2-oxotetrahydrofuran-3-yl)amino)ethyl)phenyl 2-chlorobenzoate. Prepared according to the procedure provided for 2,4-dibromo-6-(2-((2-nitrophenyl)amino)-2-oxoethyl)phenyl 2-chlorobenzoate, affording XX mg of the desired product (XX% yield). ¹H NMR (400 MHz, CDCl₃) δ 8.21 (dd, *J* = 7.9, 1.2 Hz, 1H), 7.77 (dd, *J* = 2.3, 1.2 Hz, 1H), 7.59 – 7.53 (m, 3H), 7.47 – 7.40 (m, 1H), 6.18 (s, 1H), 4.55 – 4.35 (m, 2H), 4.29 – 4.14 (m, 1H), 3.61 (s, 2H), 2.76 – 2.61 (m, 1H), 2.16 – 1.99 (m, 1H). ¹³C NMR (101 MHz, CDCl₃) δ 174.76, 169.16, 135.45, 135.02, 134.32, 133.47, 132.70, 131.78, 131.23, 127.48, 127.21, 120.57, 118.45, 66.07, 49.53, 38.19, 29.81.

2,4-dibromo-6-(2-((3-nitropyridin-4-yl)amino)-2-oxoethyl)phenyl 2-chlorobenzoate. Prepared according to the procedure provided for 2,4-dibromo-6-(2-((2-nitrophenyl)amino)-2-oxoethyl)phenyl 2-chlorobenzoate, affording XX mg of the desired product (XX% yield). ¹H NMR (400 MHz, CDCl₃) δ 10.50 (s, 1H), 9.33 (s, 1H), 8.67 (s, 2H), 8.13 (dd, 1H), 7.86 (d, *J* = 2.2 Hz, 1H), 7.59 (d, *J* = 2.3 Hz, 1H), 7.56 – 7.47 (m, 2H), 7.41 – 7.34 (m, 1H), 3.84 (s, 2H). ¹³C NMR (101 MHz, CDCl₃) δ 168.31, 162.10, 156.31, 155.69, 136.16, 134.22, 133.69, 132.54, 131.72, 129.85, 129.27, 128.07, 127.41, 127.06, 120.70, 118.99, 114.62, 40.90.

2,4-dibromo-6-(2-oxo-2-(pyrimidin-4-ylamino)ethyl)phenyl 2-chlorobenzoate. Prepared according to the procedure provided for 2,4-dibromo-6-(2-((2-nitrophenyl)amino)-2-oxoethyl)phenyl 2-chlorobenzoate, affording XX mg of the desired

product (XX% yield). ^1H NMR (400 MHz, CDCl_3) δ 8.83 (s, 1H), 8.61 (s, 1H), 8.34 (s, 1H), 8.21 – 8.14 (m, 1H), 8.10 (dd, $J = 5.8, 1.2$ Hz, 1H), 7.80 (d, $J = 2.4$ Hz, 1H), 7.57 (d, $J = 2.4$ Hz, 1H), 7.55 – 7.52 (m, 2H), 7.42 – 7.36 (m, 1H), 3.76 (s, 2H). ^{13}C NMR (101 MHz, CDCl_3) δ 168.19, 162.98, 158.59, 158.49, 156.87, 146.25, 135.79, 135.03, 134.27, 133.32, 132.57, 131.73, 130.43, 127.54, 127.12, 120.67, 118.71, 110.42, 39.79.

2-(3,5-dibromo-2-((2,6-dichlorobenzyl)oxy)phenyl)-N-(2-

nitrophenyl)acetamide. Prepared according to the procedure provided for 2,4-dibromo-6-(2-((2-nitrophenyl)amino)-2-oxoethyl)phenyl 2-chlorobenzoate, affording XX mg of the desired product (XX% yield). ^1H NMR (400 MHz, CDCl_3) δ 10.13 (s, 1H), 8.62 (dd, $J = 8.6, 1.3$ Hz, 1H), 8.13 (dd, $J = 8.5, 1.6$ Hz, 1H), 7.68 (d, $J = 2.4$ Hz, 1H), 7.59 – 7.51 (m, 1H), 7.34 (d, $J = 2.4$ Hz, 1H), 7.25 – 7.21 (m, 2H), 7.17 – 7.07 (m, 2H), 5.45 (s, 2H), 3.54 (s, 2H). ^{13}C NMR (101 MHz, CDCl_3) δ 168.67, 153.71, 137.34, 136.56, 136.06, 135.91, 134.66, 133.49, 132.13, 131.17, 131.00, 128.81, 125.79, 123.52, 122.35, 118.51, 117.84, 70.16, 39.81.

2,4-dibromo-6-(2-((2-nitrophenyl)amino)-2-oxoethyl)phenyl 2,5-

dichloroisonicotinate. Prepared according to the procedure provided for 2,4-dibromo-6-(2-((2-nitrophenyl)amino)-2-oxoethyl)phenyl 2-chlorobenzoate, affording XX mg of the desired product (XX% yield). ^1H NMR (400 MHz, CDCl_3) δ 10.39 (s, 1H), 8.68 (dd, $J = 8.5, 1.3$ Hz, 1H), 8.54 (s, 1H), 8.19 (dd, $J = 8.5, 1.6$ Hz, 1H), 7.95 (d, $J = 0.7$ Hz, 1H), 7.85 (d, $J = 2.2$ Hz, 1H), 7.68 – 7.59 (m, 2H), 7.24 – 7.16 (m, 1H), 3.79 (s, 2H). ^{13}C NMR (101 MHz, CDCl_3) δ 167.37, 165.04, 151.43, 150.39, 145.91, 143.70, 142.51, 138.80, 136.25, 135.99, 134.28, 133.96, 130.32, 125.99, 125.67, 124.04, 122.13, 121.27, 118.40, 40.97.

2,4-dibromo-6-(2-((2,3-difluorophenyl)amino)-2-oxoethyl)phenyl 2-

chlorobenzoate. Prepared according to the procedure provided for 2,4-dibromo-6-(2-((2-nitrophenyl)amino)-2-oxoethyl)phenyl 2-chlorobenzoate, affording XX mg of the desired product (XX% yield). ¹H NMR (400 MHz, Acetone-*d*₆) δ 9.17 (s, 1H), 8.11 (dd, *J* = 7.9, 1.6 Hz, 1H), 7.80 (t, *J* = 7.4 Hz, 1H), 7.76 (d, *J* = 2.3 Hz, 1H), 7.65 (d, *J* = 2.3 Hz, 1H), 7.57 – 7.46 (m, 2H), 7.38 – 7.31 (m, 1H), 7.03 – 6.94 (m, 1H), 6.94 – 6.85 (m, 1H), 3.86 (s, 2H). ¹³C NMR (101 MHz, CDCl₃) δ 167.08, 162.99, 146.01, 135.52, 135.05, 134.31, 133.18, 133.15, 132.57, 131.73, 131.12, 127.83, 127.46, 127.13, 124.21, 120.63, 118.48, 117.08, 112.62, 112.45, 39.66.

2,4-dibromo-6-(2-((2-nitrophenyl)amino)-2-oxoethyl)phenyl 3,6-

dichloropicolinate. Prepared according to the procedure provided for 2,4-dibromo-6-(2-((2-nitrophenyl)amino)-2-oxoethyl)phenyl 2-chlorobenzoate, affording XX mg of the desired product (XX% yield). ¹H NMR (400 MHz, CDCl₃) δ 10.38 (s, 1H), 8.67 (dd, *J* = 8.5, 1.8 Hz, 1H), 8.17 (dd, 1H), 7.83 – 7.78 (m, 2H), 7.65 – 7.58 (m, 2H), 7.46 (dd, *J* = 8.5, 1.4 Hz, 1H), 7.22 – 7.14 (m, 1H), 3.85 (s, 2H). ¹³C NMR (101 MHz, CDCl₃) δ 167.62, 159.73, 149.38, 146.28, 144.97, 141.72, 140.81, 139.18, 136.94, 135.92, 135.78, 134.41, 133.85, 130.49, 128.73, 125.81, 123.86, 122.75, 120.80, 40.42.

2,4-dibromo-6-(2-((2-nitrophenyl)amino)-2-oxoethyl)phenyl 5-fluoro-2-

nitrobenzoate. Prepared according to the procedure provided for 2,4-dibromo-6-(2-((2-nitrophenyl)amino)-2-oxoethyl)phenyl 2-chlorobenzoate, affording XX mg of the desired product (XX% yield). ¹H NMR (400 MHz, CDCl₃) δ 10.36 (s, 1H), 8.68 (dd, *J* = 8.5, 1.3 Hz, 1H), 8.18 – 8.10 (m, 2H), 7.81 (d, *J* = 2.3 Hz, 1H), 7.75 (dd, *J* = 7.7, 2.7 Hz, 1H), 7.64 (d, *J* = 2.3 Hz, 1H), 7.64 – 7.58 (m, 1H), 7.43 – 7.34 (m, 1H), 7.20 – 7.13 (m, 1H),

3.98 (s, 2H). ^{13}C NMR (101 MHz, CDCl_3) δ 167.86, 166.07, 161.41, 145.64, 135.93, 135.62, 134.41, 134.33, 131.20, 127.63, 127.53, 125.81, 123.78, 122.53, 121.10, 119.49, 119.25, 118.20, 117.96, 117.70, 39.87.

2,4-dibromo-6-(2-((2-nitrophenyl)amino)-2-oxoethyl)phenyl 2-bromo-4-fluorobenzoate. Prepared according to the procedure provided for 2,4-dibromo-6-(2-((2-nitrophenyl)amino)-2-oxoethyl)phenyl 2-chlorobenzoate, affording XX mg of the desired product (XX% yield). ^1H NMR (400 MHz, CDCl_3) δ 10.34 (s, 1H), 8.69 (dd, $J = 8.5, 1.3$ Hz, 1H), 8.17 (dd, $J = 8.5, 1.5$ Hz, 1H), 7.99 – 7.92 (m, 1H), 7.83 (d, $J = 2.3$ Hz, 1H), 7.63 – 7.58 (m, 2H), 7.45 – 7.30 (m, 2H), 7.22 – 7.15 (m, 1H), 3.81 (s, 2H). ^{13}C NMR (101 MHz, CDCl_3) δ 167.64, 161.84, 146.40, 138.59, 136.55, 136.08, 135.85, 134.37, 133.80, 131.53, 130.52, 128.88, 128.80, 127.94, 125.89, 123.88, 122.26, 120.84, 120.60, 118.68, 40.80.

2,4-dibromo-6-(2-((3-nitrophenyl)amino)-2-oxoethyl)phenyl 2-chlorobenzoate. Prepared according to the procedure provided for 2,4-dibromo-6-(2-((2-nitrophenyl)amino)-2-oxoethyl)phenyl 2-chlorobenzoate, affording XX mg of the desired product (XX% yield). ^1H NMR (400 MHz, CDCl_3) δ 8.41 (t, $J = 2.2$ Hz, 1H), 8.26 (d, $J = 7.4$ Hz, 1H), 8.02 (s, 1H), 7.93 (d, $J = 8.2$ Hz, 1H), 7.86 (d, $J = 8.1$ Hz, 1H), 7.81 (d, $J = 2.3$ Hz, 1H), 7.62 (d, $J = 2.3$ Hz, 1H), 7.60 – 7.53 (m, 2H), 7.51 – 7.38 (m, 2H), 3.74 (s, 2H).

2,4-dibromo-6-(2-((4-nitrophenyl)amino)-2-oxoethyl)phenyl 2-chlorobenzoate. Prepared according to the procedure provided for 2,4-dibromo-6-(2-((2-nitrophenyl)amino)-2-oxoethyl)phenyl 2-chlorobenzoate, affording XX mg of the desired

product (XX% yield). ^1H NMR (400 MHz, CDCl_3) δ 8.26 (dd, $J = 8.1, 1.5$ Hz, 1H), 8.20 – 8.15 (m, 2H), 8.14 (s, 1H), 7.81 (d, $J = 2.3$ Hz, 1H), 7.74 – 7.67 (m, 2H), 7.64 – 7.54 (m, 3H), 7.50 – 7.42 (m, 1H), 3.74 (s, 2H). ^{13}C NMR (101 MHz, CDCl_3) δ 167.37, 164.71, 145.84, 143.77, 143.73, 135.85, 135.35, 134.81, 133.17, 132.76, 131.93, 130.93, 127.32, 127.00, 125.08, 121.14, 119.31, 118.63, 39.64.

2,4-dibromo-6-(2-oxo-2-((2-oxotetrahydrofuran-3-yl)amino)ethyl)phenyl 4-(2,5-dioxo-2,5-dihydro-1H-pyrrol-1-yl)butanoate. Prepared according to the procedure provided for 2,4-dibromo-6-(2-((2-nitrophenyl)amino)-2-oxoethyl)phenyl 2-chlorobenzoate, affording XX mg of the desired product (XX% yield). ^1H NMR (400 MHz, Chloroform-d) δ 7.67 (d, $J = 2.3$ Hz, 1H), 7.58 (d, $J = 2.3$ Hz, 1H), 7.14 (s, 1H), 6.77 (s, 2H), 4.59 – 4.48 (m, 1H), 4.44 (t, 1H), 4.32 – 4.21 (m, 1H), 3.77 – 3.64 (m, 2H), 2.89 – 2.79 (m, 1H), 2.84 – 2.67 (m, 2H), 2.20 – 2.01 (m, 2H). ^{13}C NMR (101 MHz, Chloroform-d) δ 175.30, 171.77, 170.42, 169.82, 134.90, 134.56, 134.06, 131.72, 120.02, 66.36, 49.73, 37.50, 36.68, 31.16, 30.62, 30.51, 23.69.

2,4-dibromo-6-((2-nitrobenzamido)methyl)phenyl 2-chlorobenzoate. To 2-(benzyloxy)-3,5-dibromophenylmethanamine (64.0 mg, 0.173 mmol) in CH_2Cl_2 (3.45 mL, 0.05 M) under N_2 was added 2-nitrobenzoyl chloride (35.5 mg, 0.191 mmol), followed by Et_3N (58 μL , 0.415 mmol) and then DMAP (2.1 mg, 0.0173 mmol). The mixture was allowed to stir overnight at room temperature and then was diluted with CH_2Cl_2 (50 mL) and washed with HCl (25 mL, 1 M), sat. NaHCO_3 (25 mL) and then brine (25 mL). After drying over Na_2SO_4 , the material was purified via silica-gel flash chromatography, affording XX mg of the desired product (XX% yield). ^1H and ^{13}C -NMR match previously published spectra.

2,4-dibromo-6-(picolinamidomethyl)phenyl 2-chlorobenzoate. Prepared according to the procedure provided for 2,4-dibromo-6-((2 nitrobenzamido)methyl)phenyl 2-chlorobenzoate, affording XX mg of the desired product (XX% yield). ¹H NMR (400 MHz, CDCl₃) δ 8.54 (dd, *J* = 4.7, 1.4 Hz, 1H), 8.45 (s, 1H), 8.21 (dd, *J* = 7.8, 1.1 Hz, 1H), 8.15 (dd, *J* = 7.8, 1.1 Hz, 1H), 7.84 (td, *J* = 7.8, 1.8 Hz, 1H), 7.74 (d, *J* = 2.3 Hz, 1H), 7.58 (d, *J* = 2.3 Hz, 1H), 7.54 (d, 2H), 7.46 – 7.39 (m, 2H), 4.66 (d, *J* = 6.1 Hz, 2H). ¹³C NMR (101 MHz, CDCl₃) δ 164.56, 162.48, 149.41, 148.35, 145.84, 137.52, 135.04, 134.94, 133.99, 132.61, 131.78, 131.65, 127.89, 127.00, 126.59, 122.51, 120.33, 118.12, 38.74.

2,4-dibromo-6-(((2-nitrophenyl)sulfonamido)methyl)phenyl 2-nitrobenzenesulfonate. Prepared according to the procedure provided for 2,4-dibromo-6-((2 nitrobenzamido)methyl)phenyl 2-chlorobenzoate, affording XX mg of the desired product (XX% yield). ¹H NMR (400 MHz, CDCl₃) δ 8.16 (dd, 1H), 8.08 – 8.05 (m, 1H), 7.94 – 7.87 (m, 3H), 7.84 – 7.78 (m, 1H), 7.76 – 7.72 (m, 2H), 7.71 (d, *J* = 2.3 Hz, 1H), 7.61 (d, *J* = 2.3 Hz, 1H), 6.21 (s, 1H), 4.48 (s, 2H). ¹³C NMR (101 MHz, CDCl₃) δ 147.80, 144.20, 136.18, 136.13, 135.12, 133.99, 133.51, 133.35, 133.14, 132.85, 131.98, 131.00, 129.61, 125.78, 125.51, 121.88, 118.12, 43.26.

2,4-dibromo-6-(picolinamidomethyl)phenyl 4-(2,5-dioxo-2,5-dihydro-1H-pyrrol-1-yl)butanoate. Prepared according to the procedure provided for 2,4-dibromo-6-((2 nitrobenzamido)methyl)phenyl 2-chlorobenzoate, affording XX mg of the desired product (XX% yield). ¹H NMR (400 MHz, CDCl₃) δ 8.53 (dd, *J* = 4.8, 1.3 Hz, 1H), 8.41 (s, 1H), 8.19 (dd, *J* = 7.8, 1.2 Hz, 1H), 7.86 (td, *J* = 7.7, 1.7 Hz, 1H), 7.66 (d, *J* = 2.3 Hz, 1H), 7.53 (d, *J* = 2.3 Hz, 1H), 7.47 – 7.39 (m, 1H), 6.72 (s, 2H), 4.59 (d, *J* = 6.4 Hz, 2H),

3.68 (t, $J = 6.7$ Hz, 2H), 2.70 (t, $J = 7.3$ Hz, 2H), 2.10 – 1.98 (m, 2H). ^{13}C NMR (101 MHz, CDCl_3) δ 170.94, 170.02, 164.39, 149.49, 148.32, 146.02, 137.56, 134.94, 134.82, 134.31, 132.05, 126.56, 122.53, 119.96, 118.15, 38.75, 36.98, 31.20, 23.79.

2,4-dibromo-6-(picolinamidomethyl)phenyl 2-nitrobenzoate. Prepared according to the procedure provided for 2,4-dibromo-6-((2-nitrobenzamido)methyl)phenyl 2-chlorobenzoate, affording XX mg of the desired product (XX% yield). ^1H NMR (400 MHz, CDCl_3) δ 8.58 (t, $J = 6.5$ Hz, 1H), 8.55 – 8.50 (m, 1H), 8.19 – 8.12 (m, 2H), 8.02 (dd, $J = 7.7, 1.5$ Hz, 1H), 7.86 – 7.71 (m, 3H), 7.70 (d, $J = 2.3$ Hz, 1H), 7.64 (d, $J = 2.3$ Hz, 1H), 7.44 – 7.39 (m, 1H), 4.75 (d, $J = 6.5$ Hz, 2H). ^{13}C NMR (101 MHz, CDCl_3) δ 164.74, 162.45, 149.46, 148.36, 148.18, 145.10, 137.43, 135.61, 134.89, 133.39, 132.90, 132.19, 130.74, 126.50, 126.17, 124.46, 122.42, 120.79, 117.70, 38.39.

2,4-dibromo-6-((2-nitrobenzamido)methyl)phenyl 2-nitrobenzoate. Prepared according to the procedure provided for 2,4-dibromo-6-((2-nitrobenzamido)methyl)phenyl 2-chlorobenzoate, affording XX mg of the desired product (XX% yield). ^1H NMR (400 MHz, CDCl_3) δ 8.17 (dd, $J = 7.5, 1.6$ Hz, 1H), 8.00 (td, $J = 7.8, 1.3$ Hz, 2H), 7.84 (d, $J = 2.4$ Hz, 1H), 7.83 – 7.75 (m, 2H), 7.75 (d, $J = 2.3$ Hz, 1H), 7.64 (td, $J = 7.5, 1.3$ Hz, 1H), 7.59 – 7.47 (m, 2H), 6.63 (t, $J = 6.1$ Hz, 1H), 4.68 (s, 2H). ^{13}C NMR (101 MHz, CDCl_3) δ 166.66, 162.90, 148.28, 146.81, 145.30, 135.43, 134.56, 133.79, 133.72, 133.62, 133.15, 132.31, 130.88, 130.82, 128.80, 126.00, 124.70, 124.53, 121.00, 117.52, 39.06.

2,4-dibromo-6-((2,3-difluorobenzamido)methyl)phenyl 2-chlorobenzoate.

Prepared according to the procedure provided for 2,4-dibromo-6-((2-nitrobenzamido)methyl)phenyl 2-chlorobenzoate, affording XX mg of the desired product (XX% yield). ¹H NMR (400 MHz, CDCl₃) δ 8.21 (dd, 1H), 7.81 – 7.73 (m, 2H), 7.62 (d, *J* = 2.3 Hz, 1H), 7.57 – 7.53 (m, 2H), 7.46 – 7.40 (m, 1H), 7.36 – 7.27 (m, 1H), 7.21 – 7.14 (m, 1H), 7.04 (t, *J* = 11.4 Hz, 1H), 4.66 (s, 2H). ¹³C NMR (101 MHz, CDCl₃) δ 162.73, 162.47, 145.94, 135.36, 134.98, 134.44, 134.12, 132.55, 132.25, 131.69, 127.75, 127.09, 126.60, 126.57, 124.78, 124.72, 120.83, 120.65, 120.43, 118.16, 39.40.

2,4-dibromo-6-((2-chloro-N-((2-

nitrophenyl)sulfonyl)benzamido)methyl)phenyl 2-chlorobenzoate. Prepared according to the procedure provided for 2,4-dibromo-6-((2-nitrobenzamido)methyl)phenyl 2-chlorobenzoate, affording XX mg of the desired product (XX% yield). ¹H NMR (400 MHz, CDCl₃) δ 8.33 (dd, *J* = 7.9, 1.5 Hz, 1H), 8.12 (dd, *J* = 7.6, 1.1 Hz, 1H), 7.87 (dd, *J* = 7.9, 1.5 Hz, 1H), 7.80 (td, *J* = 7.6, 1.5 Hz, 1H), 7.76 – 7.69 (m, 2H), 7.57 – 7.51 (m, 3H), 7.46 – 7.39 (m, 1H), 7.37 – 7.30 (m, 1H), 7.24 (dd, *J* = 8.2, 1.1 Hz, 1H), 7.18 (td, *J* = 7.5, 1.2 Hz, 1H), 7.15 – 7.10 (m, 1H), 5.08 (s, 2H). ¹³C NMR (101 MHz, CDCl₃) δ 167.61, 165.85, 161.99, 148.04, 145.12, 135.52, 135.35, 135.32, 134.91, 133.83, 133.26, 133.21, 132.52, 132.35, 132.01, 131.90, 131.45, 131.07, 130.07, 127.98, 126.95, 126.86, 126.86, 125.08, 120.26, 118.13, 77.48, 77.16, 76.84, 47.29.

2,4-dibromo-6-(((2-nitrophenyl)sulfonamido)methyl)phenyl 2-

chlorobenzoate. Prepared according to the procedure provided for 2,4-dibromo-6-((2-nitrobenzamido)methyl)phenyl 2-chlorobenzoate, affording XX mg of the desired

product (XX% yield). ^1H NMR (400 MHz, CDCl_3) δ 8.22 (dd, 1H), 8.00 – 7.87 (m, 2H), 7.86 – 7.80 (m, 2H), 7.66 (d, $J = 2.4, 1.0$ Hz, 1H), 7.64 (dd, 1H), 7.41 – 7.27 (m, 2H), 7.06 (t, $J = 6.4$ Hz, 1H), 4.78 (d, $J = 6.4$ Hz, 2H). ^{13}C NMR (101 MHz, CDCl_3) δ 166.97, 148.57, 144.57, 136.76, 136.07, 135.78, 134.50, 133.77, 132.81, 131.94, 131.64, 131.05, 130.45, 130.14, 129.87, 127.19, 125.50, 121.89, 117.98, 39.45.

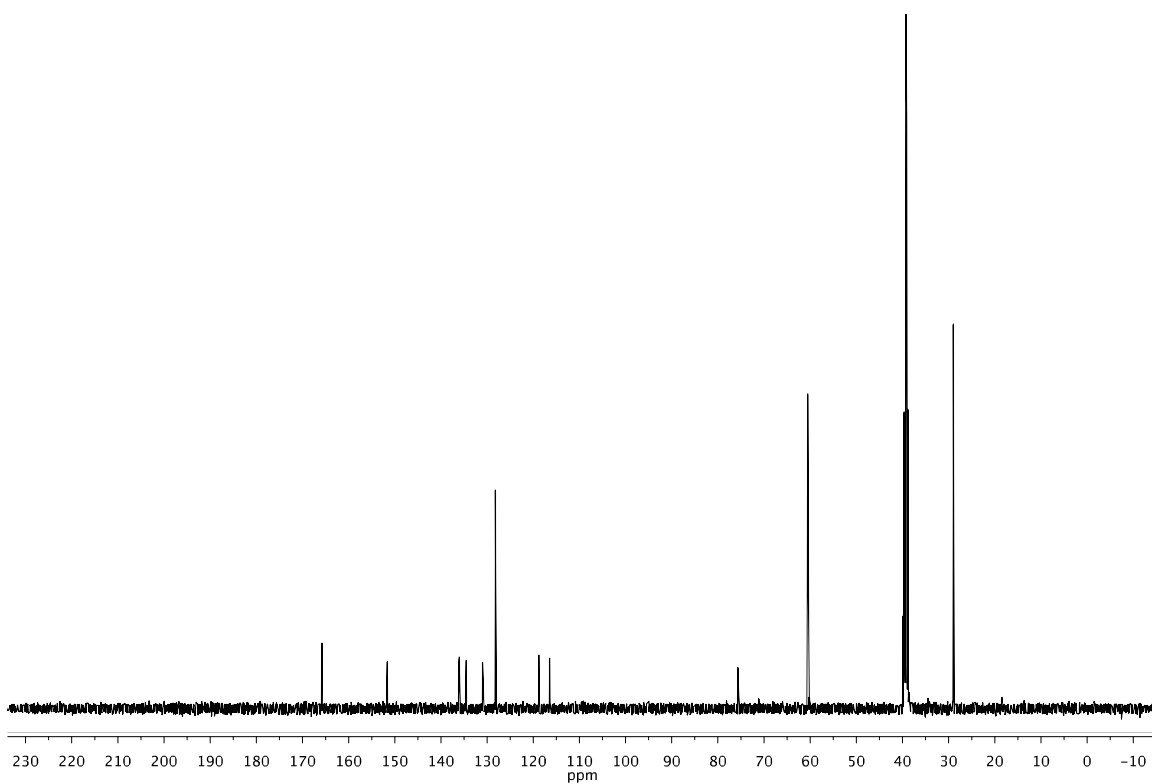
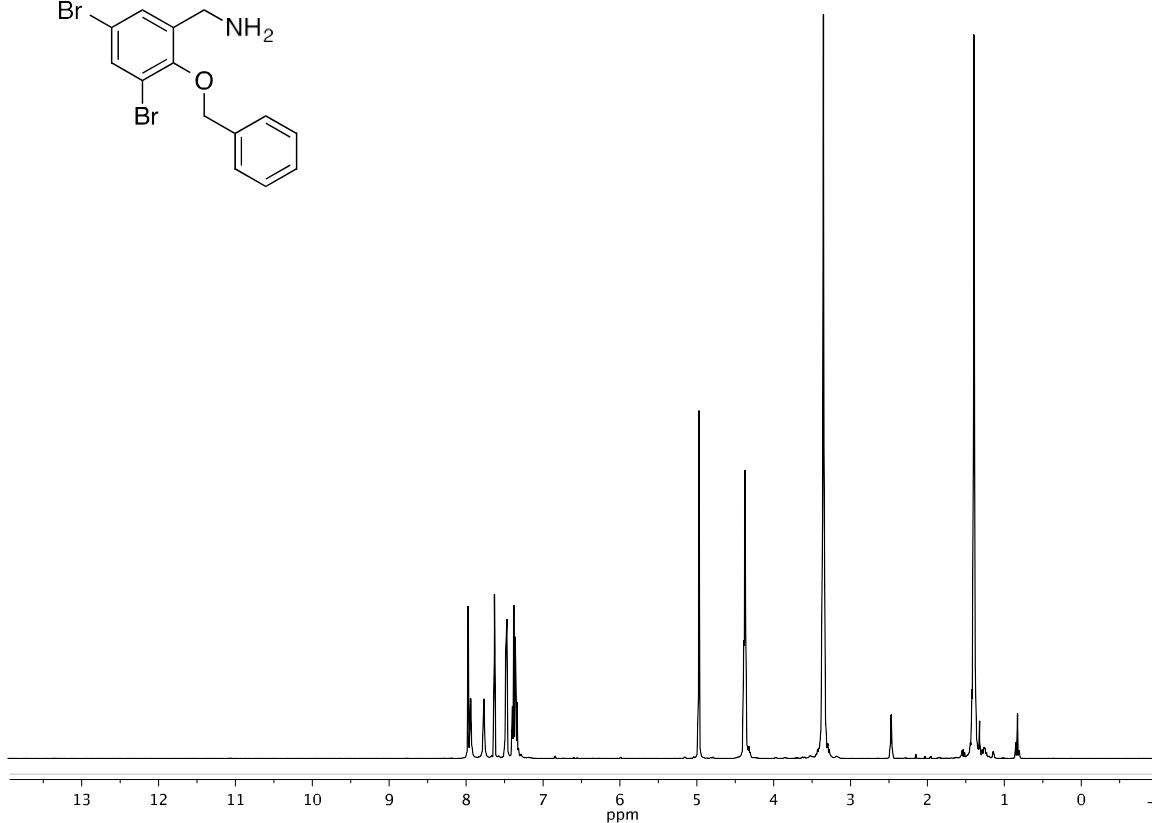
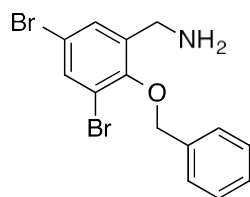
2,4-dibromo-6-(nicotinamidomethyl)phenyl 2-chlorobenzoate. Prepared according to the procedure provided for 2,4-dibromo-6-((2-nitrobenzamido)methyl)phenyl 2-chlorobenzoate, affording XX mg of the desired product (XX% yield). ^1H NMR (400 MHz, CDCl_3) δ 8.97 (s, 1H), 8.71 (s, 1H), 8.21 (dd, 1H), 8.07 (d, $J = 8.1$ Hz, 1H), 7.77 (d, $J = 2.3$ Hz, 1H), 7.62 (d, $J = 2.3$ Hz, 1H), 7.58 – 7.50 (m, 2H), 7.47 – 7.39 (m, 1H), 7.39 – 7.33 (m, 1H), 6.80 (t, 1H), 4.63 (s, 2H). ^{13}C NMR (101 MHz, CDCl_3) δ 165.40, 163.37, 152.55, 148.24, 146.10, 135.58, 135.21, 135.00, 134.32, 132.79, 132.64, 131.74, 127.52, 127.17, 123.63, 120.52, 118.19, 39.50.

2,4-dibromo-6-((pyrimidine-4-carboxamido)methyl)phenyl 2-chlorobenzoate. ^1H NMR (400 MHz, Chloroform-d) δ 9.22 (d, $J = 1.4$ Hz, 1H), 8.96 (d, $J = 5.0$ Hz, 1H), 8.38 (t, 1H), 8.20 (d, 1H), 8.06 (d, 1H), 7.76 (d, $J = 2.3$ Hz, 1H), 7.61 – 7.52 (m, 2H), 7.48 – 7.38 (m, 1H), 4.66 (d, $J = 6.3$ Hz, 2H). ^{13}C NMR (101 MHz, Chloroform-d) δ 162.91, 162.64, 159.41, 157.96, 155.96, 146.08, 135.49, 134.27, 134.21, 132.72, 132.17, 131.77, 127.84, 127.15, 126.84, 120.46, 118.87, 118.39, 39.10.

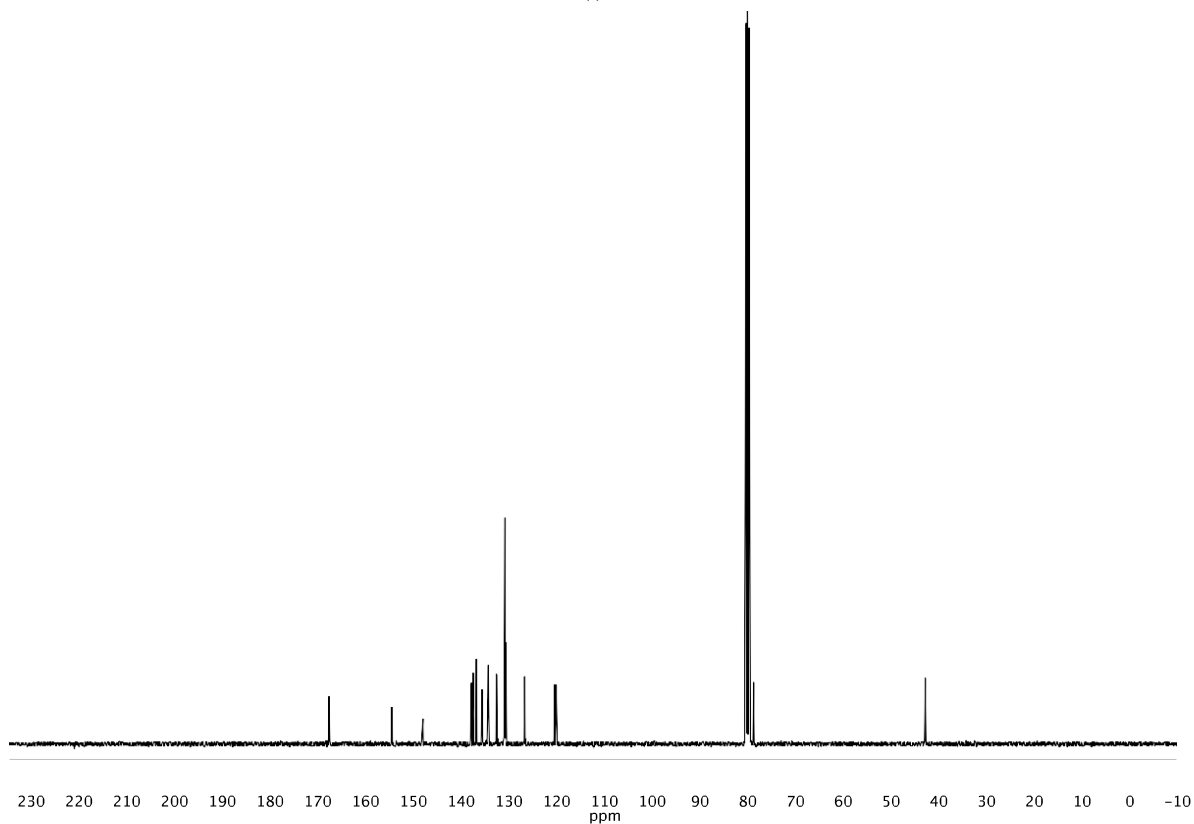
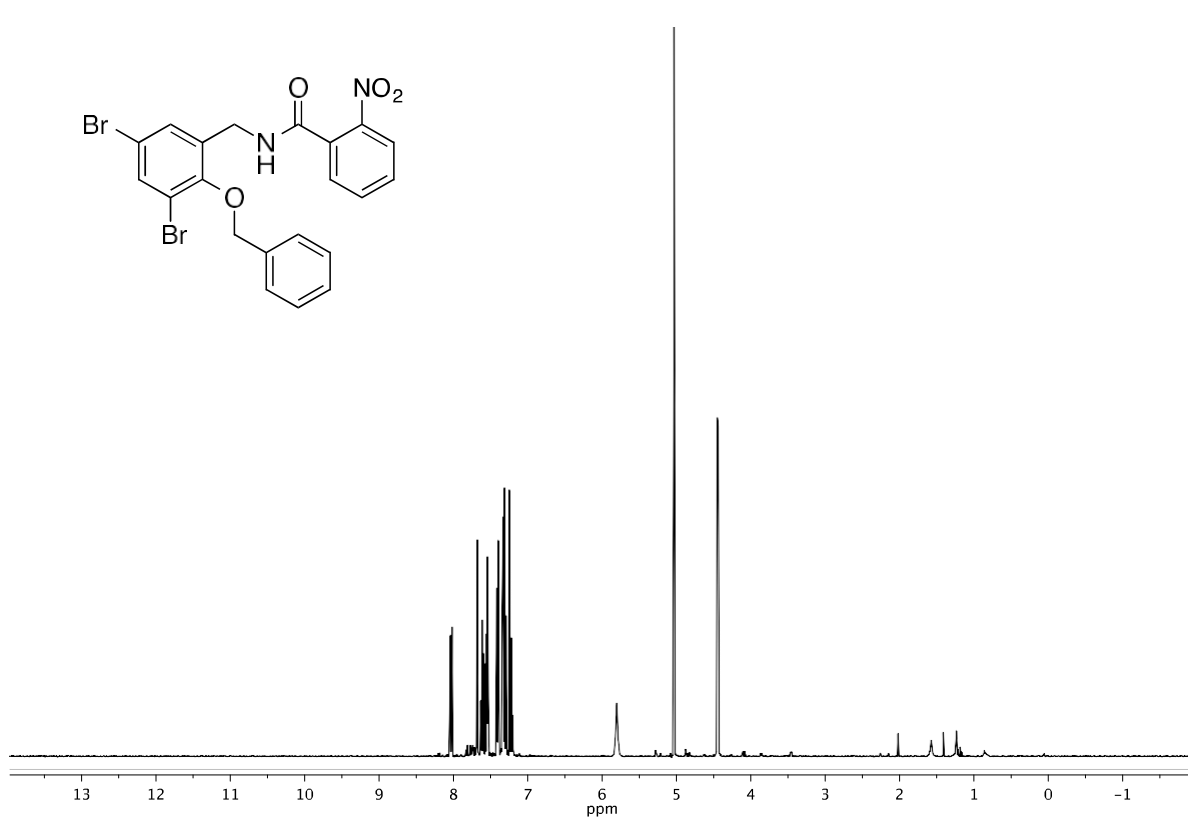
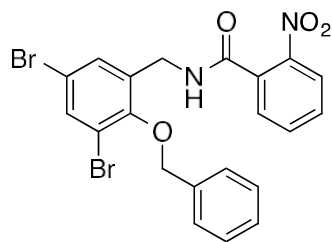
2,4-dibromo-6-(((2-cyanophenyl)sulfonamido)methyl)phenyl 2-chlorobenzoate. ^1H NMR (400 MHz, Chloroform-d) δ 8.23 – 8.14 (m, 1H), 8.01 – 7.94 (m, 1H), 7.89 – 7.82 (m, 3H), 7.69 – 7.60 (m, 2H), 7.39 – 7.32 (m, 2H), 7.12 (t, $J = 6.5$

Hz, 1H), 4.86 (d, J = 6.4 Hz, 2H), 4.53 (s, 1H). ¹³C NMR (101 MHz, Chloroform-d) δ
167.17, 144.43, 138.58, 137.11, 135.84, 135.76, 134.98, 134.71, 134.03, 133.45, 131.72,
131.20, 130.68, 130.54, 130.22, 127.29, 122.06, 117.78, 115.37, 112.35, 39.61.

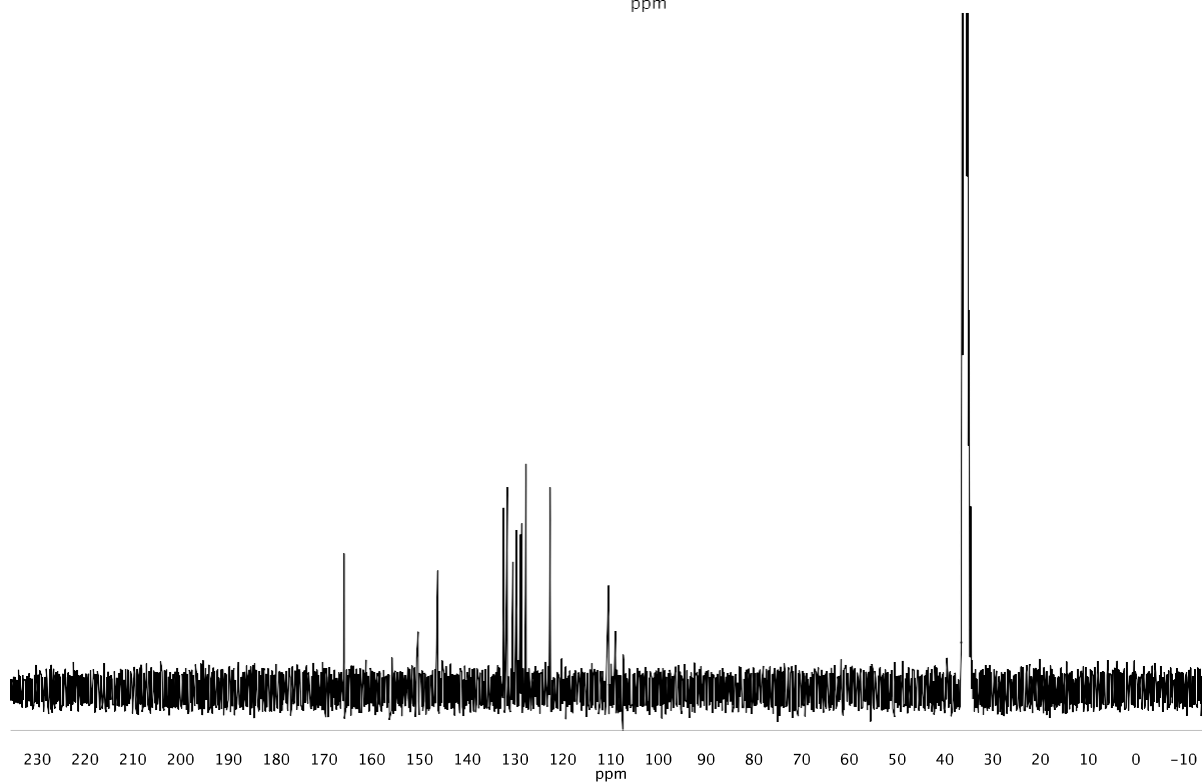
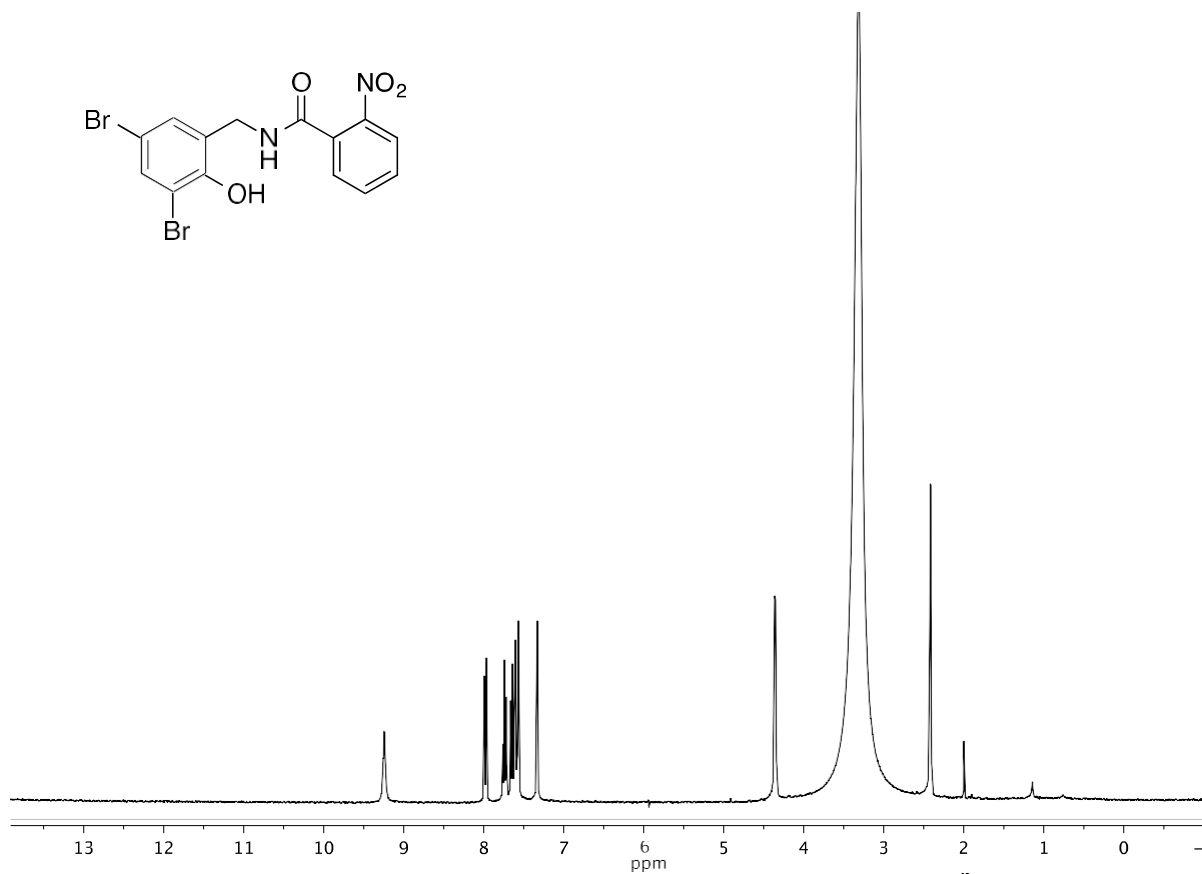
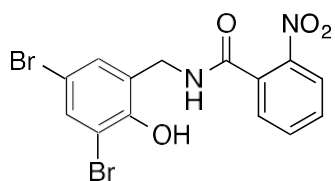
(2-(benzyloxy)-3,5-dibromophenyl)methanamine



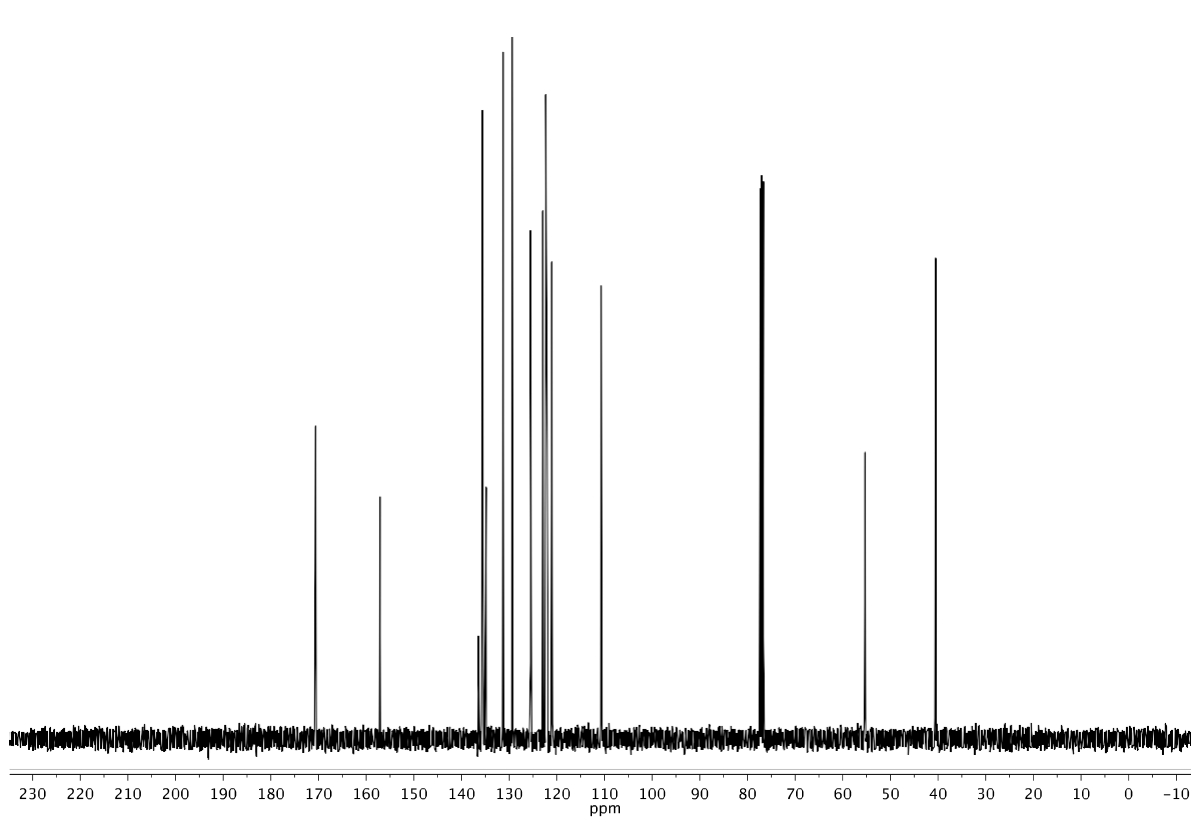
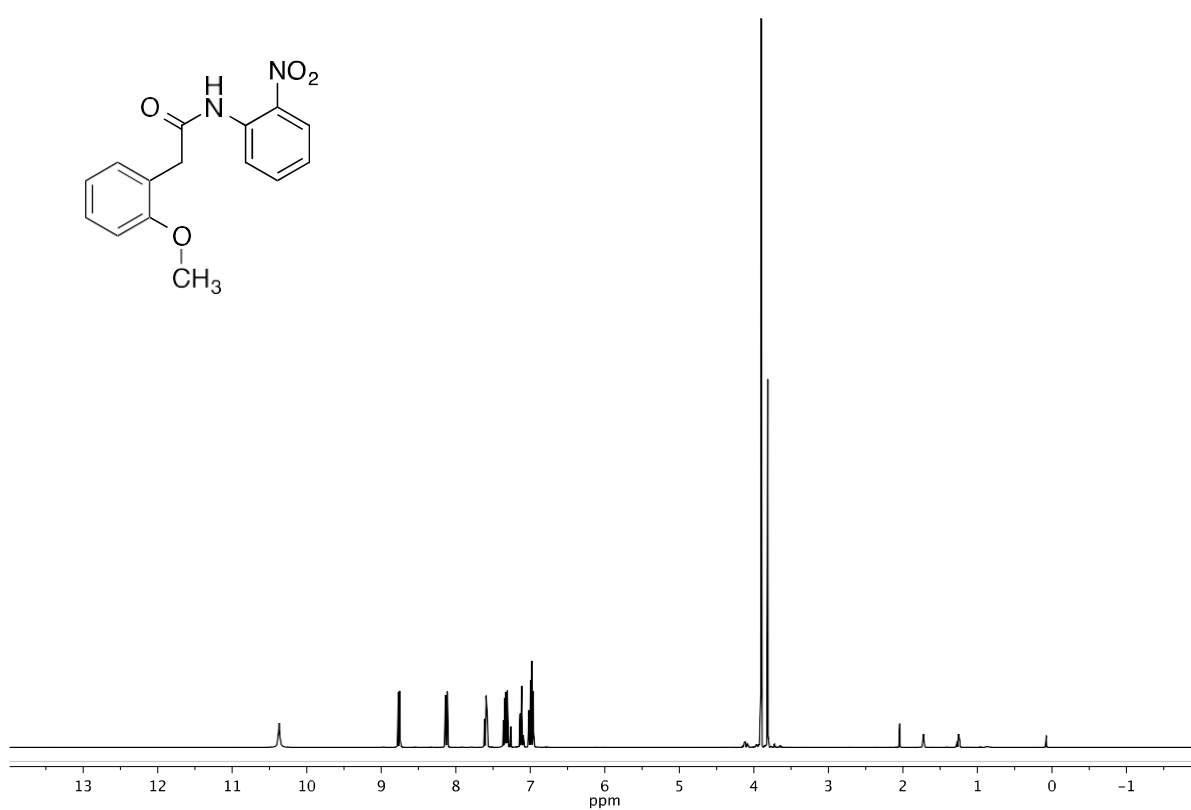
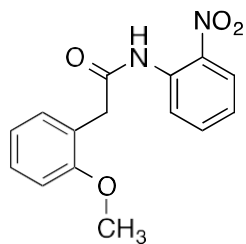
***N*-2-(benzyloxy)-3,5-dibromobenzyl)-2-nitrobenzamide**



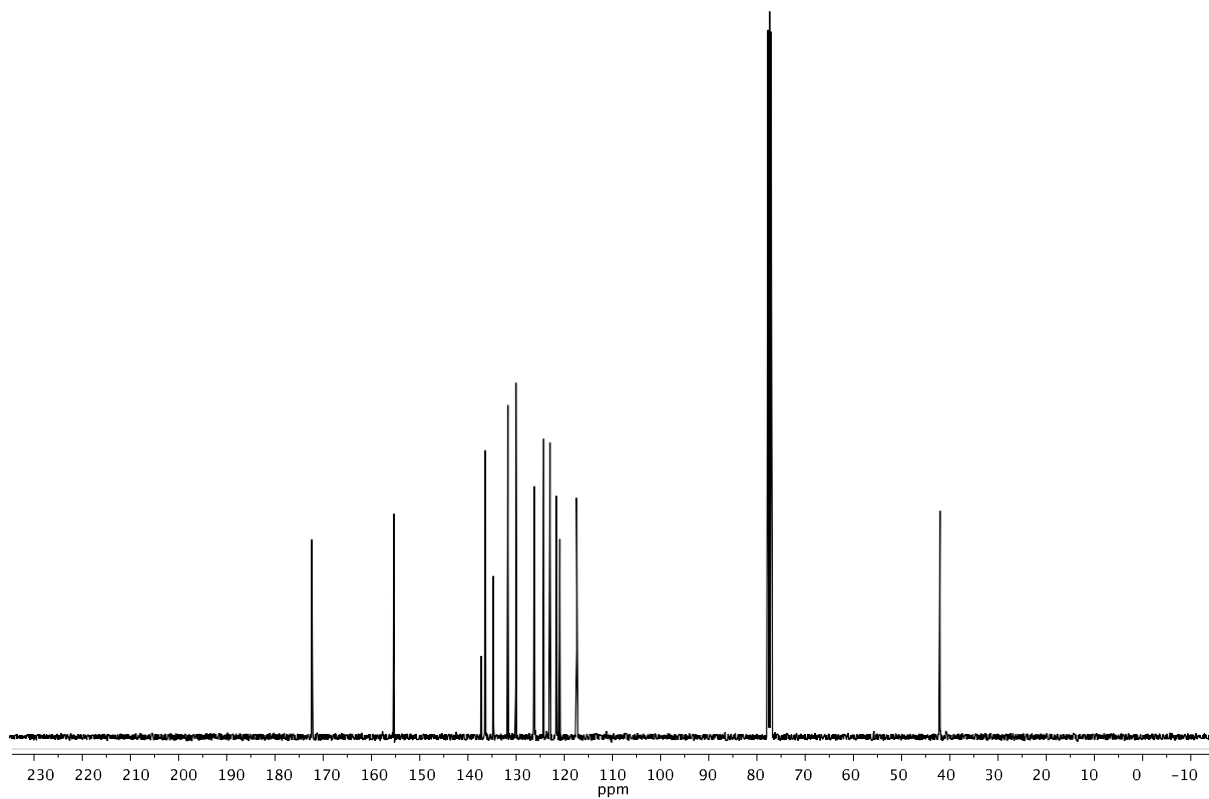
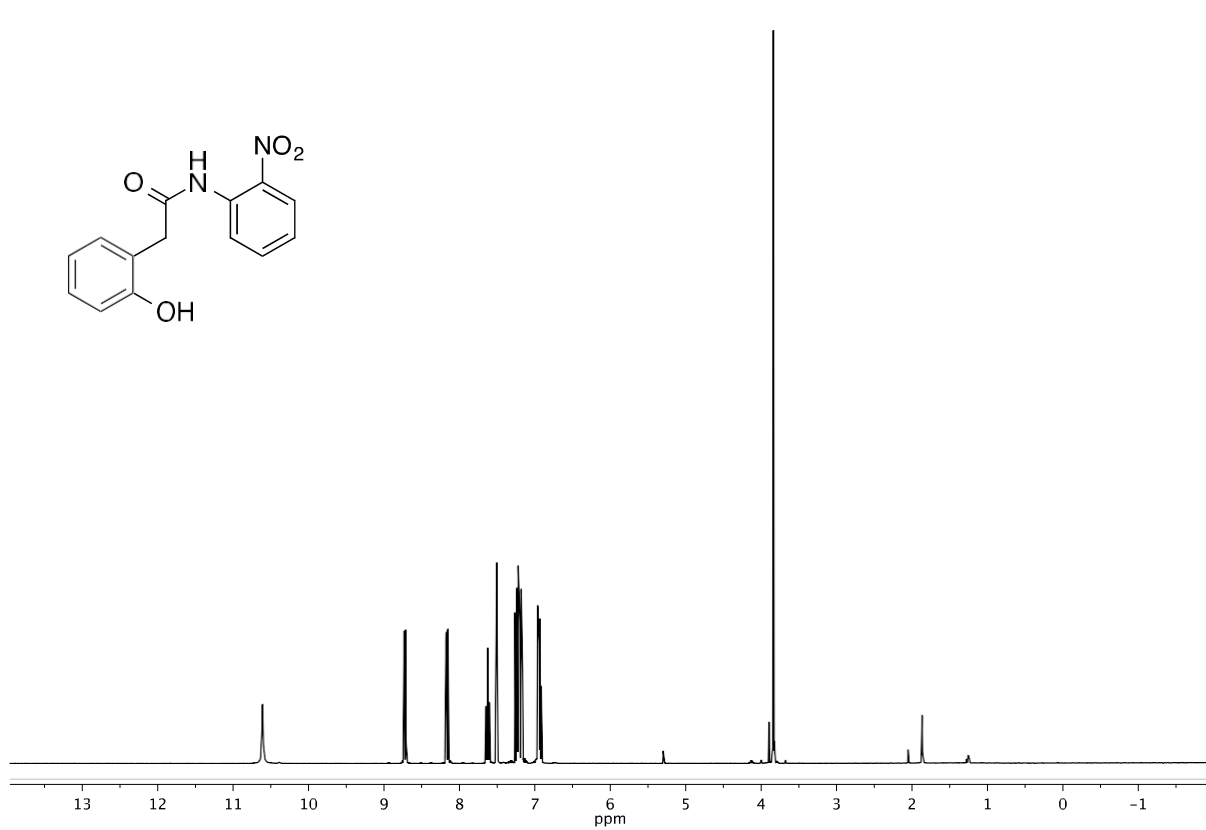
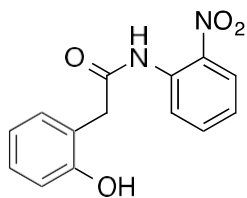
N-(3,5-dibromo-2-hydroxybenzyl)-2-nitrobenzamide



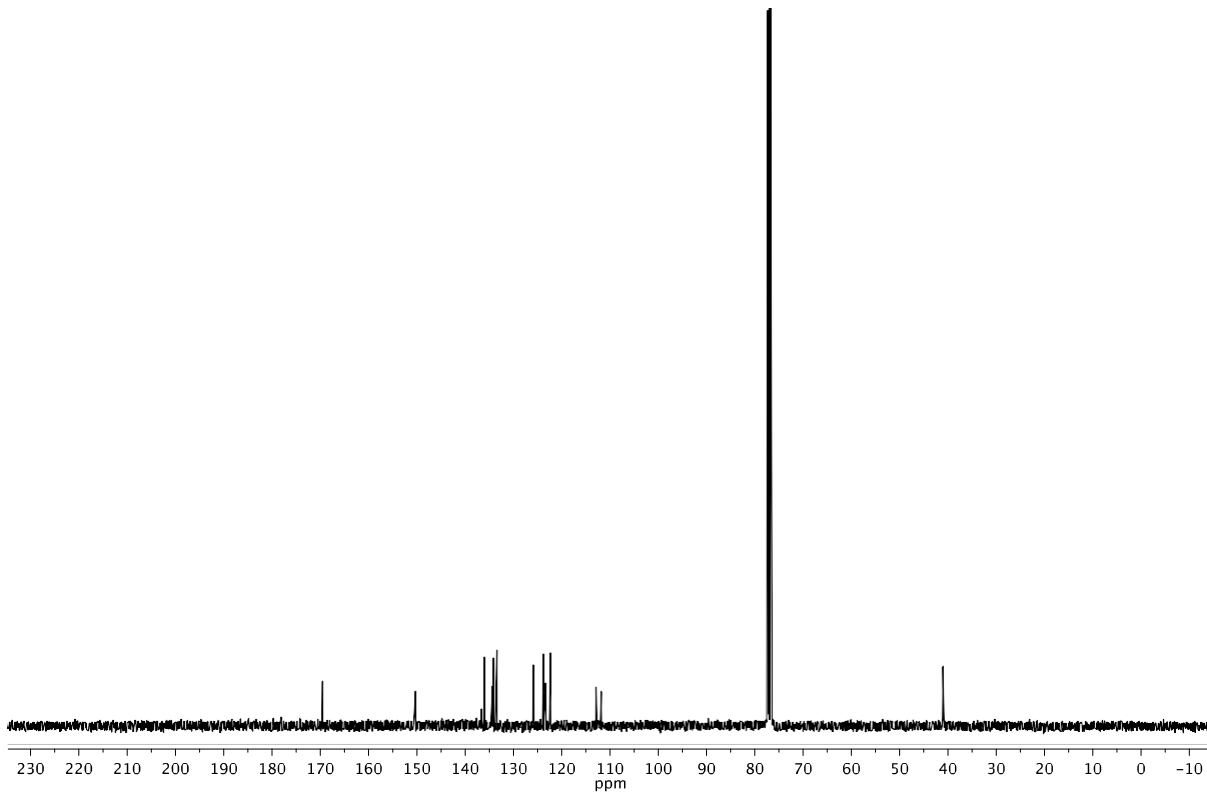
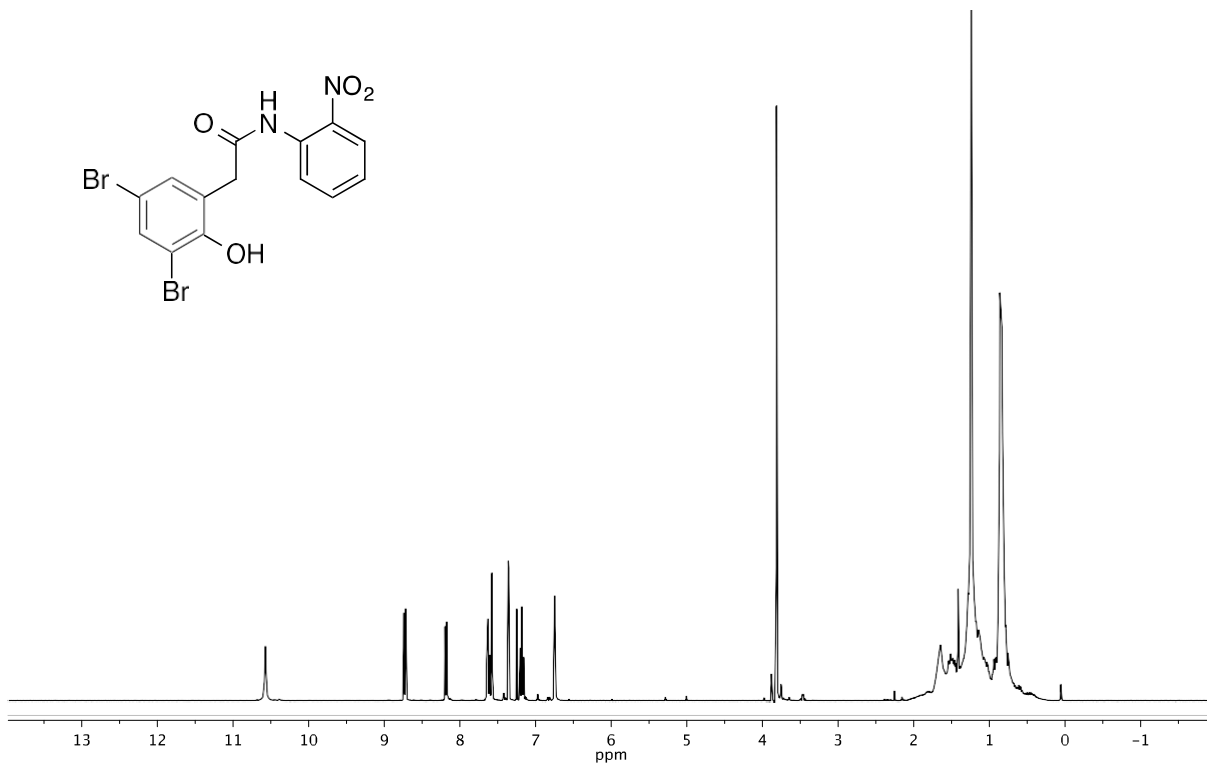
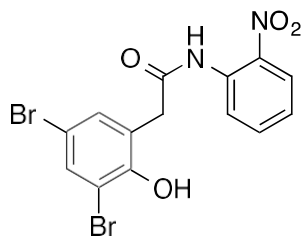
2-(2-methoxyphenyl)-N-(2-nitrophenyl)acetamide



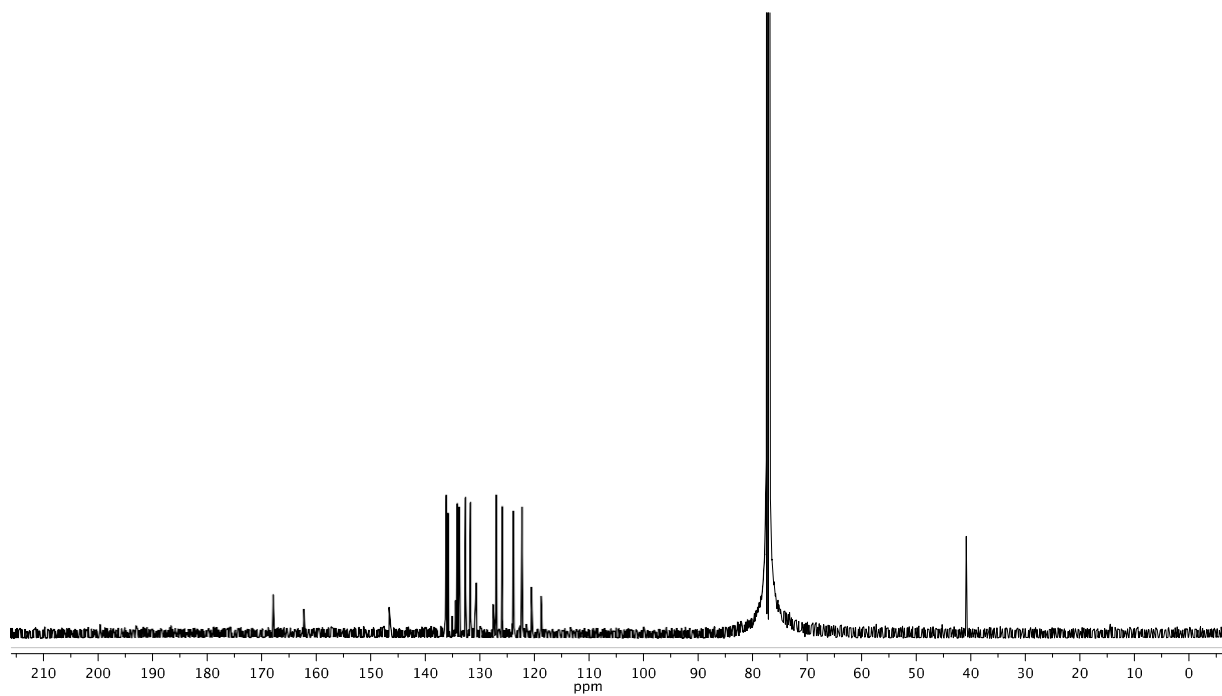
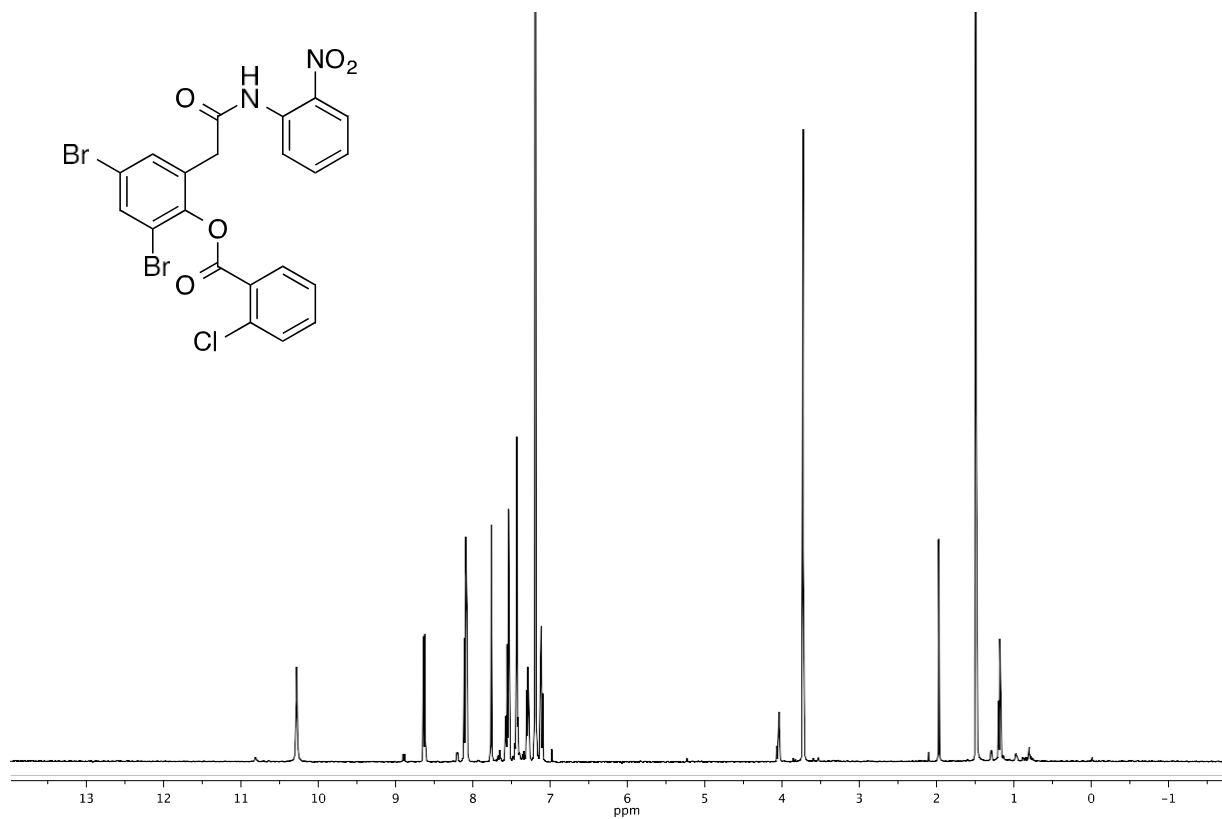
2-(2-hydroxyphenyl)-N-(2-nitrophenyl)acetamide



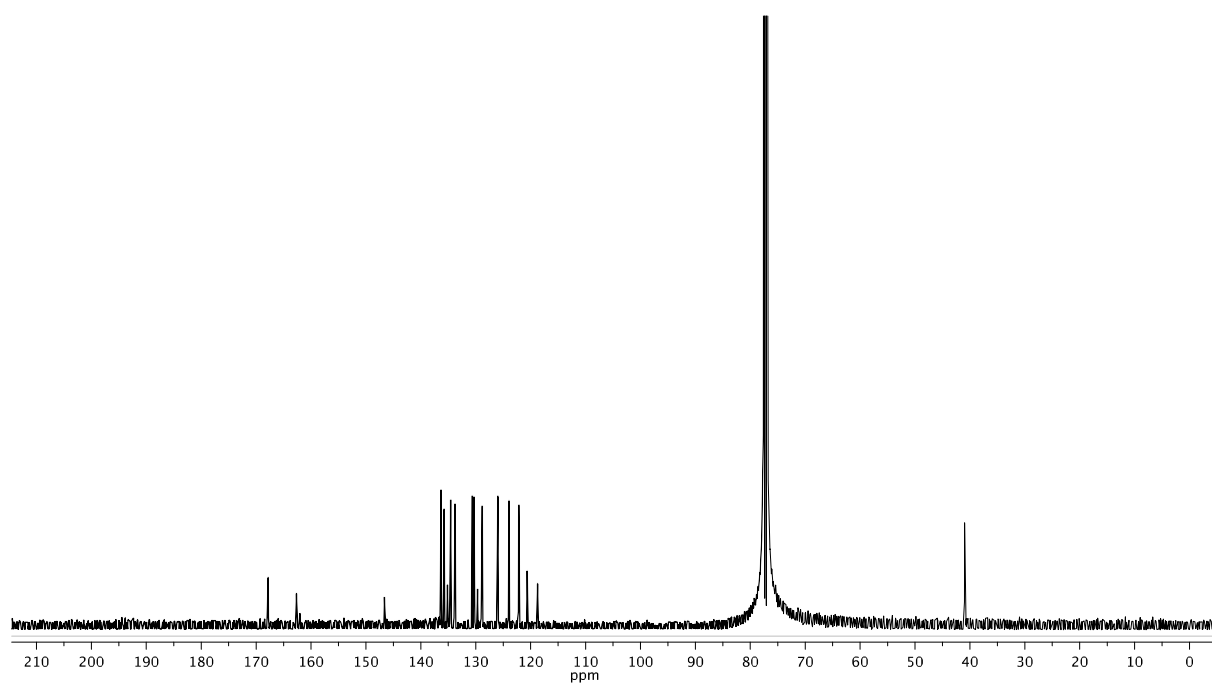
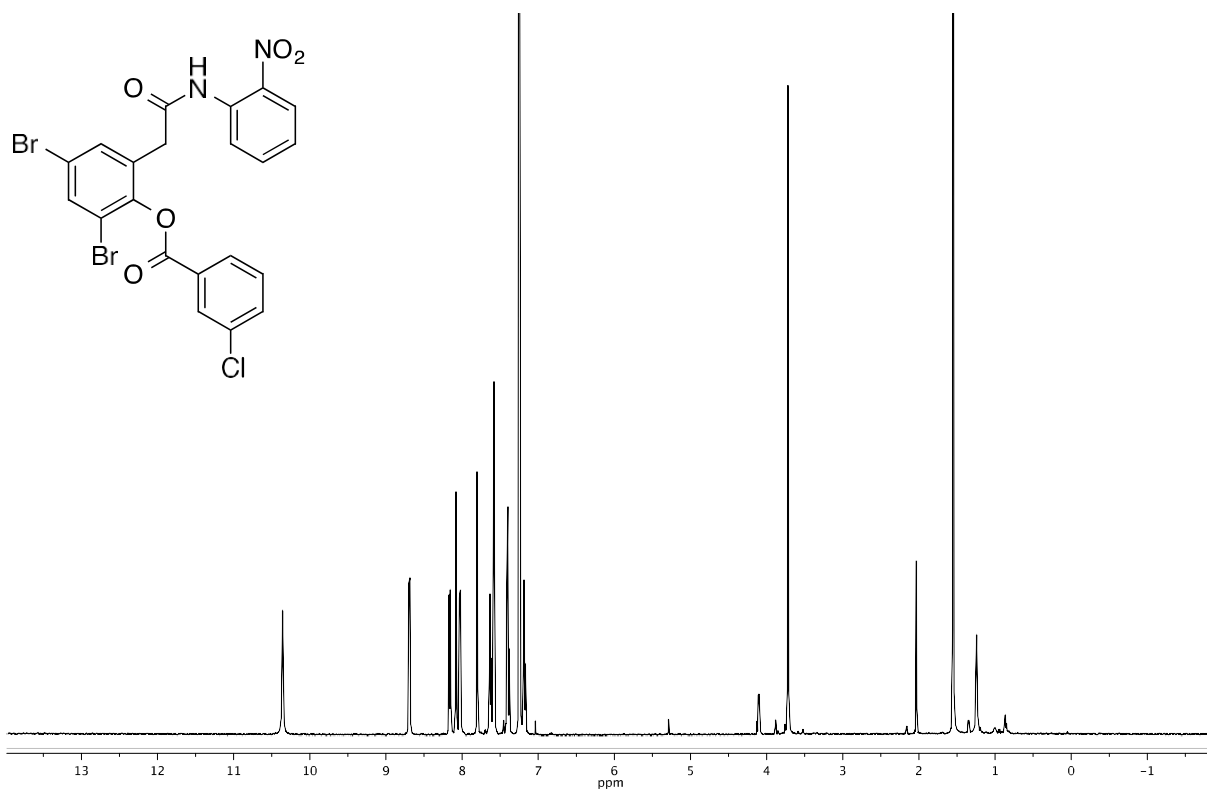
2-(3,5-dibromo-2-hydroxyphenyl)-N-(2-nitrophenyl)acetamide



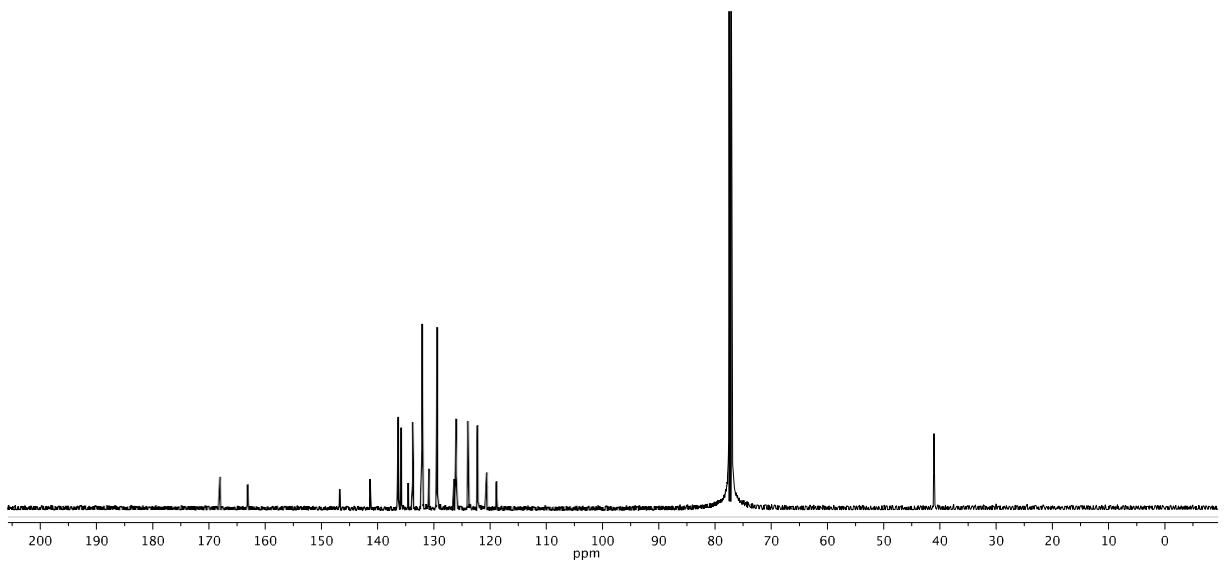
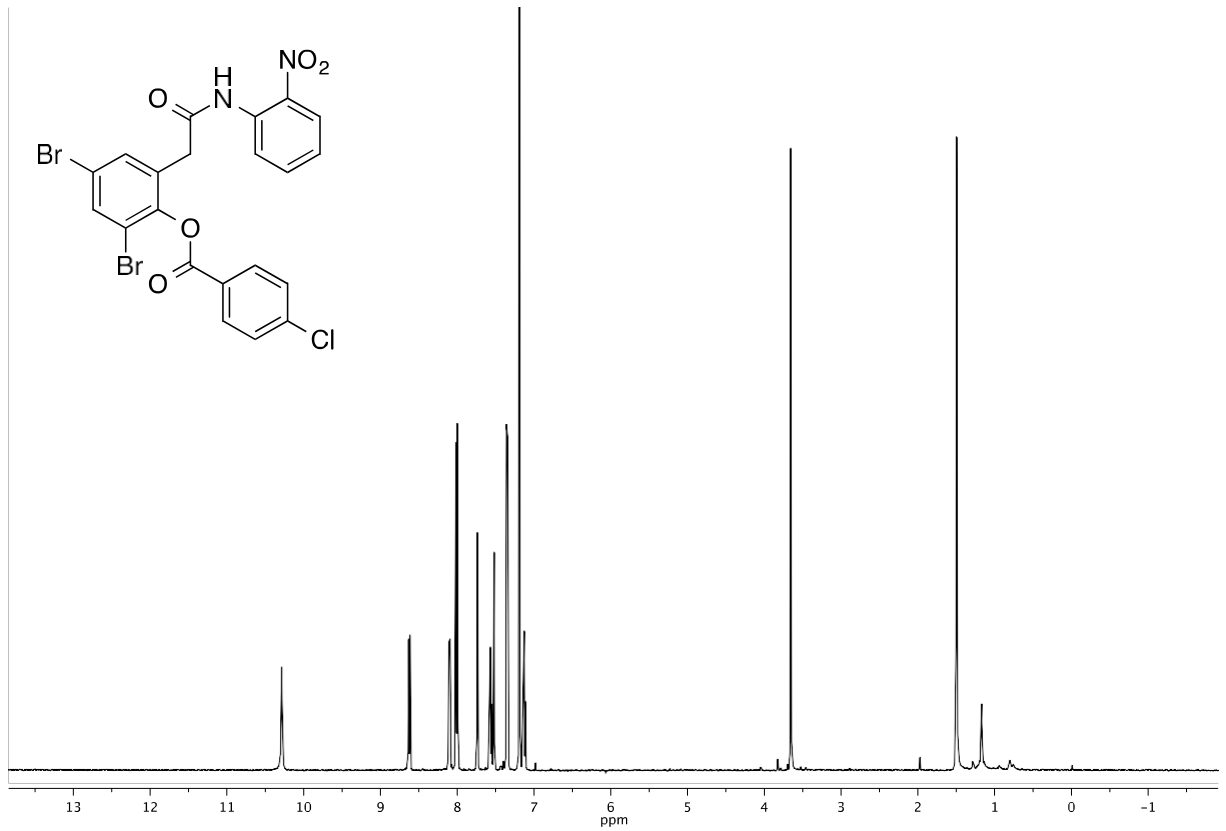
2,4-dibromo-6-(2-((2-nitrophenyl)amino)-2-oxoethyl)phenyl 2-chlorobenzoate



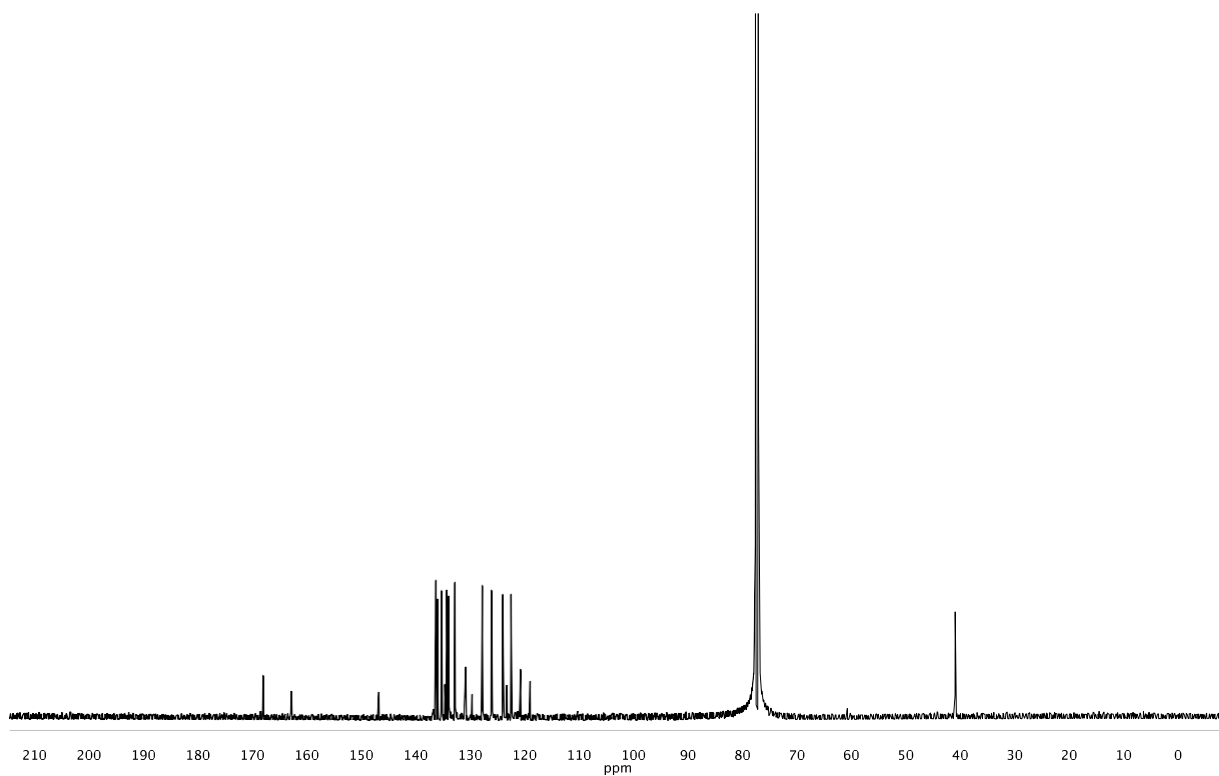
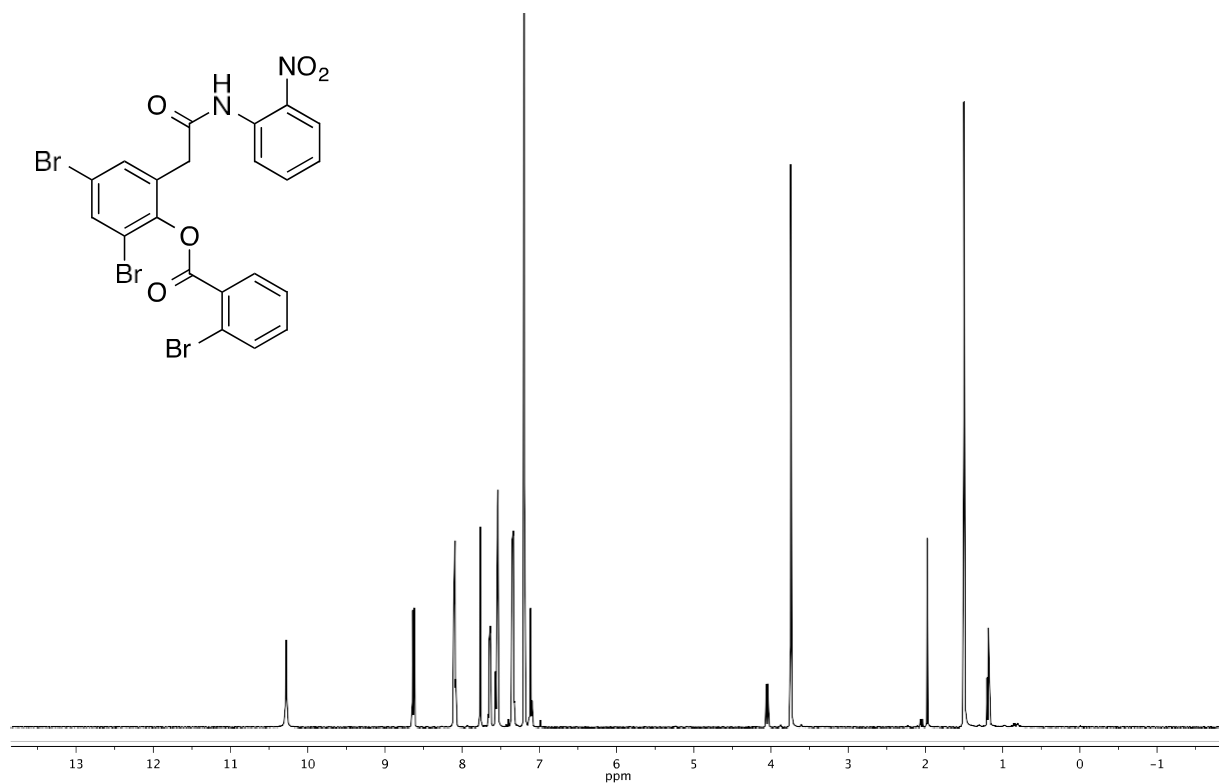
2,4-dibromo-6-(2-((2-nitrophenyl)amino)-2-oxoethyl)phenyl 3-chlorobenzoate



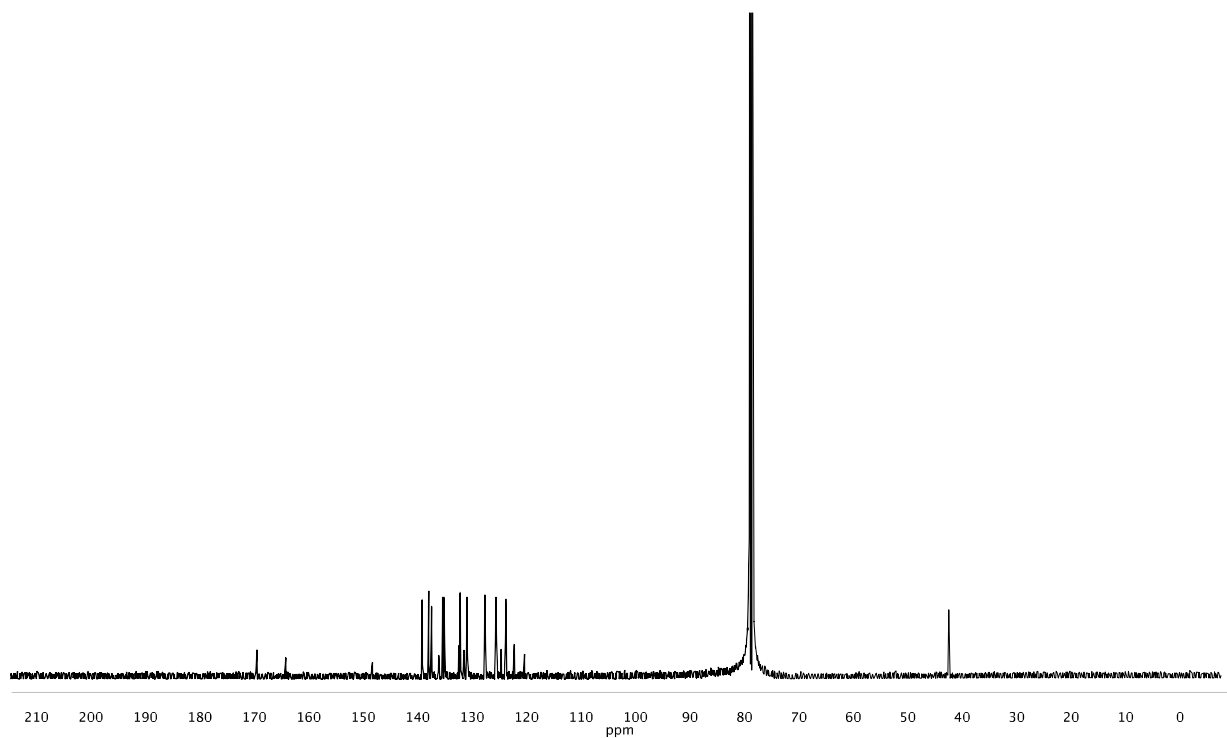
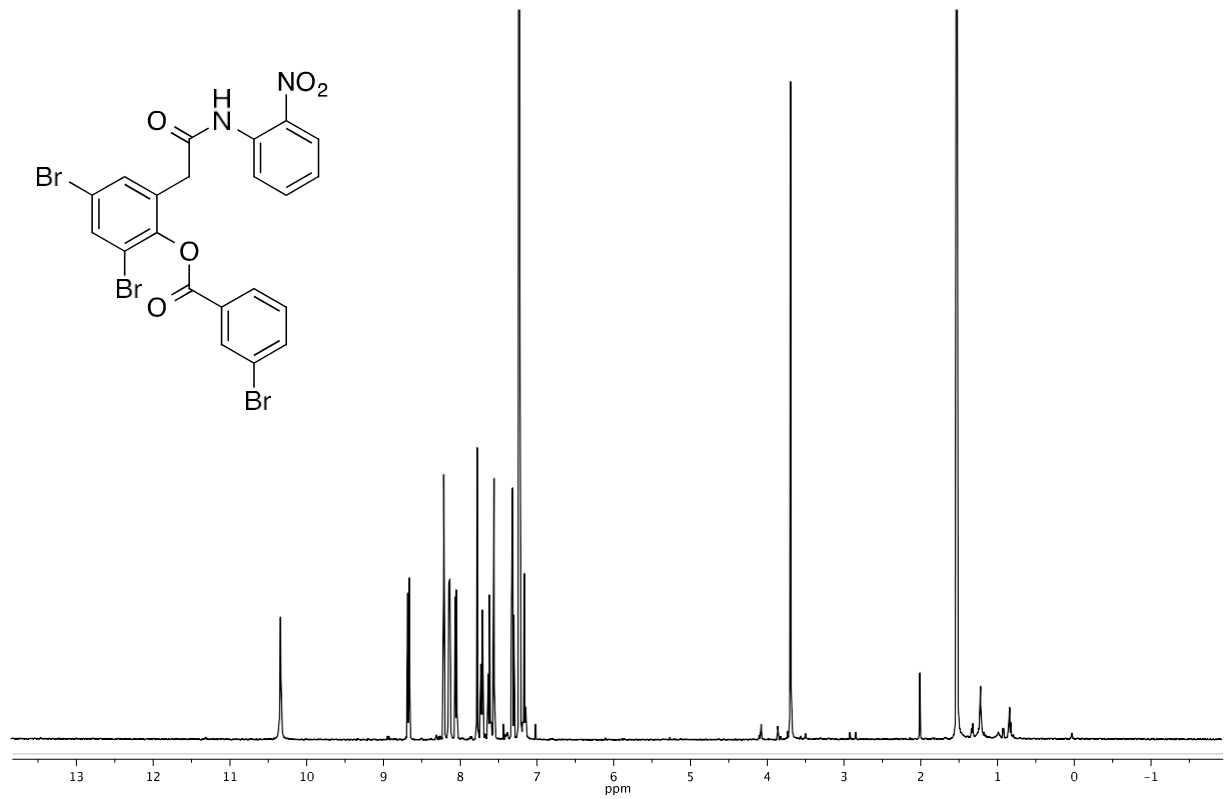
2,4-dibromo-6-(2-((2-nitrophenyl)amino)-2-oxoethyl)phenyl 4-chlorobenzoate



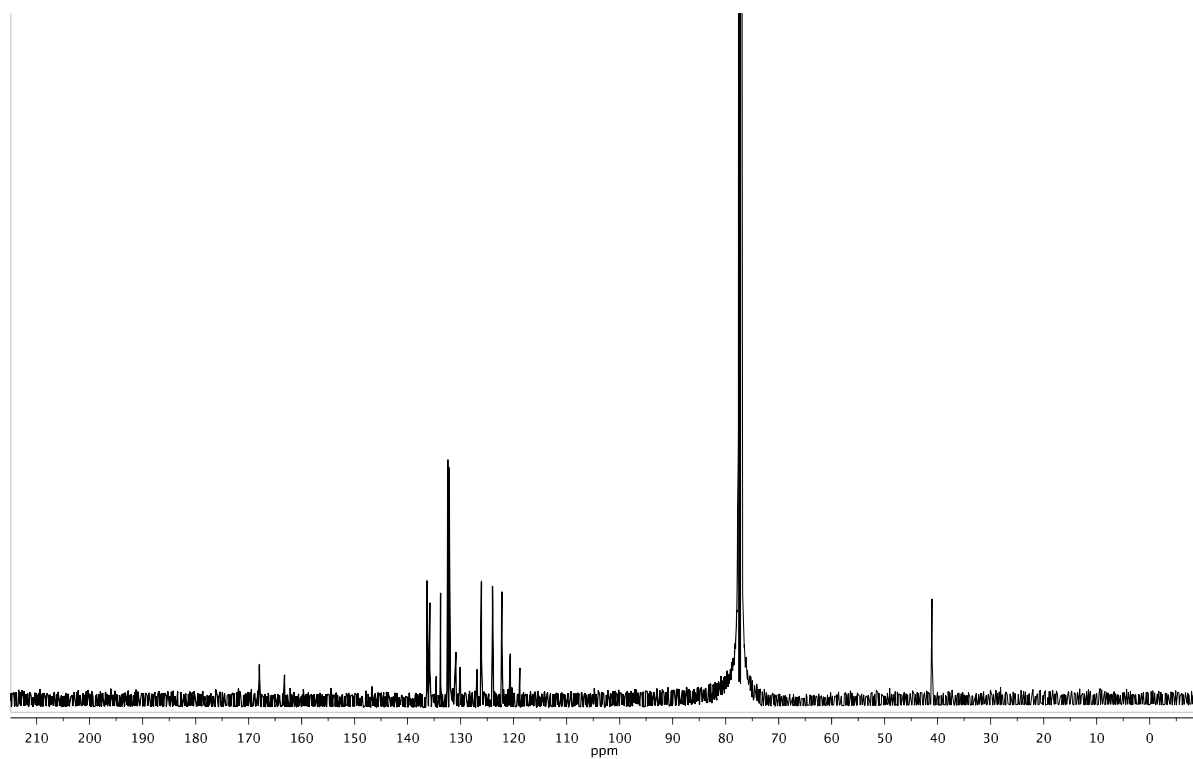
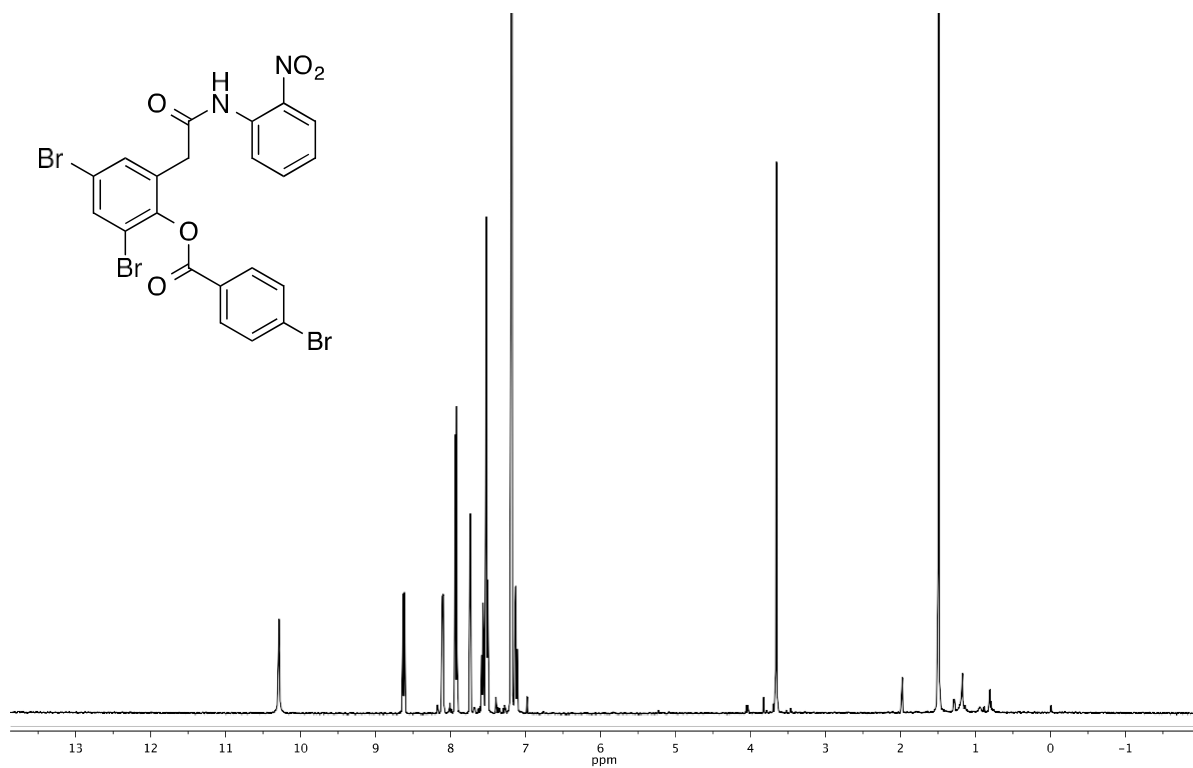
2,4-dibromo-6-(2-((2-nitrophenyl)amino)-2-oxoethyl)phenyl 2-bromobenzoate



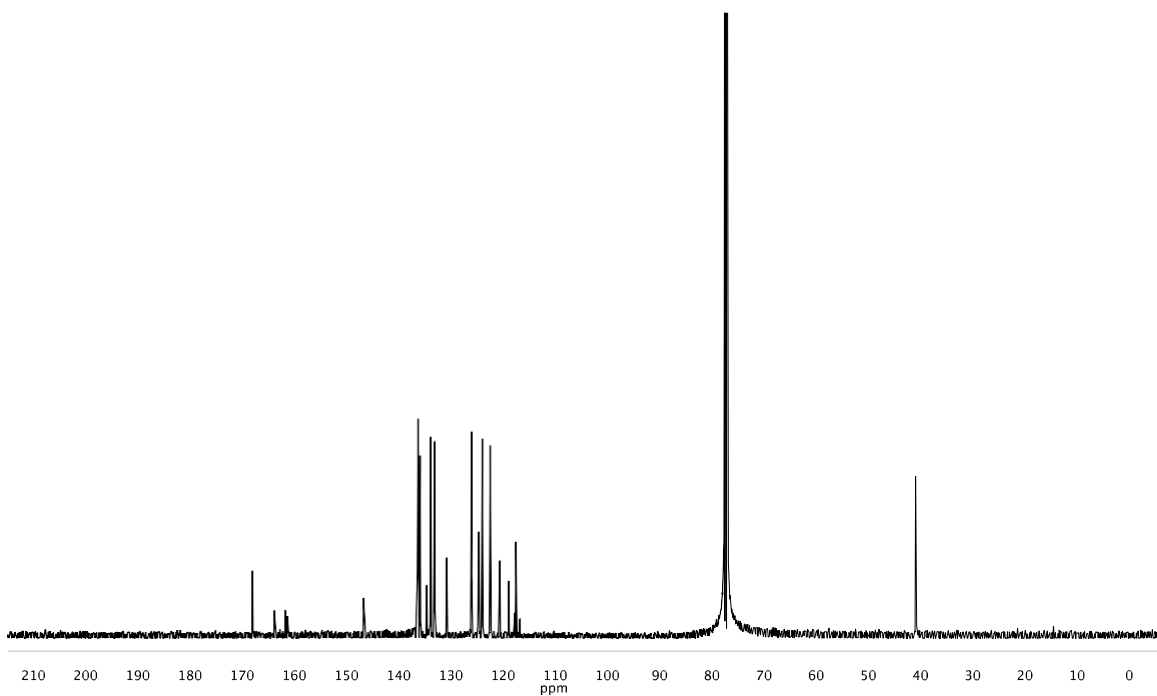
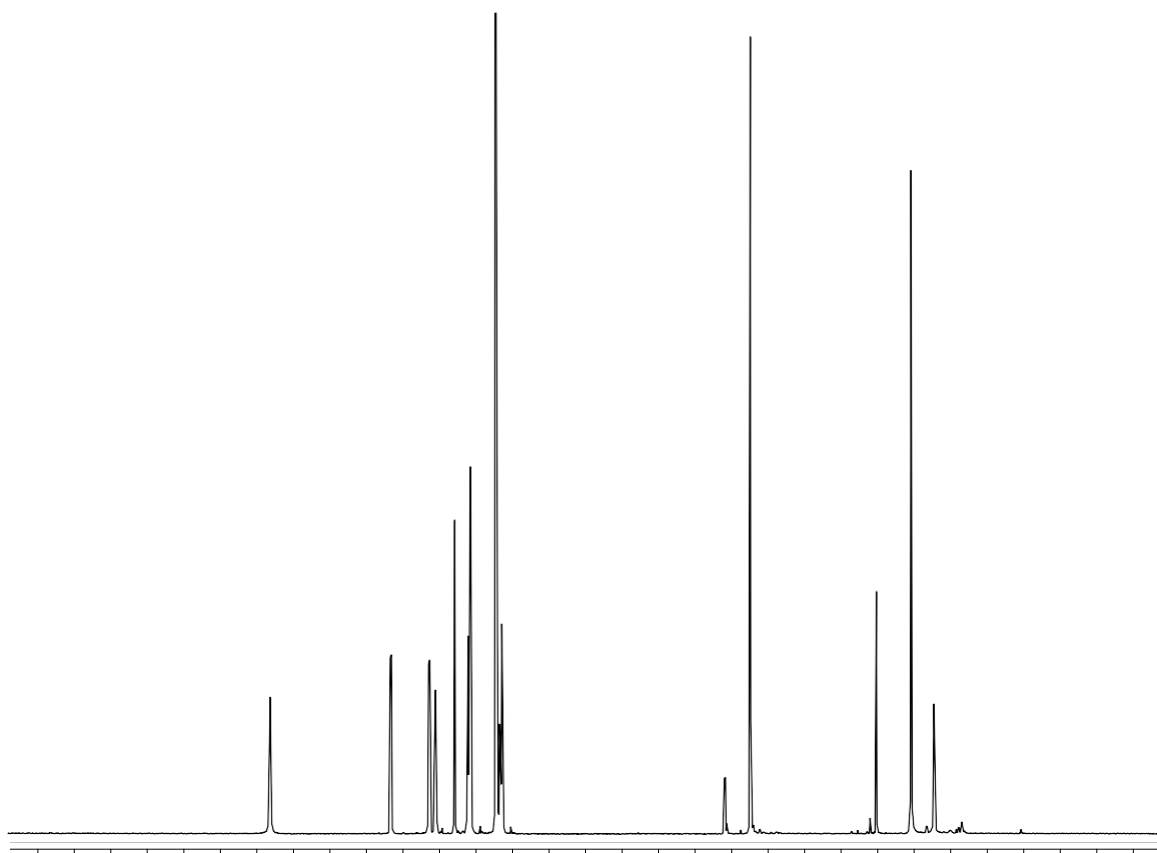
2,4-dibromo-6-(2-((2-nitrophenyl)amino)-2-oxoethyl)phenyl 3-bromobenzoate



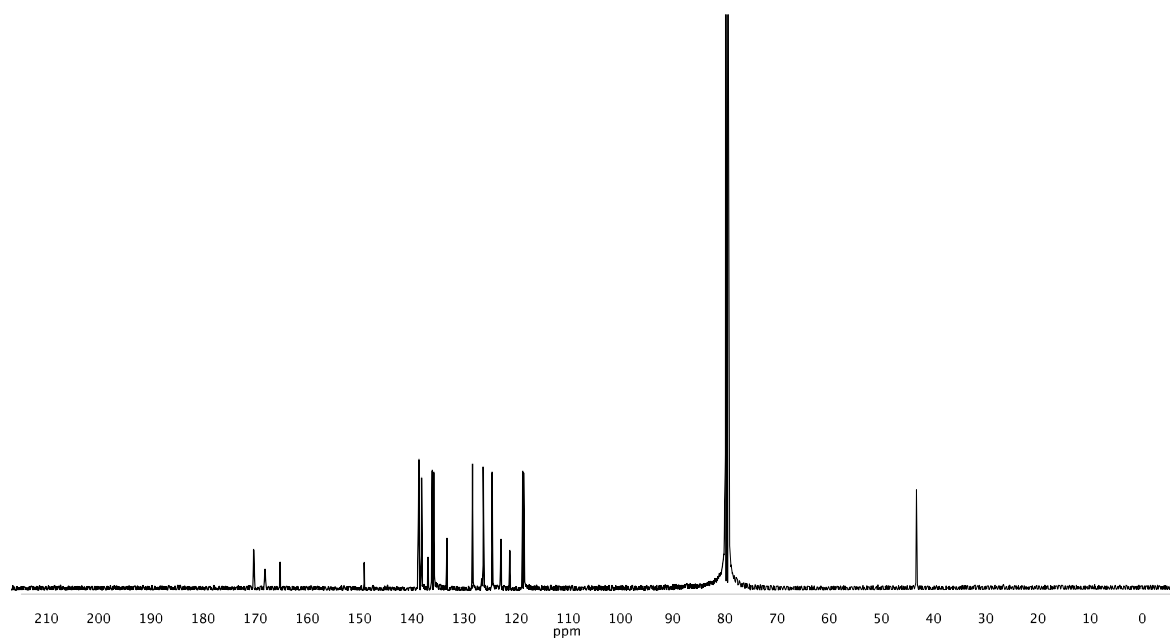
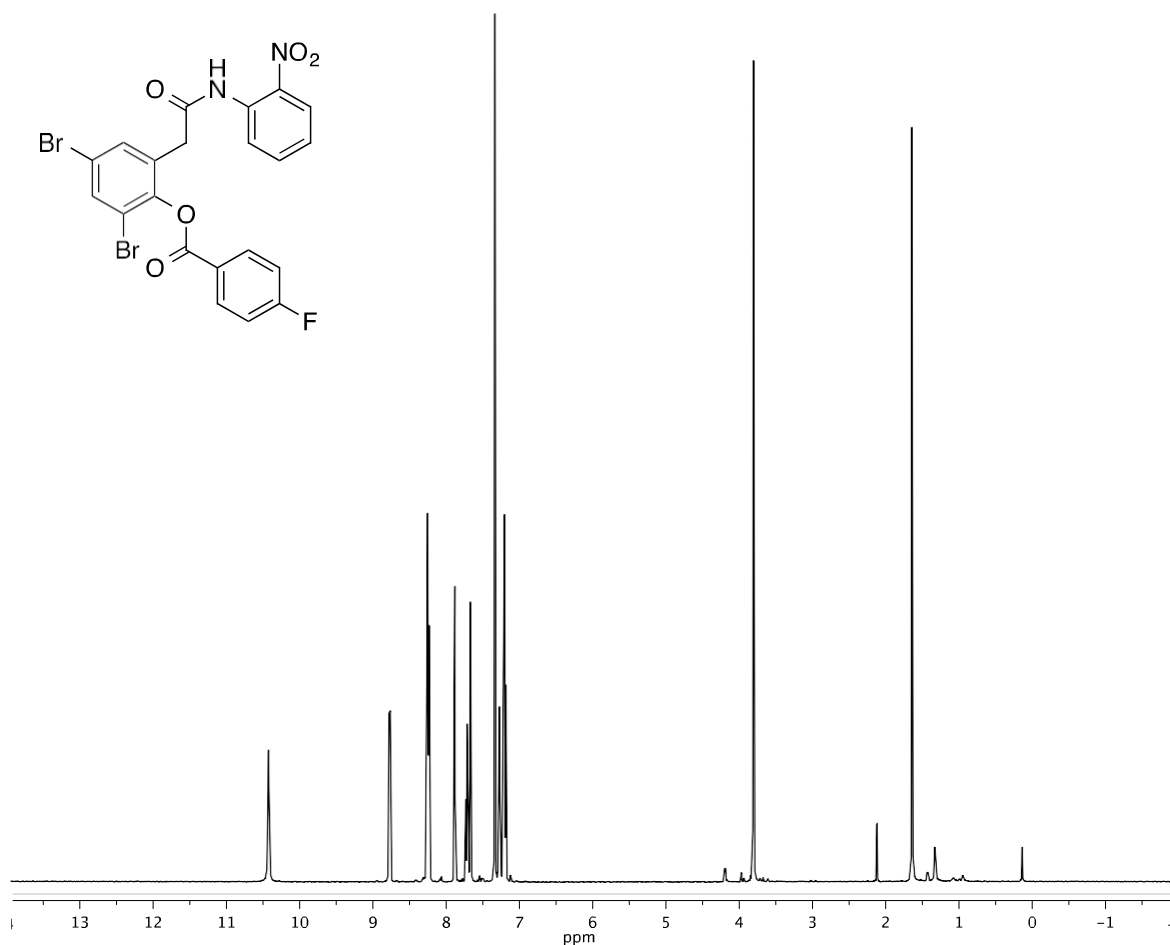
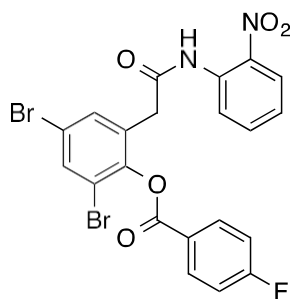
2,4-dibromo-6-(2-((2-nitrophenyl)amino)-2-oxoethyl)phenyl 4-bromobenzoate



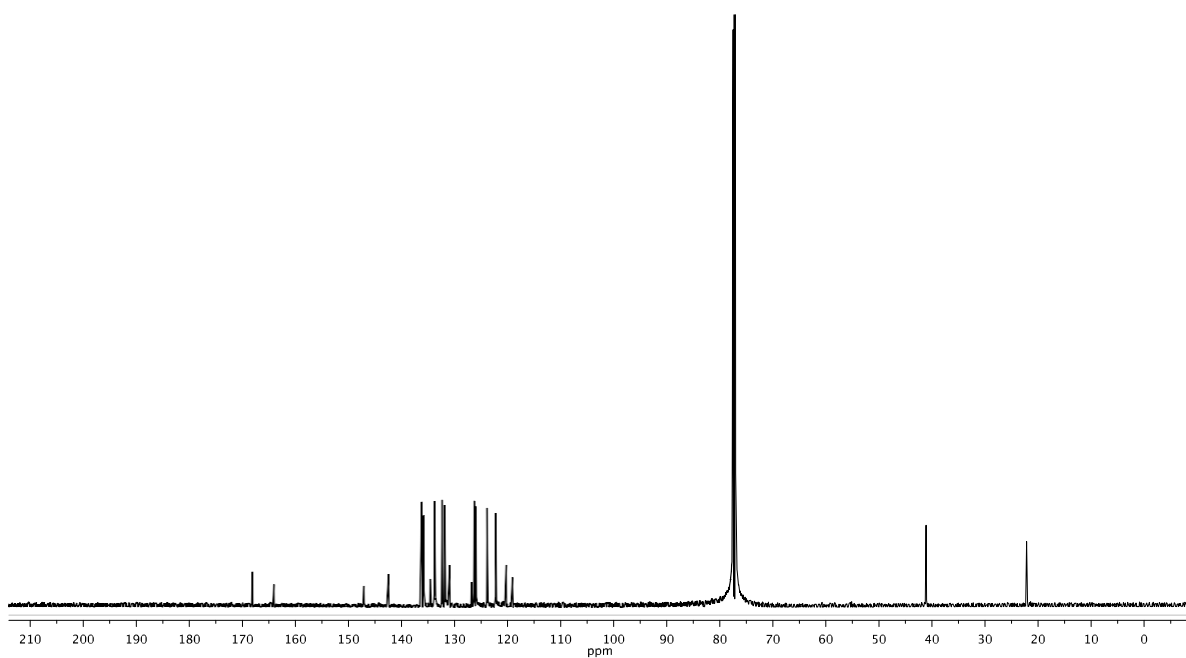
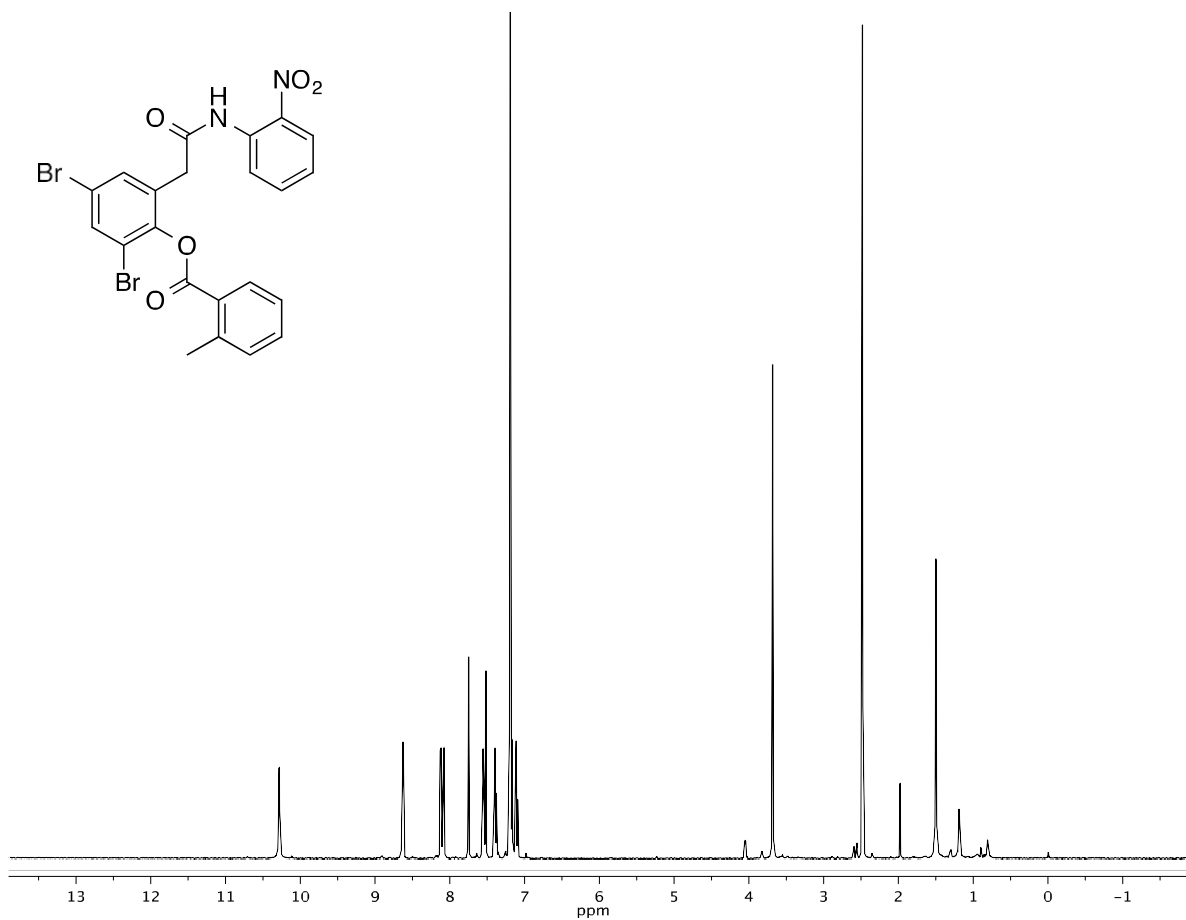
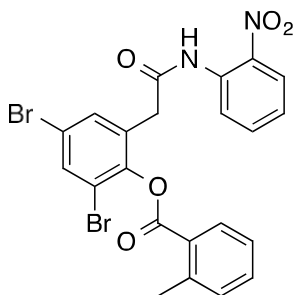
2,4-dibromo-6-(2-((2-nitrophenyl)amino)-2-oxoethyl)phenyl 2-fluorobenzoate



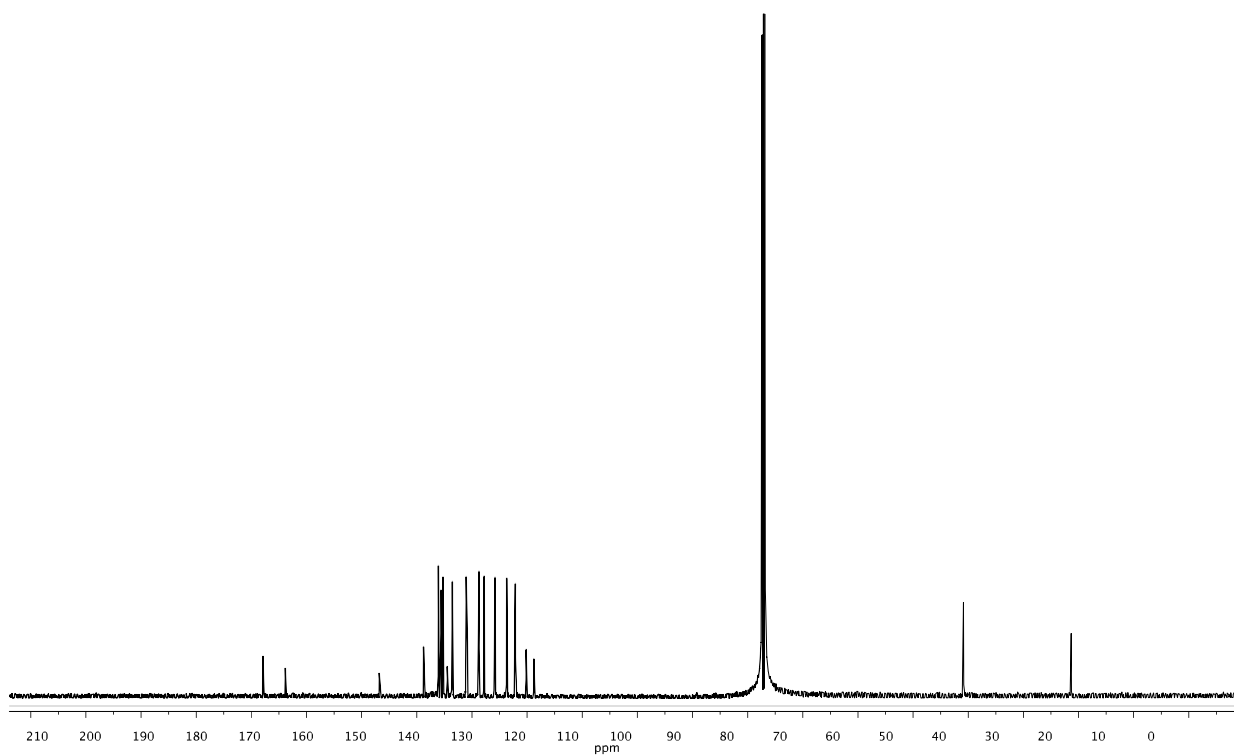
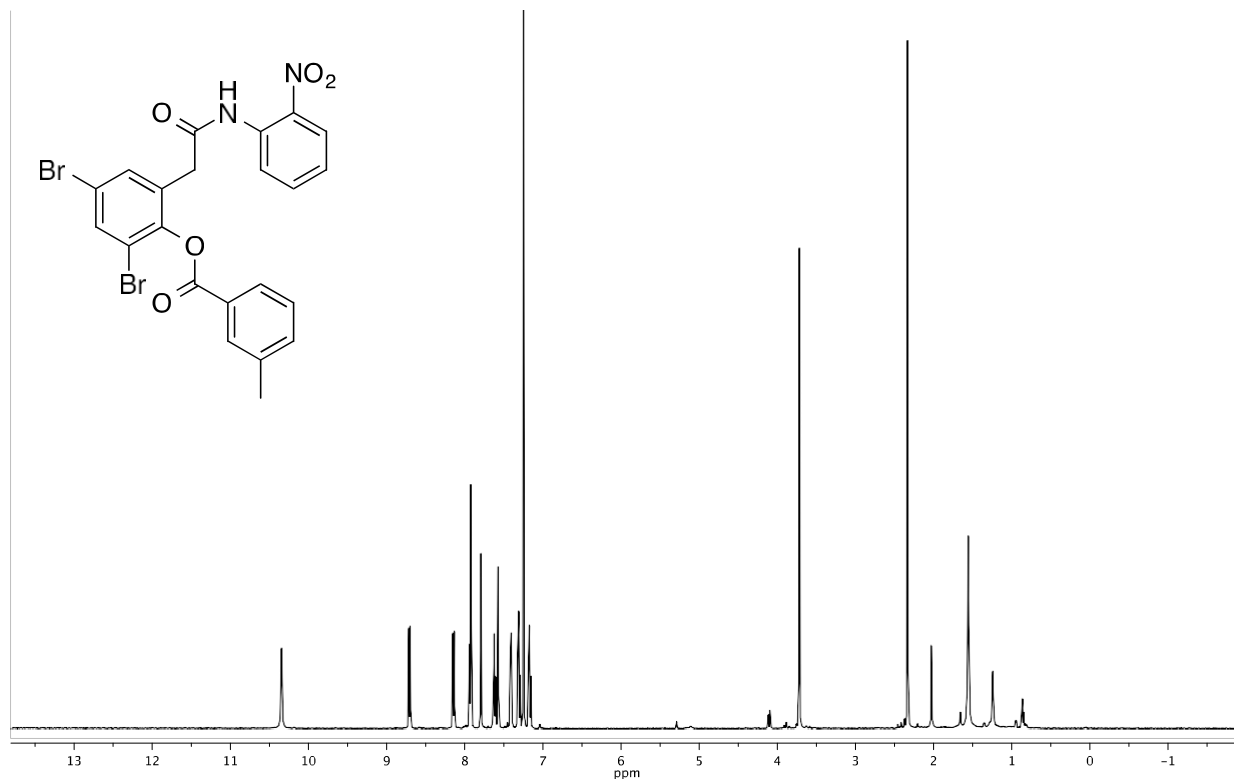
2,4-dibromo-6-(2-((2-nitrophenyl)amino)-2-oxoethyl)phenyl 4-fluorobenzoate



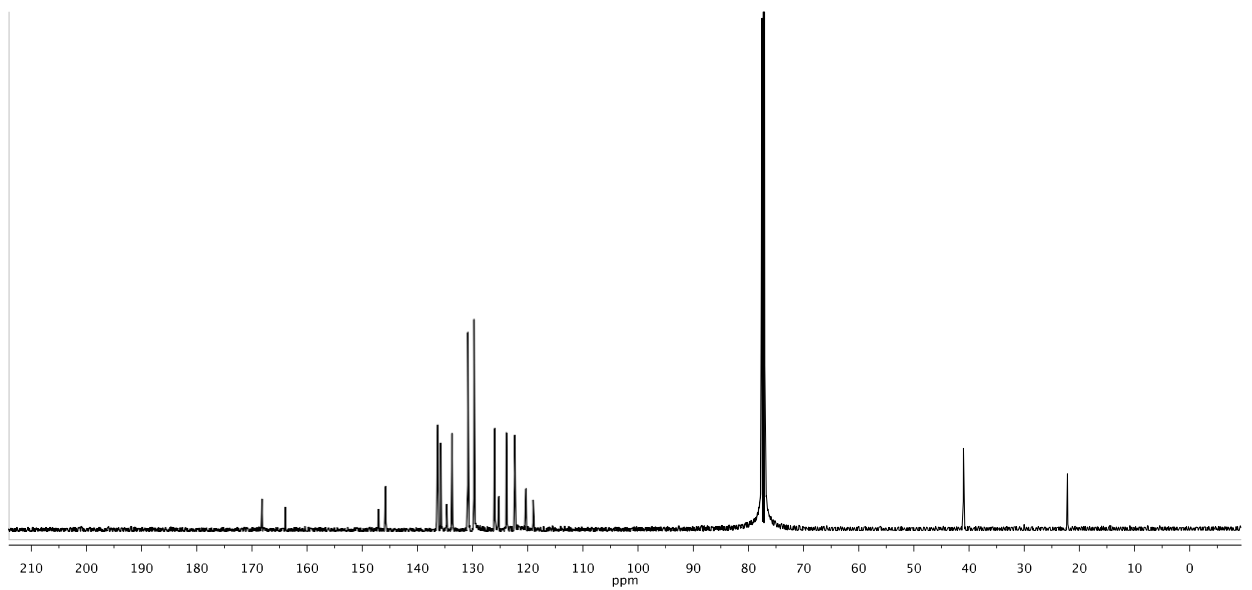
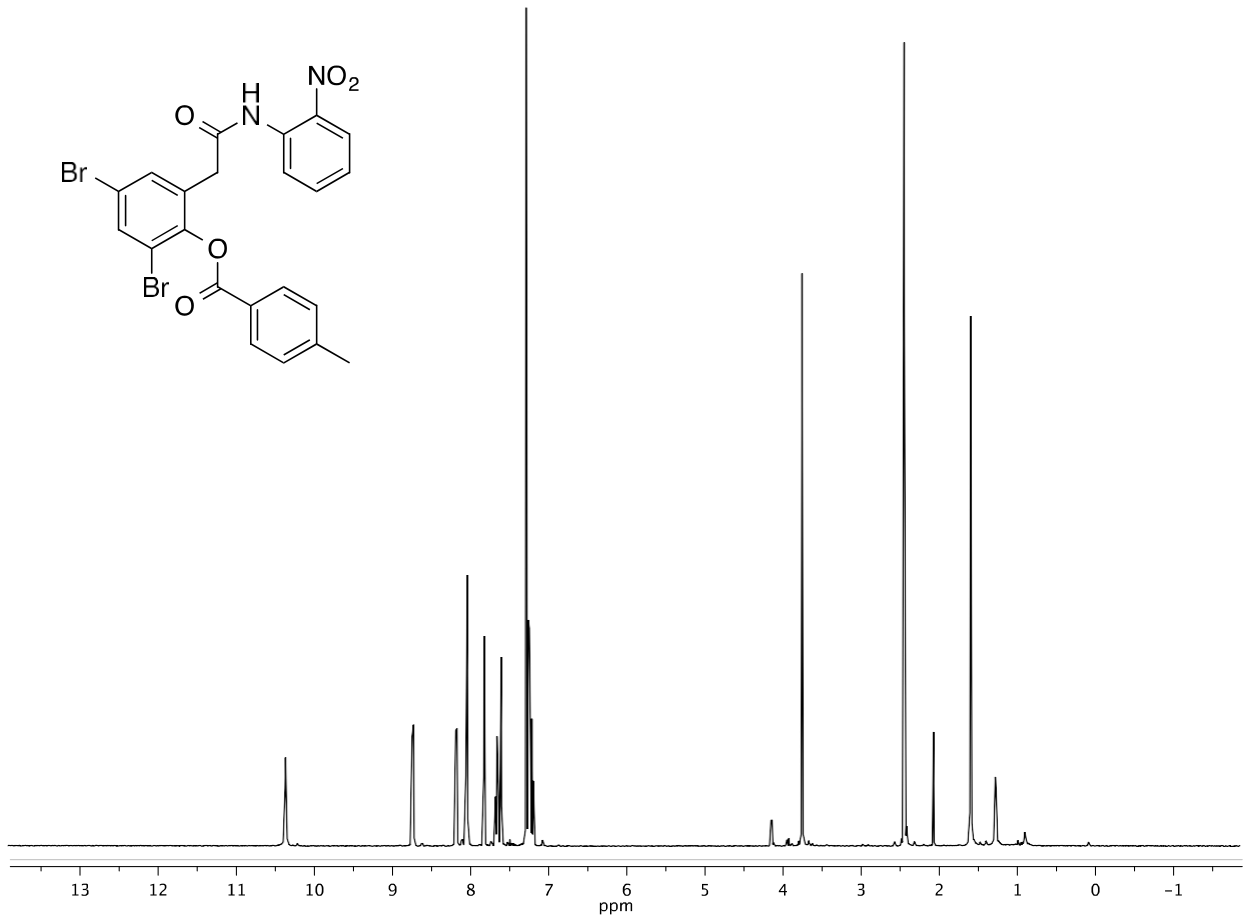
2,4-dibromo-6-(2-((2-nitrophenyl)amino)-2-oxoethyl)phenyl 2-methylbenzoate



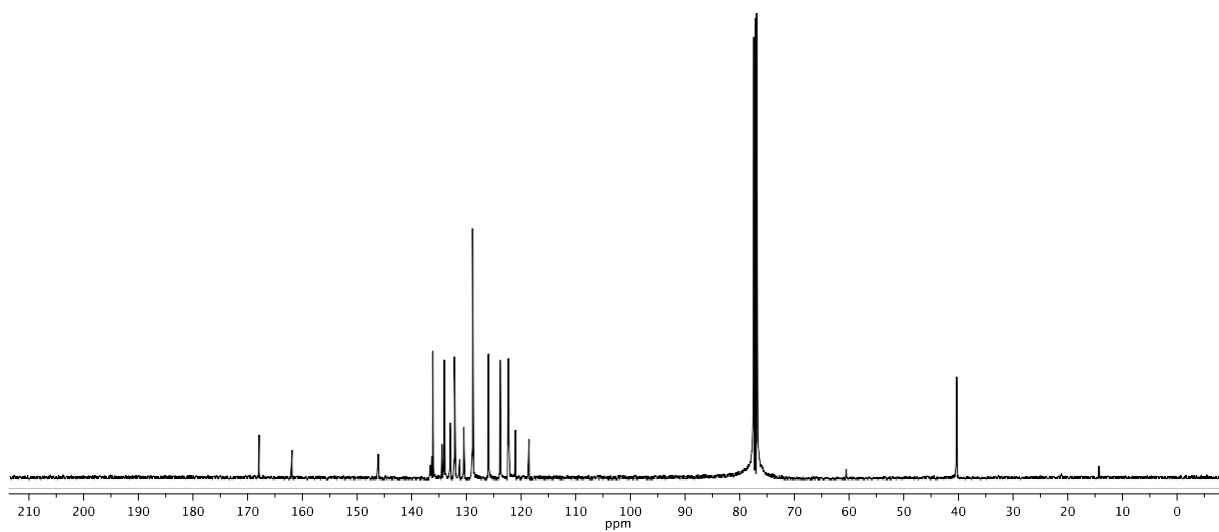
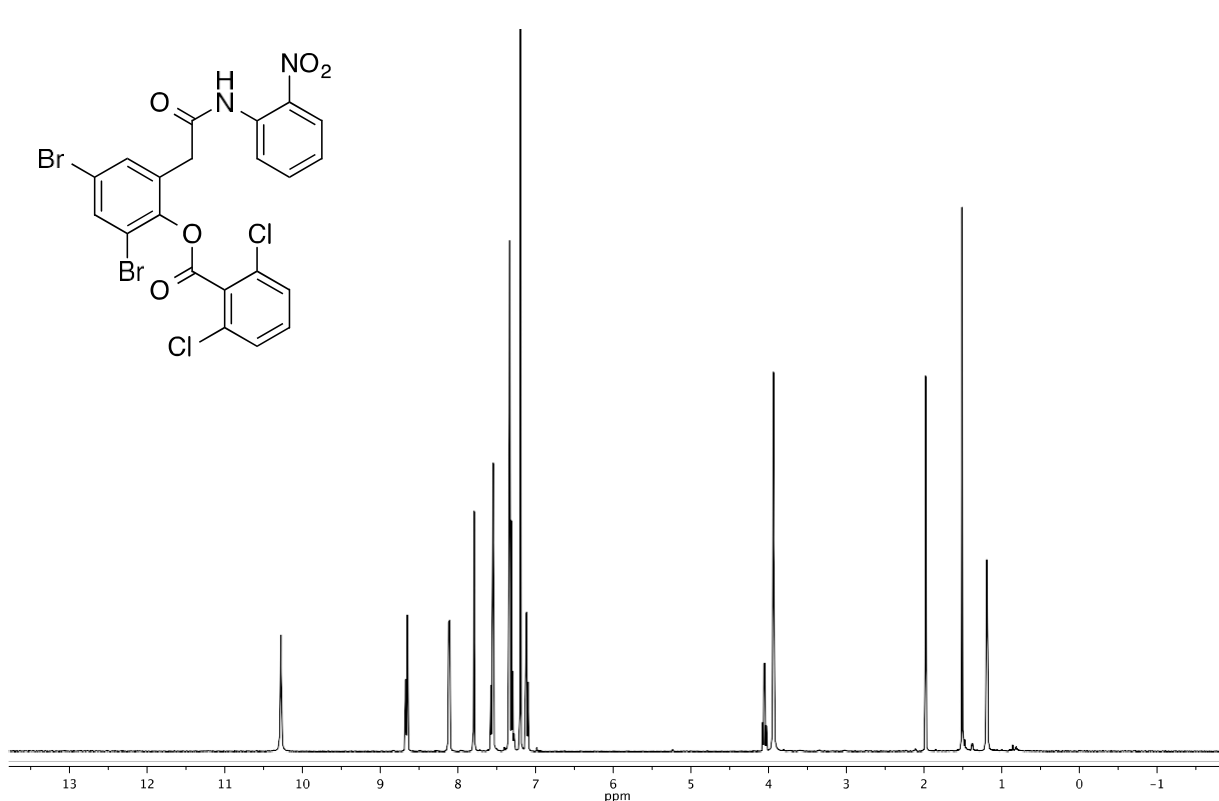
2,4-dibromo-6-(2-((2-nitrophenyl)amino)-2-oxoethyl)phenyl 3-methylbenzoate



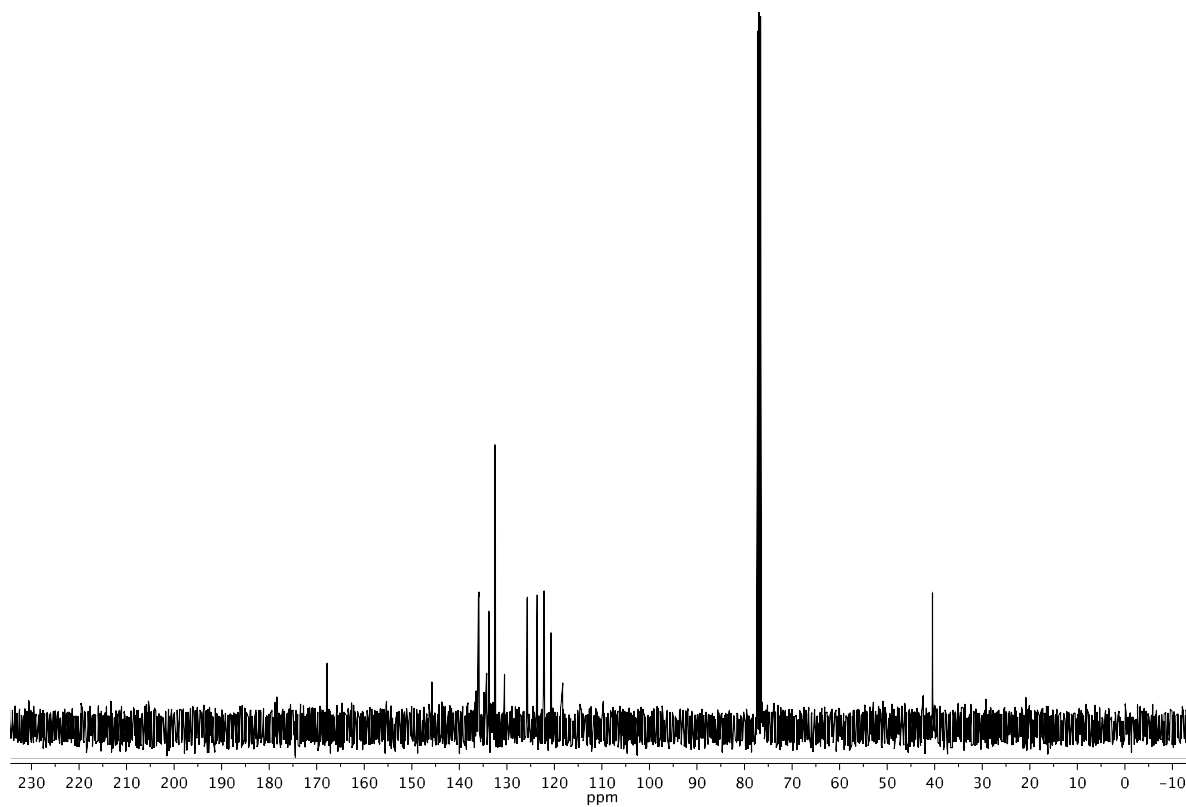
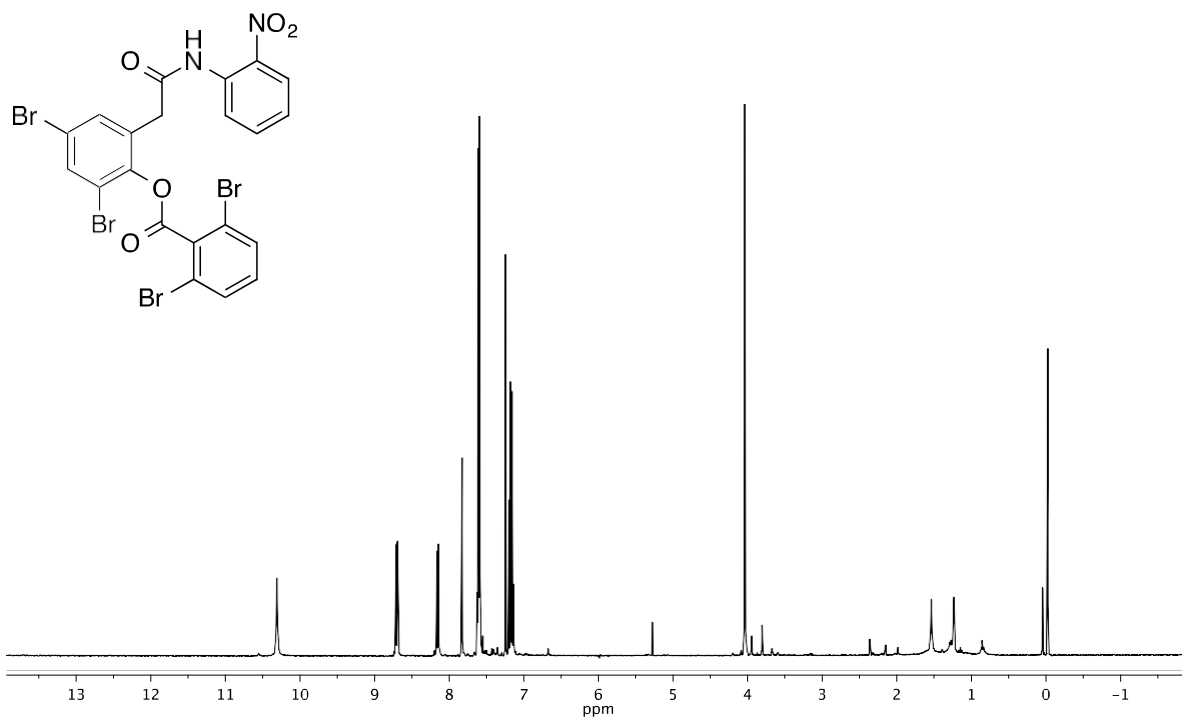
2,4-dibromo-6-(2-((2-nitrophenyl)amino)-2-oxoethyl)phenyl 4-methylbenzoate



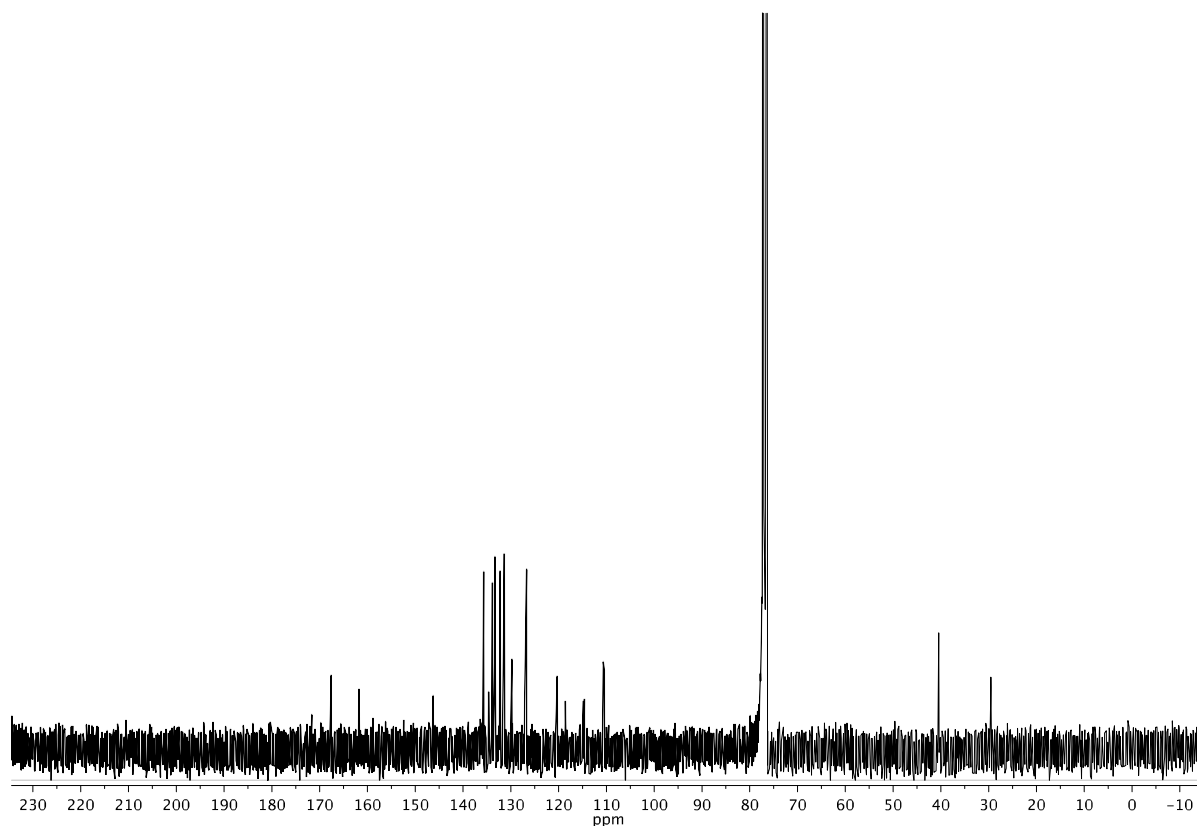
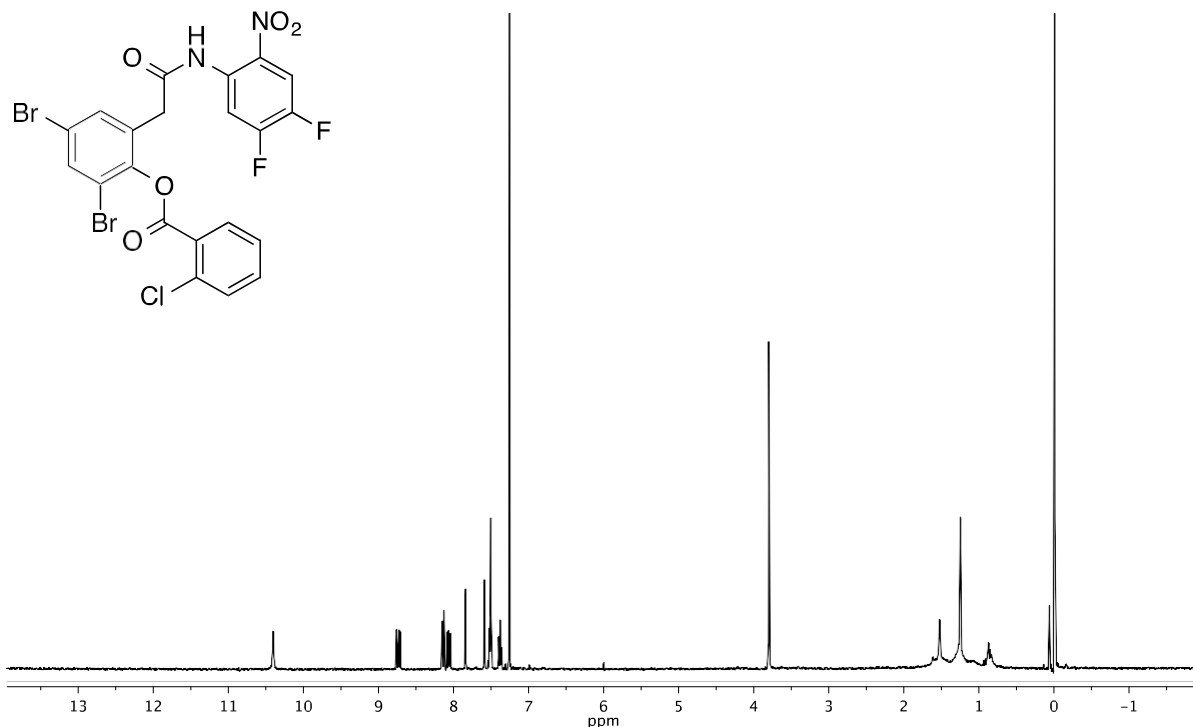
2,4-dibromo-6-(2-((2-nitrophenyl)amino)-2-oxoethyl)phenyl 2,6-dichlorobenzoate



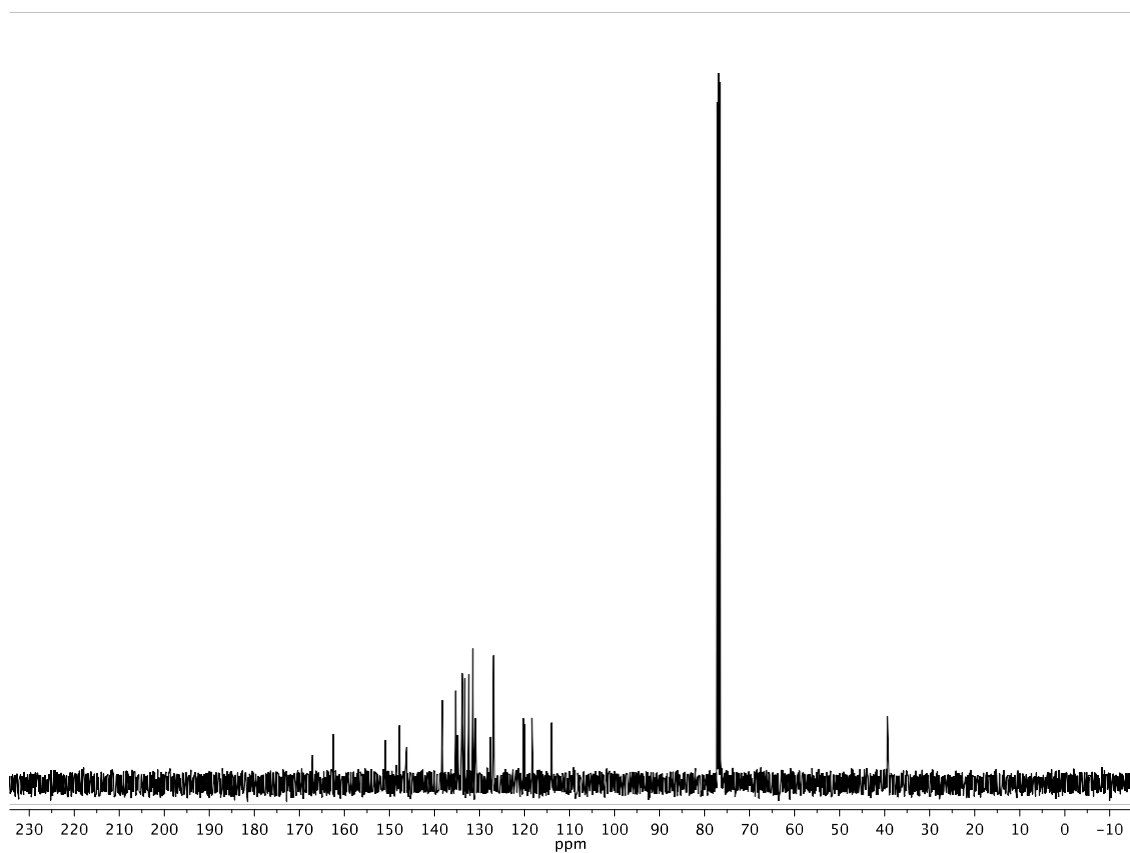
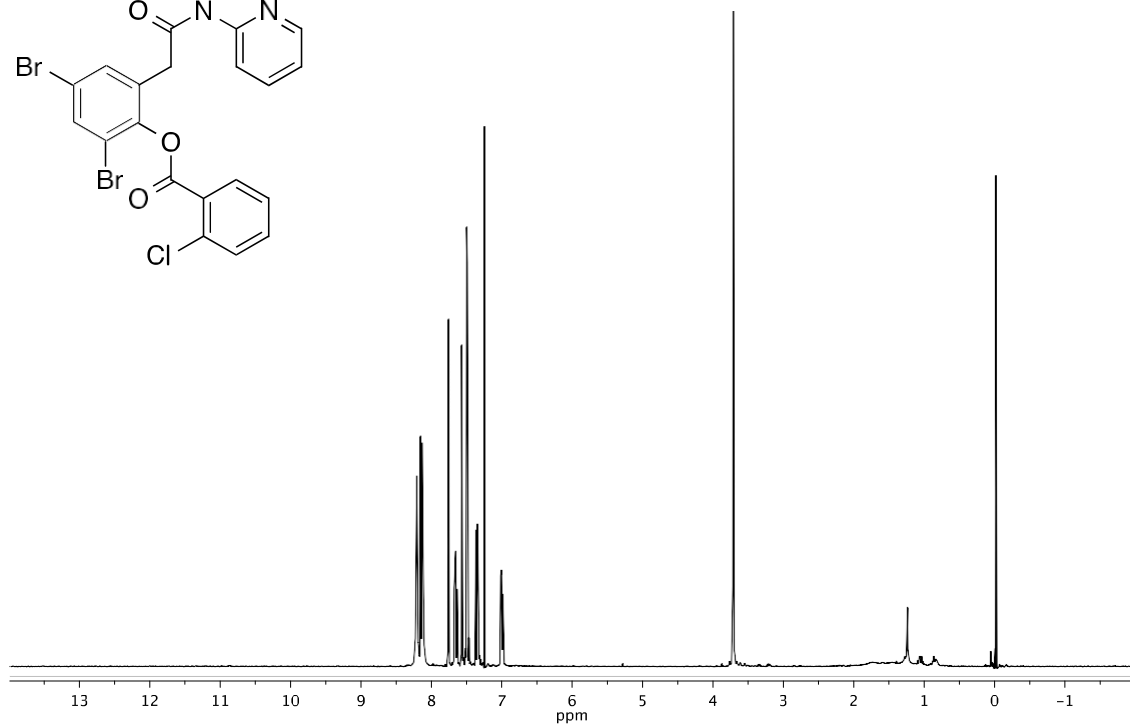
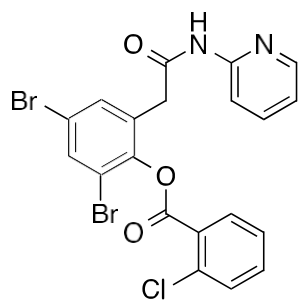
2,4-dibromo-6-(2-((2-nitrophenyl)amino)-2-oxoethyl)phenyl 2,6-dibromobenzoate



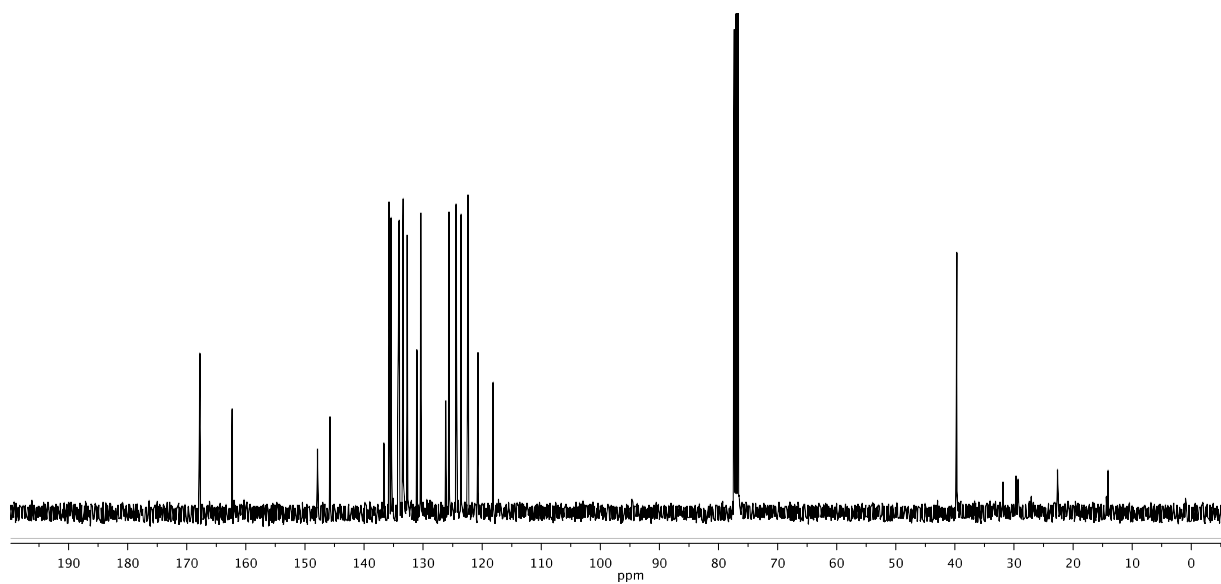
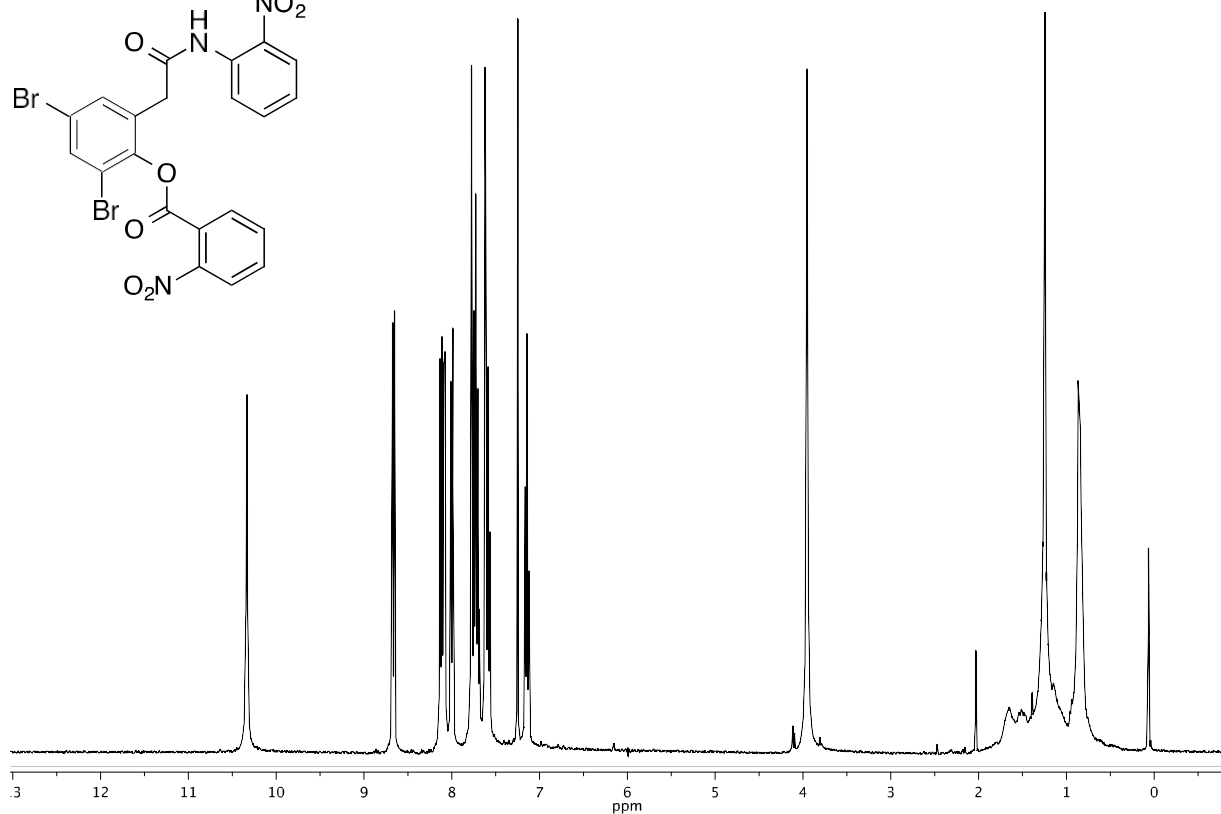
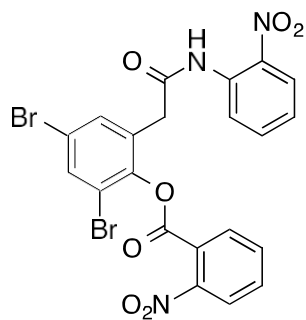
2,4-dibromo-6-(2-((4,5-difluoro-2-nitrophenyl)amino)-2-oxoethyl)phenyl 2-chlorobenzoate



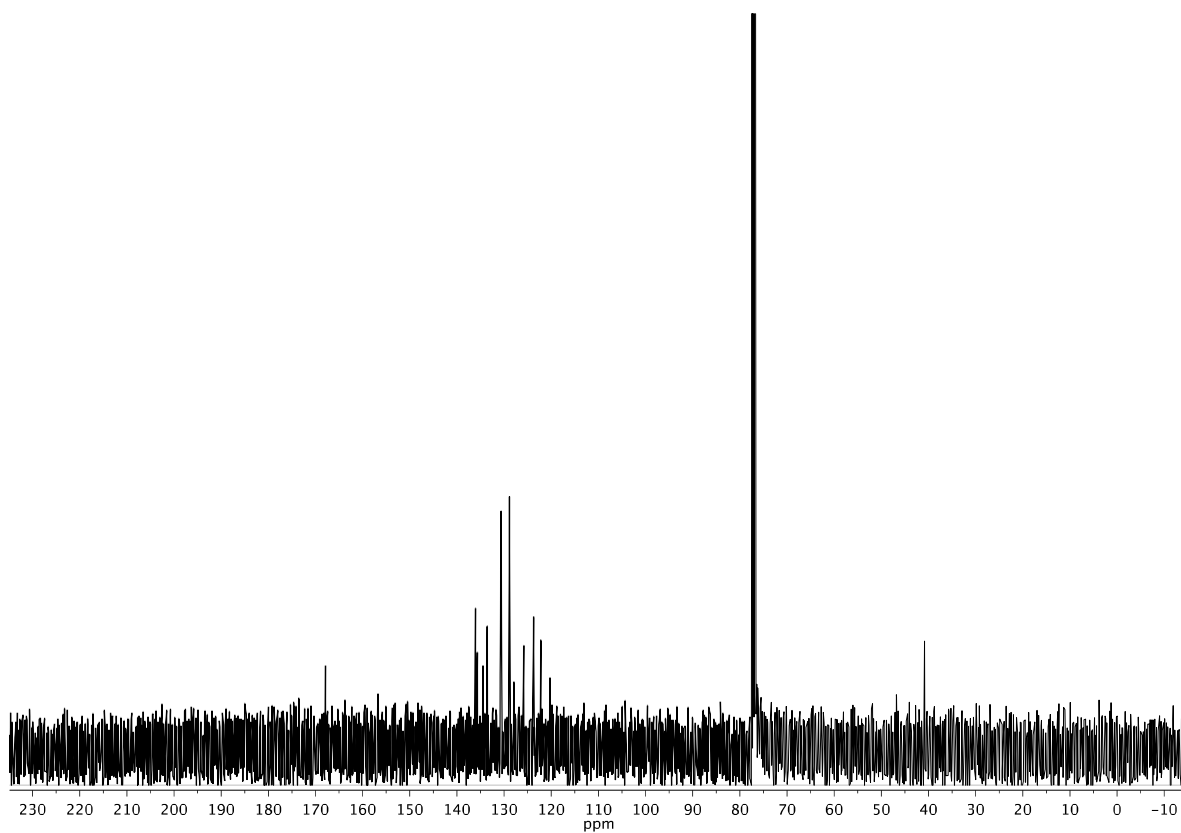
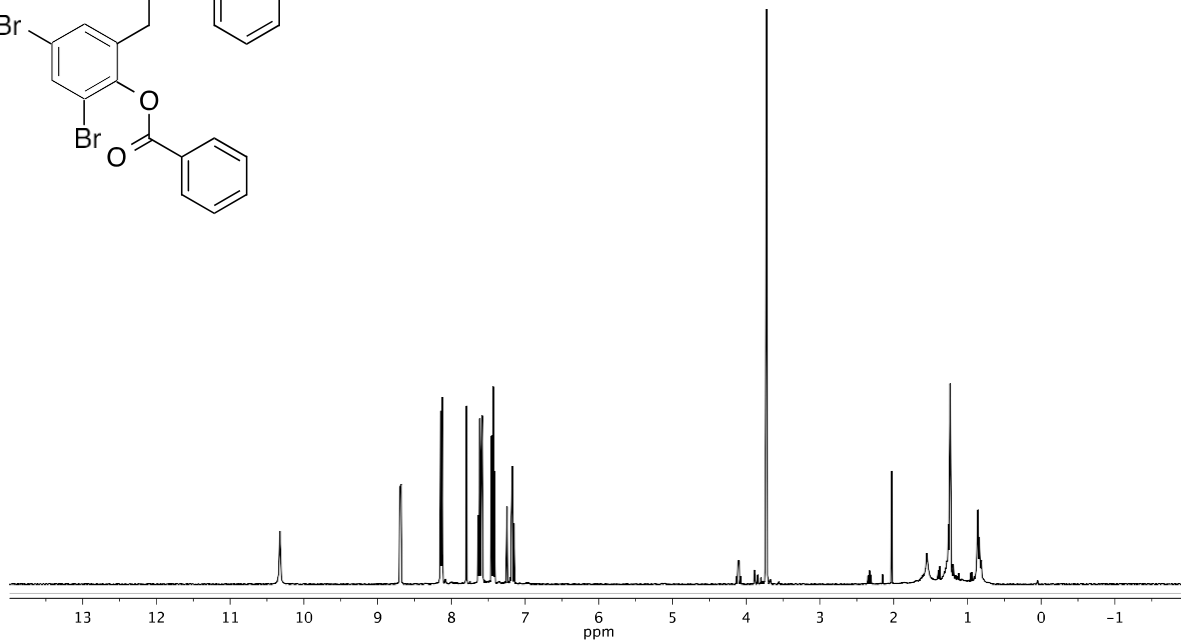
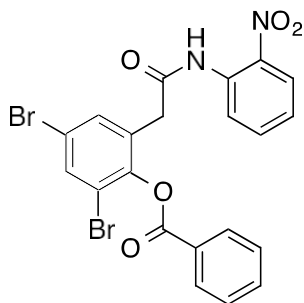
2,4-dibromo-6-(2-oxo-2-(pyridin-2-ylamino)ethyl)phenyl 2-chlorobenzoate



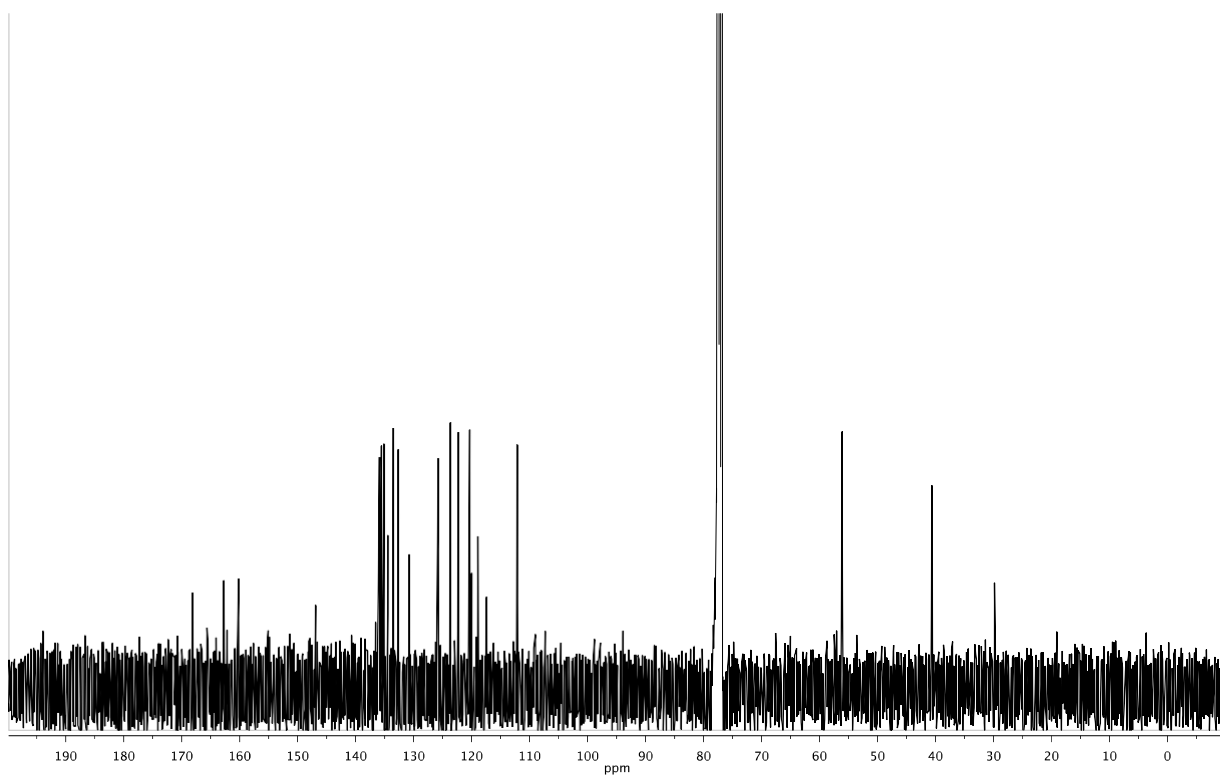
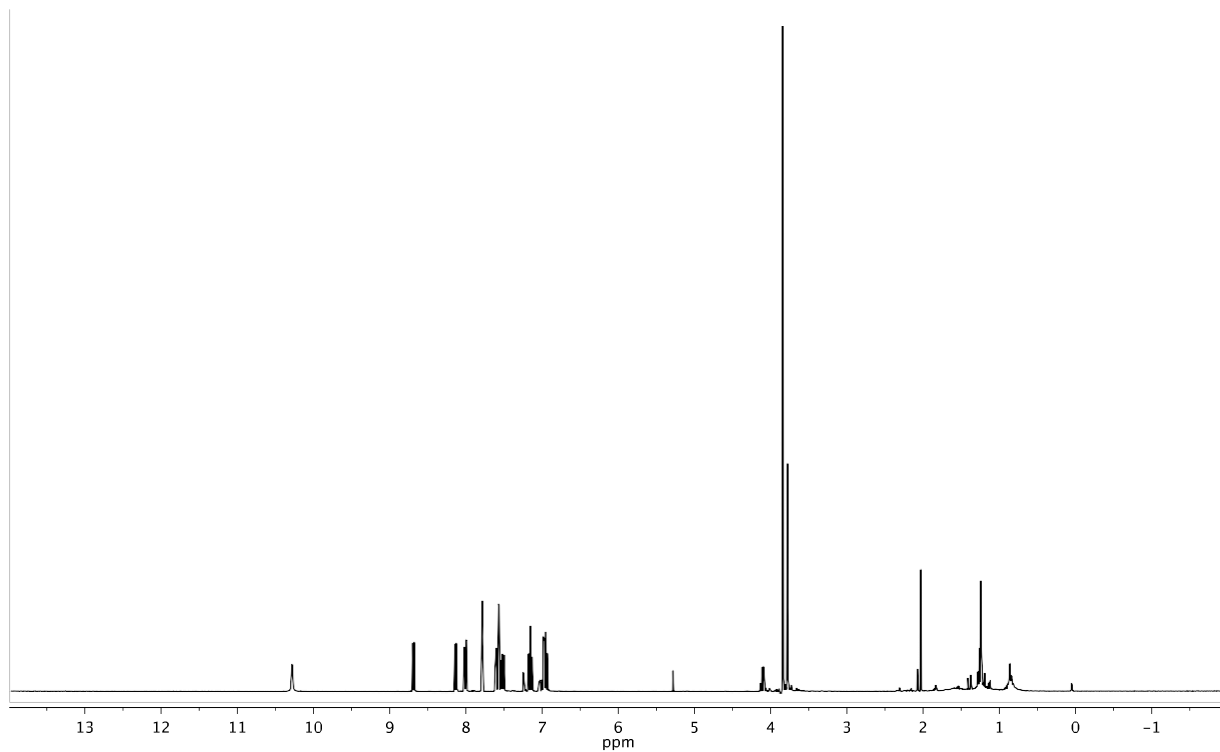
2,4-dibromo-6-(2-((2-nitrophenyl)amino)-2-oxoethyl)phenyl 2-nitrobenzoate



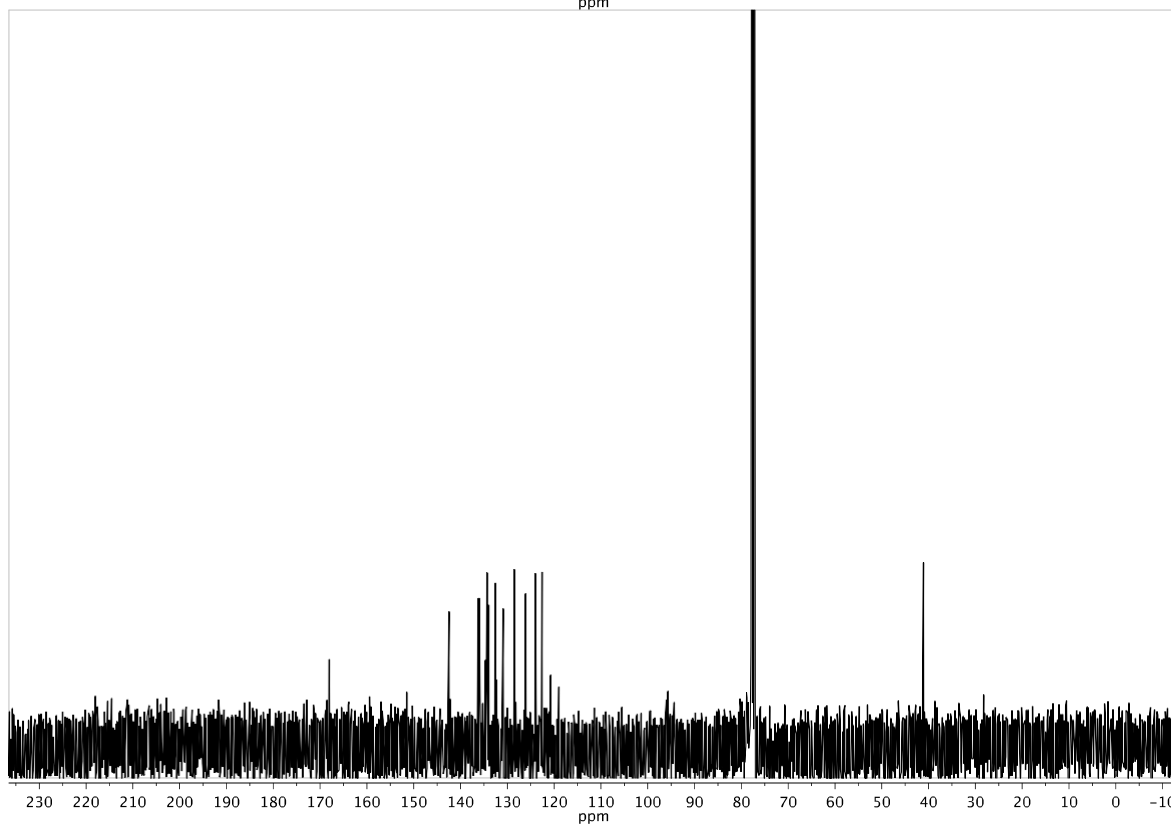
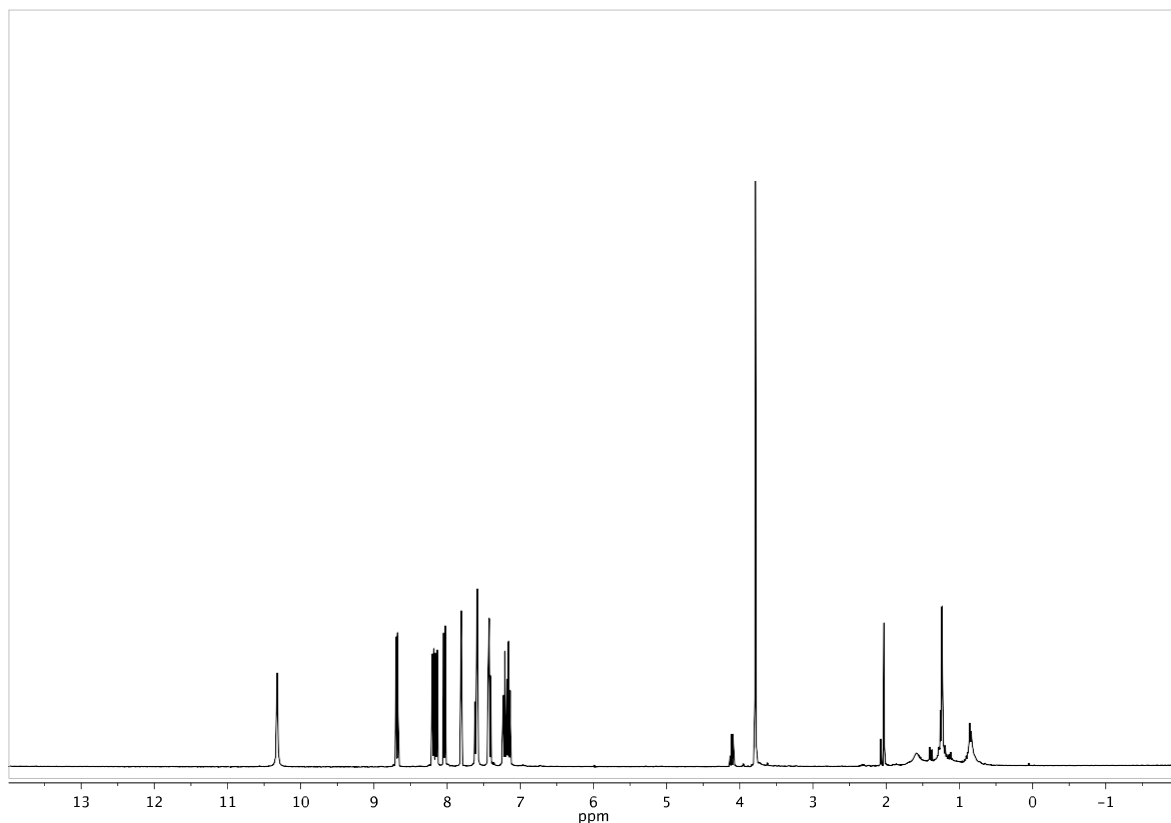
2,4-dibromo-6-(2-((2-nitrophenyl)amino)-2-oxoethyl)phenyl benzoate



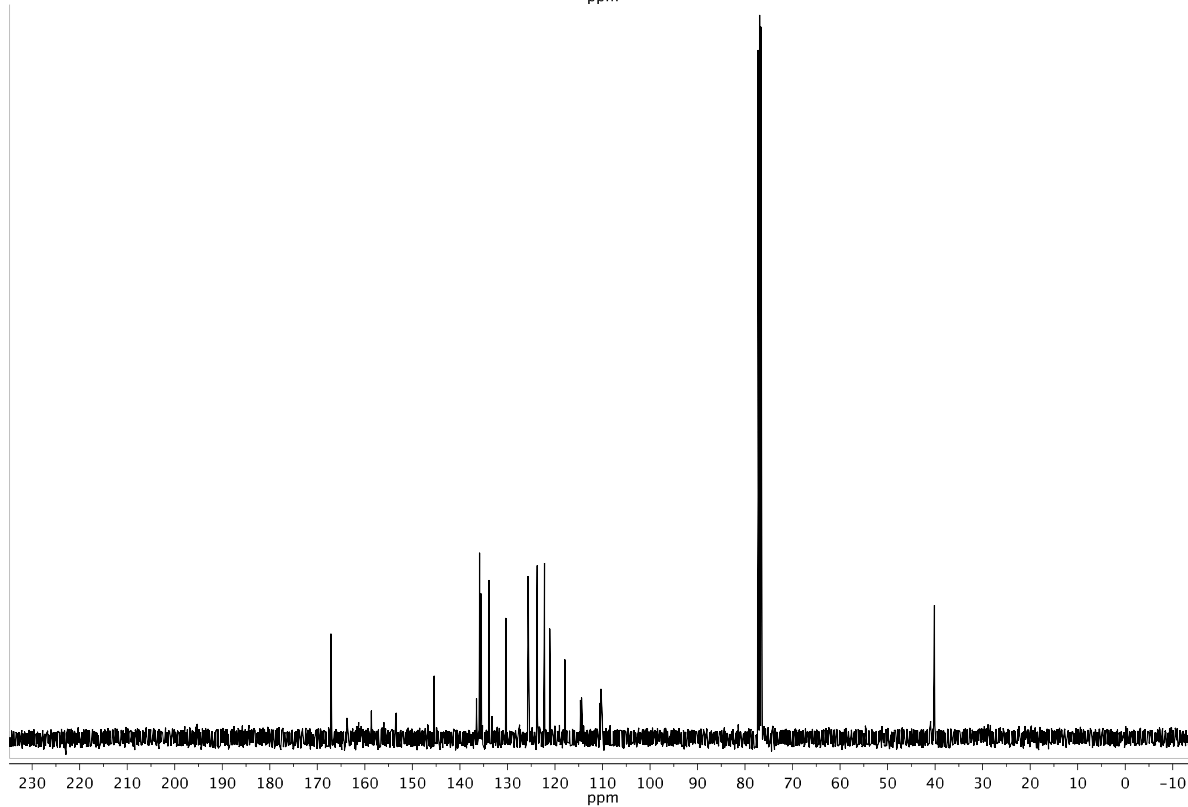
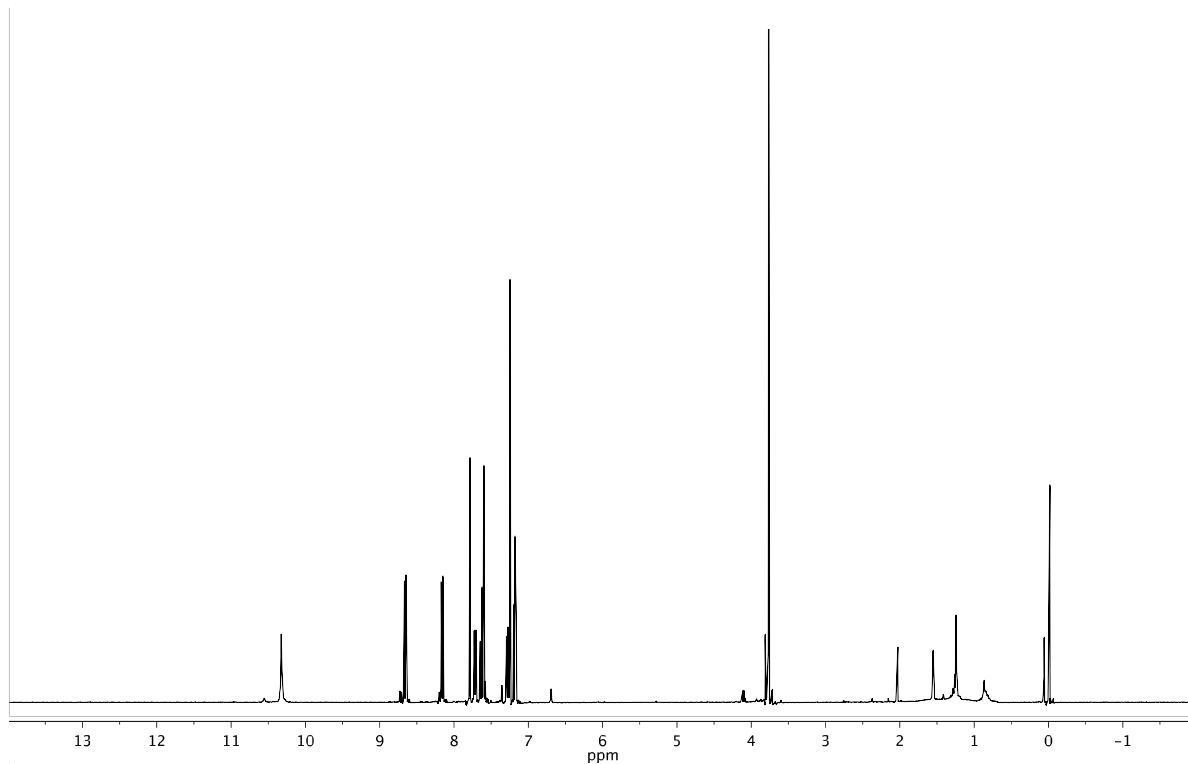
2,4-dibromo-6-(2-((2-nitrophenyl)amino)-2-oxoethyl)phenyl 2-methoxybenzoate



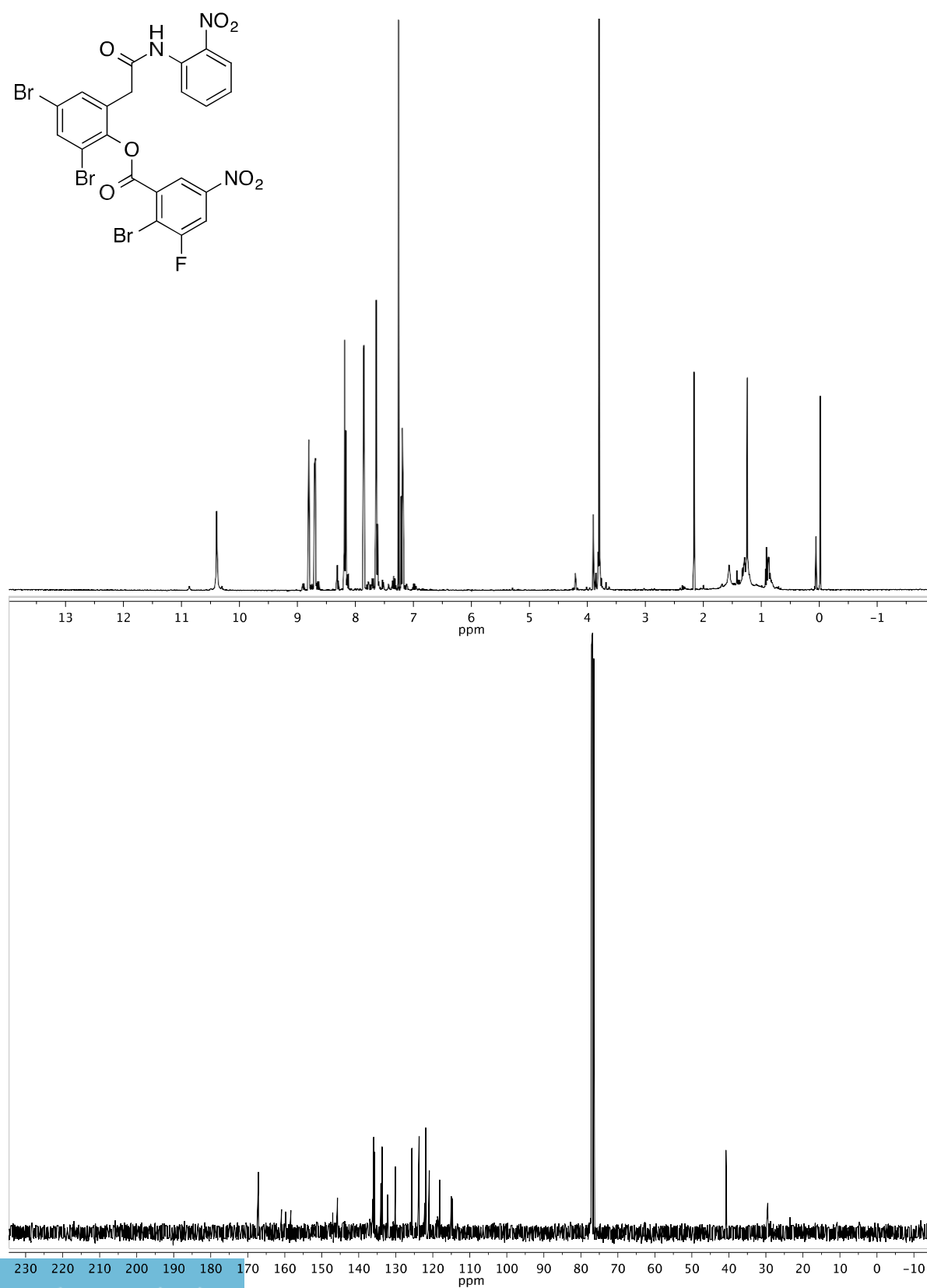
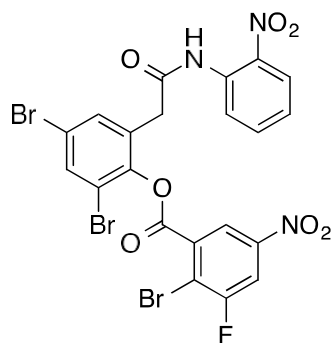
2,4-dibromo-6-(2-((2-nitrophenyl)amino)-2-oxoethyl)phenyl 2-iodobenzoate



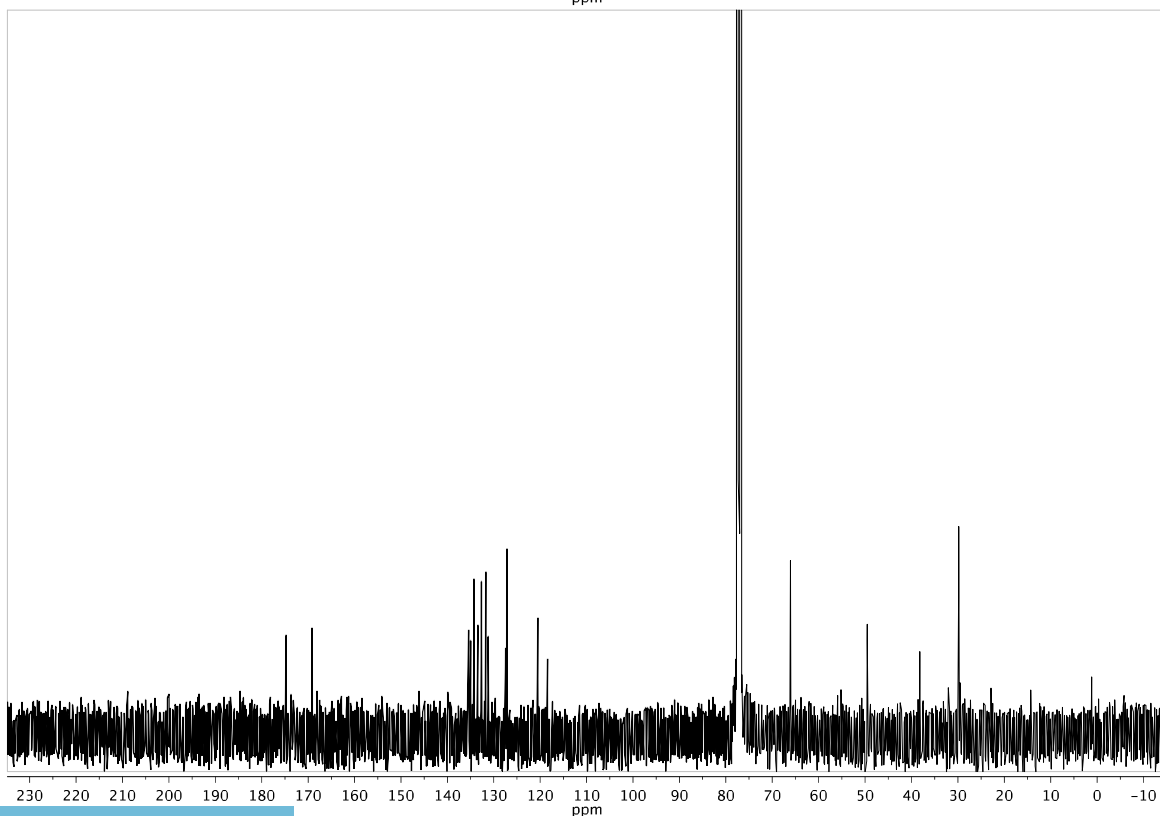
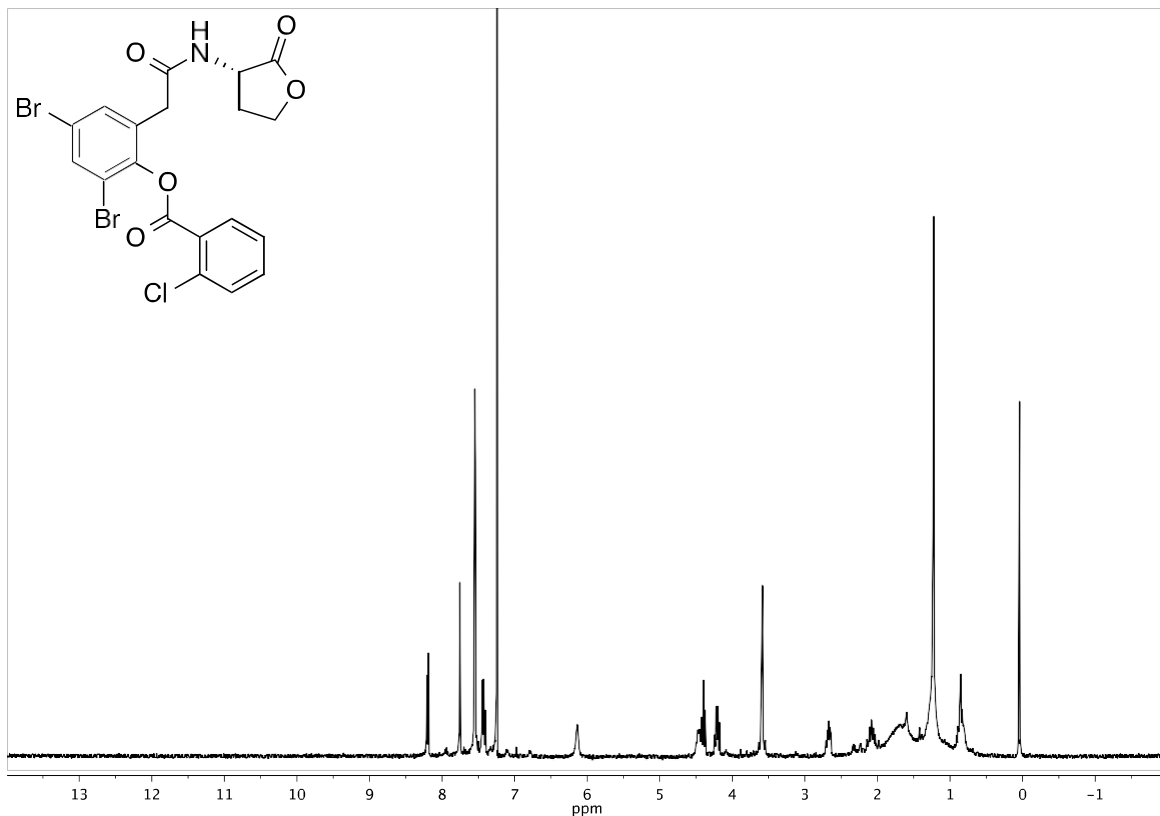
2,4-dibromo-6-(2-((2-nitrophenyl)amino)-2-oxoethyl)phenyl 3,5-difluoro-2-nitrobenzoate



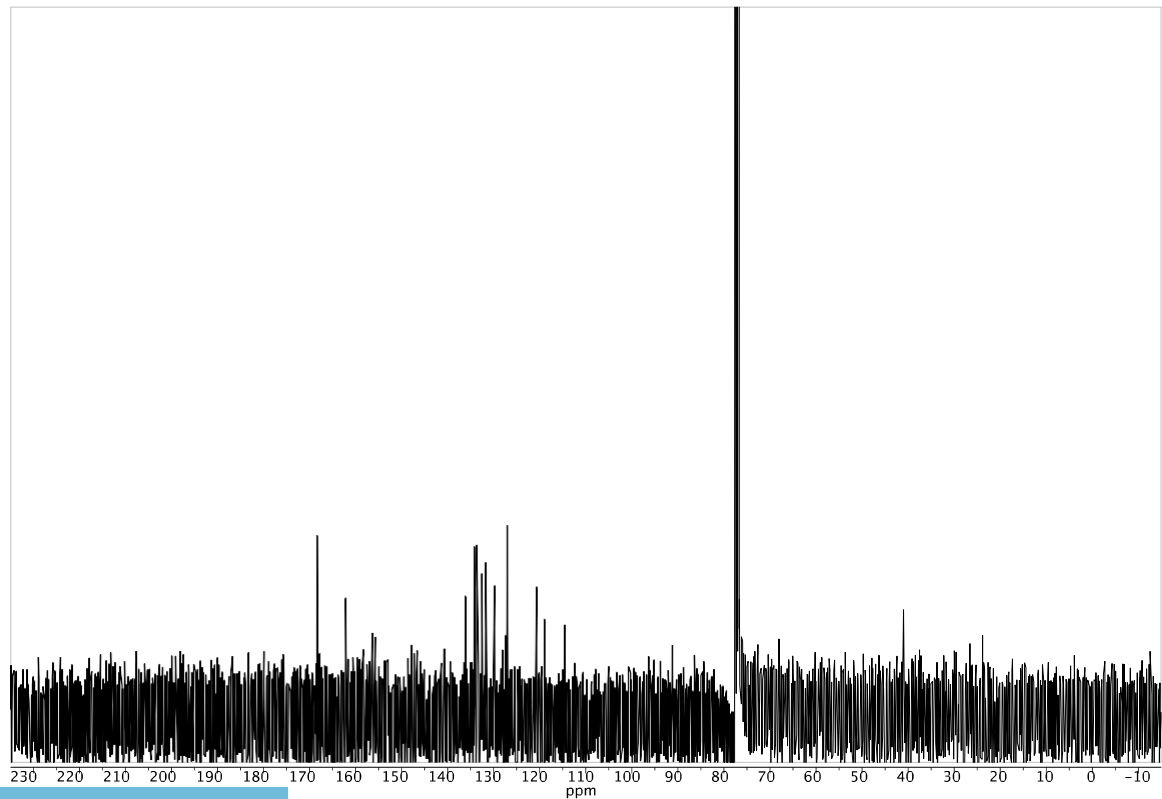
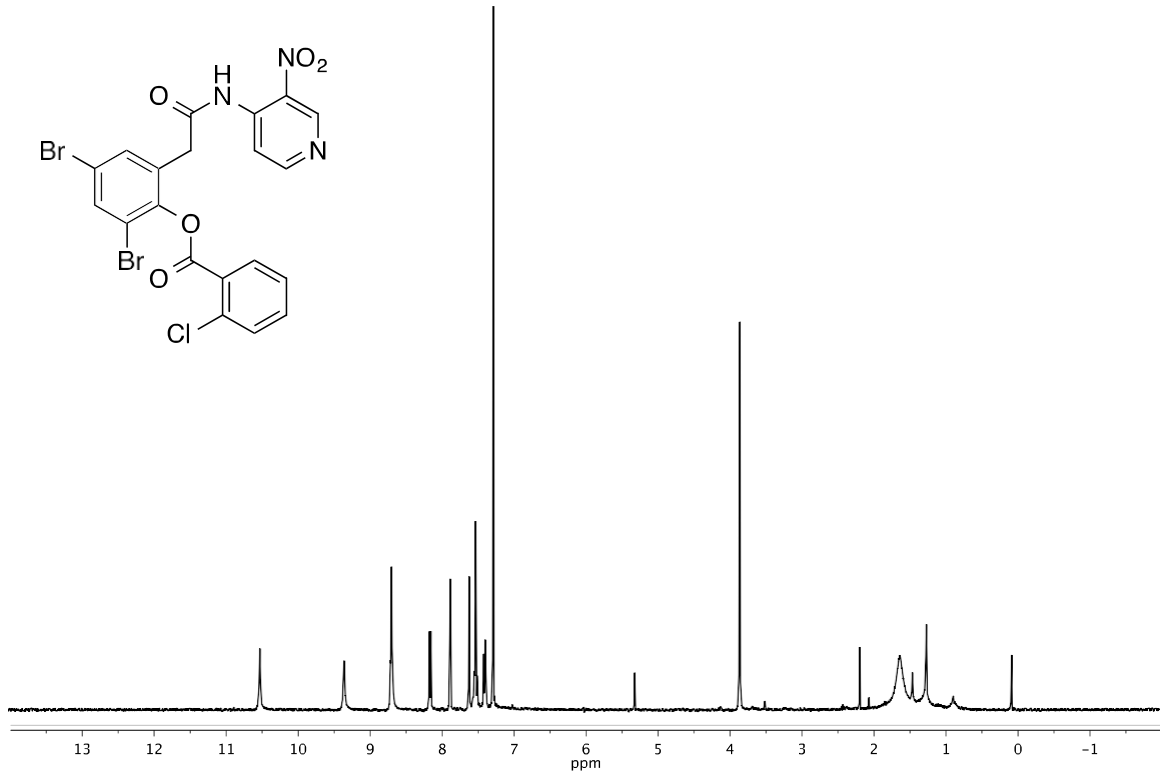
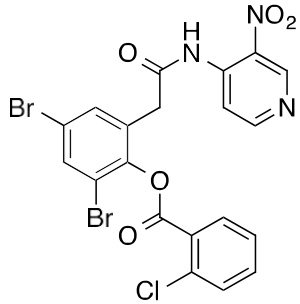
2,4-dibromo-6-(2-((2-nitrophenyl)amino)-2-oxoethyl)phenyl 2-bromo-3-fluoro-5-nitrobenzoate



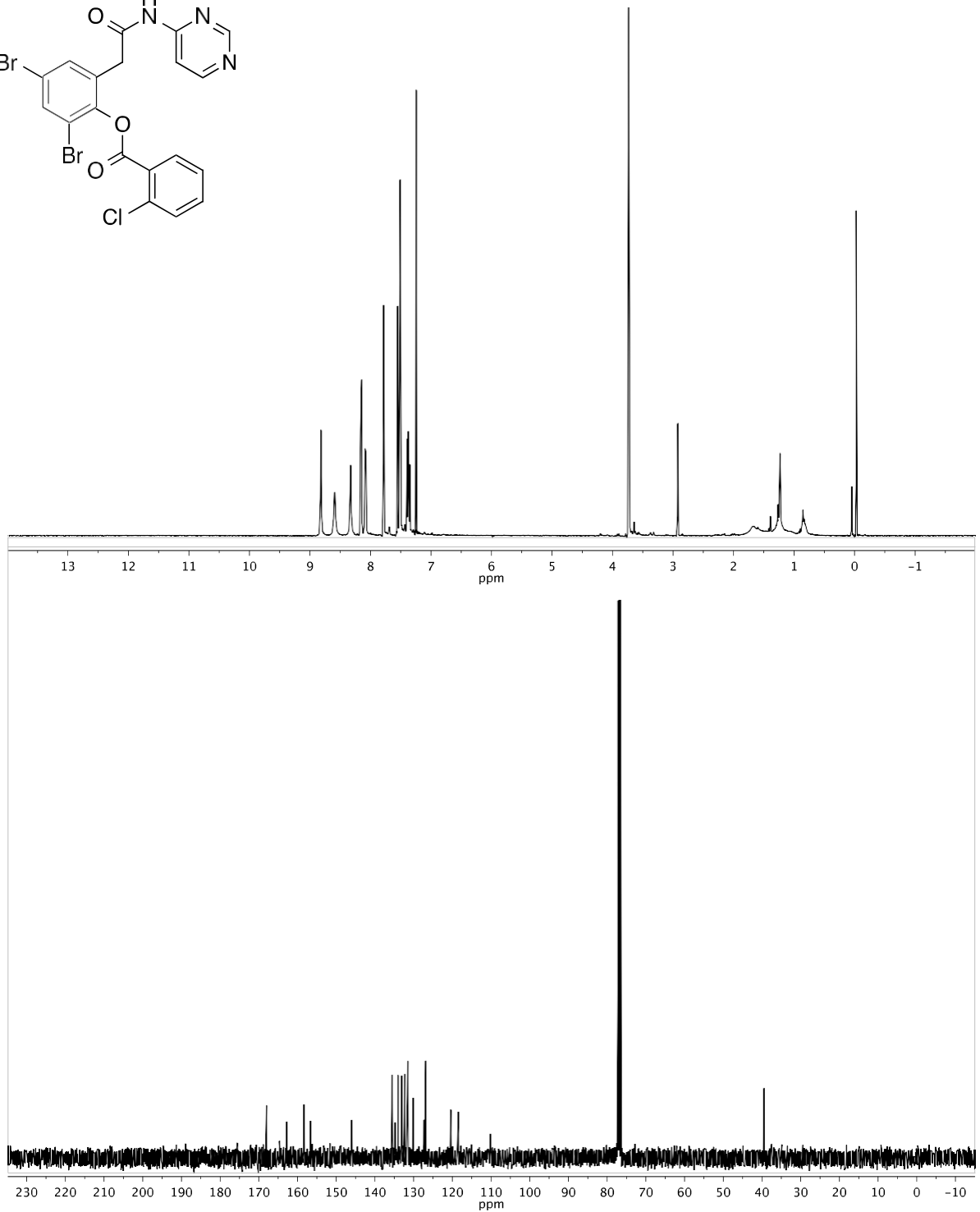
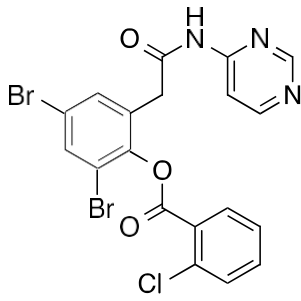
(S)-2,4-dibromo-6-(2-oxo-2-((2-oxotetrahydrofuran-3-yl)amino)ethyl)phenyl 2-chlorobenzoate



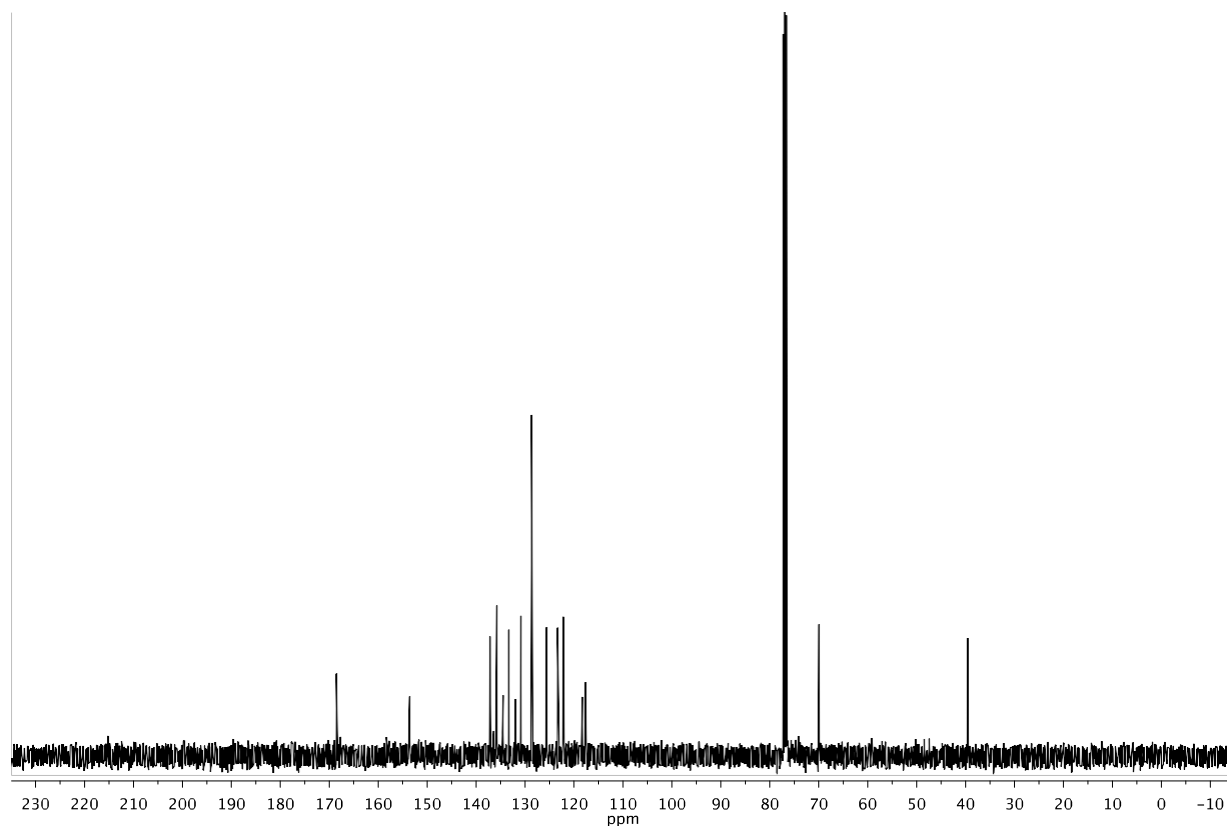
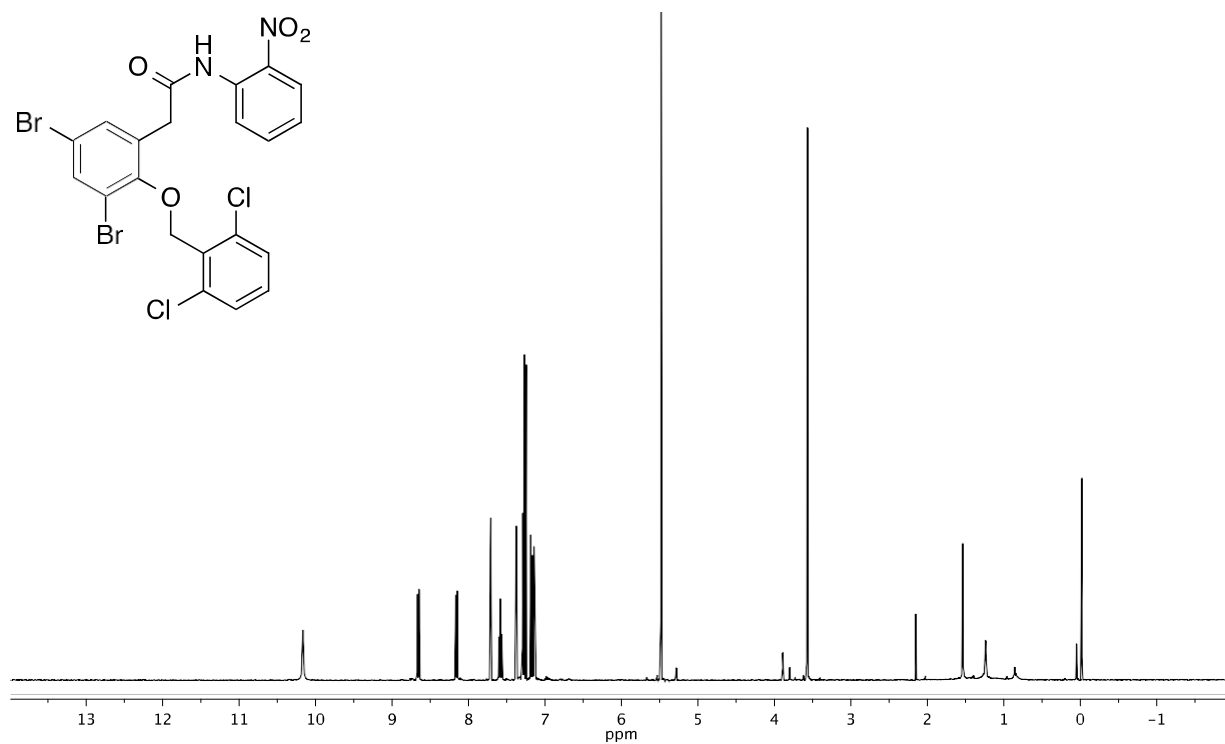
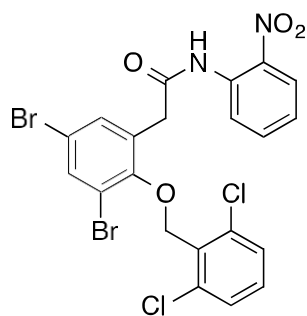
2,4-dibromo-6-(2-((3-nitropyridin-4-yl)amino)-2-oxoethyl)phenyl 2-chlorobenzoate



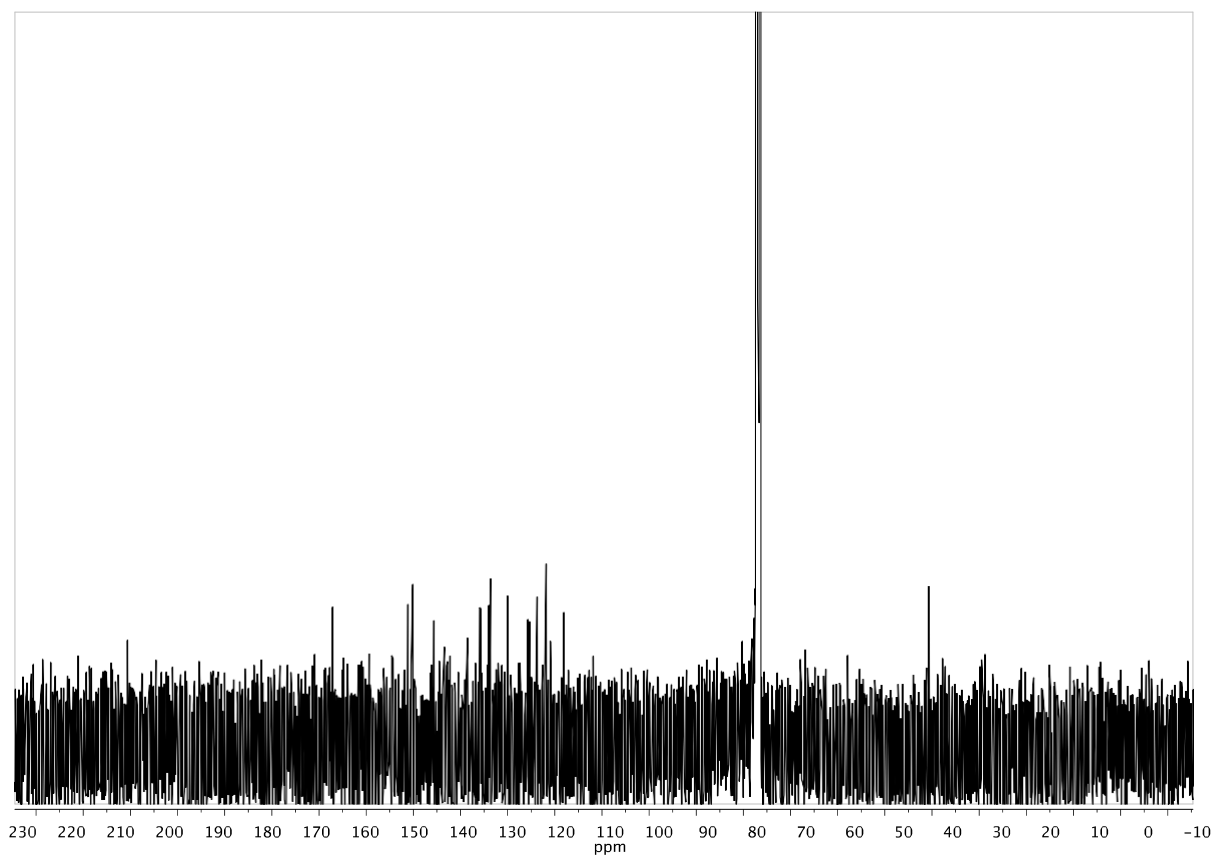
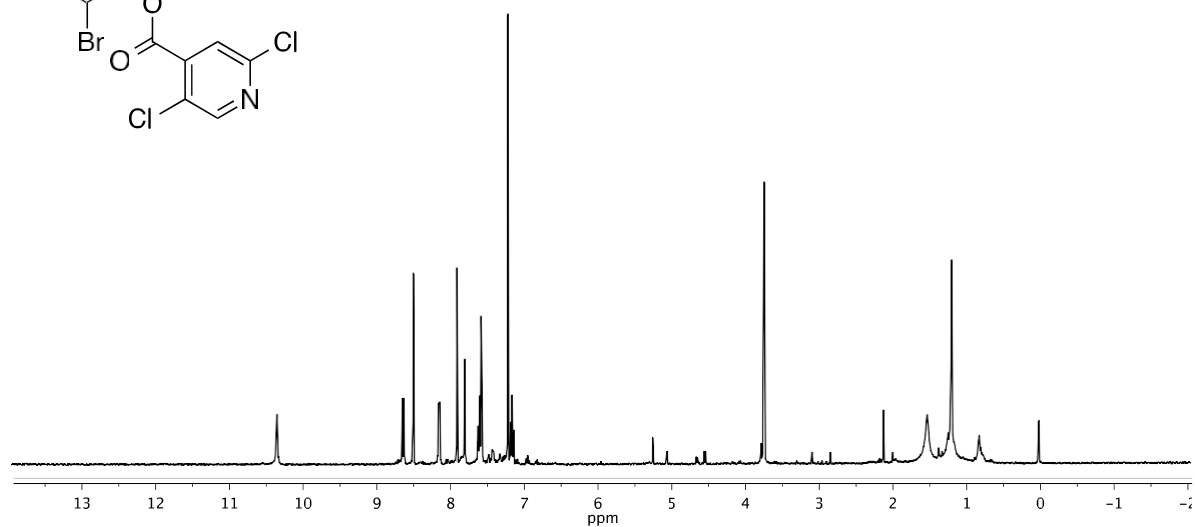
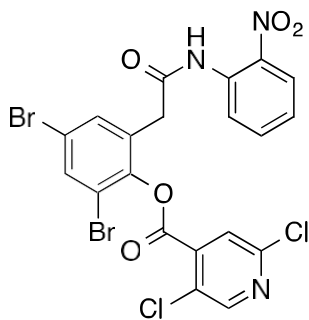
2,4-dibromo-6-(2-oxo-2-(pyrimidin-4-ylamino)ethyl)phenyl 2-chlorobenzoate



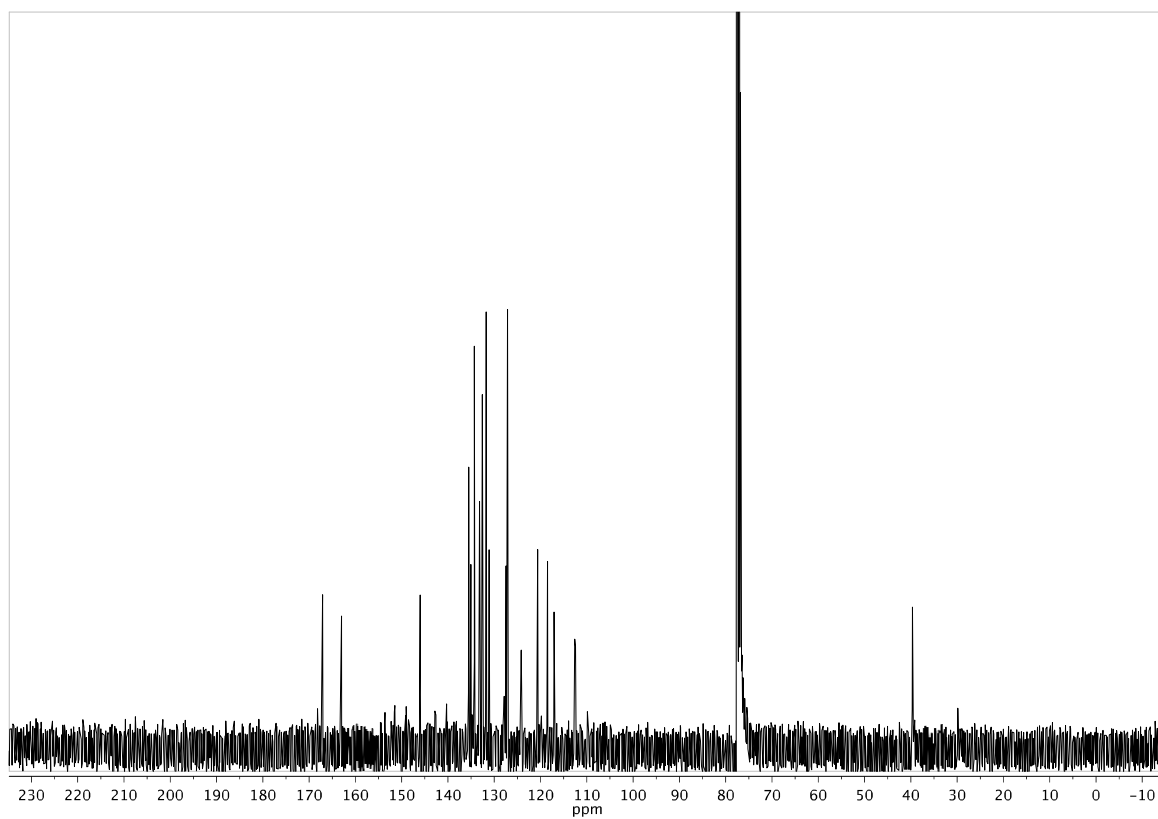
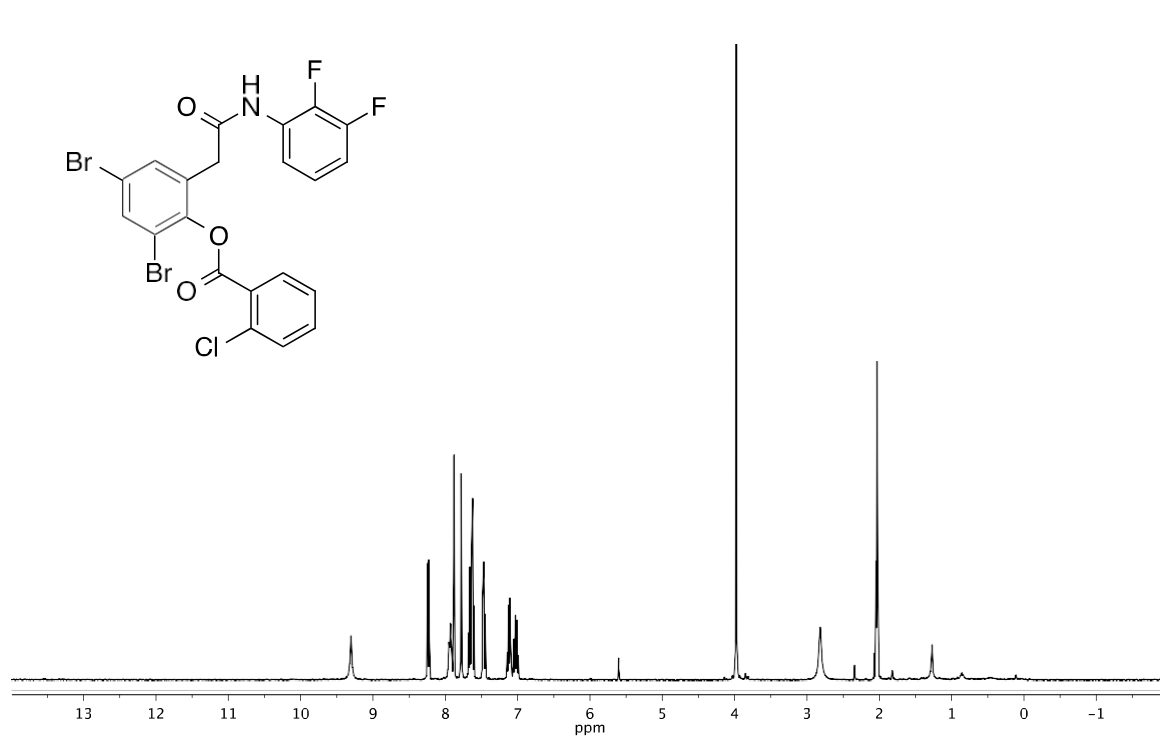
2-(3,5-dibromo-2-((2,6-dichlorobenzyl)oxy)phenyl)-N-(2-nitrophenyl)acetamide



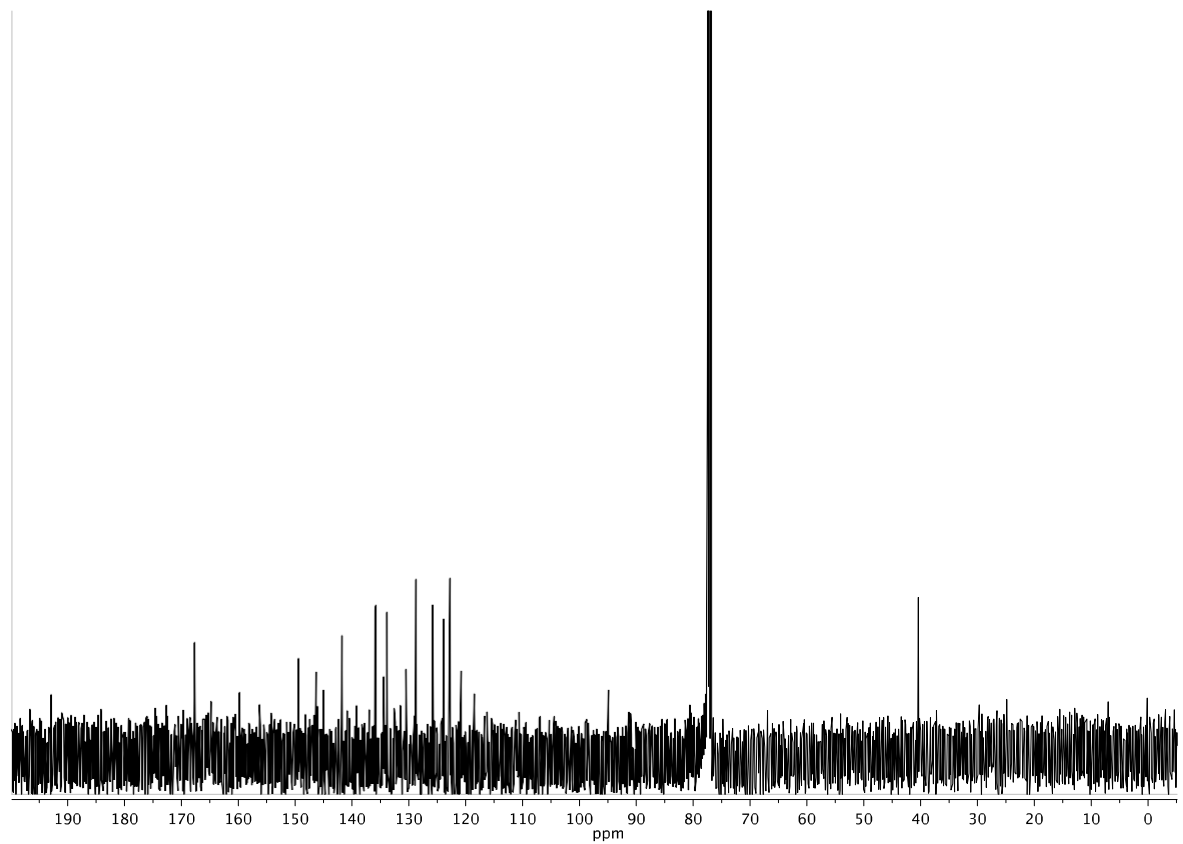
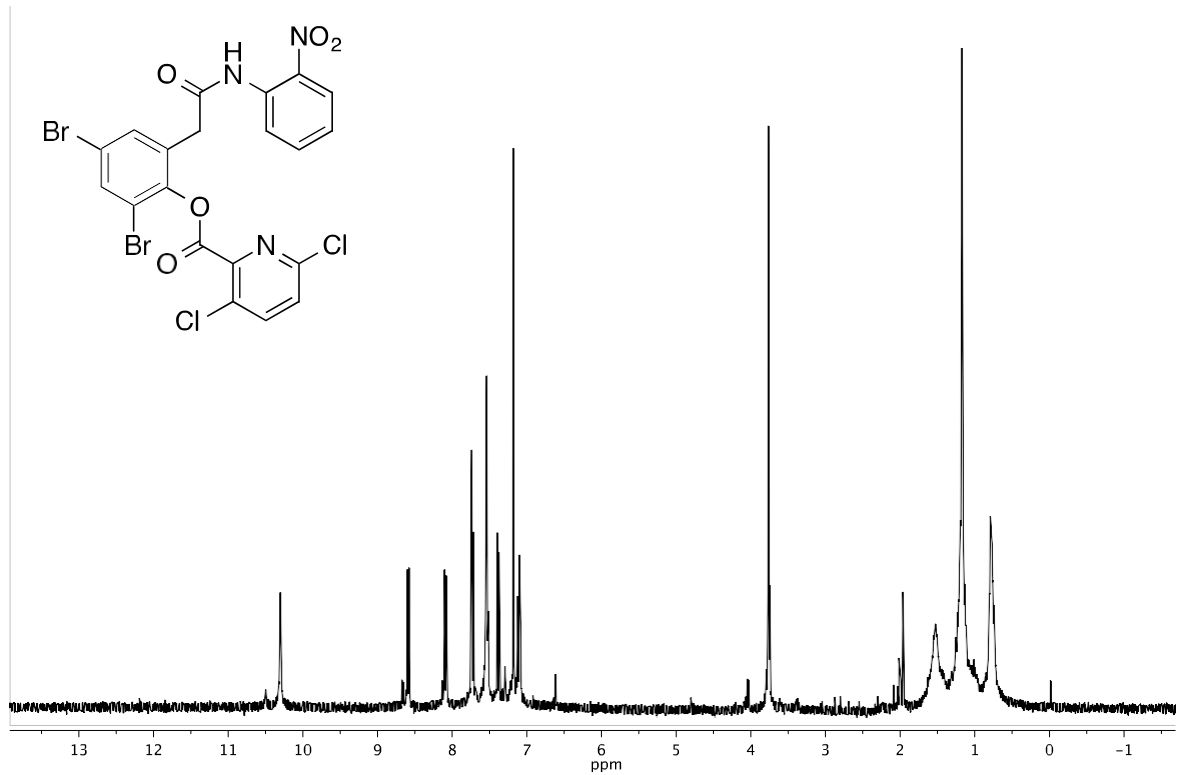
2,4-dibromo-6-(2-((2-nitrophenyl)amino)-2-oxoethyl)phenyl 2,5-dichloroisonicotinate



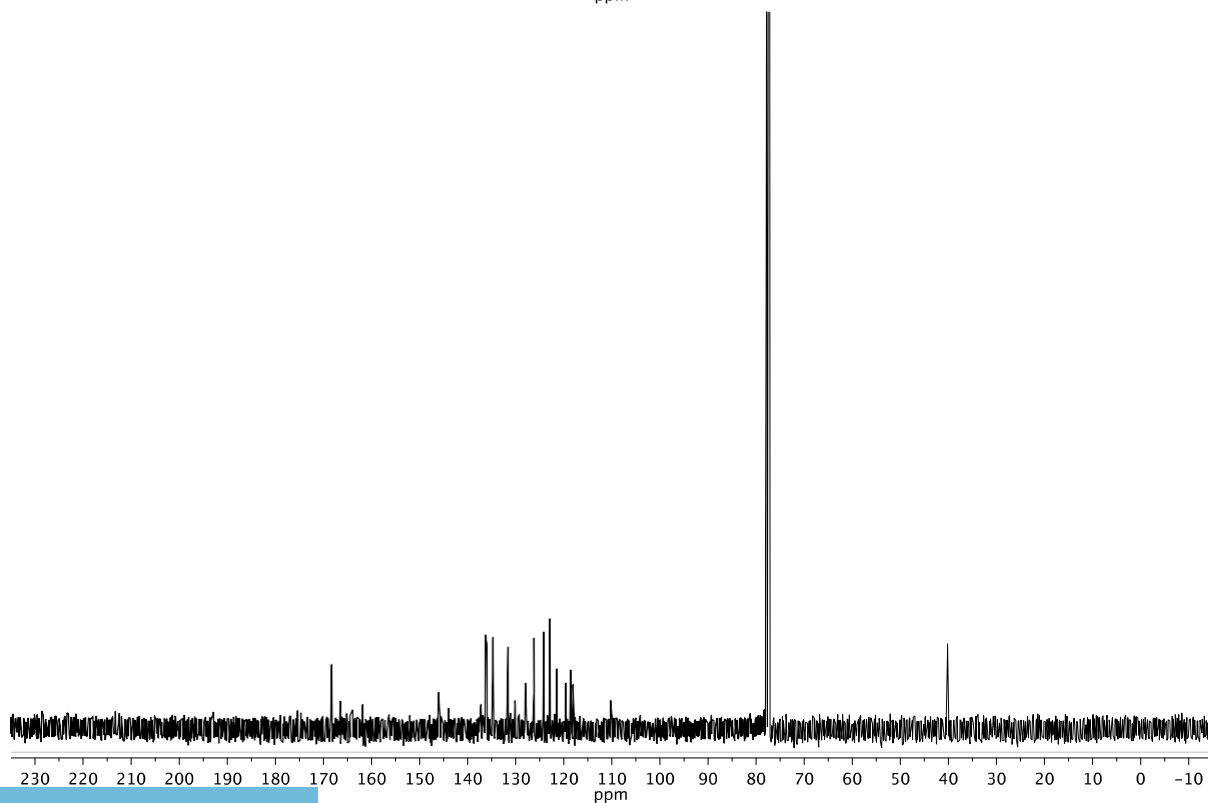
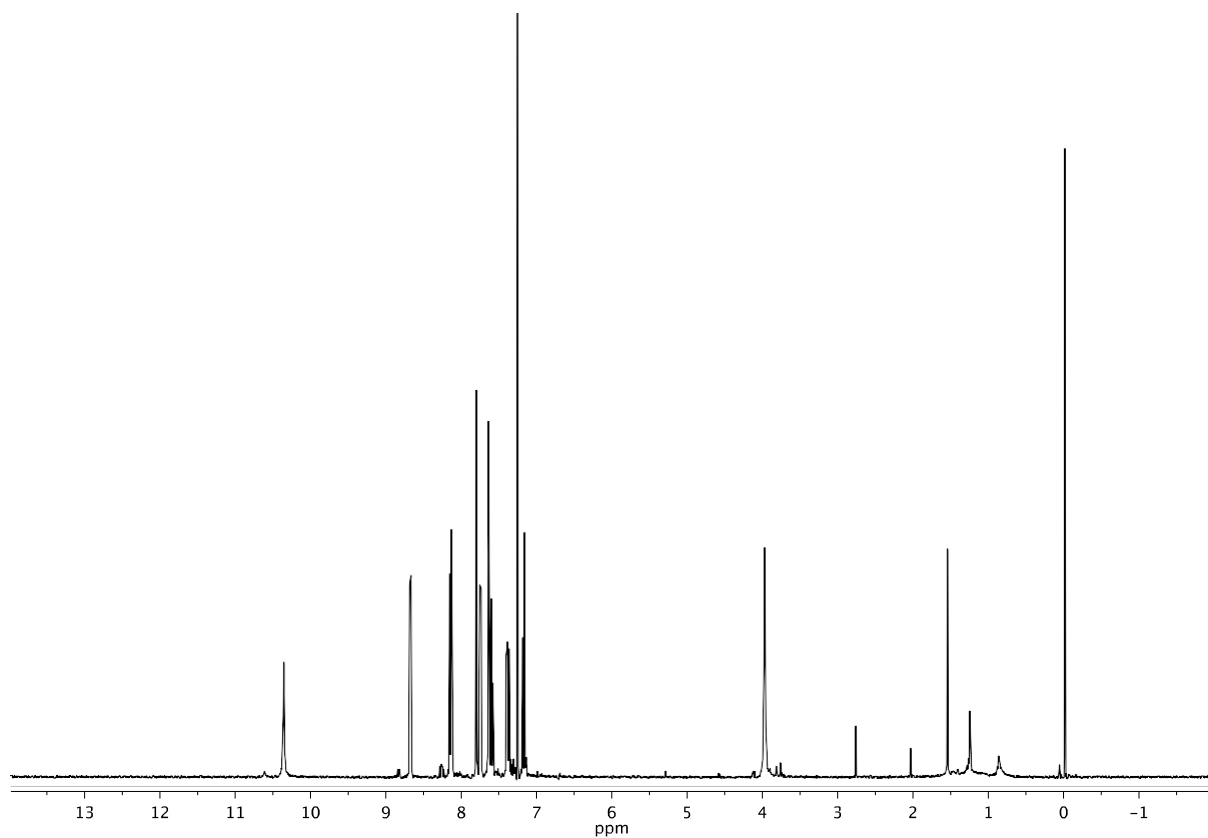
2,4-dibromo-6-(2-((2,3-difluorophenyl)amino)-2-oxoethyl)phenyl 2-chlorobenzoate



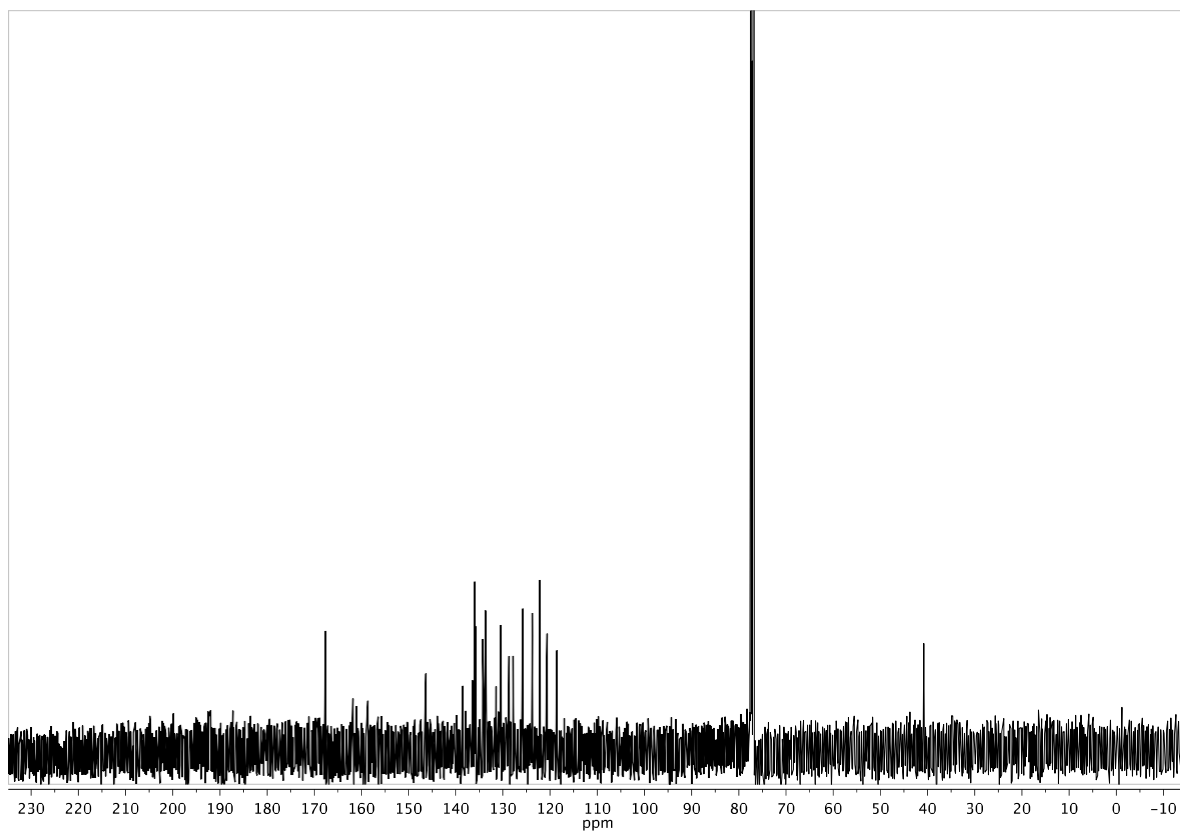
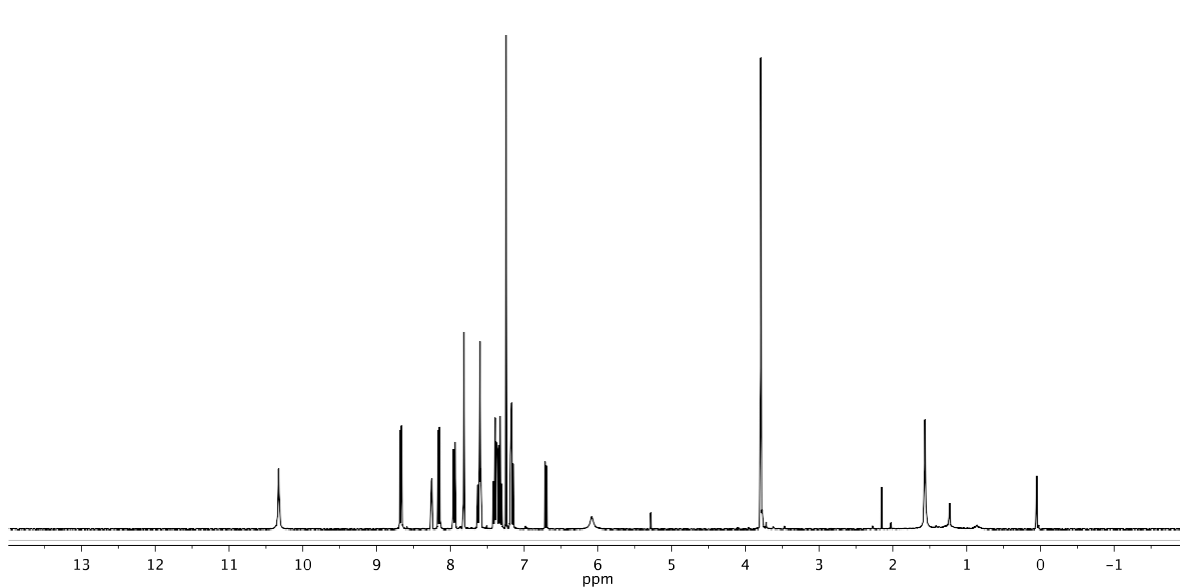
2,4-dibromo-6-(2-((2-nitrophenyl)amino)-2-oxoethyl)phenyl 3,6-dichloropicolinate



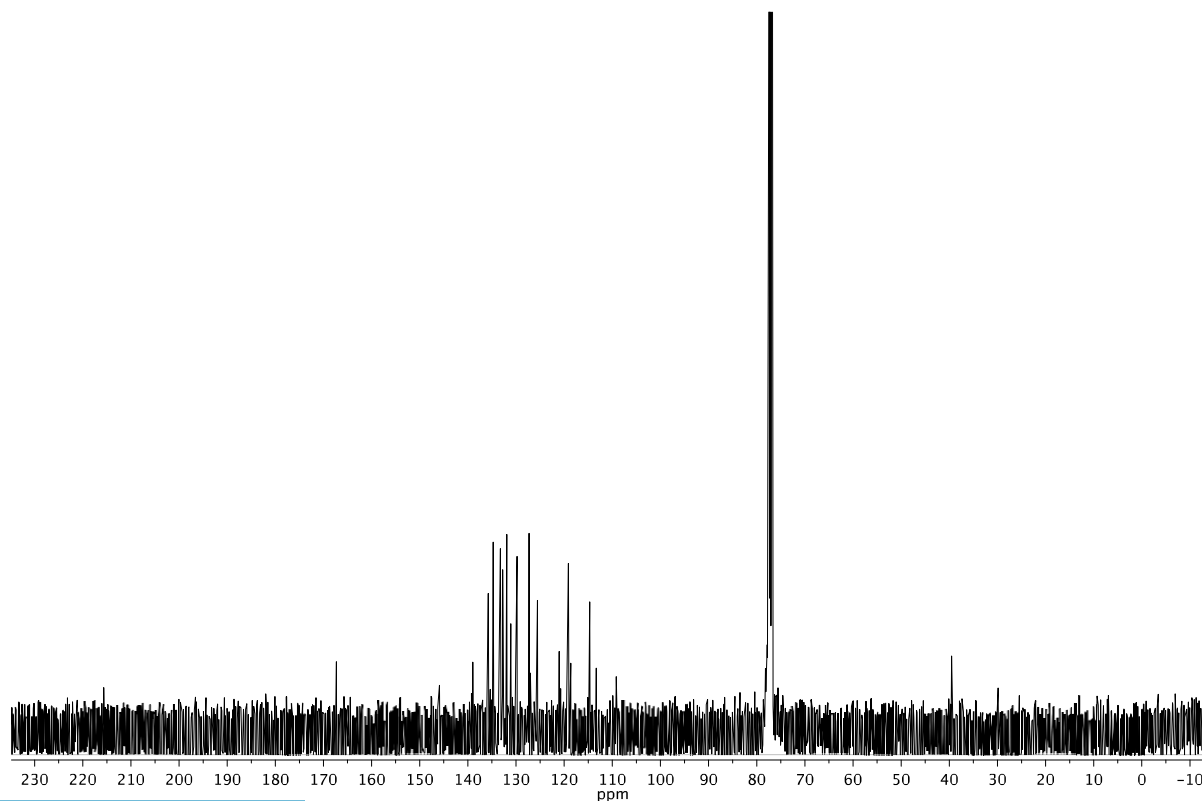
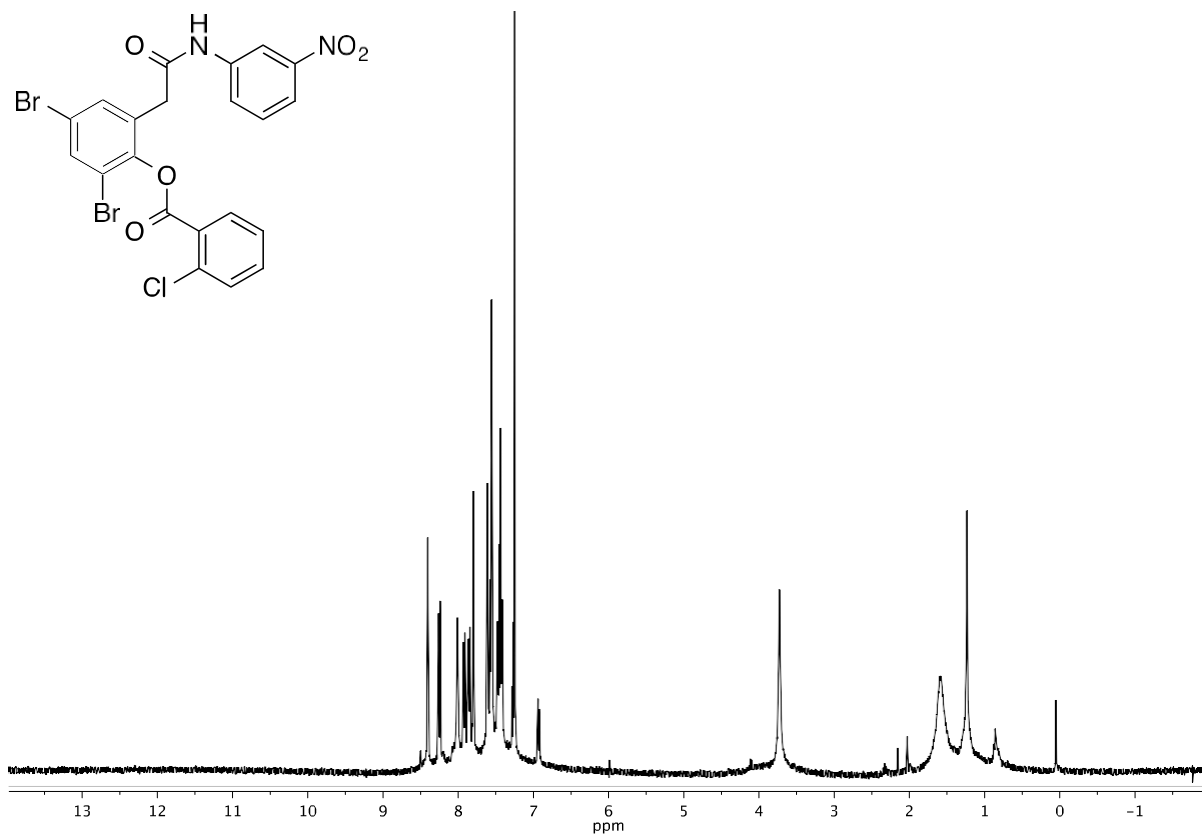
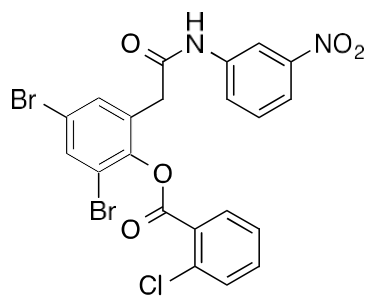
2,4-dibromo-6-(2-((2-nitrophenyl)amino)-2-oxoethyl)phenyl 5-fluoro-2-nitrobenzoate



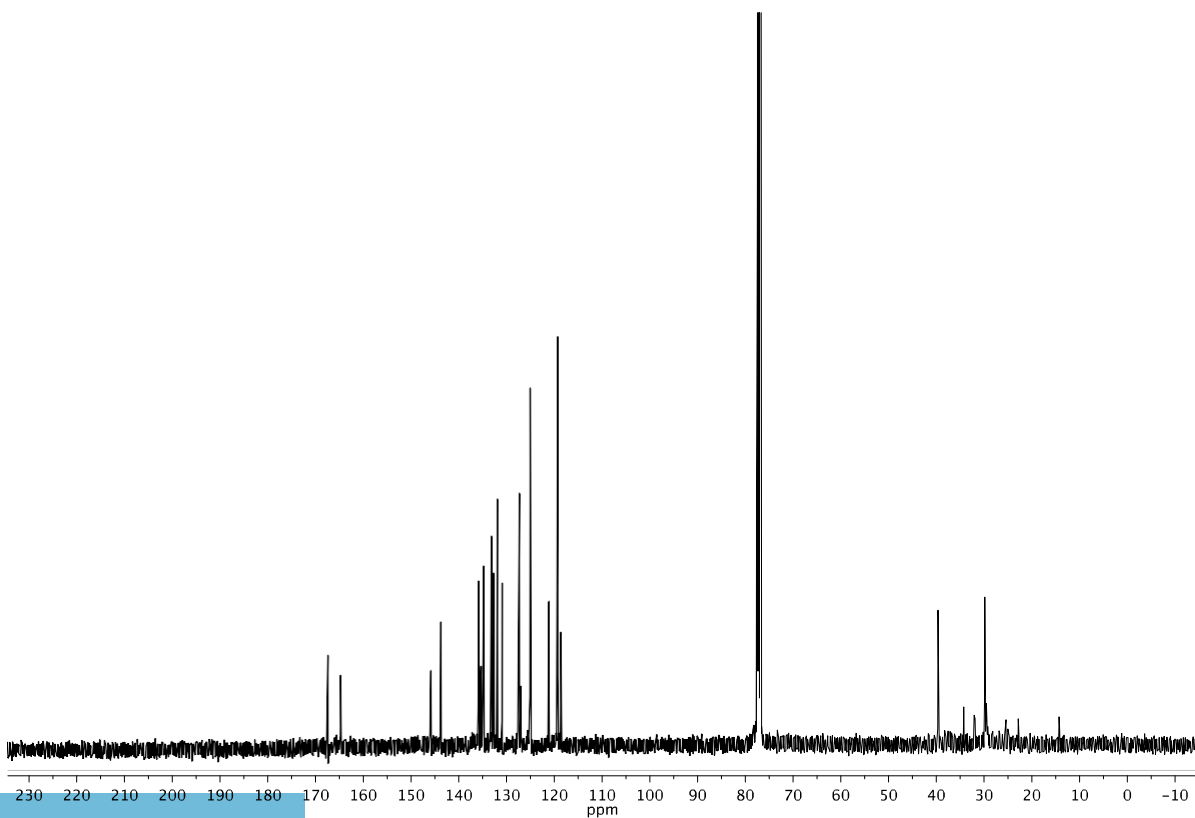
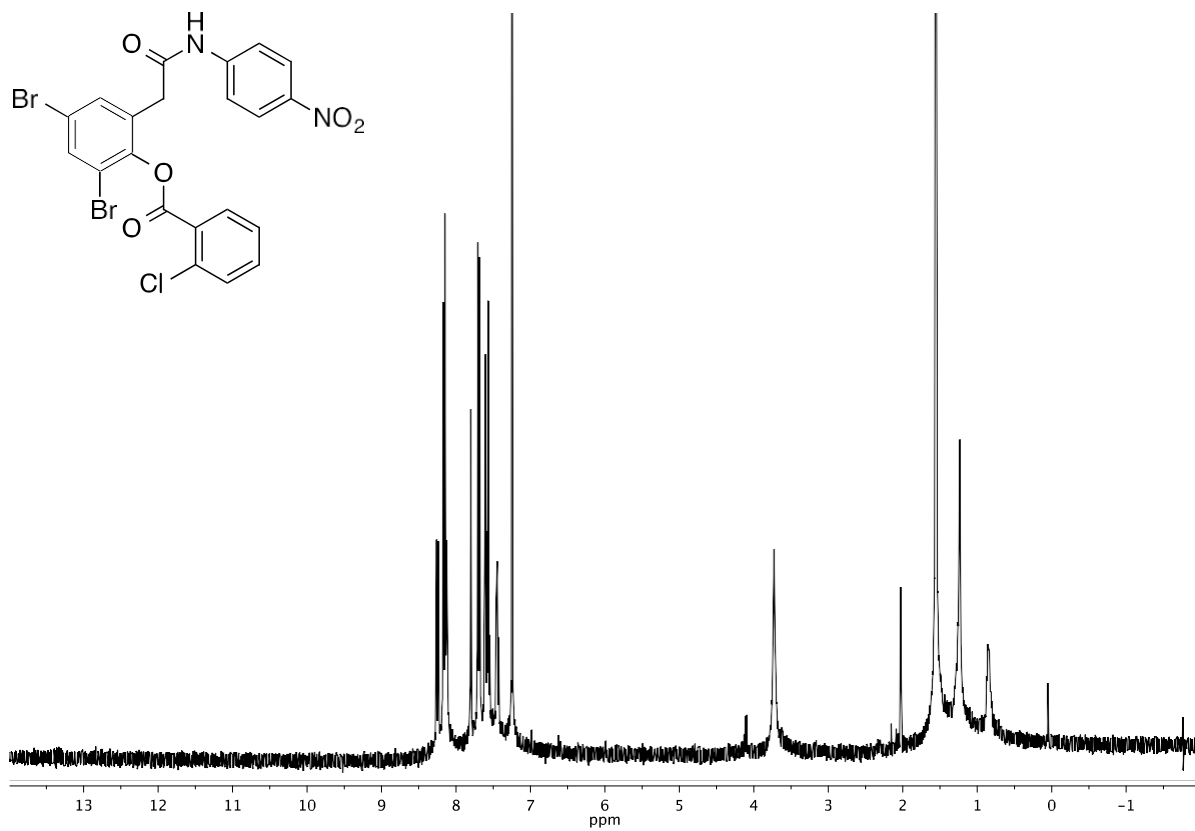
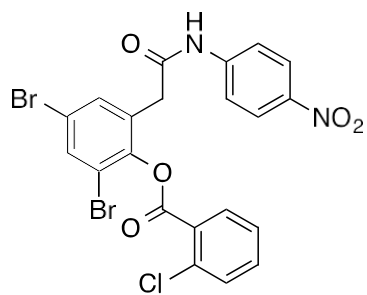
2,4-dibromo-6-(2-((2-nitrophenyl)amino)-2-oxoethyl)phenyl 2-bromo-4-fluorobenzoate.



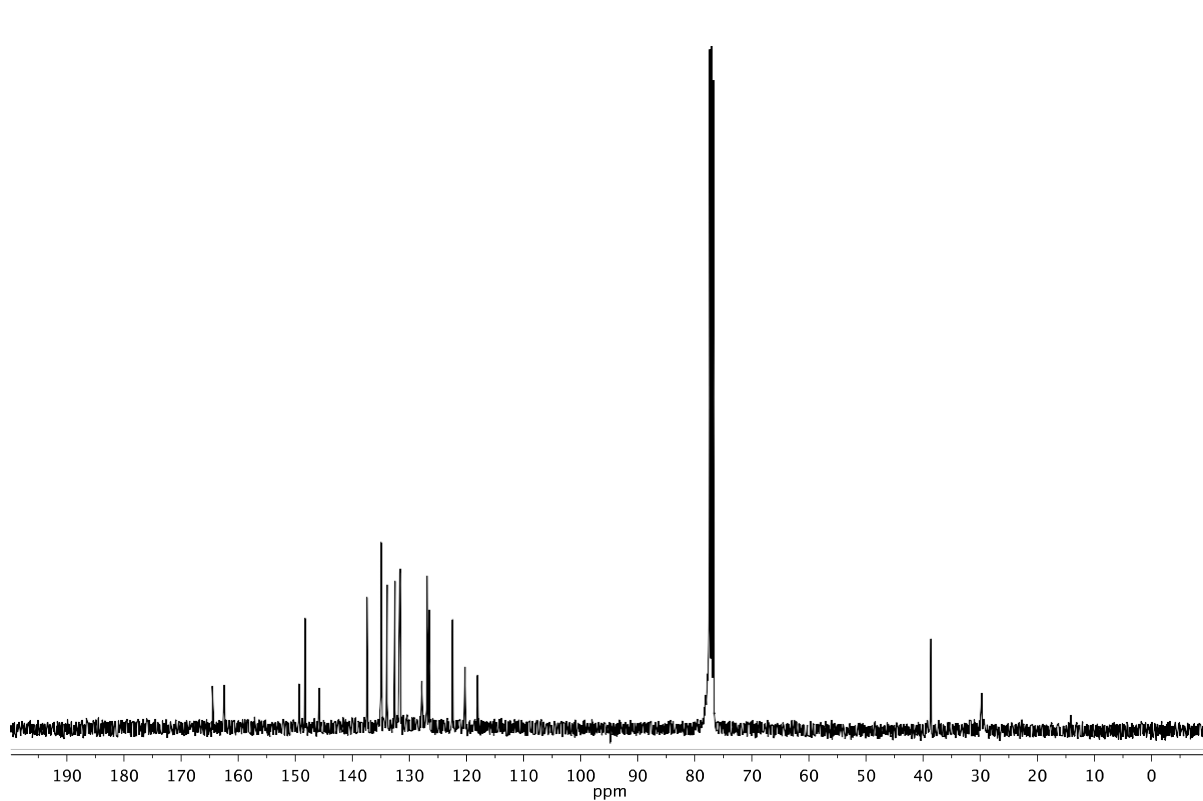
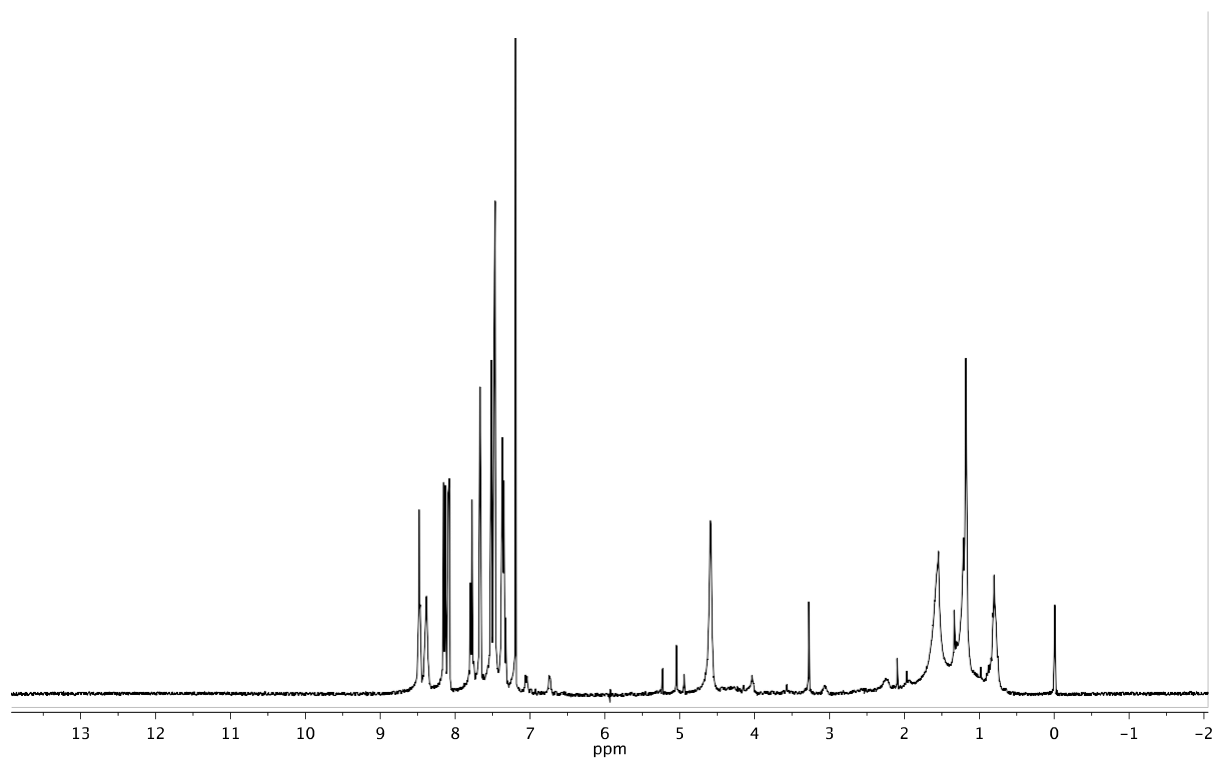
2,4-dibromo-6-(2-((3-nitrophenyl)amino)-2-oxoethyl)phenyl 2-chlorobenzoate



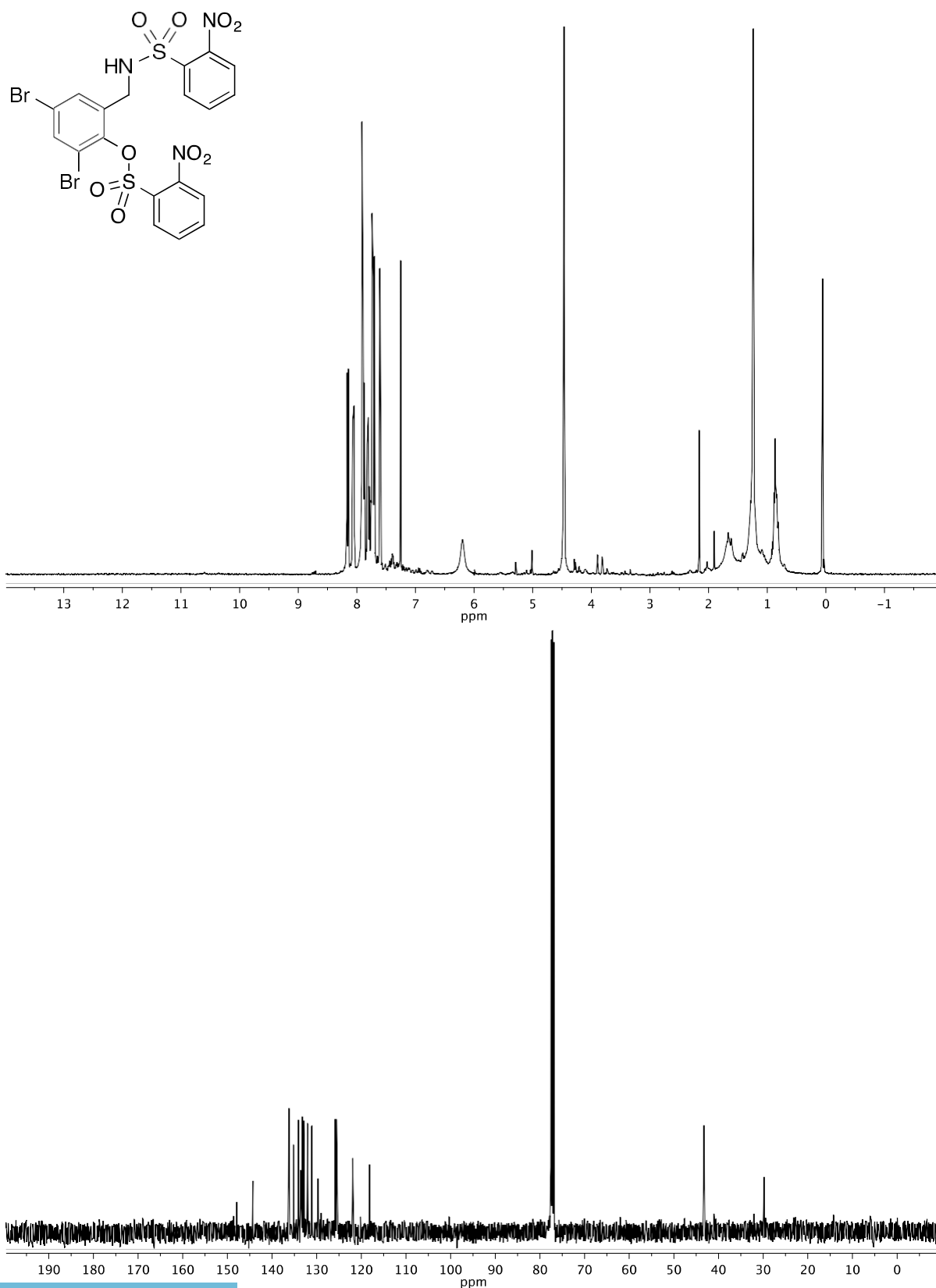
2,4-dibromo-6-(2-((4-nitrophenyl)amino)-2-oxoethyl)phenyl 2-chlorobenzoate



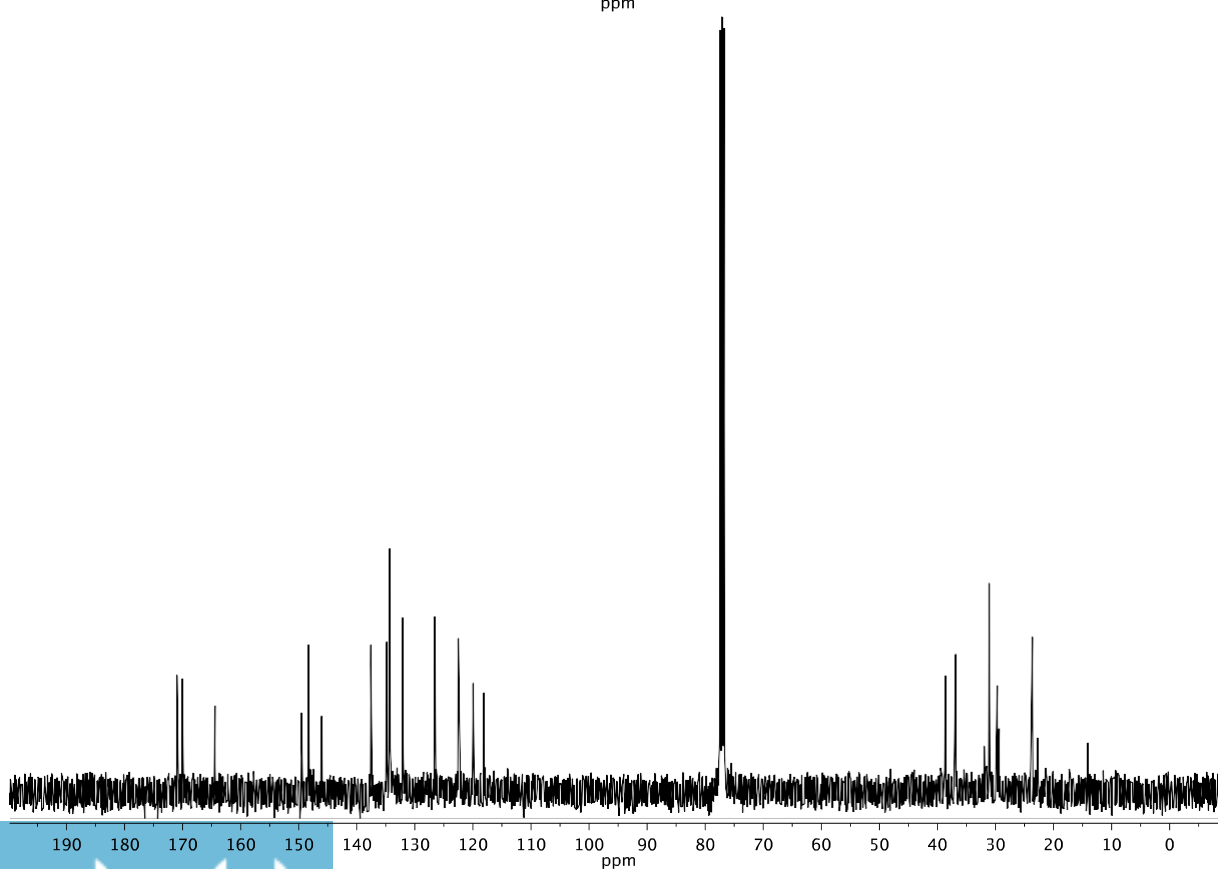
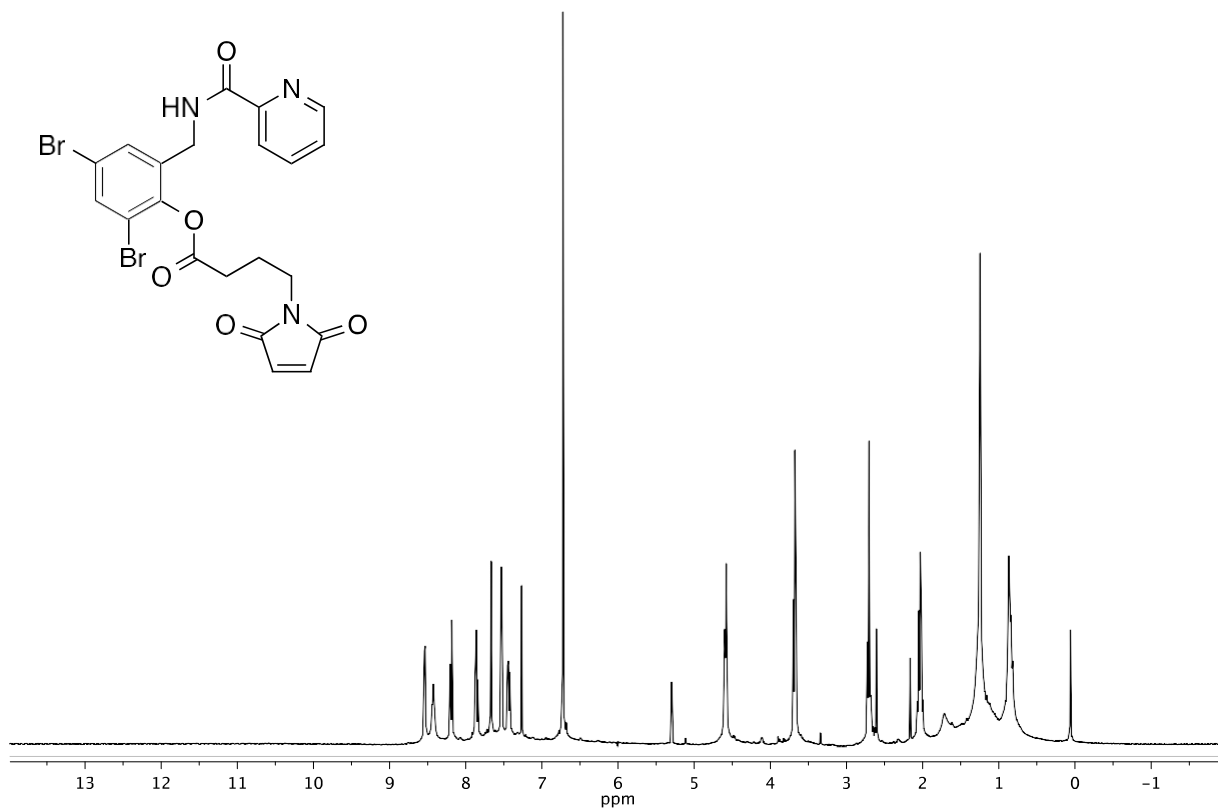
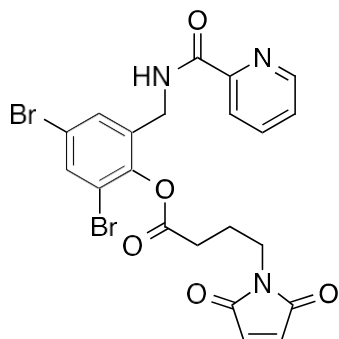
2,4-dibromo-6-(picolinamidomethyl)phenyl 2-chlorobenzoate



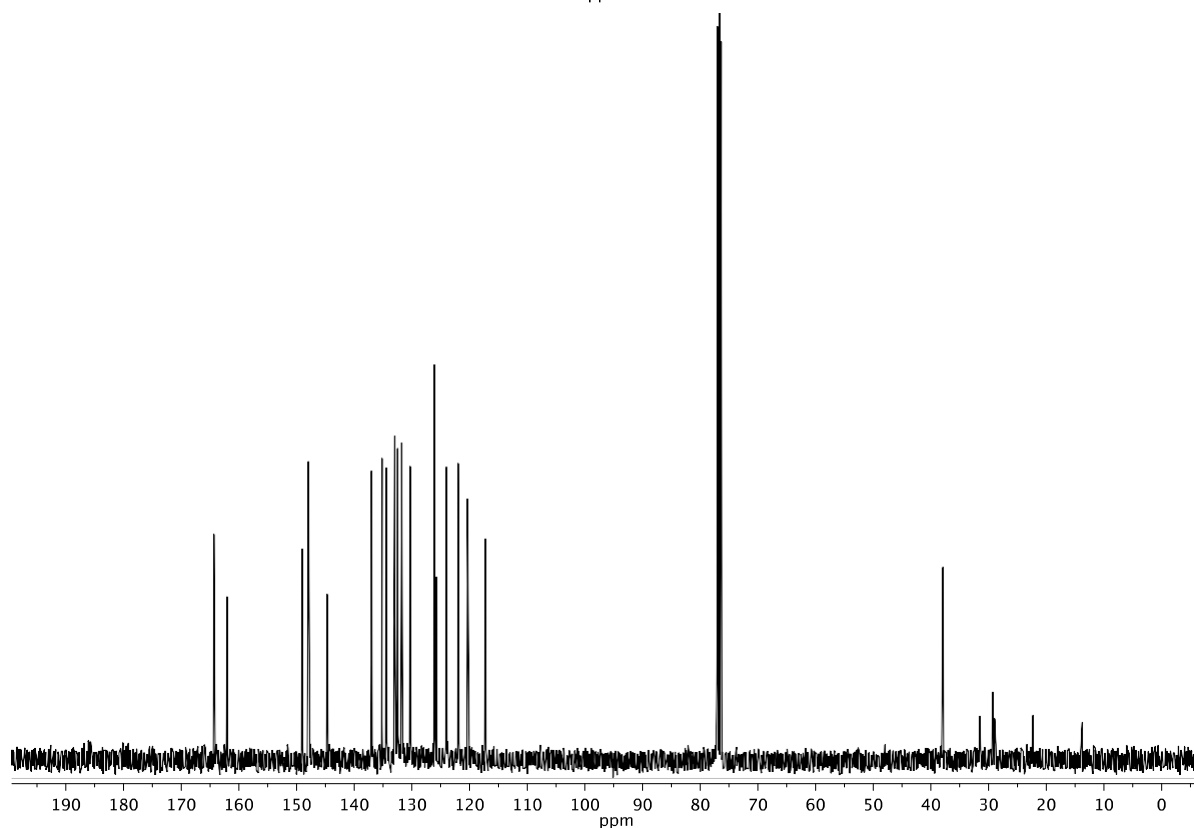
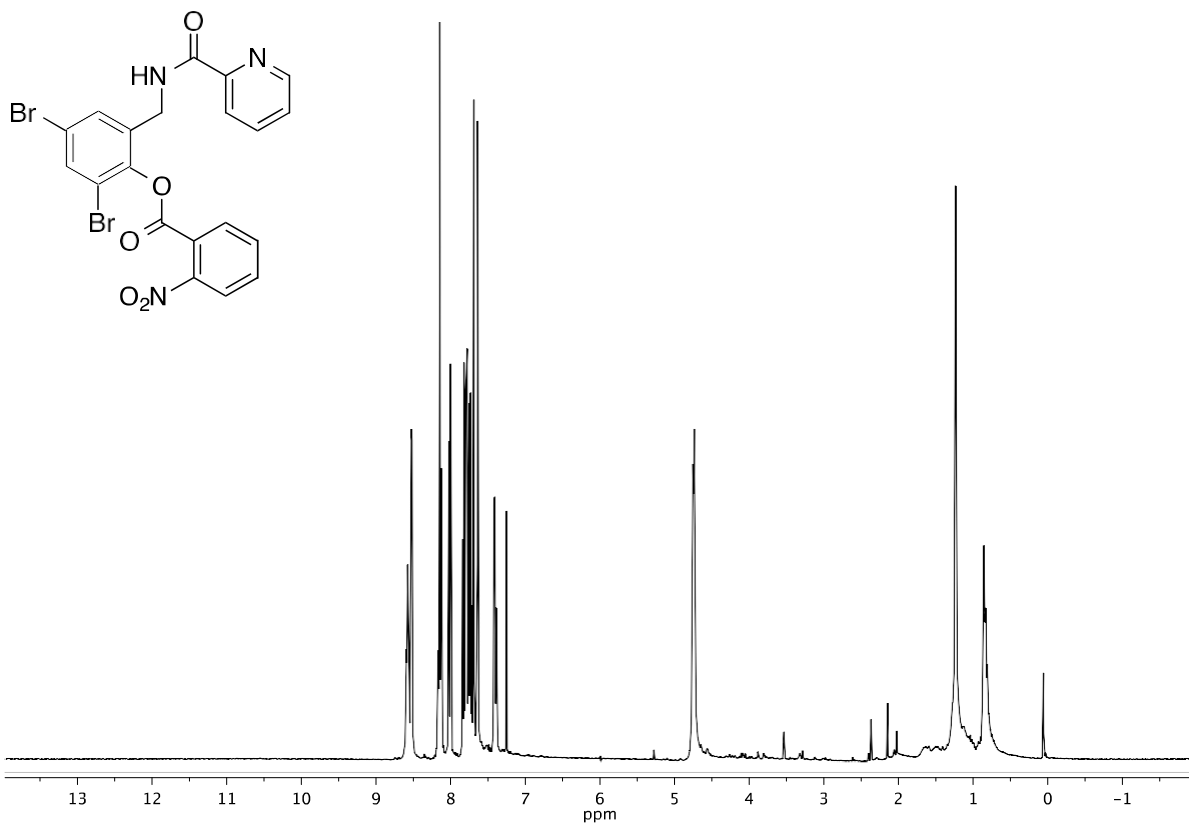
2,4-dibromo-6-(((2-nitrophenyl)sulfonamido)methyl)phenyl 2-nitrobenzenesulfonate



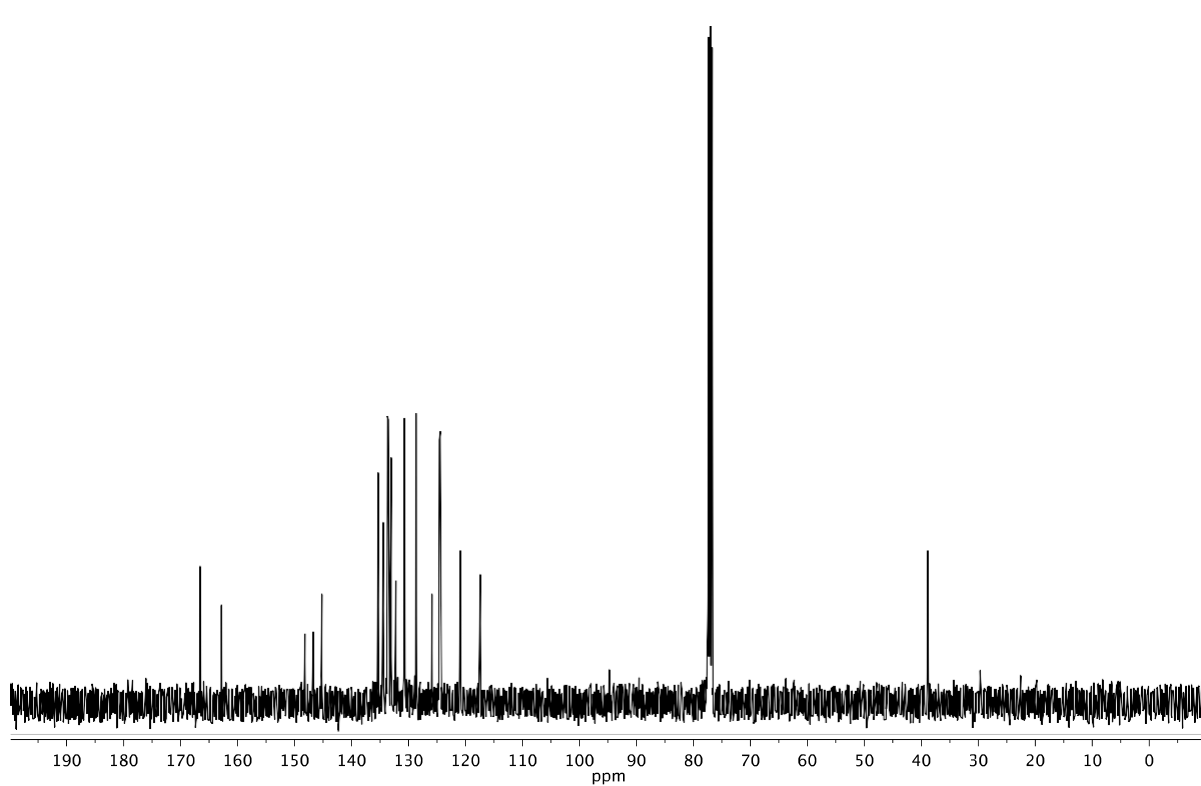
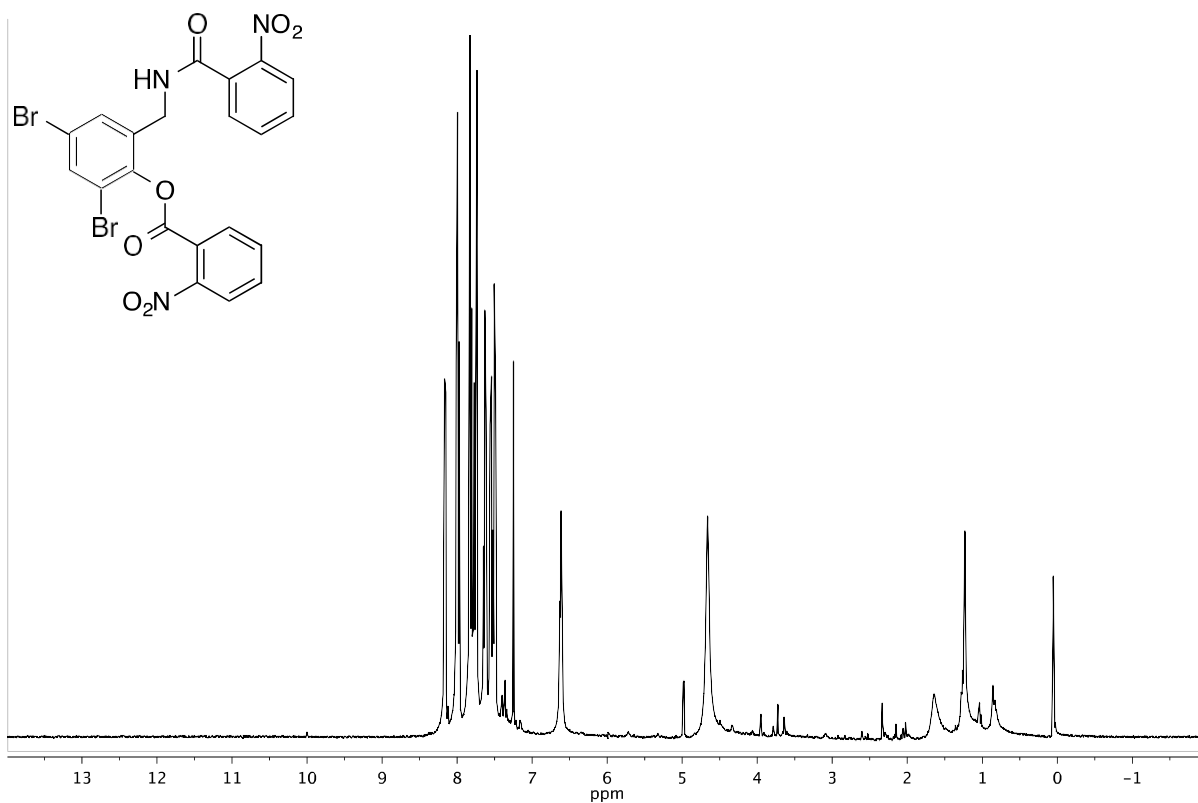
2,4-dibromo-6-(picolinamidomethyl)phenyl 4-(2,5-dioxo-2,5-dihydro-1H-pyrrol-1-yl)butanoate.



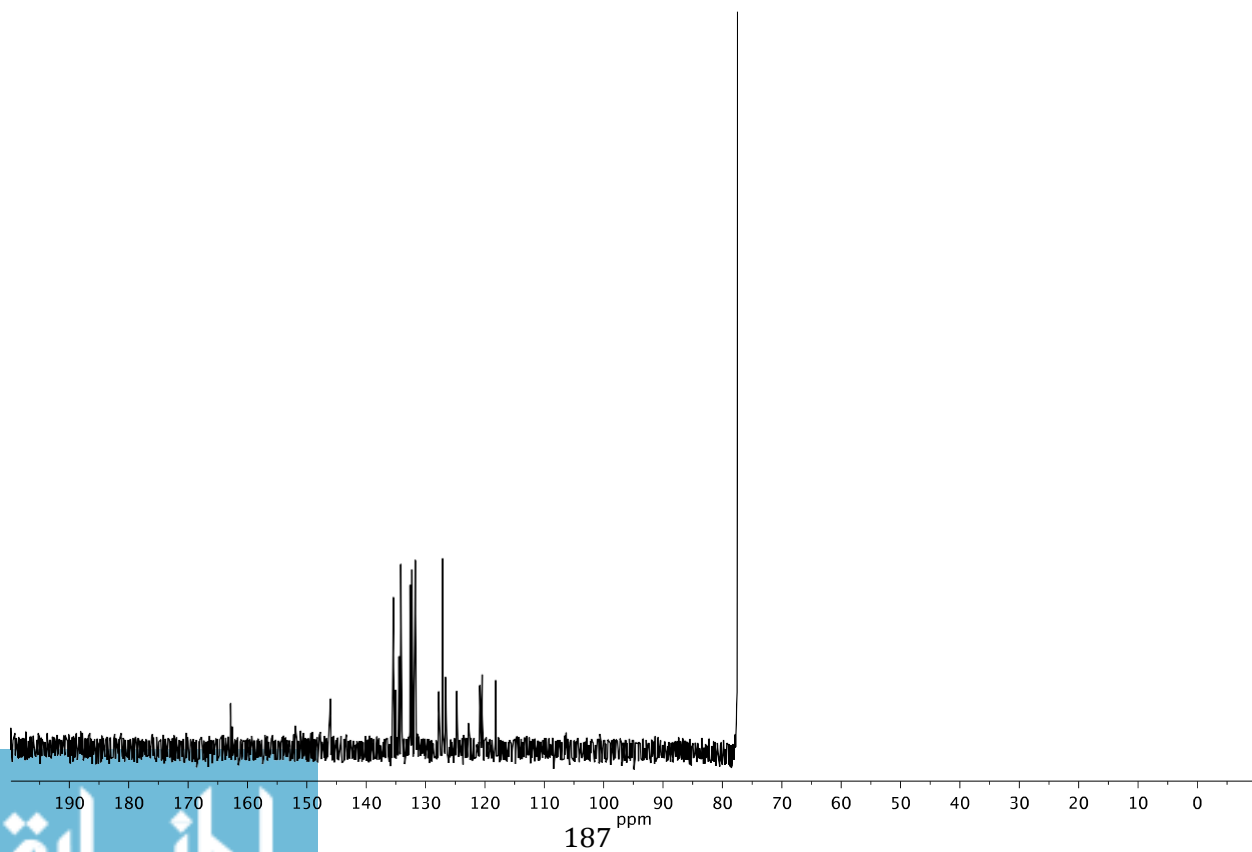
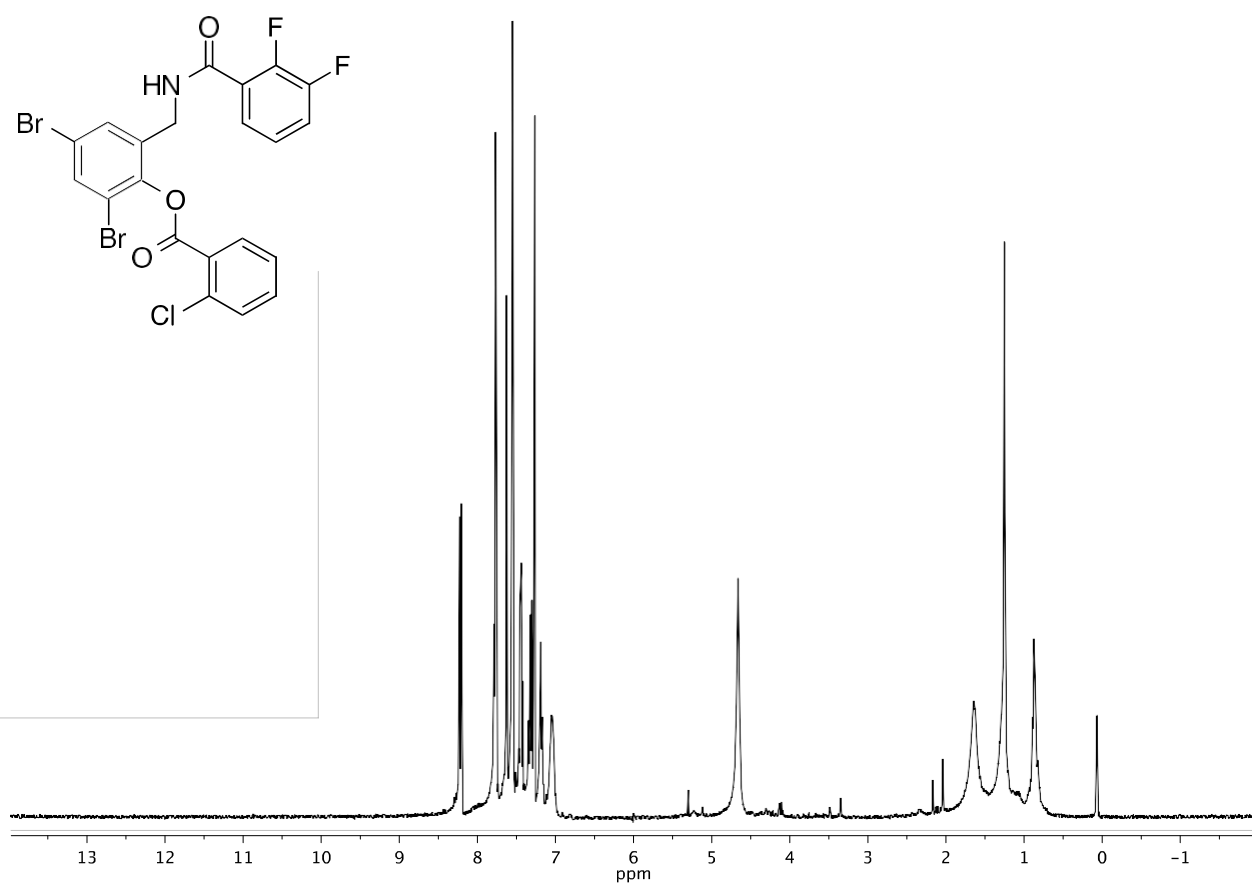
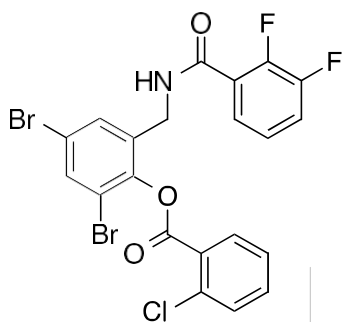
2,4-dibromo-6-(picolinamidomethyl)phenyl 2-nitrobenzoate



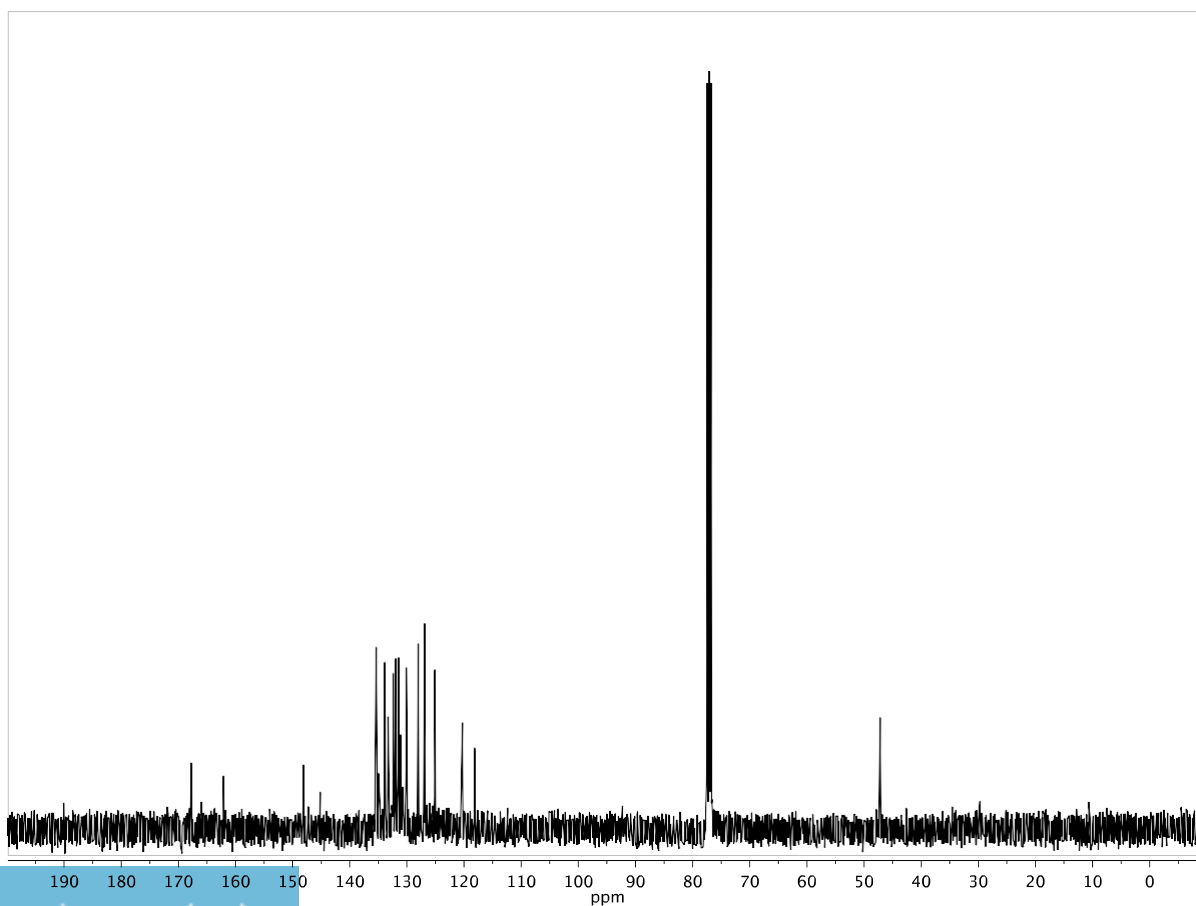
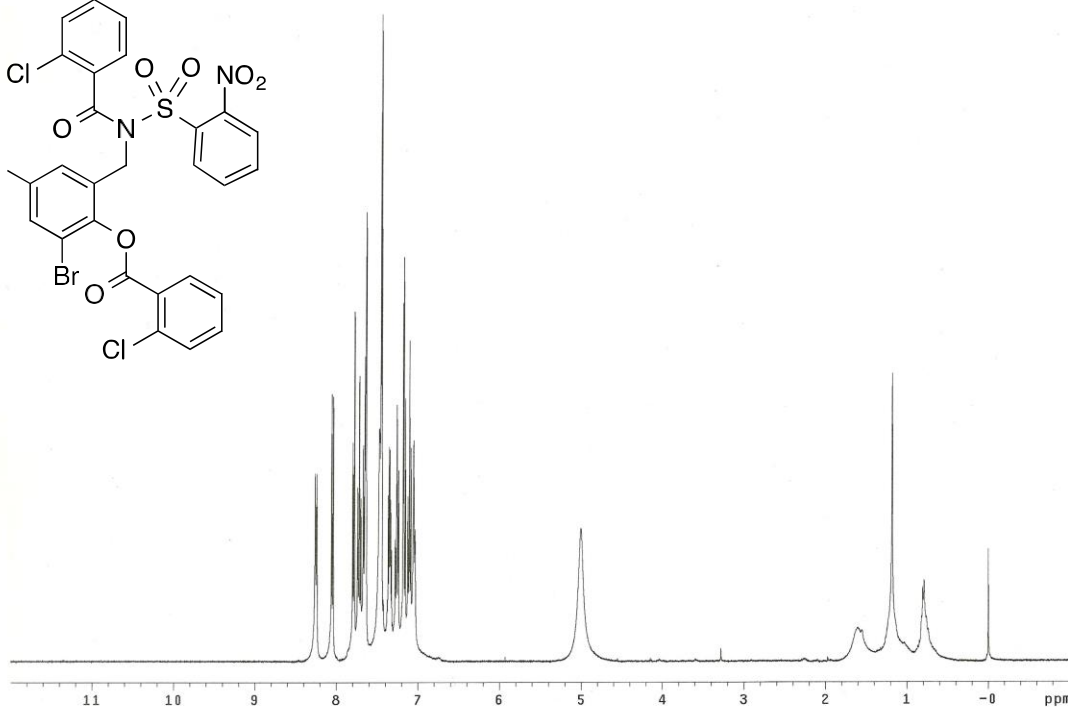
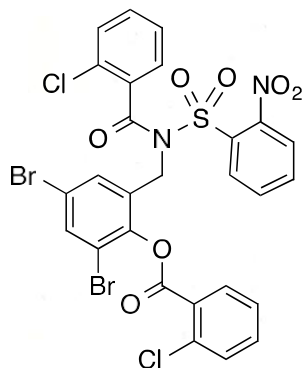
2,4-dibromo-6-((2-nitrobenzamido)methyl)phenyl 2-nitrobenzoate



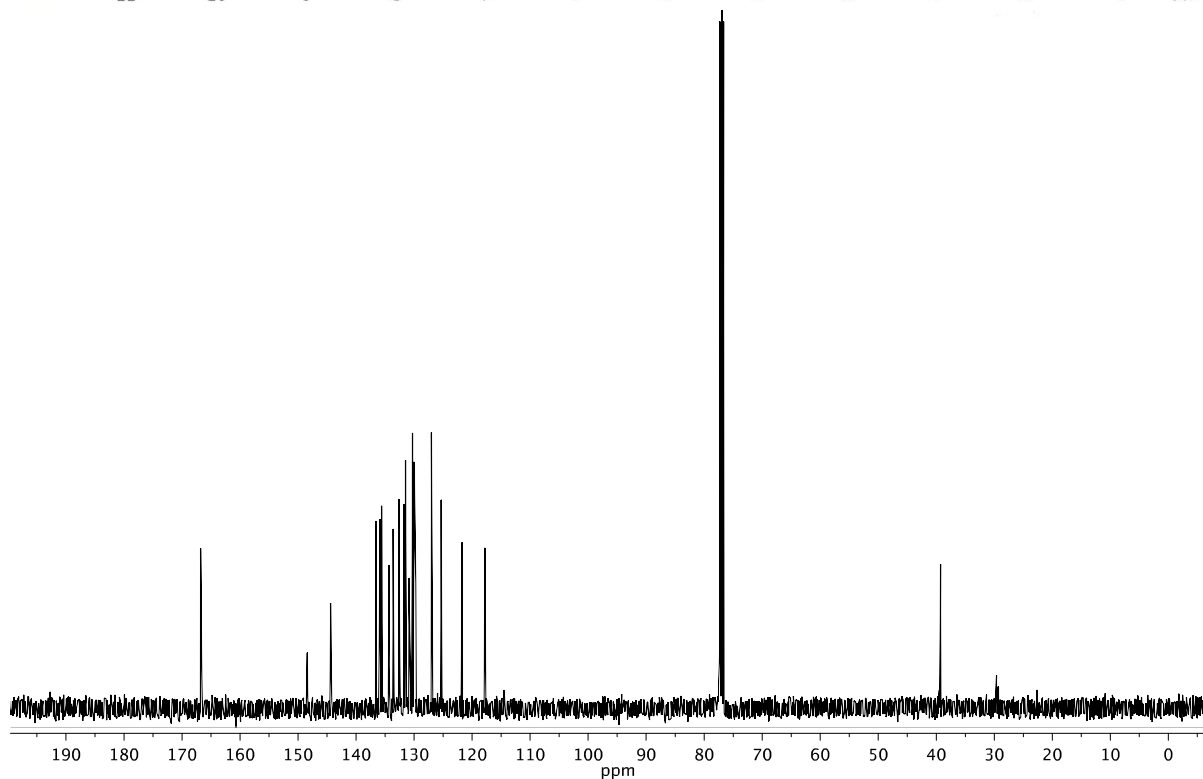
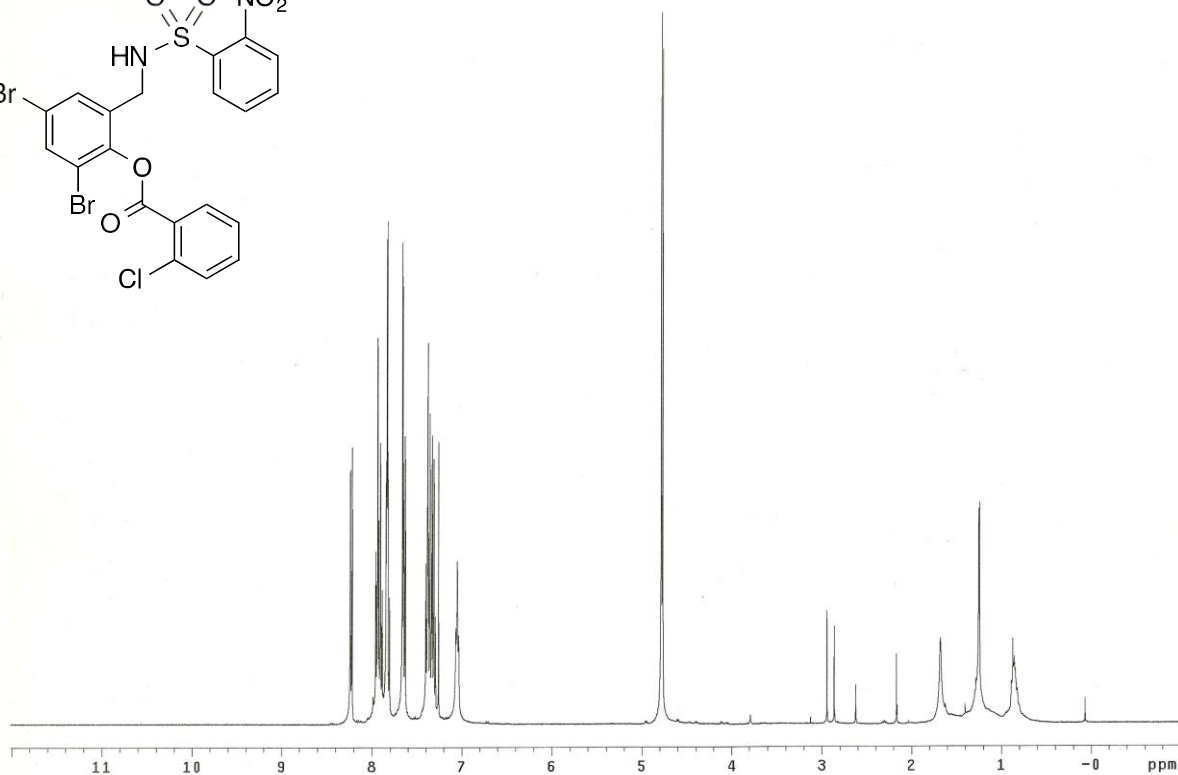
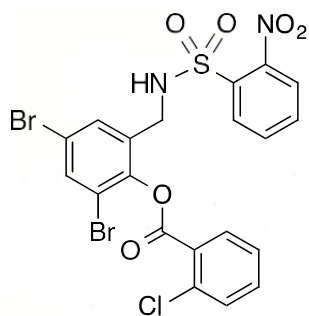
2,4-dibromo-6-((2,3-difluorobenzamido)methyl)phenyl 2-chlorobenzoate



2,4-dibromo-6-((2-chloro-N-((2-nitrophenyl)sulfonyl)benzamido)methyl)phenyl 2-chlorobenzoate



2,4-dibromo-6-(((2-nitrophenyl)sulfonamido)methyl)phenyl 2-chlorobenzoate



Chapter 5

Lipoxin A₄ augments host defense in sepsis and reduces *P. aeruginosa* virulence through quorum sensing inhibition

Introduction

In bacterial infections, signaling through pathogen associated molecular pattern (PAMP) recognition receptors activate the innate immune system¹. The subsequent increased release of inflammatory mediators such as cytokines, arachidonic acid metabolites and free radicals is critical for bacterial clearance, but if sustained, can cause tissue injury, multiple organ failure and death. Alternatively, a sustained inflammatory response may lead to a delayed dysregulation of inflammatory response, characterized by an inability of populations of lymphocytes and/or monocytes/macrophages to secrete inflammatory cytokines when stimulated²⁻⁷. In this immunocompromised condition, the host is susceptible to opportunistic infections or cannot clear preexisting infections. It is important to resolve infection as continued bacterial load will cause persistent pro-inflammatory or dysregulated inflammatory response without returning to homeostasis.

Therefore, an appropriate infection resolution can be defined as one which clears the infectious agent without causing tissue injury and/or an immunosuppressed state. The role of neutrophils in severe infections is complex. Neutrophils are first activated to combat the infectious agent. They migrate to the site of infection, release a host of pro-inflammatory mediators such as free radicals and leukotrienes, phagocytose bacteria before dying by apoptosis. Sustained neutrophil activation however can cause tissue injury and organ damage⁸⁻¹⁰. On the other hand, a paradoxical dysregulation in neutrophil function can also occur in later phases of severe infections/sepsis¹¹⁻¹⁴. Indeed, insufficient

neutrophil phagocytic activity and impaired neutrophil migration is an indicator of poor outcome in sepsis^{12,15,16}.

Inflammation resolution is an active process which involves inhibition of neutrophil activation, increased macrophage recruitment and macrophage phagocytosis of apoptotic neutrophils¹⁷⁻¹⁹. Specialized pro-resolving mediators (SPMs) such as the Lipoxins and Resolvins have been shown to resolve inflammation in sterile models of inflammation²⁰⁻²³ while reducing inflammatory response and bacterial load in various infectious models²⁴⁻³⁰. We have previously reported that Lipoxin A₄ (LXA₄) reduced blood bacterial load, decreased systemic inflammatory response and increased survival in the cecal ligation puncture (CLP) model of polymicrobial sepsis^{29,30}. LXA₄ increased bacterial clearance at least partially through promotion of neutrophil phagocytic function³¹. Fcγ receptor I (FcγRI;CD64) is an important neutrophil receptor in infection^{15,16,32} where it functions to increase uptake of bacteria^{33,35}. As increased expression has been reported to be a prognosticator of good outcome in sepsis¹⁵, we investigated if LXA₄ promoted neutrophil phagocytic activity through stimulation of FcγRI mediated phagocytosis.

During infection, in addition to host signaling pathways regulating inflammatory response there are also separate chemical regulatory pathways at work in the bacterial pathogen that are critical for the establishment and propagation of the infection. This bacterial population density-dependent process of chemical signaling is called quorum sensing (QS). The process of QS involves the bacterial production, release and detection of structurally specific small molecules and enables the bacterial pathogen to regulate its virulence by switching on genes that increase biofilm formation, toxin release and/or

antibiotic resistance^{36,43}. As anti-inflammatory agents may cause immunosuppression where the host is not able to clear pathogen and standard antibiotics do not affect inflammatory response, the most efficient treatment modality for severe bacterial infections would be to resolve inflammation and reduce bacterial virulence.

A large number of structurally distinct QS molecules in both gram-negative and gram-positive bacteria have been identified including oligopeptides, acylhomoserine lactones (AHLs), the furanosyl borate ester (AI-2), and α -amino/hydroxy ketones^{36,44}. The gram-negative bacteria pathogen, *Pseudomonas aeruginosa* utilizes at least three separate chemical signals in its regulation of a diverse array of virulence factors such as pyocyanin, elastase, HCN, rhamnolipids and biofilms. This network of QS regulation is arranged hierarchically with the LasR quorum sensing receptor which recognizes the AHL signaling molecule, *N*-3-oxododecanoyl homoserine lactone (3-oxo-C12 HSL) as its native agonist representing the master QS circuit in this bacteria⁴¹. Binding of 3-oxo-C12 HSL to the LasR QS receptor results in the activation/repression of numerous downstream genes through the action of the ligand-bound LasR as a transcription factor which upregulates the expression of virulence factors. Due to the central role of LasR in the virulence of this bacteria, inhibition of QS signaling in *P. aeruginosa* represents a novel target to reduce bacterial virulence^{45,46}. As some synthetic inhibitors/activators of LasR have similar chemical structure to LXA₄, we reasoned that LXA₄ may have quorum sensing inhibitory activity.

In this study, we investigated if the SPM, LXA₄, could modulate FcγRI mediated phagocytosis of neutrophils in the CLP model of sepsis. Additionally, we examined if LXA₄ could interfere with bacteria signaling and reduce virulence. The goal of the study

was to elucidate if LXA₄ has the unique property of modulating both host defense to increase bacterial clearance as well as reduce pathogen virulence. Such a compound could contribute a therapeutic advantage as an antimicrobial.

Results

Blood bacterial load: There is clear evidence of bacterial infection in the blood of CLP mice (Figure 1). LXA₄ (7 mg/kg) given 1h after CLP surgery reduced bacterial load significantly.

Neutrophil apoptosis and free radical production: Decreased neutrophil apoptosis as a result of infection has been well established⁵¹⁻⁵³. This increased life span of neutrophils with attendant overproduction of inflammatory mediators is thought to contribute to tissue injury associated with severe infections and sepsis^{8-10,51-53}. In our studies, blood leukocytes were isolated 24h after surgery from sham controls, CLP mice given vehicle saline or CLP + LXA₄ mice. The leukocytes were stained with the apoptosis marker Annexin V and Gr-1 as a marker for neutrophils. Neutrophil apoptosis significantly decreased at 24h after CLP surgery compared to sham controls (Figure 2a). LXA₄ completely reversed the decreased neutrophil apoptosis in CLP mice. Neutrophil ability to produce free radicals was evaluated by measuring the superoxide mediated oxidation of non-fluorescent DHR 123 to the fluorescent rhodamine 123 after PMA stimulation. CLP reduced neutrophil free radical generation ability and LXA₄ administration did not further affect superoxide generation after CLP (Figure 2b).

Neutrophil phagocytic ability and CD64 expression: As neutrophil phagocytic ability is essential for bacterial clearance, we evaluated the effect of LXA₄ on neutrophil ability to engulf fluorescently labeled *E.coli* in sham control or septic mice. Blood

leukocytes were isolated from sham controls, CLP or CLP + LXA₄ treated mice, 24h after surgery. Cells were incubated with pHrodo *E.coli* for 1h before being stained with fluorescent Gr-1 antibody to label neutrophils. Blood neutrophils from CLP mice had greater phagocytic ability compared to sham controls and LXA₄ administration increased phagocytic ability further (Figure 3a). As CD64 is a high affinity receptor which is critically important in the initiation of neutrophil phagocytosis, its expression was measured. We also measured the expression of FcγRIII and II using CD16/32 mouse antibodies. CLP increased the percentage of CD64 expressing neutrophils compared to sham controls and LXA₄ increased this further. CD16/32 expression was not affected by CLP or LXA₄ (Figure 3b).

CD64 blocking antibody studies: To confirm that CD64 is important in the LXA₄ induced increase in neutrophil phagocytosis, we incubated leukocytes with CD64 blocking antibody or vehicle saline. The results show that CD64 antibody completely abolished LXA₄-induced increase in phagocytosis (Figure 4) suggesting that the LXA₄ induced increase in neutrophil phagocytosis is mediated by CD64.

Ex vivo studies: To investigate if LXA₄ increased neutrophil phagocytosis directly, we isolated leukocytes from CLP or sham control mice 1h after surgery and incubated these cells with LXA₄ or vehicle saline for 3h before addition of fluorescent *E.coli* to measure phagocytic ability. To confirm the specificity of LXA₄, some cells were incubated with WRW4 a specific blocker of the LXA₄ formyl peptide receptor 2 (FPR2)(54). As expected, CLP mice had substantially greater percentage of neutrophils which expressed CD64 compared to sham controls (Figure 5a). Interestingly, LXA₄ did not increase the percentage of neutrophils expressing CD64. This is in contrast to the *in*

in vivo actions of LXA₄ which significantly increased the percentage of CD64 expressing cells. These data suggest that LXA₄ does not directly promote neutrophil CD64 expression. In CLP mice, LXA₄ increased neutrophil phagocytosis and this increase was completely abolished by the specific LXA₄ receptor antagonist (Figure 5b). LXA₄ however, had no effect on phagocytic ability of control neutrophils where there was minimal CD64 expression (Figure 5c). Taken together with CD64 data, the results support the postulate that LXA₄ increases CD64-dependent neutrophil phagocytosis but does not directly increase expression of CD64.

Inhibition of pyocyanin expression by LXA₄: To evaluate if LXA₄ directly influences bacterial virulence we evaluated expression levels of the exotoxin, pyocyanin, in the prominent bacterial pathogen *P. aeruginosa* (PA-14)⁵⁵. While absorbance based methods for the quantification of pyocyanin have been reported, we found this assay to be complicated by low detection limit and requirement for multiple sample manipulation steps. Accordingly, we utilized a UPLC-MS-MS based approach to determine the concentration of pyocyanin in bacterial cultures. This method provides direct ion counts of the molecular ion for pyocyanin after UPLC separation from other culture constituents and the identity of pyocyanin is further confirmed through analysis of the fragmentation pattern of the isolated molecular ion. Further, no mathematical correction needs to be applied as the concentration of pyocyanin is directly correlated to a calibration curve generated using pure pyocyanin. In this analysis, we found that in the presence of 1-5 nM of LXA₄, pyocyanin concentration in bacterial culture was decreased (Figure 6). Interestingly, we found that increasing the concentration of LXA₄ further (8 nM) abolished this effect. Taken together these results suggest a bell-shaped inhibitory curve

for LXA₄ on the expression of the bacterial virulence factor pyocyanin. This pattern of LXA₄ inhibition has been noted in other systems^{56,57}.

Inhibition of LasR QS by LXA₄: The regulation of virulence factor expression, including pyocyanin expression, in *P. aeruginosa* occurs through a complex regulatory network. The master QS receptor, LasR, plays a central role in this regulatory network and we looked to evaluate if the observed inhibition of pyocyanin by LXA₄ might be occurring through inhibition of LasR. Upon analysis using a GFP-based reporter strain for the activity of the transcription factor LasR, we found potent antagonism of LasR by LXA₄ at concentrations above 1.8 nM (Figure 7a). Generating a full dose-response curve to evaluate the antagonist activity of LXA₄ on LasR we observed partial antagonism, achieving approximately 57% inhibition at the highest concentration tested (100 nM) as compared to the known LasR antagonist, Br-HSL at 10 mM. While only partial antagonism was observed, the potency of inhibition as defined by the IC₅₀ of LXA₄ (57nM) (Table 1, supplemental data), makes LXA₄ the most potent antagonist of LasR yet described⁴³. We turned to evaluate the binding kinetics of the LasR inhibitory activity of LXA₄ using competition binding assays, locking the concentration of LXA₄ while titrating the native LasR agonist, 3-oxo-C12 HSL. In this assay we observed a shift in the EC₅₀ value for the LasR agonist 3-oxo-C12 HSL in the presence of increasing concentrations of LXA₄ (Figure 8; Table 2, supplemental data). Together, these results are consistent with LXA₄ acting as a highly potent reversible partial antagonist of the *P. aeruginosa* master QS regulator, LasR. LXA₄ is also a partial LasR agonist. The partial agonist activity of LXA₄ is anticipated from the previous assay demonstrating partial antagonist activity for this compound. In this assay the native agonist was not fully

titrated leading to the incomplete dose-response curve for this control compound, however the different levels of maximal activation expected from LXA₄ acting as a partial agonist are clearly defined.

Discussion

Effective resolution of infection and/or inflammation is now believed to be an active process^{18,19,58}. As part of the early innate immune system, neutrophils are activated to help clear the invading pathogen. Excessive neutrophil activation however, may lead to tissue injury and damage while impaired neutrophil activity which can occur later in sepsis, may result in reduced bacterial clearance¹¹⁻¹⁴. Ideally therefore, neutrophil activation and subsequent apoptosis are critical for inflammation resolution and to achieve homeostasis in the host^{44,59,60}.

SPMs have been reported to have significant pro-resolution effects in various non-infectious, infectious and sepsis models^{20-22,25,26,28-30,45,61-64}. The underlying mechanism for these beneficial effects is believed to be due to the resolution effects on different populations of cells including neutrophils and macrophages^{25-27,29,30,60,61,65-67}. With respect to infection, we and others have consistently shown that SPMs such as LXA₄ could simultaneously reduce bacterial load and inflammatory response²⁸⁻³⁰. The timing of administration may be of importance because overly robust down regulation of neutrophil function may produce unwanted bacterial spread⁵⁴.

CD64 expression is important for neutrophil activation and phagocytic ability (33,68). There is evidence that neutrophil CD64 expression can be used as a selective biomarker for infection where highest levels of expression were found in patients with infection compared to patients with autoimmune disorders which were themselves

significantly higher than normal patients or patients with inactive disease⁶⁹. In addition, studies have now linked increased neutrophil CD64 expression with better outcome in sepsis¹⁵. The possible reason for this is because neutrophil phagocytic action is increased and may augment bacterial clearance. In our studies, *in vivo* administration of LXA₄ to CLP mice increased neutrophil phagocytic ability and CD64 expression without altering CD16/32 expression. In addition, use of CD64 blocking antibody abolished the increase in phagocytic ability in neutrophils isolated from LXA₄-treated animals. These results correlated with a significant decrease in blood bacterial load suggesting that augmented CD64-dependent neutrophil phagocytic ability may be partially responsible for the decreased bacterial load with LXA₄ administration. The increase in phagocytic ability is consistent with the action of a related SPM, Resolvin E1 which was also reported to increase neutrophil phagocytic ability²⁵.

To study the effects of LXA₄ on neutrophils further, peripheral blood neutrophils taken from CLP mice after 1h, were incubated with different concentrations of LXA₄. Under these conditions, LXA₄ increased neutrophil phagocytic ability without affecting expression of CD64. Importantly, LXA₄ did not affect neutrophil phagocytic ability in cells taken from control animals where CD64 expression was minimal. These results suggest that LXA₄ directly increased CD64-dependent neutrophil phagocytic ability providing evidence that concentrations of LXA₄ that produce a significant biological effect in neutrophils only affected the phagocytic activity of already activated neutrophils. These results are consistent with *in vitro* studies showing that LXA₄ inhibited stimulated neutrophil chemotactic responses⁶⁵ but do not directly affect quiescent neutrophil phagocytic activity⁶⁶. Use of a specific LXA₄ receptor (FPR-2)

blocker completely abolished LXA₄ effects on neutrophil phagocytic ability confirming the receptor binding specificity of the LXA₄ in these studies. These *ex vivo* results differ from our *in vivo* data in that administration of LXA₄ *in vivo* resulted in an increased CD64 expression in neutrophils. The mechanism for this difference is unknown but may indicate that LXA₄ by itself is unable to increase CD64 expression in neutrophils or that neutrophils from LXA₄ treated septic mice are more responsive to CD64 inducing agents such as IFN-g or G-CSF. Although the incubation time of 3h for these *ex vivo* studies was shorter than the 24h of the *in vivo* experiments, it is unlikely that the shorter time frame contributed to the fact that LXA₄ did not augment CD64 expression. This is because CD64 expression can clearly be enhanced in the time period used, as can be seen in Figure 5 where neutrophils taken 1h after CLP had substantially greater CD64 expression compared to neutrophils taken from control mice. These results would argue that the conditions allowed enough time for there to be an increase in CD64 expression.

Apart from increasing peripheral blood neutrophil phagocytic ability, LXA₄ reversed the decline in blood apoptosis commonly found in sepsis and did not affect PMA stimulated superoxide generation. These results confirm previous work by us that LXA₄ increases neutrophil phagocytic activity and restores apoptosis activity without excessive free radical production in CLP rats³¹.

P. aeruginosa is a virulent bacterial strain which causes various infections that can result in sepsis especially in immunocompromised individuals⁷⁰. The coordinated behavior for colonization of higher organisms and virulence of *P. aeruginosa* is mediated by binding of 3-oxo-C12 HSL to its native QS receptor, the bacterial transcription factor LasR. Through this receptor signaling mechanism, *P. aeruginosa* bacteria coordinate the

gene expression and release of virulence factors such as exoproteases, siderophores, exotoxins and secondary metabolites^{42,44,71-74}). In addition, biofilm formation is also coordinated through this mechanism^{42,43}. Apart from coordinating signals between bacteria, 3-oxo-C12 HSL activates the hosts' immune system through stimulation of T-cell production of interferon-gamma (IFN-g) in resting cells⁷⁵. On the other hand, if macrophages are co-stimulated with bacterial endotoxin, 3-oxo-C12 HSL increases production of IL-10, an anti-inflammatory cytokine⁷⁶ which has been shown to reduce neutrophil phagocytic ability. These results strongly suggest that 3-oxo-C12 HSL is not only an important mediator of bacterial virulence by stimulating the expression and release of virulence factors but can also modulate host, immune responses. Our results here add to this intriguing *inter*-kingdom chemical communication crosstalk by demonstrating that LXA₄ with primary activity in the resolution of inflammatory signaling in the host inhibits the activity of a bacterial QS receptor, LasR, and decreases the expression of virulence factors in this bacteria. The potency of this inhibition by LXA₄ as evaluated by comparison of IC₅₀ values is several orders of magnitude greater than any reported LasR antagonist⁷⁷, and occurs at physiologically relevant concentrations of LXA₄⁶⁴. Interestingly, not only is LXA₄ an antagonist but it also has partial agonist activity against LasR (Figure 8b). This property is particularly intriguing because there is very little structural similarity between LXA₄ and a known antagonist, Br-HSL (Figure 8a) or the endogenous agonist 3-oxo-C12 HSL. The results suggest that LXA₄ acts as a partial agonist and a competitive antagonist at the LasR binding site. Investigation of related lipid mediators to examine the specificity of LXA₄ for LasR is a subject of current study.

Pyocyanin is an exotoxin produced by *P. aeruginosa*. It is one of many virulence factors regulated by quorum sensing pathways and the release of pyocyanin is completely necessary for *P.aeruginosa* lung infections⁷⁸. It is therefore a good marker of *P. aeruginosa* virulence. *In vitro* studies have shown that pyocyanin inhibits cell respiration and disrupts calcium homeostasis⁷⁹. Our results show that LXA₄ reduced pyocyanin release from *P. aeruginosa* at concentrations of 1 – 5 nM LXA₄. Taken together with our results showing that LXA₄ inhibits the activity of expression of pyocyanin mediated by the QS receptor LasR, these observations strongly suggest that LXA₄ at physiologically relevant concentrations can reduce *P. aeruginosa* virulence.

It is noteworthy that there was a concentration-dependent effect of LXA₄ on pyocyanin release until the highest concentration of LXA₄ (8 nM). This bell shaped curve is characteristic and consistent of previous reports showing that LXA₄ effects stop at higher concentrations^{56,57}. This effect may be due to the partial agonist activity of LXA₄ on LasR at higher concentrations of this ligand or could result from potential interactions with cellular targets in *P. aeruginosa* in addition to LasR.

Importantly, *P. aeruginosa* has been reported to possess a secretable 15-lipoxygenase enzyme which has been demonstrated to convert arachidonic acid to 15-hydroxyeicosatetraenoic acid (15-HETE)⁸⁰. This would suggest that when *P. aeruginosa* is in the vicinity of host neutrophils (which possess the 5-lipoxygenase enzyme), transcellular biosynthesis of LXA₄ can occur. Taken together with our studies, host-bacteria cross-talk may occur to control virulence.

Experimental Section

All experiments were performed in adherence to protocols approved by the Institutional Animal Care and Use Committee of Rowan University and strictly complied with the National Institutes of Health guidelines on the use of experimental animals.

Synthesis of LXA₄

LXA₄ was prepared synthetically by previously published methods⁴⁷. The purity of the compound was measured by HPLC-Mass Spectrometry and determined to be > 98% and 1 mg was dissolved in 500 ml sterile saline on days of experiment.

CLP-sepsis model:

CLP was performed on male CD1 mice (25 – 30g) using modified methods as previously published (29,30,48). On day of surgery, mice were anesthetized with 2.5% isofluorane (with oxygen). A 1-cm-long midline incision was made in the abdomen to expose the cecum. The distal half of the cecum was ligated with 3.0 surgical silk. Using a 21-gauge needle, the cecum was punctured twice, through and through. A small amount of fecal matter was massaged out of the cecum through these holes, to ensure patency of the punctures. The cecum was placed back into the abdomen, which was then closed in 2 layers. For sham controls, ceca were isolated but not ligated or punctured. Saline (4 ml/100g; s.c.) was injected to replace any fluids lost during surgery. 1h after surgery, CLP mice were anesthetized and injected with LXA₄ (7 mg/kg), or saline vehicle, intravenously via the tail vein. This concentration of LXA₄ was derived from published *in vivo* work in rodents^{29,30,49}.

The CLP model is widely regarded as the gold standard to study sepsis because it can be manipulated to different levels of severity and demonstrates bacteremia, a pro-

inflammatory phase and an immunosuppressive phase^{5,7,48}.

Isolation of blood leukocytes.

After 24h, mice were anesthetized with ketamine/xylazine (50/10 mg/kg, i.p.). 1 mL of whole blood was drawn by cardiac puncture into 0.05 M EDTA (final concentration). Blood was lysed using RBC lysis buffer and filtered through a 100 µm cell strainer. Lysed blood was centrifuged (500 x g, 5 min, room temperature), cells were resuspended in 2 mL of PBS/10% fetal calf serum kept on ice and total cell counts (gated at > 7 µm), were performed (Beckman Coulter counter Z4; Brea, CA, USA).

Bacterial load

1:10 serial dilutions of blood were made and aseptically spread on tryptic soy agar plates (Sigma-Aldrich; St. Louis, MO, USA) to measure aerobic bacteria growth. The plates were incubated overnight at 37⁰C. At the end of the incubation period, colony forming units (CFU) were counted by operators blind to the treatment groups.

Neutrophil free radical production and apoptosis assays

To determine effects of LXA₄ on neutrophil free radical production during sepsis, we performed dihydrorhodamine 123 (DHR123) flow cytometry assays. Initially, 0.5 µg of phycoerythrin (PE) labeled anti-mouse granulocyte antibody, Gr-1 (Biolegend, San Diego, CA, USA), was added to 100 µl of total leukocytes from blood. Debris was gated out according to their forward and side scatter parameters. The remaining non-debris population was designated as total leukocyte population. Neutrophils were initially identified by forward and side scatter parameters (low forward, high side scatter), followed by Gr-1 surface immunostaining for flow cytometry. Results are reported as Gr-1⁺ cells derived from Gr-1⁺ cells gated from total leukocyte population. The Gr-1

antibody (RB6-8C5 clone) has high affinity for Ly6G and low affinity for Ly6C (manufacturer's details). Furthermore, the epitope recognized by this Gr-1 Ab overlapped with Ly6G but not with Ly6C and has been used as a blood neutrophil marker (49).

To determine the appropriate voltage for cells positive for rhodamine, total leukocytes (1×10^6 /mL) were incubated with 1 μ M phorbol 12-myristate 13-acetate (PMA; Sigma, St, MO) at 37°C for 15 min, followed by addition of DHR123 (Invitrogen, Grand Island NY, USA) (5 μ M), at 37°C for 5 min. The reaction was stopped by washing cells twice with ice cold PBS (500xg, 3 min). Cells from sham, CLP, CLP+LXA₄ mice were stained with DHR123 only (37°C, 5 min), Cells undergoing apoptosis and/or necrosis were determined by staining with Annexin V (4 ml/sample) as recommended by manufacturer (Biolegend, San Diego, CA, USA), while non-viable/necrotic cells were detected with 7-amino-actinomycin D (7AAD; Biolegend, San Diego, CA, USA). Positive Annexin V⁺ gating was standardized by incubating total leukocytes from each experimental group with staurosporine (1 μ M, 37°C, 5% CO₂, 3h). All samples were analyzed within 1h of adding Annexin V. In all assays, 10,000 events were collected in total leukocyte population for each sample using an Accuri C6 flow cytometer (BD Biosciences; Franklin Lakes, NJ, USA). All assays for determination of neutrophil free radical and apoptosis were performed in duplicate for each animal and an average for each parameter was determined for each individual animal.

Neutrophil Phagocytic ability

E. coli bioparticles (pHrodo; Invitrogen, Grand, Island, NY, USA) were opsonized with *E. coli* opsonizing reagent for 1h at 37°C (1:1 ratio). pHrodo bioparticles were washed twice (1200 x g, 15 min) to remove any unbound IgGs. Opsonized

bioparticles were added to unlabeled total leukocytes from peritoneum and blood (3:1 ratio, bioparticles to leukocytes). Incubations (1h, 37⁰C; 1h, on ice) were stopped by washing with ice cold PBS twice. Three different time points (30, 60 and 90 min) were carried out to determine the optimal incubation period for phagocytosis assay. It was determined that 60 min was the optimum incubation time. Cells that internalized *E. coli* were separated from cells that did not internalize *E. coli* by comparing voltage intensities between samples placed on ice (negative control) and 37⁰C. Samples were resuspended and fixed with 0.4% paraformaldehyde and analyzed by flow cytometry the following day. Immunostaining of Gr-1, FcγRI (CD64) and FcγRIII/II (CD16/32) were performed after the phagocytosis assays as described above. Similar to free radical and apoptosis, phagocytosis assays were performed in duplicate for each individual mouse and an average of the duplicates were calculated. The phagocytic ability is expressed as phagocytic index. Mean number of *E. coli* ingested by neutrophils containing *E.coli* = mean fluorescence intensity. Therefore

Phagocytic index = % neutrophils ingesting at least 1 *E. coli* cell X mean fluorescence intensity

In separate studies, 8 mg of CD64 blocking Ab or isotype antibody controls was incubated for 1h with cells isolated from CLP + LXA₄ mice prior to phagocytosis assays.

Ex vivo experiments

1h after performing CLP or sham surgery, total leukocytes from blood were processed according to methods mentioned above. For *ex vivo* studies, total leukocytes (10⁵ cells) were suspended in 1 ml RPMI media. Either LXA₄ (1, 10 nM) or PBS were added and the cells incubated at 37⁰C, 5% CO₂ for 3h. To confirm the specificity of

LXA₄ actions, a specific LXA₄ receptor blocker (50 mM WRW4; Tocris, Loughborough, UK) was incubated together with cells prior to phagocytosis assays. Reactions were stopped by adding ice cold PBS/2% fetal calf serum, followed by two washes (500 x g, room temperature, 4 min). Samples were kept on ice before performing assays in duplicate to measure phagocytic index as described above for *in vivo* studies. Cells were then stained for Gr-1 and CD64. All assays were performed in duplicate and the average of the duplicates calculated.

Pyocyanin analysis

Overnight *P. aeruginosa* PA-14 cultures were prepared in cation-adjusted Mueller-Hinton broth at 37°C with shaking at 300 rpm. The overnight culture was diluted 100 fold into the same medium with the appropriate compounds. The positive control for pyocyanin included DMSO at the highest concentration used in the assay. LXA₄ was added at 8 nM, 5 nM, 1 nM, and 0.2 nM. All solutions were prepared in duplicates and were incubated at 37°C with shaking at 300 rpm for 36h. For High Performance Liquid Chromatography Mass Spectrometry Mass Spectrometry (HPLC-MS-MS) quantification, 1 mL from each overnight culture was transferred into a 2 mL microcentrifuge tubes and centrifuged at 12,000 X g for 15 min at 21°C. Using a syringe, 500 µL of the cell-free supernatant was removed and transferred into new tubes. Chloroform (400 µL) was added to each tube and then centrifuged at 12,000 x g for 1 min. A portion of the bottom organic layer (200 uL) was transferred into a vial for Ultra Performance Liquid Chromatography Mass Spectrometry Mass Spectrometry (UPLC-MS-MS) analysis. The samples were subjected to HPLC separation through an in-line Waters 2795 Separations Module on a BETASIL 5 mm Phenyl-Hexyl HPLC column (Thermo Scientific,

Waltham, MA, USA) using a linear gradient of ACN/H₂O (0.1% formic acid modified, 5% to 95% ACN) and were analyzed in positive ion mode on a Waters Micromass Quattro MS-MS by evaluating the TIC for the presence of pyocyanin molecular ion at m/z 211.28. The identity of pyocyanin was further confirmed by monitoring the presence of a characteristic fragmentation peak at m/z 168.33. The concentration of pyocyanin was determined by recording the TIC for m/z 211.28 of triplicate injections of the duplicate samples by comparison to an external calibration curve generated using pure pyocyanin (Aldrich, St. Louis, MO, USA).

LasR Reporter Strain Bioassay

The LasR reporter strain bioassay was performed as described previously (43) with modifications. The reporter strain was kindly provided by Bonnie L. Bassler (Princeton University). This *E. coli* strain was grown overnight at 37°C in Luria broth (LB) (Fisher Scientific) maintained with 100 µg/mL ampicillin and 50 µg/mL of kanamycin. The overnight culture was subcultured 1:40 for bioassay analysis. For agonist assays compounds were added to the diluted overnight reporter strain in 96-well black microplates with clear bottoms (Corning) at the starting concentrations described and titrated by serial dilution. Plates were incubated with shaking at 37°C for 4-6h and were evaluated for fluorescence (ex485/em538) and absorbance (A600) using a Molecular Devices SpectraMax M5 microplate reader. The native LasR agonist, N-3-oxo-dodecanoyl-L-homoserine lactone was utilized as the positive control for this assay. For antagonism assays, the native LasR agonist, 3-oxo-C12 HSL was employed at a constant concentration of 50 nM. The previously described antagonist, (S)-2-(4-bromophenyl)-N-(2-oxotetrahydrofuran-3-yl) acetamide (Br-HSL) was used as the positive control for

antagonism (50). LXA₄ or control compounds were added to the diluted overnight reporter strain containing 3-oxo-C12 HSL, titrated by serial dilution and analyzed as described for the agonist assay.

Statistical analyses:

One way analysis of variance (ANOVA) was used to analyze all data with more than 2 groups, using GraphPad Prism 6 software. Differences between groups were then ascertained using Newman-Keuls test of significance. In cases when there were only 2 groups, significance was analyzed using the unpaired t-test. For bacteria load, the Mann-Whitney U test for non-parametric data was used. In *ex vivo* studies, changes were expressed as percentage increase from controls samples incubated without LXA₄. Dose-response curves for the LasR-reporter strain studies were fit to the data using standard nonlinear regression data fitting settings in GraphPad Prism 6. Differences between groups are considered significant at $p < 0.05$.

Conclusion

This study provides evidence that LXA₄ increases host response against infection by augmenting neutrophil CD64 mediated phagocytic ability as well as reducing bacterial virulence. This novel dual property of LXA₄ working on both host defense and pathogen virulence warrants further investigation. Future studies on LXA₄ and related pro-resolving mediators may lead to discovery of a new class of antimicrobial which upregulates host defense and simultaneously reduces bacterial virulence.

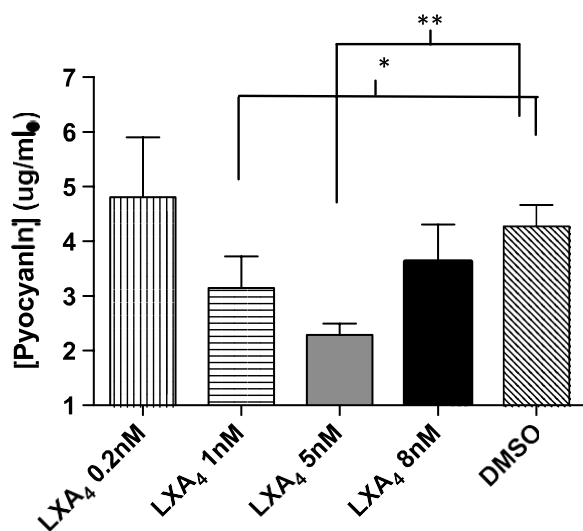


Figure 22. LXA₄ inhibits the expression of *P. aeruginosa* virulence factor, pyocyanin. Pyocyanin concentrations were determined by integration of the LC-MS total ion chromatogram (m/z, 211.2) on the basis of the correlation with a standard curve that was prepared by using pure pyocyanin. The data are presented as means \pm 6 SD of n = 3. *P, 0.05; **P, 0.01.

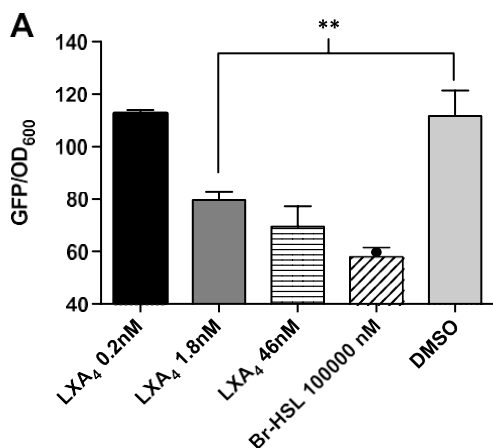
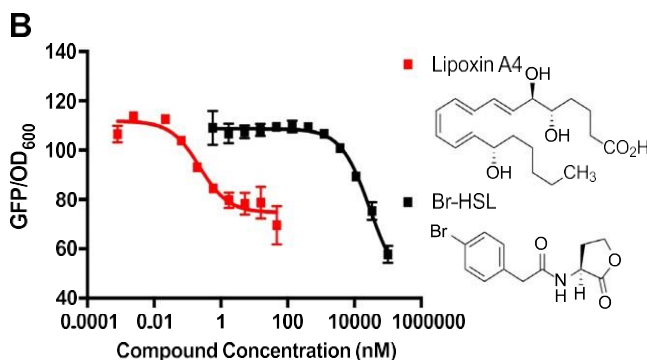


Figure 23. A) LXA₄ inhibits the LasR QS receptor. Inhibition values determined employing the green fluorescent protein (GFP)-based LasR antagonist bioassay. Inhibition of LasR at the compound concentrations indicated is shown as means \pm 6 SD of n = 3. **B)** Antagonism dose-response curve for LXA₄ and Br-HSL (known LasR antagonist) in the presence of 50 nM of the native LasR agonist, 3-oxo-C12 HSL. OD, optical density. Data points are means of n=3. **P, 0.01.



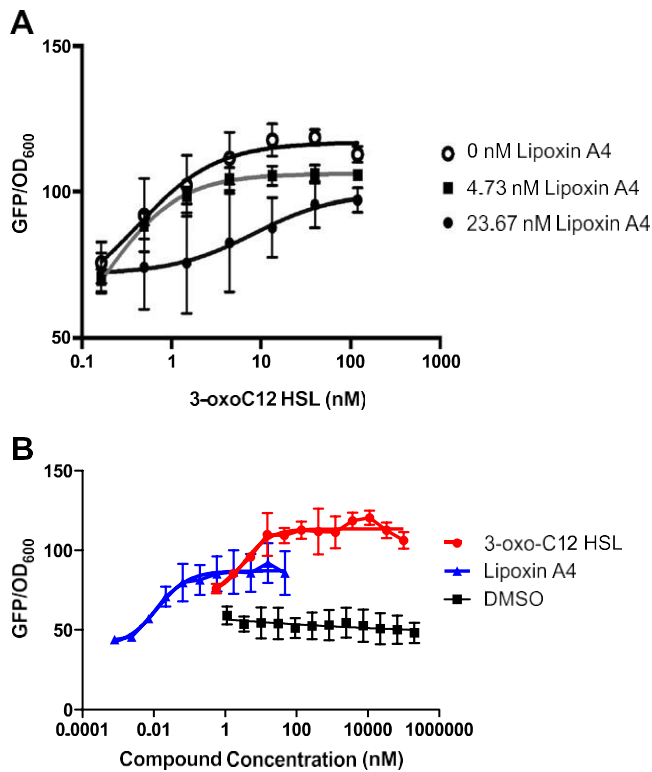


Figure 24. A) Competition binding assay for LXA₄ inhibition of LasR. The native LasR agonist, 3-oxo-C12 HSL, was titrated against fixed concentrations of LXA₄. Increasing values for the titration of the native agonist in the presence of increasing concentrations of inhibitor is consistent with LXA₄ acting as a reversible antagonist of this receptor. B) LasR agonist assays were performed by using LXA₄, 3-oxo-C12 HSL, and DMSO. LXA₄ is a partial agonist of LasR in *P. aeruginosa* in which maximum response is less than the maximum response of the endogenous ligand, 3-oxo-C12 HSL. GFP, green fluorescent protein; OD, optical density. All data points are means \pm 6 SD of $n = 3$.

References

- [1] El-Mowafi, Shaima A.; Alumasa, John N.; Ades, Sarah E.; Keiler, Kenneth C. Cell-Based Assay To Identify Inhibitors of the Hfq-sRNA Regulatory Pathway. *Antimicrobial Agents and Chemotherapy*. **2014**. 58: 5501-5509.
- [2] Bardill J, Xiaonan Z, Hammer J. The *Vibrio cholerae* quorum sensing response is mediated by Hfq-dependent sRNA/mRNA base pairing interactions. *Molecular Microbiology*. **2011**. 80:1381-1394.
- [3] Tu, Kimberly C.; Bassler, Bonnie L. Multiple small RNAs act additively to integrate sensory information and control quorum sensing in *Vibrio harveyi*. *Genes & Dev*. **2007**. 21: 221-233.
- [4] Vincent, Helen A.; Henderson, Charlotte A.; Stone, Carlanne M.; Cary, Peter D.; Gowers, Darren M.; Sobott, Frank; Taylor, James E.; Callaghan, Anastasia J. The low-resolution solution structure of *Vibrio cholerae* Hfq in complex with Qrr1 sRNA. *Nucleic Acids Research*. **2012**. 40: 8698–8710.
- [5] Sakai, Norio; Shimamura, Kazuyori; Ikeda, Reiko; Konakahara, Takeo. Hf(OTf)₄-Catalyzed Regioselective N-Aminomethylation of Indoles and Related NH-Containing Heterocycles. *J. Org. Chem*. **2010**. 75: 3923–3926.
- [6] Love, Brian. Facile Synthesis of N-Dialkylaminomethyl-Substituted Heterocycles. *J. Org. Chem*. **2007**. 72: 630-632.
- [7] Wen, Xiaoan; El Bakali, Jamal; Deprez-Poulain, Rebecca; Deprez, Benoit. Efficient propylphosphonic anhydride (T3P) mediated synthesis of benzothiazoles, benzoxazoles and benzimidazoles. *Tetrahedron Letters*. **2012**. 53: 2440–2443.
- [8] Young, Douglas D.; Deiters, Alexander. Photochemical hammerhead ribozyme activation. *Bioorganic & Medicinal Chemistry Letters*. **2006**. 16: 2658-2661.
- [9] Lusic, Hrvoje; Young, Douglas D.; Lively, Mark O.; Deiters; Alexander. Photochemical DNA Activation. *Organic Letters*. **2007**. 9: 1903-1906.
- [10] Young DD, Deiters A. Photochemical control of biological processes. *Org Biomol Chem*. **2007**. 5: 999-1005.
- [11] Zhao, X., Koestler, B. J., Waters, C. M., & Hammer, B. K. Post-transcriptional activation of a diguanylate cyclase by quorum sensing small RNAs promotes biofilm formation in *Vibrio cholerae*. *Molecular Microbiology*. **2013**. 89(5): 989-1002.
- [12] Shao, Y., & Bassler, B. L. Quorum regulatory small RNAs repress type VI secretion in *Vibrio cholerae*. *Molecular Microbiology*. **2014**. 92(5): 921-930.

- [13] Singh, Naorem Santa; Kachhap, Sangita; Singh, Richa; Chandra Mishra, Rahul; Singh, Balvinder; Raychaudhuri, Saumya. The length of glycine-rich linker in DNA-binding domain is critical for optimal functioning of quorum-sensing master regulatory protein HapR. *Molecular Genetics and Genomics*. **2014**. 289(6): 1171-1182.
- [14] Fuson, Reynold C.; Bull, Benton A. The Haloform Reaction. *Chem. Rev.* **1934**. 15(3): 275–309.
- [15] Sarma, Manas Jyoti; Borah, Arun Jyoti; Rajbongshi, Kamal Krishna; Phukan, Prodeep. Formation of new C–O and C–N bonds via base promoted Csp²–Csp³ bond cleavage of α -nitro ketone. *Tetrahedron Letters*. **2015**. 56(50): 7008–7011.
- [16] Ballini, Roberto; Bosica, Giovanna; Fiorini, Dennis. Uncatalyzed conversion of linear α -nitro ketones into amides by reaction with primary amines under solventless conditions. *Tetrahedron*. **2003**. 59: 1143–1145.
- [17] Maab, Ran; Heab, Liang-Nian; Liuab, An-Hua; Songab, Qing-Wen. Cu(II)-catalyzed esterification reaction via aerobic oxidative cleavage of C(CO)–C(alkyl) bonds. *Chem. Commun.* **2016**. 52: 2145-2148.
- [18] Lesic B, Lépine F, Déziel E, Zhang J, Zhang Q, Padfield K, et al. Inhibitors of pathogen intercellular signals as selective anti-infective compounds. *PLoS Pathog*. 2007 Sep 14;3(9):1229–39. PMID: PMC2323289
- [19] Rasmussen TB, Givskov M. Quorum-sensing inhibitors as anti-pathogenic drugs. *Int. J. Med. Microbiol*. 2006 Apr;296(2-3):149–61.
- [20] Lyon GJ, Muir TW. Chemical signaling among bacteria and its inhibition. *Chemistry & Biology*. Elsevier; 2003;10(11):1007–21.
- [21] Manefield M, de Nys R, Kumar N, Read R, Givskov M, Steinberg P, et al. Evidence that halogenated furanones from *Delisea pulchra* inhibit acylated homoserine lactone (AHL)-mediated gene expression by displacing the AHL signal from its receptor protein. *Microbiology (Reading, Engl.)*. 1999 Feb;145 (Pt 2):283–91.
- [22] Müh U, Hare BJ, Duerkop BA, Schuster M, Hanzelka BL, Heim R, et al. A structurally unrelated mimic of a *Pseudomonas aeruginosa* acyl-homoserine lactone quorum-sensing signal. *Proc. Natl. Acad. Sci. U.S.A. National Acad Sciences*; 2006;103(45):16948–52.
- [23] Müh U, Schuster M, Heim R, Singh A, Olson ER, Greenberg EP. Novel *Pseudomonas aeruginosa* quorum-sensing inhibitors identified in an ultra-high-

throughput screen. *Antimicrobial Agents and Chemotherapy*. 2006 Nov;50(11):3674–9. PMID: PMC1635174

- [24] Geske GD, O'Neill JC, Miller DM, Wezeman RJ, Mattmann ME, Lin Q, et al. Comparative Analyses of N-Acylated Homoserine Lactones Reveal Unique Structural Features that Dictate Their Ability to Activate or Inhibit Quorum Sensing. *ChemBioChem*. 2008 Feb 15;9(3):389–400.
- [25] Geske GD, O'Neill JC, Miller DM, Mattmann ME, Blackwell HE. Modulation of Bacterial Quorum Sensing with Synthetic Ligands: Systematic Evaluation of N-Acylated Homoserine Lactones in Multiple Species and New Insights into Their Mechanisms of Action. *J. Am. Chem. Soc.* 2007 Nov;129(44):13613–25.
- [26] Smith RS, Iglewski BH. *P. aeruginosa* quorum-sensing systems and virulence. *Current Opinion in Microbiology*. 2003 Feb;6(1):56–60.
- [27] Hentzer M, Wu H, Andersen JB, Riedel K, Rasmussen TB, Bagge N, et al. Attenuation of *Pseudomonas aeruginosa* virulence by quorum sensing inhibitors. *EMBO J.* 2003 Aug 1;22(15):3803–15. PMID: PMC169039
- [28] Smith KM, Bu Y, Suga H. Library Screening for Synthetic Agonists and Antagonists of a *Pseudomonas aeruginosa* Autoinducer. *Chemistry & Biology*. 2003 Jun;10(6):563–71.
- [29] Schuster M, Lostroh CP, Ogi T, Greenberg EP. Identification, timing, and signal specificity of *Pseudomonas aeruginosa* quorum-controlled genes: a transcriptome analysis. *Journal of Bacteriology*. 2003 Apr;185(7):2066–79. PMID: PMC151497
- [30] Lambert PA. Mechanisms of antibiotic resistance in *Pseudomonas aeruginosa*. *Journal of the Royal Society of Medicine*. Royal Society of Medicine Press; 2002;95(Suppl 41):22.
- [31] Kollef MH, Golan Y, Micek ST, Shorr AF, Restrepo MI. Appraising contemporary strategies to combat multidrug resistant gram-negative bacterial infections—proceedings and data from the Gram-Negative Resistance Summit. *CLIN INFECT DIS*. Oxford University Press; 2011;53(suppl 2):S33–S55.
- [32] Biodefense Category A, B, C Pathogens, NIAID, NIH [Internet]. niaid.nih.gov. [cited 2013 Oct 23]. Retrieved from: <http://www.niaid.nih.gov/topics/biodefenserelated/biodefense/pages/cata.a.spx>
- [33] Defoirdt T, Boon N, Bossier P. Can bacteria evolve resistance to quorum sensing disruption? *PLoS Pathog*. 2010;6(7):e1000989. PMID: PMC2900297

- [34] Khmel IA, Metlitskaya AZ. Quorum sensing regulation of gene expression: A promising target for drugs against bacterial pathogenicity. *Mol Biol.* 2006 Mar;40(2):169–82.
- [35] Clatworthy AE, Pierson E, Hung DT. Targeting virulence: a new paradigm for antimicrobial therapy. *Nat Chem Biol* [Internet]. Nature Publishing Group; 2007 Sep;3(9):541–8. Retrieved from: <http://www.nature.com/nchembio/journal/v3/n9/full/nchembio.2007.24.html>
- [36] Rasko DA, Sperandio V. Anti-virulence strategies to combat bacteria-mediated disease. *Nature Reviews Drug Discovery.* Nature Publishing Group; 2010 Jan 18;9(2):117–28.
- [37] Zakhari JS, Kinoyama I, Struss AK, Pullanikat P, Lowery CA, Lardy M, et al. Synthesis and Molecular Modeling Provide Insight into a *Pseudomonas aeruginosa* Quorum Sensing Conundrum. *J. Am. Chem. Soc.* 2011 Mar 23;133(11):3840–2.
- [38] Zou Y, Nair SK. Molecular Basis for the Recognition of Structurally Distinct Autoinducer Mimics by the *Pseudomonas aeruginosa* LasR Quorum-Sensing Signaling Receptor. *Chemistry & Biology.* Elsevier Ltd; 2009 Sep 25;16(9):961–70.
- [39] Meanwell NA. Synopsis of Some Recent Tactical Application of Bioisosteres in Drug Design. *J. Med. Chem.* [Internet]. 2011 Apr 28;54(8):2529–91. Retrieved from: <http://pubs.acs.org/doi/pdf/10.1021/jm1013693>
- [40] Amara N, Mashiach R, Amar D, Krief P, Spieser SAH, Bottomley MJ, et al. Covalent Inhibition of Bacterial Quorum Sensing. *J. Am. Chem. Soc.* 2009 Aug 5;131(30):10610–9.
- [41] Geske GD, Mattmann ME, Blackwell HE. Evaluation of a focused library of N-aryl l homoserine lactones reveals a new set of potent quorum sensing modulators. *Bioorganic & Medicinal Chemistry Letters.* Elsevier Ltd; 2008 Nov 15;18(22):5978–81.
- [42] Ni N, Li M, Wang J, Wang B. Inhibitors and antagonists of bacterial quorum sensing. *Med. Res. Rev.* 2009 Jan;29(1):65–124.
- [43] Mattmann ME, Blackwell HE. Small Molecules That Modulate Quorum Sensing and Control Virulence in *Pseudomonas aeruginosa*. *J. Org. Chem.* 2010 Oct 15;75(20):6737–46.
- [44] Fink, M.P., and Warren, H.S. (2014) Strategies to improve drug development for sepsis. *Nature Reviews* **13**, 741-758

- [45] Ayala, A., Perrin, M.M., Kisala, J.M., Ertel, W., and Chaudry, I.H. (1992) Polymicrobial sepsis selectively activates peritoneal but not alveolar macrophages to release inflammatory mediators (IL-1, IL-6 and TNF). *Circ. Shock* **36**, 191-199
- [46] Ayala, A., Kisala, J.M., Felt, J.A., Perrin, M.M., and Chaudry, I. H. (1992) Does endotoxin tolerance prevent the release of inflammatory monokines (interleukin 1, interleukin 6 or tumor necrosis factor) during sepsis? *Arch. Surg.*, **127**, 191-196
- [47] Docke, W.D., Randow, F., Syrbe, U., Krausch, D., Asadullah, K., Reinke, P., Volk, H. D., and Kox, W. (1997) Monocyte deactivation in septic patients: restoration by IFN-gamma treatment. *Nat. Med.* **3**, 678-681
- [48] Ellaban, E., Bolgos, G., and Remick, D. (2004) Selective macrophage suppression during sepsis. *Cell Immunol.* **231**, 103-111
- [49] Pahuja, M., Tran, C., Wang, H., and Yin, K. (2008) Alveolar macrophage suppression in sepsis is associated with HMGB1 migration. *Shock* **29**, 754-760
- [50] Reddy, R.C., Chen, G.H., Newstead, M.W., Moore, T., Zeng, X., Tateda, K., and Standiford, T.J. (2001) Alveolar macrophage deactivation in murine septic peritonitis: role of interleukin 10. *Infect. Immun.* **69**, 1394-1401
- [51] Liaw, W.J., Chen, T.H., Lai, Z.Z., Chen, S.J., Chen, A., Tzao, C., Wu, J.Y., and Wu, C.C. (2005) Effects of a membrane permeable radical scavenger, tempol, on intraperitoneal sepsis-induced organ injury in rats. *Shock* **23**, 88-96
- [52] Ritter, C., Andrades, M.E., Reinke, A., Menna-Barreto, S., Moreira, J.C., and Dal-Pizzol, F. (2004) Treatment with N-acetylcysteine plus deferoxamine protects rats against oxidative stress and improves survival in sepsis. *Crit. Care Med.* **32**, 342-349
- [53] Yang, Q., Ghose, P., and Ismail, N. (2013) Neutrophils mediate immunopathology and negatively regulate protective immune responses during fatal bacterial infection-induced toxic shock. *Infect. Immun.* **81**, 1751-1763
- [54] Alves-Filho, J.C., Freitas, A., Spiller, F., Souto F.O., and Cunha, F.Q. (2008) The role of neutrophils in severe sepsis. *Shock* **30** (suppl. 1), 3-9
- [55] Craciun, F.L., Schuller, E.R., and Remick, D.G. (2010) Early enhanced local neutrophil recruitment in peritonitis-induced sepsis improves bacterial clearance and survival. *J. Immunol.* **185**, 6930-6938
- [56] Kasten, K.R., Prakash, P.S., Unsinger, J., Goetzman, H.S., England, L.G., Cave, C.M., Seitz, A.P., Mazuski, C.N., Zhou, T.T., Morre, M., Hotchkiss, R.S.,

Hildeman, D.A., and Caldwell, C.C. (2010) Interleukin-7 (IL-7) treatment accelerates neutrophil recruitment through gamma delta T-cell IL-17 production in a murine model of sepsis. *Infect. Immun.* **78**, 4714-4722

- [57] Robertson, C. M., Perrone, E. E., McConnell, K. W., Dunne, W. M., Boody, B., Brahmabhatt, T., Diacovo, M. J., Van Rooijen, N., Hogue, L. A., Cannon, C. L., Buchman, T. G., Hotchkiss, R. S., and Coopersmith, C. M. (2008) Neutrophil depletion causes a fatal defect in murine pulmonary Staphylococcus aureus clearance. *J. Surg. Res.* **150**, 278-285
- [58] Danikas, D.D., Karakantza, M., Theodorou, G. L., Sakellaropoulos, G.C., and Gogos, C.A. (2008) Prognostic value of phagocytic activity of neutrophils and monocytes in sepsis: Correlation to CD64 and CD14 antigen expression. *Clin. Exp. Immunol.* **154**, 87-97
- [59] Cid, J., Garcia-Pardo, G., Aguinaco, R., Sanchez, R., and Llorente, A. (2001) Neutrophil CD64: diagnostic accuracy and prognostic value in patients presenting to the emergency department. *Eur. J. Clin. Microbiol. Infect. Dis.* **30**, 845-852
- [60] Godson, C., Mitchell, S., Harvey, K., Petasis, N. A., Hogg, N. A., and Brady, H. R. (2000) Cutting edge: lipoxins rapidly stimulate nonphlogistic phagocytosis of apoptotic neutrophils by monocyte-derived macrophages. *J Immunol.* **164**:1663-1667
- [61] Serhan, C. N., and Chiang, N. (2004) Novel endogenous small molecules as the checkpoint controllers in inflammation and resolution: entrée for resolomics. *Rheum. Dis. Clin. North Am.* **30**, 69-95
- [62] Serhan, C. N., Chiang, N., and Van Dyke, T. E. (2008) Resolving inflammation: dual anti-inflammatory and pro-resolution lipid mediators. *Nat. Rev. Immunol.* **8**, 349-361
- [63] Bannenberg, G., Moussignac, R.L., Gronert, K., Devchand, P.R., Schmidt, B.A., Guilford, W.J., Bauman, J.G., Subramanyam, B., Perez, H.D., Parkinson, J.F., and Serhan, C.N. (2004) Lipoxins and novel 15-epi-lipoxin analogs display potent anti-inflammatory actions after oral administration. *Br. J. Pharmacol.* **143**, 43-52
- [64] Gewirtz, A.T., Collier-Hyams, L.S., Young, A.N., Torsten, K., Guilford, W.J., Parkinson, J.F., Williams, I.R., Neish, A.S., and Madara, J.L. (2002) Lipoxin A₄ analogs attenuate induction of intestinal epithelial proinflammatory gene expression and reduce the severity of dextran sodium sulfate-induced colitis. *J. Immunol.* **168**, 5260-5267

- [65] Leonard, M.O., Hannan, K., Burne, M.J., Lappin, D.W.P., Doran, P., Coleman, P., Stenson, C., Taylor, C.T., Daniels, .F, Godson, C., Petasis, N.A., Rabb, H., and Brady, H.R. (2002) 15-epi-16-parafluorophenoxy lipoxin A₄ methyl ester, a synthetic analogue of 15-epi-lipoxin A₄ is protective in experimental ischemic acute renal failure. *J. Am. Soc. Nephrol.* **13**, 1657-1662
- [66] Mitchell, S., Thomas, G., Harvey, K., Cottell, D., Reville, K., Berlasconi, G., Petasis, N. A., Erwig, L., Rees, A. J., Savill, J., Brady, H. R., and Godson, C. (2002) Lipoxins, aspirin-triggered epi-lipoxins, lipoxin stable analogues, and the resolution of inflammation: stimulation of macrophage phagocytosis of apoptotic neutrophils in vivo. *J. Am. Soc. Nephrol.* **13**, 2497-2507
- [67] Chiang, N., Fredman, G., Backhed, F., Oh, S.F., Vickery, T., Schmidt, B.A., and Serhan, C.N. (2012) Infection regulates pro-resolving mediators that lower antibiotic requirements. *Nature* **482**, 524-528
- [68] El Kebir, D., Gjorstrup, P., and Filep, J. G. (2012) Resolvin E1 promotes phagocytosis-induced neutrophil apoptosis and accelerates resolution of pulmonary inflammation. *Proc. Natl. Acad. Sci. USA* **109**, 14983-14988
- [69] Pouliot, M., Clish, C.B., Petasis, N.A., Van Dyke, T.E., and Serhan, C.N. (2000) Lipoxin A₄ analogues inhibit leukocyte recruitment to *Porphyromonas gingivalis*: a role for cyclooxygenase-2 and lipoxins in periodontal disease. *Biochemistry* **39**, 4761-4768
- [70] Spite, M., Norling, L.V., Summers, L., Yang, R., Cooper, D., Petasis, N.A., Flower, R. J., Perretti, M., and Serhan, C.N. (2009) Resolvin D2 is a potent regulator of leukocytes and controls microbial sepsis. *Nature* **461**, 1287-1291
- [71] Ueda, T., Fukunaga, K., Seki, H., Miyata, J., Arita, M., Miyasho, T., Obata, T., Asaon, K., Betsuyaku, T., and Takeda, J. (2014) Combination therapy of 15-Epi-Lipoxin A₄ with antibiotics protects mice from *Escherichia coli* –Induced sepsis. *Crit. Care Med.* **42**, e288-e295
- [72] Walker, J., Dichter, E., Lacorte, G., Kerner, D., Spur, B., Rodriguez, A., and Yin, K. (2011) Lipoxin A₄ increases survival by decreasing systemic inflammation and bacterial load in sepsis. *Shock* **36**, 410-417
- [73] Wu, B., Walker, J., Temmermand, D., Mian, K., Spur, B., Rodriguez, A., Stein, T.P., Banerjee, P., and Yin, K. (2013) Lipoxin A₄ promotes more complete inflammation resolution in sepsis compared to stable Lipoxin A₄ analog. *Prost. Leukot. Essent. Fatty Acids* **89**, 47-53
- [74] Wu, B., Walker, J., Spur, B.W., Rodriguez, A., and Yin, K. (2015) Effects of Lipoxin A₄ on antimicrobial actions of neutrophils in sepsis. *Prost. Leukot. Essent. Fatty Acids* **94**, 55-64

- [75] Qureshi, S., Lewis, S., Gant, V., Treacher, D., Davis, B., and Brown, K. (2001) Increased distribution and expression of CD64 on blood polymorphonuclear cells from patients with the systemic inflammatory response syndrome (SIRS). *Clin. Exp. Immunol.* **125**, 258-265
- [76] Garcia-Garcia E., and Rosales, C. (2002) Signal transduction during Fc receptor-mediated phagocytosis. *J. Leukocyte Biol.* **72**, 1092-1108
- [77] Indik, Z.K., Hunter, S., Huang, M.M., Pan, X.Q., Chien, P., Kelly, C., Levinson, A.I., Kimberly, R.P., and Schreiber, A.D. (1994). The high affinity Fc γ receptor (CD64) induces phagocytosis in the absence of its cytoplasmic domain: the gamma subunit of Fc γ RIIIA imparts phagocytic function to Fc γ RI. *Exp. Hematol.* **22**, 599-606
- [78] Indik, Z.K., Park, J.G., Hunter, S., and Schreiber, A.D. (1995) Structure/function relationships of Fc-gamma receptors in phagocytosis. *Semi. Immunol* **7**, 45-54
- [79] Galloway, W.R.J.D., Hodgkinson J.T., Bowden, S.D., Welch, M., and Spring, D.R. (2011) Quorum sensing in Gram-negative bacteria: small-molecule modulation of AHL and AI-2 quorum sensing pathways. *Chem. Rev.* **111**, 28–67
- [80] Gonzalez, Barrios A.F., Zuo, R., Hashimoto, Y., Yang, L., Bentley, W.E., and Wood, T.K. (2006) Autoinducer 2 controls biofilm formation in *Escherichia coli* through a novel motility quorum-sensing regulator (MqsR, B3022). *J. Bacteriology* **188**, 305-316
- [81] Gonzalez, J.E., and Keshavan, N.D. (2006) Messing with bacterial quorum sensing. *Microbiol. Molecular Biol. Reviews* **70**, 859-874
- [82] Henke, J.M., and Bassler, B.L. (2004) Three parallel quorum sensing systems regulate gene expression in vibrio harveyi. *J. Bacteriol.* **186**, 6902-6914
- [83] Lowery, C.A., Salzameda, N.T., Sawada, D., Kaufmann, G.F., and Janda, K.D. (2010). Medicinal chemistry as a conduit for the modulation of quorum sensing. *J. Med. Chem.* **53**, 7467–7489
- [84] Jimenez, P.N., Koch, G., Thompson, J.A., Xavier, K.B., Cool, R.H., and Quax, W.J. (2012) The multiple signaling systems regulating virulence in *Pseudomonas aeruginosa*. *Microbiol. Mol. Bio. Rev.* **76**, 46–65
- [85] Ng, W.-L., and Bassler B.L. (2009) Bacterial quorum-sensing network architectures. *Annu. Rev. Genet.* **43**, 197–222

- [86] O'Loughlin, C.T., Miller, L.C., Siryaporn, A., Drescher, K., Semmelhack, M. F., and Bassler, B. L. (2013) A quorum-sensing inhibitor blocks *Pseudomonas aeruginosa* virulence and biofilm formation. *Proc. Natl. Acad. Sci. USA* **110**, 17981-17986
- [87] Kalia, V.C. (2012) Quorum sensing inhibitors: An overview. *Biotechnology Advances* **31**, 224-245
- [88] Lesic, B., Lépine, F., Déziel, E., Zhang, J., Zhang, Q., Padfield, K., Castonguay, M.H., Milot, S., Stachel, S., Tzika A.A, Tompkins, R.G., and Rahme, L.G. (2007) Inhibitors of pathogen intercellular signals as selective anti-infective compounds. *PLoS Pathog.* **3**,1229–1239
- [89] Rasmussen, T. B., and Givsko, M. (2006) Quorum-sensing inhibitors as anti-pathogenic drugs. *Int. J. Med. Microbiol.* **296**, 149–161
- [90] Rodríguez, A., Nomen, M., Spur, B.W., Godfroid, J.-J., and Lee, T.-H. (2000) Total synthesis of lipoxin A₄ and lipoxin B₄ from butadiene. *Tetrahedron Lett.* **41**, 823-826
- [91] Rittirsch, D., Huber-Lang, M.S., Flieri, M.A., and Ward, P.A. (2009) Immunodesign of experimental sepsis by cecal ligation and puncture. *Nat. Protoc.* **4**, 31-36
- [92] Ribechini, E., Leenen, P.J.M. and Lutz, M.B. (2009) Gr-1 antibody induces STAT signaling, macrophage marker expression and abrogation of myeloid-derived suppressor cell activity in BM cells. *Eur. J. Immunol.* **39**, 3538-3551.
- [93] Geske, G.D., O'Neill, J.C., Miller, D.M., Mattmann, M.E., and Blackwell, H.E. (2007) Modulation of bacterial quorum sensing with synthetic ligands: systematic evaluation of N-acylated homoserine lactones in multiple species and new insights into their mechanisms of action. *J. Am. Chem. Soc.* **129**, 13613–13625
- [94] Paunel-Gorgulu, A., Kirichevska, T., Logters, T., Windolf, J., and Flohe, S. (2012) Molecular mechanisms underlying delayed apoptosis in neutrophils from multiple trauma patients with and without sepsis. *Mol. Med.* **18**, 325-335
- [95] Fox, S., Leitch, A., Duffin, R., Haslett, C., and Rossi A.G. (2010) Neutrophil apoptosis: Relevance to innate immune response and inflammatory disease. *J. Innate Immun.* **2**, 216-227
- [96] Kennedy, A.D., and DeLeo, F.R. (2009) Neutrophil apoptosis and the resolution of infection. *Immunol. Res.* **43**, 25-61

- [97] Sordi, R., Menezes-de-Lima Jr, O., Horewica, V., Sceschowitsch, K., Santos, L.F., and Assreuy J. (2013) Dual role of lipoxin A₄ in pneumosepsis pathogenesis. *Int. Immunopharmacol.* **17**, 283-292
- [98] Allen, L., Dockrell, D.H., Pattery, T., Lee, D.G., Cornelis, P., Hellewell, P.G. and Whyte, M.K.B. (2005) pyocyanin production by *Pseudomonas aeruginosa* induces neutrophil apoptosis and impairs neutrophil host defenses in vivo. *J. Immunol.*, **174**, 3643-3649
- [99] Fierro, I.M., Colgan, S.P., Bernasconi, G., Petasis, N.A., Clish, C.B., Arita, M., and Serhan, C.N. (2003) Lipoxin A₄ and aspirin-triggered 15-epi-lipoxin A₄ inhibit human neutrophil migration: comparisons between synthetic 15 epimers in chemotaxis and transmigration with microvessel endothelial cells and epithelial cells. *J. Immunol.* **170**, 2688-2694
- [100] Maddox, J.F., and Serhan C.N. (1996) Lipoxin A₄ and B₄ are potent stimuli for human monocyte migration and adhesion: selective inactivation by dehydrogenation and reduction. *J. Exp. Med.* **183**, 137-146
- [101] Levy, B., Clish, C.B., Schmidt, B., Gronert, K., and Serhan, C.N. (2001) Lipid mediator class switching during acute inflammation signals in resolution. *Nature Immunol.* **2**, 612-619
- [102] Dransfield, I., Rossi, A.G., Brown, S.B., and Hart S.P. (2005) Neutrophils: dead or effete? Cell surface phenotype and implications for phagocytic clearance. *Cell Death Differ.*, **12**, 1363-1367
- [103] El Kebir, D., Jozsef, L., Pan, W., Petasis, N.A., Serhan, C.N., and Filep, J.G.. (2007) Aspirin-triggered lipoxins override the apoptosis–delaying action of serum amyloid A in human neutrophils: A novel mechanism for resolution of inflammation. *J. Immunol.* **179**, 616-622
- [104] Dufton, N., Hannon, R., Brancalone, V., Dalli, J., Patel, H. B., Gray, M., D’Acquisto, F., Buckingham, M., Perretti, M., and Flower R. J. (2010) Anti-inflammatory role of the murine formyl-peptide receptor 2: ligand-specific effects on leukocyte responses and experimental inflammation. *J. Immunol.* **184**, 4092-4098
- [105] El Kebir, D., Jozsef, L., and Filep, J.G. (2008) Opposing regulation of neutrophil apoptosis through the formyl peptide receptor-like 1/lipoxin A₄ receptor: implications for resolution of inflammation. *J. Leuk. Biol.* **84**, 600-606
- [106] Jin, S.-W., Zhang, L., Lian, Q.-Q., Liu, D., Wu, P., Yao, S.-L., and Ye, D.-Y. (2007) Posttreatment with aspirin-triggered lipoxin A₄ analog attenuates lipopolysaccharide-induced acute lung injury in mice: the role of heme oxygenase-1. *Crit. Care and Trauma*, **104**, 369-377

- [107] Dalli, J., Chiang N. and Serhan C.N. (2015) Elucidation of novel 13-series resolvins that increase with atorvastatin and clear infections. *Nature Medicine*, **21**, 1071-1075.
- [108] Lee, T.H., Horton, C.E., Kyan-Aung, U., Haskard, D., Crea, A.E.G., and Spur B.W. (1989) Lipoxin A₄ and lipoxin B₄ inhibit chemotactic responses of human neutrophils stimulated by leukotriene B₄ and N-formyl-L-methionyl-L-leucyl-phenylalanine. *Clin. Sci.* **77**, 195–203
- [109] Maderna, P., Cottell, D.C., Berlasconi, G., Petasis, N.A., Brady, H.R., and Godson C. (2002). Lipoxins induce actin reorganization in monocytes and macrophages but not in neutrophils. *Am. J. Pathol.* **160**, 2275-2283
- [110] Serhan, C.N., Maddox, J.F., Petasis, N.A., Akritopoulou-Zanze, I., Papayianni, A., Brady, H.R., Colgan, S.P., and Madara, J.L. (1995) Design of lipoxin A₄ stable analogs that block transmigration and adhesion of human neutrophils. *Biochemistry* **34**, 14609–14615
- [111] Looney, M.R., Su, X., Van Ziffle, J.A., Lowell, C.A., and Matthay, M.A. (2006) Neutrophils and their Fcγ receptors are essential in a mouse model of transfusion-related acute lung injury. *J. Clin. Invest.* **116**, 1615-1623
- [112] Hussein, O.A., El-Toukhy, M.A., and El-Rahman, H.S. (2010). Neutrophil CD64 expression in inflammatory autoimmune diseases: its value in distinguishing infection from disease flare. *Immunol. Invest.* **39**, 699-712
- [113] Fergie, J.E., Shema, S.J., Lott, L., Crawford, R., and Patrick, C.C. (1994) *Pseudomonas aeruginosa* bacteremia in immunocompromised children: analysis of factors associated with poor outcome. *Clin. Infect. Dis.*, **18**, 390-394
- [114] Mishra, M., Byrd, M.S., Sergeant, S., Azad, A.K., McPhail, L., Schlesinger, L.S., Parsek, M.R., and Wozniak D.J. (2012) *Pseudomonas aeruginosa* Psi polysaccharide reduces neutrophil phagocytosis and the oxidative response by limiting complement-mediated opsonization. *Cell Microbiol.* **14**, 95-106
- [115] Moore, J.D., Rossi, F.M., Welsh, M.A., Nyffeler, K.E., and Blackwell, H.E. (2015) A comparative analysis of synthetic quorum sensing modulators in *Pseudomonas aeruginosa*: new insights into mechanism, active efflux susceptibility, phenotypic response, and next-generation ligand design, *J. Am. Chem. Soc.* **137**, 14626–14639
- [116] Prince, L.R., Bianchi, S.M., Vaughan, K.M., Bewley, M.A., Marriott, H.M., Walmsley, S.R., Taylor, G.W., Buttle, D.J., Sabroe, I., Dockrell, D.H., and Whyte, M.K. (2008) Subversion of a lysosomal pathway regulating neutrophil apoptosis by a major bacterial toxin, pyocyanin. *J. Immunol.* **180**, 3502-3511

- [117] Pearson, J.P., Gray, K.M., Passador, L., Tucker, K.D., Eberhard, A., Iglewski, B.H., and Greenberg, E.P. (1994). Structure of the autoinducer required for expression of *Pseudomonas aeruginosa* virulence genes. *Proc. Natl. Acad. Sci. USA* **91**, 197–201
- [118] Smith, R.S., Harris, S.G., Phipps, R., and Iglewski, B. (2002) The *Pseudomonas aeruginosa* quorum-sensing molecule N-(3-oxododecanoyl) homoserine lactone contributes to virulence and induces inflammation in vivo. *J. Bacteriology* **184**, 1132-1139
- [119] Glucksam-Galnoy, Y., Sananes, R., Silberstein, N., Krief, P., Kravchenko, V.V., Meijler, M.M., and Zor, T. (2013) The bacterial quorum-sensing signal molecule n-3-oxo-dodecanoyl-L-homoserine lactone reciprocally modulates pro- and anti-inflammatory cytokines in activated macrophages. *J. Immunol.* **191**, 337-344
- [120] O'Brien, K.T., Noto, J.G., Nichols-O'Neill, L., and Perez, L.J. (2015) Potent irreversible inhibitors of quorum sensing regulated virulence in *Pseudomonas aeruginosa*. *ACS Med. Chem. Lett.* **6**, 162-167
- [121] Lau, G. W., Ran, H., Kong, F., Hassett, D. J., and Mavradi, D. (2004) *Pseudomonas aeruginosa* pyocyanin is critical for lung infection in mice. *Infect. Immun.* **71**, 4275-4278
- [122] Sorensen, R.U., and Klinger, J.D. (1987) Biological effects of *Pseudomonas aeruginosa* phenazine pigments. *Antibiot. Chemother.* **39**, 113-124
- [123] Vance, R.E., Hong, S., Gronert, K., Serhan, C.N. and Mekalanos, J.T. (2004) The opportunistic pathogen *pseudomonas aeruginosa* carries a secretable arachidonate 15-Lipoxygenase. *Proc. Natl. Acad. Sci., USA* **101**, 2135-2139.